Quantum Brownian Motion in Bose-Einstein Condensates

Submitted in partial fulfillment of the requirements

of the degree of

Doctor of Philosophy

by

Christos Charalambous

Supervisor

Prof. M. Lewenstein

Co-Supervisor

Dr. M.-A. Garcia-March

UNIVERSITAT POLITECNICA DE CATALUNYA

(2020)

Dedicated to

"$\mathcal{FAMILY}$"

Acknowledgments

"*...I hope for nothing, I fear for nothing, I am free...*" N. Kazantzakis

This PhD thesis is the result of my "Brownian motion" in life, starting from Cyprus, moving through London, Zurich and finally Barcelona, where certain forces that pushed me towards my current state appear to be less random than others and worth explicit mentioning. I first thank my supervisor Maciej Lewenstein for giving me the opportunity to undertake this PhD in his group, allowing me to pursue the research directions that I found interesting. I also thank my cosupervisor Miguel-Angel Garcia-March for supporting me in the difficult moments of my PhD and encouraging me in my first steps as a researcher. Without doubt, important contributions to the completion of this thesis had Aniello Lampo, Gorka Muñoz-Gil, Mohammad Mehboudi and Arnau Riera.

Χωρίς αμφιβολία όμως, έχοντας ξεκινήσει ένα διδακτορικό στα 27 μου, ήμουνα ήδη μια καλά διαμορφωμένη προσωπικότητα και ως εκ τούτου θεωρώ ότι ένα μεγάλο μέρος των ευχαριστιών μου πρέπει να αποδοθεί σε όλες εκείνες τις "δυνάμεις' που συνέβαλαν στον σχηματισμό της προσωπικότητας που είμαι σήμερα, πριν ξεκινήσω τις διδακτορικές μου σπουδές. Ηλίου φαεινότερο είναι ότι πρώτοι στην λίστα με αυτούς τους οποίους οφείλω να ευχαριστήσω βρίσκονται οι γονείς μου. Αναμφίβολα, η συνεισφορά τους στην ζωή μου μπορεί μόνο να χαρακτηρισθεί εως σαν την σταθερής κατεύθυνσης αυτοφυής δύναμη που συναντά κανείς στην κίνηση των "ενεργών σωματιδίων του Μπράουν". Ο παραλληλισμός αυτός θεωρώ ότι είναι ακριβής μιας και ξέρω ότι πάντα ένα κομμάτι του εαυτού μου θα καθοδηγείται σταθερά από τις αξίες και το ήθος που μου έχουν εμφυσήσει και για τα οποία θα τους είμαι αιώνια ευγνώμων. Μητέρα Πατέρα σας αγαπώ και σας ευχαριστώ εκ βάθους καρδίας. Χωρίς εσάς τίποτα από όσα έχω καταφέρει δεν θα ήταν εφικτό. Οφείλω επίσης να ευχαριστήσω όλα τα άτομα που με τον ένα ή τον άλλο τρόπο πίστεψαν σε εμένα, και με τον τρόπο τους ο καθένας, μου έδωσαν την απαραίτητη αυτοπεποίθηση για να πετύχω ότι έχω πετύχει μέχρι σήμερα. Σε αυτή την κατηγορία περιλαμβάνονται προφανώς όλα τα άτομα της οικογένειας μου στην Κύπρο, όπου με τον όρο οικογένεια δεν αναφέρομαι μόνο στα άτομα που συνδέομαι εξ αίματος. Ευχαριστώ όλους τους ανθρώπους που γνώρισα στο Λονδίνο, την Ζυρίχη και την Βαρκελώνη και τους οποίους μπορώ να αποκαλώ πραγματικούς φίλους. Προφανώς αυτοί που θα το διαβάσουν ξέρουν σε ποιούς αναφέρομαι. Τέλος πρέπει να ευχαριστήσω την κοπέλα μου Λάουρα που σε αυτό το τελευταίο έτος του διδακτορικού μου υπήρξε ένα ασφαλές λιμάνι όπου πάντα ήξερα ότι μπορούσα να αντιμετωπίσω τις φουρτούνες που έρχονταν. Σας ευχαριστώ όλους όσους συνεισφέρατε με τον ένα ή τον άλλο τρόπο στο να έχει η Μπραουνιανή μου κίνηση μια τόσο όμορφη κατεύθυνση τελικά!

C. Charalambous

LIST OF PUBLICATIONS

Journal Papers included in this Thesis

1. C. Charalambous, M. A. García-March, G. Munoz-Gil, P. R. Grzybowski and M. Lewenstein, (2019), Control of anomalous diffusion of a Bose polaron in a coherently coupled two-component BEC, arxiv:1910.01571 (Submitted to Quantum).

2. C. Charalambous, M. A. García-March, M. Mehboudi and M. Lewenstein, (2019), Heat current control in trapped BEC, *New J. of Physics*, **21** (8), 083037.

3. M. Mehboudi, A. Lampo, C. Charalambous, L. A. Correa, M. A. García-March and M. Lewenstein,(2019), Using polarons for sub-nk quantum non-demolition thermometry in a Bose-Einstein condensate, *Phys. Rev. Lett.* **122** (3), 030403.

4. C. Charalambous, M. A. García-March, A. Lampo, M. Mehboudi and M. Lewenstein, (2019), Two distinguishable impurities in BEC: squeezing and entanglement of two Bose polarons, *SciPost* **6** (10).

Other Journal Papers

5. A. Lampo, C. Charalambous, M. A. García-March and M. Lewenstein, (2018),Non-Markovian polaron dynamics in a trapped Bose-Einstein condensate, *Phys. Rev. A* **98** (6), 063630.

6. T. R. de Oliveira, C. Charalambous, D. Jonathan, M. Lewenstein and A. Riera, (2018), Equilibration time-scales in closed many-body quantum systems, *New J. of Physics* **20** (3), 033032.

7. G. Muñoz-Gil, C. Charalambous, M. A. García-March, M. F. Garcia-Parajo, C. Manzo, M. Lewenstein and A. Celi, (2017), Transient subdiffusion from an Ising environment, *Phys. Rev. E* **96**, 052140.

8. C. Charalambous, G. Muñoz-Gil, A. Celi, M. F. Garcia-Parajo, M. Lewenstein, C. Manzo, and M. A. García-March, (2017), Nonergodic subdiffusion from transient interactions with heterogeneous partners, *Phys. Rev. E* **95**, 032403 .

Abstract

English version

Quantum Brownian motion is one of the most prominent examples of an open quantum system, a system which cannot be treated in isolation, due to the unavoidable interaction with the surrounding environment. There are a number of methods to study the dynamics of a system undergoing such a type of motion, and recently it was shown that the simplest one that satisfies Heisenberg Uncertainty principle is the approach of Quantum Generalized Langevin Equations (QGLE). This is also the method used throughout this thesis. A Quantum Brownian motion approach was used to study a plethora of systems, among them the Bose polaron problem. In this case, one transforms the original problem into one where the impurities are treated as quantum Brownian particles interacting with a bath composed of the Bogoliubov modes of the condensate. Then by deriving the relevant QGLE, it was shown that the dynamics of the Bose polaron exhibit memory effects. This was studied for both a free BEC and a harmonically trapped one. Taking advantage of this recent theoretical development, we study a number of phenomena that can be examined under this prism and show how various microdevices can be constructed and controlled.

In the first project, we study the creation of entanglement and squeezing of two uncoupled impurities that are immersed in a single common Bose-Einstein condensate (BEC) bath. We treat these impurities as two quantum Brownian particles as explained above. We study two scenarios:(i) In the absence of an external potential, we observe sudden death of entanglement;(ii) In the presence of an external harmonic potential, where entanglement survives even at the asymptotic time limit. In our study we consider experimentally tunable parameters.

In our second work, we studied the diffusive behavior of a Bose Polaron immersed in a coherently coupled two-component BEC. The particle superdiffuses if it couples in the same manner to both components, i.e. if it couples either attractively or repulsively to both of them. This is the same behavior of an impurity immersed in a single BEC. Conversely, we find that it exhibits a transient nontrivial subdiffusive behavior if it couples attractively to one of the components and repulsively with the other. We show how the magnitude of the anomalous exponent reached and the duration of the subdiffusive interval can be controlled with the Rabi frequency of the coherent coupling between the two components and the coupling strength of the impurity to the BEC.

Then we proceeded with the construction of two microdevices, a quantum sub-nk thermometer and a heat diode. In the first project, we introduced a novel minimally disturbing method for sub-nK thermometry in a Bose-Einstein condensate (BEC). Our technique again was based on the Bose polaron model where an impurity embedded in the BEC acts as the thermometer. We propose to detect temperature fluctuations from measurements of the position and momentum of the impurity. Crucially, these cause minimal backaction on the BEC and hence, realize a nondemolition temperature measurement. Following the paradigm of the emerging field of quantum thermometry, we combine tools from quantum parameter estimation and the theory of open quantum systems to solve the problem in full generality. We thus avoid any simplification, such as demanding thermalization of the impurity atoms, or imposing weak dissipative interactions with the BEC. Our method is illustrated with realistic experimental parameters common in many labs, thus showing that it can compete with state-of-the-art destructive techniques, even when the estimates are built from the outcomes of accessible (suboptimal) quadrature measurements.

In our final work, we investigated the heat transport and the control of heat current among two spatially separated trapped Bose–Einstein Condensates (BECs), each of them at a different temperature. To allow for heat transport among the two independent BECs we consider a link made of two harmonically trapped impurities, each of them interacting with one of the BECs. Since the impurities are spatially separated, we consider long-range interactions between them, namely a dipole–dipole coupling. We study this system under theoretically suitable and experimentally feasible assumptions/parameters. The dynamics of these impurities is treated within the framework of the quantum Brownian motion model as before. We address the dependence of heat current and current–current correlations on the physical parameters of the system. Interestingly, we show that heat rectification, i.e. the unidirectional flow of heat, can occur in our system, when a periodic driving on the trapping frequencies of the impurities is considered. Therefore, our system is a possible setup for the implementation of a phononic circuit. Motivated by recent developments on the usage of BECs as platforms for quantum information processing, our work offers an alternative possibility to use this versatile setting for information transfer and processing, within the context of phononics, and more generally in quantum thermodynamics.

Spanish version

El movimiento Browniano, es uno de los ejemplos mas prominentes de un sistema abierto, es decir un sistema que no se puede tratar en aislamineto, debido a la inevidable interaccion con su ambiente. Existe una multitud de metodos para estudiar la dinamica de un sistema que realiza dicho tipo de movimiento, y recientemente se ha demostrado

que el metodo mas simple que cumple el principio de la incertidumbre de Heisenberg es el de Quantum Generalized Langevin Equations (QGLE). Este es tambien el metodo que se usa en esta tesis. La perspectiva de Quantum Brownian motion se ha usado para estudiar una plethora de sistemas, entre ellos el probema de Bose polaron. En este caso, uno pasa el problema original a uno donde las impurezas se tratan como Quantum Brownian particulas interactuando con un baño compuesto de modos de Bogoliubov del condensado. Despues de derivar la QGLE relevante, se habia demostrado que la dinamica del Bose polaron muestra efectos de memoria. Esto se ha estudiado tanto en un BEC libre como en uno atrapado en un trapo harmonico. Aprovechando de este reciente desarrollo, estudiamos muchos phenomenos que se pueden investigar bajo este prisma y mostramos como se pueden constuir y controlar varios microdispositivos.

En el primer proyecto, estudiamos la creacion de enlazamiento y squeezing de dos impurezas no copladas, immersas en un unico Bose-Einstein condensate baño comun. Tratamos estas dos impurezas como dos particulas quantum Brownianas. Estudiamos dos scenarios: (i) en la ausencia de un potencial externo, donde observamos la muerte repentina del enlazamiento (ii) en la presencia de un trapo externo harmonico, donde el enlazamiento sobrevive incluso en el limite asimptotico de largos tiempos. En nuestros estudios, hemos considerado parametros que se pueden ajustar en un experimento.

En nuestro segundo trabajo, estudiamos el comportamiento difusivo de un Bose polaron inmerso en un BEC de dos componentes que estan acopladas coherentemente. La particula es superdiffusa si se acopla en la misma manera a los dos componentes, i.e. si se acopla attractivamente o repulsivamente a los dos. Este es el mismo comportamiento a una impureza inmersa en un unico BEC. Al contrario, encontramos que la particula muestra un comportamiento transitorio non-trivial cuando se acopla a los dos componentes attractivamente al uno y repulsivamente al otro. Mostramos como la magnitud del exponente anomalo y la duracion del periodo transiente se pueden controlar a traves de la frequencia Rabi del acoplamiento coherente entre los dos componentes y la fuerza del acoplamiento de la impureza a los dos componentes del BEC.

En seguida, procedemos con la construccion de dos microdispositivos, un termometro quantico y un diodo termico. En el primer proyecto, hemos introducido un nuevo metodo de minimo disturbio, que sirve para termometria en temperaturas sub-nK en un BEC. Nuestra technica esta basada otra vez en el modelo de Bose polaron, donde esta vez la impureza immersa en un BEC sirve como un termometro. La propuesta es detectar fluctuaciones de la temperatura de las medidas de la posicion y el momentum de la impureza. Crucialmente, estas causan una reaccion minima en el BEC y por lo tanto, realizan una medida de la temperatura no demoledora. Siguiendo el paradigma del emergente campo de termometria cuantica, combinamos herramientas de la estimacion de parametros cuan-

tica y de la teoria de sistemas abiertos para resolver el problema en generalidad completa. Por lo tanto evitamos cualquiera simplificacion, como la imposicion de la termalizacion de la impureza, o del acoplamiento debil de la impureza con el BEC. Nuestro metodo esta illustrado con parametros experimentales realistas commun en muchos laboratorios, demostrando que puede competir con las tecnicas destructivas mas modernas, incluso cuando las medidas estan construidas de los resultados de las medidas hechas en las cuadraduras accesibles (suboptimas).

En el ultimo trabajo, investigamos el transporte de calor y el control de corrientes de calor entre dos BECs espacialmente separados y atrapados harmonicamente, cada uno en una temperatura distinta. Para permitir el flujo de de calor entre los dos independientes BECs, consideramos un vinculo establecido atraves de dos impurezas harmonicamente atrapadas, cada una interactuando con su propio BEC. Dado que las impurezas estan espacialmente separadas, consideramos interacciones de largo rango entre ellas, en particular un acoplamiento de dipolo-dipolo. Estudiamos este sistema bajo supuestos- parametros que estan experimentalmente factibles. Tratamos la dinamica de estas impurezas en el marco de referencia del movimiento Browniano cuantico. Examinamos la dependencia del corriente de calor y sus correlaciones en los parametros fisicos del sistema. Mostramos que la rectificacion del corriente del calor, i.e. el flujo de calor unidireccional, puede ocurir en el sistema, cuando aplicamos una conduccion periodica en las frequencias de los trapos de las impurezas. Por lo tanto, nuestro sistema es una posible configuracion para la implementacion de un circuito fononico. Motivados de los recientes avances en el uso de plataformas de BECs para el procesamiento de informacion cuantico, nuestro trabajo ofrece una posibilidad alternativa para usar este aparato en la transferencia y el procesamiento de informacion, dentro del contexto de la ciencia de "phononics", y mas general dentro del campo de la termodinamica cuantica.

TABLE OF CONTENTS

CHAPTER 1

INTRODUCTION

In physics the "system" is the small part of the universe on which we have some control. In other words, it is the part of "interest" that we measure and/or manipulate. Knowing the system Hamiltonian, H_S, we can calculate its time evolution and find the future state of the system, as well as telling its past (how it reached the current state). The system of interest can be, for instance, an electron, an atom, a piece of metal, a cup of coffee, or the solar system. Admittedly, in many cases the effects of the environment can be neglected, and the dynamics is then determined by the system Hamiltonian alone. Often, however, we are forced to take into account that our system is not isolated, but coupled to its surroundings (Weiss, 2012, Zwanzig, 2001). In this scenario, it is usually the case that either because we do not know the evolution of the environment (on which we have not control), or because we only look at the system dynamics, we do not have complete info on the whole (system plus bath).

One such example of a phenomenon where the environment is of paramount importance in determining the dynamics of the system, is Brownian motion, also referred to as pedesis. This phenomenon, regards the phenomenologically random motion of heavy particles suspended in some medium (a liquid or a gas) resulting from their collision with the fast-moving molecules that constitute the medium. The first decisive study that established the fact that this random motion of particles should be attributed to the dynamics of the constituent particles, (and not to some property of living organisms, neither to currents appearing due to other phenomena e.g. evaporation in the experiment of Ingenhousz (Ingen-Housz, 1785)) was undertaken in 1827 by the botanologist

Robert Brown (Brown, 1828), while he was looking through a microscope at pollen grains in water. Many years later, Albert Einstein, in a paper published in one of his "annus mirabilis" papers, explained through a statistical theory these observations, by making use of his contemporary "discontinuists" view on nature that the world is made out of atoms and molecules. The proposition of Einstein was the following: If heat is due to kinetic fluctuations of atoms, and if the particle of interest, the later called Brownian particle, undergoes an enormous number of random bombardments by the surrounding fluid particles, then this should perform a diffusive motion for which certain predictions can be made. Smoluchowski almost simultaneously, developed a kinetic model to explain Brownian motion (von Smoluchowski, 1906).

In particular, Einstein by using arguments of thermodynamics and the concept of osmotic pressure of suspended particles, he managed to evaluate a particle diffusion constant by balancing a diffusion current with a drift current (through Stokes' law). In doing so, he obtains a relation between two transport coefficients: the particle diffusion constant and the fluid viscosity, or friction. This relation, known as the Einstein relation (Einstein, 1905), was generalized later on in terms of the famous fluctuation-dissipation theorem by Callen and Welton (Callen and Welton, 1951), and with the linear response theory by Kubo (Kubo, 1957). This enabled him to extract an independent estimate of the atomistic important, and much debated Avogadro- Loschmidt number $N_{Avogadro}$, by just making a measurement of the diffusion constant – i.e. by measuring distance traveled rather than velocity. With the experimental confirmation from Perrin of Einstein's theory, and the verification of the prediction of Einstein regarding the Avogadro number, Brownian motion became a well established theory. In the years to come this became an important model aimed to approach a large set of different contexts characterized by a non-deterministic behavior, or where dissipative processes occur, as result of the unavoidable interaction with the environment around (Weiss, 2012, Mazo, 2002, Gardiner, 2009).

However, this theory of classical Brownian motion, in the context of modern physics is often inadequate. In many cases, particularly at low temperatures, this theory ignores important quantum effects, such as quantum noise arising from quantum fluctuations, which play a crucial role in noise assisted tunneling and transfer of electrons and quasiparticles. Yet another aspect of the subject which has come to the fore in recent years is the quantum mechanics of macroscopic quantum variables such as the decay of a zero voltage state in a biased Josephson junction, flux quantum transitions in a SQUID (Hänggi *et al.*, 1990) and the possible reversal by quantum tunneling of the magnetization of a single domain ferromagnetic particle as used to store data. In addition to this, it is known that quantum mechanics is incompatible with frictional forces, which appears in the stochastic modeling of Brownian motion, therefore the two should somehow made consistent, in the framework

of a theory of quantum Brownian motion. Finally, the ability to trace quantum phenomena in the Brownian motion model, which is a many-body setting, could potentially reveal insights in the fundamental physics of the quantum to classical transition problem (Weiss, 2012, Kohen *et al.*, 1997). For all of these considerations, the development of a theory of quantum Brownian motion was of paramount importance.

A quantum theory of Brownian motion, was indeed established through the work of Caldeira and Leggett (Caldeira and Leggett, 1981). The Caldeira-Leggett model is a Hamiltonian system that exhibits dissipation by coupling to a continuum. In its most general formulation, this model essentially refers to the sum of the Hamiltonian of a central system of interest (which is either a continuous variable system such as quantum harmonic oscillator or a free particle, or a discrete variable system such as a spin or a qubit), the Hamiltonian of continuous bath of quantum harmonic oscillators (or fermions/spins), and a bilinear coupling term between them. The central degree of freedom corresponds to a macroscopic system and the bath represents the environment. The coupling causes the central system to damp by transference of energy to the continuum. This system has become a standard model for studying the physics of low temperature quantum systems, and has played a crucial role both in revealing fundamental physics phenomena in this setting, as well as in designing microdevices in which quantum phenomena play an important role.

1.1 Quantum Brownian Motion and Bose polarons

An immediate application of the QBM theory concerns ultracold quantum gases. Quantum gases have sparked off intense scientific interest in recent years, both from the theoretical and experimental point of view. They are an excellent test-bed for many-body theory, and are particularly useful to investigate strongly coupled and correlated regimes, which remain hard to reach in the solid state field.

In particular QBM may be useful to approach the polaron problem. The concept of polaron has been introduced by Landau and Pekar to describe the behaviour of an electron in a dielectric crystal (Landau and Pekar, 1948a). The motion of the electron distorts the spatial configuration of the surrounding ions, which let their equilibrium positions to screen its charge. The movement of the ions is associated to phonon excitations that dress the electron. The resulting system, which consists of the electron and its surrounding phonon cloud, is called polaron. The concept of polaron has been extended to describe a generic particle, the impurity, in a generic material, e.g. a conductor, a semiconductor or a gas. One important example is that of an impurity embedded in an ultracold gas. This system has been widely studied both theoretically and experimentally, in the case of a ultracold Fermi or Bose gas.

In the QBM framework, the impurity plays the role of the Brownian particle, while the bath consists of the degrees of freedom related to the gas. The main reason to study this system from the open quantum systems point of view lies in the possibility to better describe the motion of the impurity, rather than its spectral quantities, such as ground state, energy levels and so on, like in the majority of the literature nowadays. The interest in the motion of the impurity is motivated by a recent class of experiments aimed to measure observable related to the impurity dynamics, for instance that in. (Catani *et al.*, 2012a). Here, the physics of an impurity in a gas in one dimension is considered, and its position variance is measured, evaluating in a quantitative manner important features of the motion, such as oscillations, damping and slope. To evaluate this kind of behavior a continuous-variable model such as QBM is appropriate. The application of QBM to the Bose polaron system (an impurity in a Bose gas) is another fundamental motivation of the present work.

1.2 Projects

In this thesis, we study both fundamental physics phenomena regarding Bose polarons seen under the prism of QBM:

1. Entanglement between two impurities in a common BEC bath
2. Control of the diffusion of an impurity in a coherently coupled two-component BEC,

as well as applications, namely the proposal of two microdevices:

1. A sub-nk quantum thermometer in a BEC
2. A quantum heat diode in BECs

1.2.1 Two distinguishable impurities in BEC: squeezing and entanglement of two Bose polarons

Entanglement represents a necessary resource for a number of protocols in quantum information and for other quantum technologies, which are expected to be implemented in the foreseeable future for various practical applications (Horodecki *et al.*, 2009a, Sarovar *et al.*, 2010, Jozsa and Linden, 2003, Gauger *et al.*, 2011, Holland and Burnett, 1993). The entangled parties of a composite quantum system evolve, under realistic conditions, coupled to external degrees of freedom, which may be treated as a *bath*. In this *open quantum system*, the bath acts as a source of decoherence, leading to the destruction of quantum coherence among the states of the entangled subsystems (Schlosshauer, 2007a). Indeed, to reach a relevant technological level, one of the main obstacles is the difficulty to ensure such a coherence despite the interaction of the system with the bath. However, the presence of the bath can produce other potentially useful phenomena. For instance, two non-interacting particles immersed in a common bath can be entangled as a consequence

of an effective interaction induced by the bath (Duarte and Caldeira, 2006, 2009). A number of situations have been considered, where indeed entanglement is observed in the aforementioned setting (Braun, 2002, Plenio and Huelga, 2002, Benatti *et al.*, 2003, 2010, Doll, R. *et al.*, 2006, Shiokawa, 2009, Wolf *et al.*, 2011, Kajari *et al.*, 2012, Doll *et al.*, 2007).

Here we investigate the bath-induced entanglement among two distinguishable impurities embedded in a common homogeneous Bose-Einstein condensate (BEC) in 1D. Such an issue recently attracted a lot of attention, e.g, the study of impurities in double-wells in a BEC (Cirone *et al.*, 2009), the study of entanglement and the measurement of non-Markovianity between a pair of two-level localized impurities in a BEC (Debarba and Fanchini, 2017, McEndoo *et al.*, 2013), particle number entanglement between regions of space in a BEC (Heaney *et al.*, 2007), or the environment-induced interaction for impurities in a lattice (Galve and Zambrini, 2018, Sarkar *et al.*, 2018). Moreover, in a number of experiments (Fadel *et al.*, 2018, Kunkel *et al.*, 2018, Lange *et al.*, 2018) performed this same year, entanglement between regions of a BEC was observed. In these works discrete observables were considered, while on the contrary, in our studies we will focus on entanglement of continuous variables in BEC.

1.2.2 Control of anomalous diffusion of a Bose Polaron in a coherently coupled two-component Bose-Einstein condensate

The phenomenon of anomalous diffusion attracts a growing interest in classical and quantum physics, appearing in a plethora of various systems (Hanggi *et al.*, 2005, Sokolov and Klafter, 2005). In classical systems, there has been a considerable effort to elucidate the properties and conditions of anomalous diffusive behaviour, with a large emphasis given to the question of how this anomalous diffusion could potentially be controlled. In many models, the appearance of the anomalous diffusion is attributed to some random component of the system-environment set-up, usually distributed with a power-law. Examples include continuous time random walks (Scher and Montroll, 1975), diffusion on a fractal lattice (Bunde and Havlin, 1994), diffusivity (i.e. diffusion coefficient) that is inhomogeneous in time (Saxton, 1993, 1997), or space (Leyvraz *et al.*, 1986, Hottovy *et al.*, 2012, Cherstvy and Metzler, 2013, Cherstvy *et al.*, 2013, 2014) in a regular or random manner, the patch model (Massignan *et al.*, 2014a, Manzo *et al.*, 2014), hunters model (Charalambous *et al.*, 2017), etc. In quantum systems, a paradigmatic instance of a highly controlled system is that of a Bose Einstein Condensate (BEC). It was shown that BEC with tunable interactions, are promising systems to study a number of diffusion-related phenomena, such as Anderson Localization (AL) in disordered media (Min *et al.*, 2012, Roati *et al.*, 2008, Jendrzejewski *et al.*, 2012), the expansion of 1D BEC in dis-

ordered speckle potentials (Aspect *et al.*, 2009, Sanchez-Palencia and Lewenstein, 2010, Modugno, 2010, Billy *et al.*, 2008, Roati *et al.*, 2008, Jendrzejewski *et al.*, 2012, Deissler *et al.*, 2010, Lucioni *et al.*, 2011, Min *et al.*, 2012, Donsa *et al.*, 2017), the subdiffusive behavior of the expansion of a wave packet of a 1D quantum, chaotic and nonlinear system (Shepelyansky, 1993, Kopidakis *et al.*, 2008, Pikovsky and Shepelyansky, 2008, Flach *et al.*, 2009, Skokos *et al.*, 2009, Veksler *et al.*, 2009, Mulansky and Pikovsky, 2010, Laptyeva *et al.*, 2010, Iomin, 2010, Larcher *et al.*, 2009, Lucioni *et al.*, 2011, Min *et al.*, 2012), the Brownian motion of solitons in BEC (Aycock *et al.*, 2017), as well as the superdiffusive motion of an impurity in a BEC studied in (Lampo *et al.*, 2017a, 2018, Charalambous *et al.*, 2019a).

In this work, we study how an impurity in a coherently coupled two-component BEC shows a transient anomalous diffusing behaviour. We study this phenomenon under experimentally realistic conditions and we show that this behavior can be controlled through the strength of the interactions and the coherent coupling. To this end, we treat the Bose Polaron problem within an open quantum system framework. The open quantum system approach has been used recently in the context of ultracold quantum gases to study the diffusion of an impurity and two impurities in a BEC (Lampo *et al.*, 2017a, 2018, Charalambous *et al.*, 2019a), for the movement of a bright soliton in a superfluid in one dimension (Efimkin *et al.*, 2016a), see also(Hurst *et al.*, 2017a, Keser and Galitski, 2018, Bonart and Cugliandolo, 2012a)). On the other hand, the effect of contact interactions, dipole-dipole interactions and disorder on the diffusion properties of 1D dipolar two-component condensates were studied in (Bai and Xue, 2015), identifying again the conditions for subdiffusion. The study of the diffusive behaviour of a 2D two-component BEC in a disordered potential was undertaken in (Xi *et al.*, 2014). Finally, an important study on an impurity immersed in a two-component BEC was reported in (Ashida *et al.*, 2018).

1.2.3 Using polarons for sub-nK quantum nondemolition thermometry in a Bose-Einstein condensate

The ongoing efforts in the development of quantum technologies is strongly fueled by their many anticipated practical applications (Celi *et al.*, 2016). In the process, we are already benefiting from striking experimental advances and much deeper theoretical insights. In particular, ultracold atomic gases are a key platform for quantum technologies due to their potential for quantum simulation (Bloch *et al.*, 2008, Lewenstein *et al.*, 2012). Nonetheless, operating a quantum simulator requires very precise tuning of the parameters of the experiment, so as to ensure that the simulated system behaves as intended. In particular, a precise temperature control is essential, for instance, for the reconstruction of the equation of state of the system (Bloch *et al.*, 2012).

In current experimental setups, the main thermometric techniques are based on time-of-flight measurements either directly on the BEC (Leanhardt *et al.*, 2003, Gati *et al.*, 2006), or on impurities embedded in it (Olf *et al.*, 2015, Spiegelhalder *et al.*, 2009). In the former case, temperatures of few nK, or even sub-nK might be estimated efficiently, although at the price of destroying the BEC. On the contrary, the latter protocols are less destructive, albeit efficient at relatively "large" temperatures of $\sim 100\ nK$. Interestingly, recent proposals have discussed minimally disturbing interferometric set-ups in which the temperature is mapped onto a relative phase on a probe (Stace, 2010, Martín-Martínez *et al.*, 2013, Sabín *et al.*, 2014), however, the underlying models are very simple.

An effective non-demolition thermometric technique in the sub-nK regime is thus still missing. Any such strategy should be build upon a *comprehensive theoretical description* and be capable of informing the choice of the most sensitive temperature-dependent quantities to be measured. Here, we propose what is, to the best of our knowledge, the first experimentally feasible quantum non-demolition technique to measure the temperature of a BEC in the sub-nK domain. It is based on the Bose polaron problem, i.e., interrogation of an impurity that is embedded in the condensate, while causing minimal disturbance to the cold atomic gas. The impurity problem has been intensively studied in the context of polaron physics in strongly-interacting Fermi (Schirotzek *et al.*, 2009a, Kohstall *et al.*, 2012a, Koschorreck *et al.*, 2012, Massignan *et al.*, 2014b, Lan and Lobo, 2014, Levinsen and Parish, 2014, Schmidt *et al.*, 2012) or Bose gases (Côté *et al.*, 2002, Massignan *et al.*, 2005, Cucchietti and Timmermans, 2006a, Grusdt *et al.*, 2014, Grusdt and Demler, 2015, Grusdt *et al.*, 2017a, 2015, 2017b, Shchadilova *et al.*, 2016a, Shashi *et al.*, 2014a, Shchadilova *et al.*, 2016c, Lampo *et al.*, 2017b, Pastukhov, 2017, Yoshida *et al.*, 2018, Guenther *et al.*, 2018a, Lampo *et al.*, 2018), as well as in solid state physics (Landau and Pekar, 1948b, Devreese and Alexandrov, 2009b, Alexandrov and Devreese, 2009), and mathematical physics (Lieb and Yamazaki, 1958, Lieb and Thomas, 1997a, Frank *et al.*, 2010, Anapolitanos and Landon, 2013a, Lim *et al.*, 2018). We specifically *avoid* any unjustified simplifications—such as complete thermalization of the impurities at the BEC temperature—and investigate the problem in its full generality.

1.2.4 Heat current control in trapped BEC

Control of heat transport has enormous potential applications, beyond the traditional ones in thermal insulation and efficient heat dissipation. It has been suggested as a resource for information processing, giving rise to striking technological developments. A series of smart heat current control devices, such as thermal diodes (Terraneo *et al.*, 2002, Li *et al.*, 2004, 2005, Hu *et al.*, 2006), thermal transistors (Li *et al.*, 2006), thermal pumps (Segal and Nitzan, 2005a, Marathe *et al.*, 2007, Ren *et al.*, 2010), thermal logic gates (Wang and Li, 2007) or thermal memories (Wang and Li, 2008b), have been proposed in the past decade. A key underlying idea in some of these devices is that

heat transport associated to phonons can realistically be used to carry and process information. The science and engineering of heat manipulation and information processing using phonons is a brand new subject, termed phononics (Wang and Li, 2008a, Li *et al.*, 2012a, Dubi and Di Ventra, 2011). In the emerging field of quantum thermodynamics, the issues of heat transfer and heat rectification are basic ingredients for the understanding and designing heat engines or refrigerators at nanoscales. Besides the technological interests, highly controlled platforms for heat transport can potentially enable the study of fundamental theoretical questions, which will shed light on the study of thermodynamics of nonequilibrium systems (Binder *et al.*, 2019). In particular, heat conduction in low-dimensional systems has attracted a growing interest because of its multifaceted fundamental importance in statistical physics, condensed matter physics, material science, etc (Giazotto *et al.*, 2006, Dhar, 2008, Lepri *et al.*, 2003, Li *et al.*, 2012b).

In past years, advanced experimental techniques have allowed for the miniaturization of heat transport platforms down to the mesoscopic/microscopic scale. Experimentally, a nanoscale solid state thermal rectifier using deposited carbon nanotubes has been realized recently (Chang *et al.*, 2006), and a heat transistor—heat current of electrons controlled by a voltage gate—has also been reported (Saira *et al.*, 2007). Furthermore, it has been shown that thermal rectification can appear in a two-level system asymmetrically coupled to phonon baths (Segal and Nitzan, 2005b,a). In general, various models for thermal rectifiers/diodes that allow heat to flow easily in one direction have been proposed (Terraneo *et al.*, 2002, Li *et al.*, 2004, 2005, Hu *et al.*, 2006, Segal and Nitzan, 2005b, Lan and Li, 2006, Hu and Yang, 2005, Yang *et al.*, 2007). Among such platforms, interesting examples are those based on ultracold atomic systems, both at the theoretical level (Wang *et al.*, 2018, Jaramillo *et al.*, 2016, Ye *et al.*, 2017, Li *et al.*, 2018) as well as at the experimental one (Brantut *et al.*, 2013). In these works, the paradigm of the model used is that of tailored time dependent protocols performing a heat cycle (often an Otto cycle). A cycle here consist of a series of steps performed in finite time where thermodynamic parameters are controlled such that heat is transferred from one bath into another. Frequently, the energy that one needs to spend in implementing the aforementioned protocols is too large for the amount of heat transferred. In addition, in such a heat cycle, the Hamiltonian must be modified as adiabatically as possible to avoid unwanted excitations. We remark that for the goals of the present work considering adiabatic changes in the Hamiltonian will require long timescales, and therefore it can have drawbacks, such as exceeding the life time of the BECs. Even though attempts have been made to overcome this problem (Li *et al.*, 2018, Torrontegui *et al.*, 2013, Deffner *et al.*, 2014), our proposal in (Charalambous *et al.*, 2019b) circumvents it altogether by considering a rather different paradigm. Instead of cycles, we consider autonomous heat platforms, where the working medium is permanently coupled to different baths and under the influence of external time-dependent

driving.

Hence, the motivation for the project in (Charalambous *et al.*, 2019b) was two-fold. Firstly, we were motivated by the need for simple, analytically tractable, physical models in which one can study fundamental questions regarding heat transport in low-dimensional systems. In the literature, a number of theoretical studies exist regarding these transport problems but they are all dealing with oversimplified abstract systems. We wanted to propose a concrete system for these studies based on the treatment of the Bose polaron system as a quantum Brownian particle. Secondly, we were motivated by the increasing interest in autonomous platforms on which one can construct thermal devices, such as for example heat diodes and heat engines, as for example in (Riera-Campeny *et al.*, 2019).

1.3 Plan of the thesis

The thesis is organized as following. In Chapters 2-4 we introduce the necessary background to understand our work, such as the concepts of Classical and Quantum Brownian motion and the idea of a Bose Einstein Condensate and the related Bose-polaron problem. In Chapters 5-8 we present the original work pursued during the completion of this doctoral thesis.

In chapter 2 we resume the essentials of classical Brownian motion. This part of the thesis does not contain any original result, but it is important to present the main results of the classical Brownian motion in order to make the manuscript self-consistent. We give a brief historical overview of the main milestones in the development of classical Brownian motion, and then we proceed by going in more detail through the theoretical study of Einstein, who wrote an equation for the density probability of the pollen grains. In this way he computed the mean square displacement of the pollen grains, predicting a linear dependence on time (diffusion effect). Actually Einstein was not the only one who tried to propose a theoretical explanation of Brownian motion. Other scientists, such as Marian Von Smoluchowski and then Paul Langevin, dealt with the same problem, although with different techniques, for which we also give a short introduction. In particular, Langevin treated Brownian motion by means of a stochastic differential equation ruling the temporal evolution of the grains position. He also found diffusion effect for the mean square displacement. This was detected in experiments in 1909 by Perrin, confirming the theory of Brownian motion and providing a convincing evidence of the atomistic essence of matter.

In chapter 3 we give an overview of QBM. We first motivate the development of QBM, by discussing the pitfalls of the classical theory. The physics of QBM may be explored by means of different formal tools. Among these, the most common is the master equation, i.e. an equation ruling the temporal evolution of the reduced density matrix of the central

system, here represented by the quantum Brownian particle. The master equation is a fundamental object in the field of open quantum systems and permits to evaluate in a quantitative manner both decoherence and dissipation, as well as the average values of the observables. However, in many cases the structure of a master equation may result complicated and the procedure to solve it is often not so easy. Therefore, one usually looks into a particular class of approximated master equations, allowing to deal with a certain problem in a mathematical simple manner. An important example is provided by the Born-Markov master equation, based on the absence of self-correlations within the environment (Markov approximation) and the assumption that the global state of the system plus the bath remains separable at all times (Born approximation). In the majority of the situations this kind of equations can be solved analytically providing a description of the behaviour of the central system. Comparisons with experiments suggested that the predictions of this model are reasonable in many cases. We discuss the relevant problems of the aforementioned approximations, as well as attempts to overcome them. We furthermore comment on a representation in phase space of the stationary solution of such a master equation, by making use of the Gaussian Wigner function. We briefly also discuss the path integral treatment of QBM. After this short review of these methods, where we note their advantages and disadvantages, we focus on the study of the quantum generalized Langevin equation approach to QBM. This is the main method used in our studies, for a number of reasons, mainly because in comparison to the Born-Markov master equation, it permits us to study the low temperature strong coupling regimes of QBM and because in comparison to the path integral approach is considerably much simpler to treat analytically. In this chapter we present the main tools that are used in the works undertaken in this thesis, such as the spectral density, the Kramers-Kronig relations, the linear response function and the fluctuation dissipation theorem.

In Chapter 4, we present a short introduction to the basics of the physics of BEC with the aim to obtain a better understanding of the concept of a Bose polaron, which plays the role of the working material in our studies. We begin by a definition as well as a historical overview of an ideal BEC, and we then extend the relevant concepts in the weakly interacting regime, which is experimentally more relevant, and is the setting we assume in this thesis. The most important point here is that weakly interacting BEC can be characterized by just one more parameter compared tot he ideal gas, and that is the scattering length. We then comment on trapped BEC, giving particular emphasis in harmonically trapped BEC and the Thomas-Fermi limit, which is used in Chapters 7 and 8. From this we proceed to the details of how one can consider BEC of reduced dimensions, since in our work for the sake of simplicity and in order to follow theoretical studies that would be as analytic as possible, we focus on 1D BEC. Upon establishing the conditions and assumptions that go into the BEC that we will consider in our work

as the medium for the QBM, we continue with a section on Bose polarons. These are basically divided into two types, large and small polarons, where the distinction is made according to how the radius of the polaron compares with the lattice distance, if we assume the polarons to move on a lattice. There is also a distinction between weak and strong coupling polarons depending on the strength with which the impurity couples to its surrounding cloud, which is properly defined in the section. The large polaron is also referred to as the continuum polaron, and this is the setting we will consider in this thesis, i.e. we will be working with continuous bath variables. We then focused on the Frohlich Hamiltonian description of Bose polarons, which is valid under the assumption of weak interaction between the impurity and the bath, where we explain what weak means in this context (it is a different definition of weak compared to what weak means in the Born-Markov approximation). We also discuss various approaches that allow one to go beyond the Frohlich Hamiltonian paradigm, even though we do not consider this case in this thesis.

In Chapter 5 and 6 we focus on phenomena regarding Bose polarons that one can reveal by treating the Bose polaron as a QBP. Specifically, in Chapter 5 we study how introducing two impurities of ultracold atoms in a common bath, the bath being a BEC, can lead to entanglement between these impurities. In particular, we start from a physical Hamiltonian and through a Bogoliubov transformation and by making the dipole approximation we convert the system into that of two QBP described by a Caldeira-Leggett type Hamiltonian. By studying the relevant quantum Langevin equations we see that the two impurities become effectively coupled due tot their common interaction with the bath, which has been shown in the literature to lead to the emergence of entanglement between them in the long time limit under certain scenarios. We study two cases, namely the impurities being either free or harmonically trapped. In the former case, we study the dynamical evolution of the entanglement, and we find that there is no entanglement in the long time limit. However for the latter, even though we were not able to obtain the dynamical evolution of entanglement, we prove that indeed entanglement can survive in the long time limit, and we study how this is affected by the various parameters of the system. The results of this study might be interesting in the implementation of various quantum information protocols in ultracold gases platforms. In Chapter 6, we focus on the dynamics, in particular the diffusive behaviour, of an impurity immersed in a coherently coupled two component BEC. In this case a rather more complicated Bogoliubov transformation has to be undertaken, for which we essentially present an overview at the beginning of the chapter. Upon doing so, we realize that depending on the way the impurity couples to the two components of the bath, it can couple to two distinct modes of the bath. Namely if the impurity couples in the same way, either attractively or repulsively to both components, then it interacts with the "density" mode of the bath, which essentially

leads to a diffusive behaviour similar to coupling to a single BEC. On the other hand if the impurity couples differently to the two components, then it interacts with the spin mode of the bath, which is characterized by a spectral density that is gapped, and that above the gap the spectrum grows with the square root of the bath oscillators' frequencies. This gap depends on the frequency of the coherent coupling between the two components and results in a transiently subdiffusive behaviour for the impurity. We study how the parameters of the system affect this behaviour.

In Chapter 7 and 8, we focus on the construction of microdevices using Bose polarons that are treated as QBP. Specifically, in Chapter 7, we introduce a novel minimally-disturbing method for sub-nK thermometry in a Bose-Einstein condensate (BEC)(Mehboudi *et al.*, 2019a). To be able to study our system in an exact manner, once again, we treat the Bose polaron in a trapped BEC as a QBP, following the treatment of (Lampo *et al.*, 2017a) and the assumptions therein. We then use the fluctuations of the position and momentum of this impurity to obtain an estimation of the temperature fluctuations of the BEC. To be able to present our results, we give a short introduction of the basic notions in quantum thermometry, such as the Quantum Cramer Rao bound, the Quantum Fisher Information (QFI) as well as the symmetric logarithmic derivative. We focus in the long time limit of the dynamics of the impurity. The BEC is assumed to always be in a thermal state and thanks to the way we treat the problem, we avoid making the common assumption in such thermometric protocols of the impurity equilibrating with the bath. From the QBM theory, we evaluate the second moments of the position and momentum, which, for a Gaussian quantum mechanical system as this, is enough to evaluate the QFI which gives an estimate of the accuracy of our thermometry. Measuring such fluctuations, does not requires destroying the BEC sample, since we only need to make measurements on the impurity, hence our method is a non-demolition one. Finally, we study the effects of the strength of the coupling of the impurity and the BEC on the accuracy of the measuring protocol, and we examine which fluctuation and hence which measurement, of position or of momentum, is more informative about the temperature of the BEC. In Chapter 8, we study the control of heat currents between two BECs through the introduction of a driving field, creating hence a heat diode made out of BECs (Charalambous *et al.*, 2019b). To do so, we again consider two harmonically trapped BECs that are spatially separated and kept at different temperatures. We assume a harmonically trapped impurity immersed in each one of these two BECs, and we allow these impurities to interact through dipole-dipole interactions. After a series of well controlled assumptions, we shown how this system can be described by an equation of motion describing two spring like coupled harmonic oscillators. We then proceed with a brief description of the main quantities of interest in such a system, namely the heat current and the current fluctuations, and we discuss them in both a static scenario, and under the influence of a periodically driving

force. We then numerically evaluate these quantities and study how they are affected upon varying the various parameters of the system. For the driven case, we also evaluate the rectification coefficient under various parameter regimes, and we show that our set-up can be used as a heat diode.

CHAPTER 2

CLASSICAL BROWNIAN MOTION

The term Brownian motion, originally, refers to the random movement of a particle suspended in a fluid, with the nowadays terminology referring to a multitude of systems where a single entity appears to perform a random motion in its phase space. This could be as diverse as a particle in a fluid, the changes in the decisions of a person, as well as the fluctuations of a stock in the stock market. Focusing on its implications in physics, this phenomenon played a very important role in the history of science because it leaded to the idea that matter is made up by atoms.

In this chapter we briefly present the fundamental results concerning classical Brownian motion, focusing on a description of the original observations and of the main theoretical attempts to study it. Even though no new results are presented here, the main features of the phenomenon are presented, such as diffusion and the Fluctuation-Dissipation theorem, which will allow us to obtain an intuition for their quantum counterparts which will be presented in the next section and which have indeed been used in deriving the results of this thesis.

We start by doing a historical overview of the main results concerning Brownian motion, starting from the initial experimental observation of Brown, the theoretical explanation of it and the foundations of the theory given almost simultaneously by Einstein and Smoluchowski, and moving on to important subsequent works on the stochastic dynamics of Brownian particles given by Langevin. In particular, Einstein developed a statistical theory that served to describe how the probability distribution of the position of the par-

ticle evolved in time. On the other hand, Smoluchowski, developed a kinetic model to explain Brownian motion in terms of the collisions of the constituents of the fluid embedding the pollen grains, which in a sense involved a higher level of description of the motion as we will see later in this Chapter. Finally, Langevin developed his own theory to study the phenomenon, giving a description on the single trajectory level, rather than a statistical one, by making developing a stochastic differential equation for the purpose. All of these works studied as an observable verification of their theory the mean square displacement of the Brownian particle, and they all agreed that it should depend linearly on time. Such a prediction was indeed verified experimentally by Perrin in 1908 and represents a strong confirmation of the theories of Brownian motion. Thanks to this result Perrin won the Nobe prize in 1909 providing a strong evidence for the atomist hypothesis of the matter.

2.1 Historical overview and important contributions

In the year 1905 (Einstein, 1905), thanks to Einstein's intuition, the phenomenon observed by the Scottish botanist Robert Brown in 1827 (Brown, 1828), becomes the spark for the development of a probabilistic formulation of statistical mechanics and the birth of a well-established subject of physical investigation, the so-called Brownian motion (BM). By balancing a diffusion current with a drift current through Stokes' law, Einstein evaluated a particle diffusion constant, which he related to the fluid's viscosity, or friction. For completeness, we note that in this original work of Einstein, the mass of the particle under investigation was ignored. The aforementioned derived relation, known as the Einstein relation (Einstein, 1905), was generalized later on to the famous fluctuation-dissipation theorem derived by Callen and Welton (Callen and Welton, 1951), and also by making use of the linear response theory by Kubo (Kubo, 1957). Furthermore, from a heuristic derivation of the (overdamped) diffusion equation, he deduced his famous prediction that the Mean Square Displacement (MSD) of suspended particles is proportional to time. This non ballistic motion, i.e. that the MSD does not grow as the square of time, was later on also interpreted as a consequence of the fact that, the trajectories of a normal Brownian Particle (BP) can be regarded as memory-less and non-differentiable (Einstein, 1908). Another consequence of the relation derived by Einstein, was that a measurement of the diffusion constant, which only required a much easier to obtain measurement of the distance traveled rather than the much more difficult to get measurement of velocity, enabled the extraction of an independent estimate of the atomistic important, and much debated Avogadro- Loschmidt number $N_{avogadro}$. The first experiment verifying Einstein's theory came from Perrin (Perrin, 1909), which led to the measurement of Avogadro's number and thus proved the existence of molecules. This work won Perrin the Nobel Prize in Physics in 1926. We should note that, soon after Einstein, Von Smoluchowski (von Smoluchowski, 1906) gave an alternate explanation in terms of a random walk, taking into

account the fact that Einstein's work ignored the inertia of the BP. Langevin (Langevin, 1908) used Smoluchowski's random walk to recover Einstein's result through the use of the now famous Langevin equation. There are a number of review works where one can study the history of BM that go into much more detail than this thesis (Hanggi *et al.*, 2005, Bian *et al.*, 2016).

Without any doubt, the problem of Brownian motion has played a central role in the development of both the foundations of thermodynamics and the dynamical interpretation of statistical physics. A milestone in doing so, has been the work of Callen and Welton (Callen and Welton, 1951), and subsequently by Nyquist and Johnson(Nyquist, 1928). There, a generalization of the relations by Einstein was considered for the voltage fluctuations, in order to include quantum effects. In their fundamental work, they established a quite generally valid connection between the response function and the associated equilibrium quantum fluctuations, i.e. the quantum fluctuation-dissipation theorem. Another key development must be credited to Lars Onsager. In his work, via his regression hypothesis, he linked the relaxation of an observable in the presence of weak external perturbations, to the decay of correlations between associated microscopic variables (Onsager, 1931). This resulted in the family of relations commonly known as the Green-Kubo relations (Kubo, 1957, Green, 1952). An important point to make about all of these approaches, is that the fluctuation properties of the corresponding variables (response-fluctuation theorems) can be extended to arbitrary (dynamical and non-dynamical) systems that operate far from equilibrium (Hänggi and Thomas, 1982).

Finally, a powerful scheme to describe and characterize statistical non-linear dynamics from microscopic first principles was also later developed. The related works made use of the non-Markovian, generalized Langevin equations or equivalently of its associated generalized master equations. Such strategies have by now been well developed and understood, but unfortunately they can only be used for thermal equilibrium systems. A much more general approach, of which the generalized Langevin equation is a special case, that is free of this problem but technically much more involved, is the projection operator technique (Zwanzig, 1961, 2001). This method is used to eliminate the non-relevant (phase space) degrees of freedom and yields a clear-cut method to obtain the formal equations for either the rate of change of the probability or the reduced density operator, i.e. the generalized (quantum) master equation or the non-linear generalized (quantum) Langevin equation (Mori, 1965). This latter approach proved very useful to characterize the complex relaxation dynamics in glasses and related systems (Kawasaki, 1970).

2.2 Approaches to classical normal Brownian motion

Einstein's theory of the Brownian motion(Einstein, 1905) is based on the notion that the BP, a large particle, as e.g. a pollen grain, suspended in a colloidal suspension performs a discrete time random walk. The walk is a result of the very large number of impacts of the surrounding molecules on the BP. In other words the displacement of the BP is a sum of random variables, each having arbitrary distributions. Therefore, the theory developed by Einstein may be defined as a statistical one, namely it does not rely on a microscopic kinetic model, but it refers to generic probability distributions. This is exactly what gives this model both its strength and its weakness. The strength is that it is applicable to a wide range of circumstances and is easily generalizable. The weakness is that it does not carry so much insight on what is happening at the microscopic dynamical time scale.

Einstein's theory can be characterized as a mesoscopic one: it refers to timescales long enough to contain many elementary events, yet short enough to be effectively infinitesimal on an observational scale. Precisely, one can introduce a characteristic time, short compared to macroscopically observable times, yet long with respect to the inverse collision frequency, such that the particle's movements in two consecutive time intervals are independent. In practice, this is understood as following: After a collision between the Brownian particle and a constituent of the environment, the latter interacts with a large number of other constituents, such that its dynamical state becomes scarcely dependent on its state before the previous collision with the Brownian one. One can better understand this, if he considers the original example studied by Einstein, which would be a test-particle immersed in an ideal gas of non-interacting particles.

It is customary, to assume the initial state being a temperature equilibrium state, $e^{-\beta H_B}$, where H_B is the bath Hamiltonian and $\beta = 1/k_B T$ is the inverse temperature. In other words, the initial data of the heat-bath particles are given by this equilibrium measure at inverse temperature β. The scaling limit necessary to reduce the chance of recollisions, in this case, could be $m/M \to 0$, where M and m are the mass of the test-particle and the heat-bath particles, respectively. In this case, a collision with a single light particle does not have sizeable effect on the motion of the heavy particle, and hence this way memory effect is reduced. However, the rate of collisions has to be increased in parallel with $m/M \to 0$ to have a sizeable total collision effect [1]. In effect, this destroys the suspended Brownian particle dependence on its initial conditions. In other words we say that the process described above is Markovian. Of course Einstein never used such a term, because the famous work of Markov(Markov, 1906) concerning Markov chains came

[1] There is a natural scaling limit, where non-trivial limiting dynamics was proven by Durr, Goldstein and Lebowitz (D. Durr and Lebowitz, 1981)

two years later.

In summary, Einstein whose work can be thought in terms of an unbiased discrete random walk model essentially, made the following series of assumptions in order to derive his results, namely:

1. the independence of individual BPs (infinite diluteness assumption);
2. the existence of a sufficiently small time scale beyond which individual displacements are statistically independent;
3. the particle displacements happen in multiples of an average value called the typical mean free path, the average collision-free distance traveled by the BP;
4. the displacements are distributed symmetrically in all directions; and
5. the variance of the particle displacement at each step remains finite.

These assumptions, together with the assumptions that the time between successive observations is always larger than and such that a sufficiently large number of steps have taken place, are essentially the assumptions for the Central Limit Theorem (CLT) to be valid (Vulpiani A. and D., 2014). They guarantee that the fluctuations on the probability distribution $p(x;t)$ of the position x of the BP at any time t will be negligibly small, and therefore that a deterministic continuous equation about the evolution of the probability distribution should be derivable, which we present in more detail in the next section.

2.2.1 Diffusion equation and Fokker-Planck equation

Diffusion equation

As we stated in the beginning of the section, Einstein's framework is not based on a kinetic model, but employs probability distributions. Let $p(x;t)$ be the probability density that the particle be at position x at time t. There is no external force so the system is homogeneous, i.e. $p(x;t) = p(-x;t)$. Let $\phi(L;\delta t)$ be the probability of the particle moving a distance L in time δt (δt is supposed to be so large, that the motion of the random walker is independent of its motion at time $t \pm \delta t$, yet δt is supposed very small compared to the observation time intervals). The hypothesis of a Markov process permits to write a Chapman-Kolmogorov equation for it:

$$p(x;t+\delta t) = \int p(x-L;t)\,\phi(L;\delta t)\,dL \tag{2.1}$$

The above integral equation, called the Smoluchowski integral equation (W. T. Coffey and Waldron, 2004), is a particular form of the Boltzmann equation introduced by Boltzmann in 1872 (W. T. Coffey and Waldron, 2004) in order to demonstrate that whatever the

initial distribution of an assembly of molecules in phase space, the ultimate result would be the Maxwell-Boltzmann distribution. Eq. (2.1) must be solved for $p(x;t)$ given an initial distribution for it. Also a mechanism or physical cause for the random process must be given i.e. $\phi(L;\delta t)$ must be specified. By assuming a Gaussian state for the displacements of the system, $\phi(L;\delta t)$ (justified by the central limit theorem (Mulligan, 2007), since the resulting displacement L of the walker is the sum of the elementary displacements arising from the molecular collisions (supposed statistically independent) which take place in time δt so that the central limit theorem of probability theory applies.) and that L and δt approach zero (extremely small displacements in infinitesimally short times) in such a way that:

$$\lim_{\substack{L \to 0 \\ \delta t \to 0}} \frac{\langle L^2 \rangle}{2\delta t} = D, \tag{2.2}$$

one can derive from Eq. (2.1) the diffusion equation

$$\frac{\partial p(x;t)}{\partial t} = D \frac{\partial^2 p(x;t)}{\partial x^2}. \tag{2.3}$$

The fundamental solution of Eq. (2.3) also called the Green function or propagator is:

$$p(x;t \mid x_0,t_0) = \frac{1}{\sqrt{4\pi D\,|t-t_0|}} e^{-\frac{[x(t)-x(t_0)]^2}{4D|t-t_0|}} \tag{2.4}$$

which is a centered Gaussian distribution with variance:

$$\left\langle [x(t)-x(t_0)]^2 \right\rangle = 2D\,|t-t_0|\,. \tag{2.5}$$

To continue, Einstein essentially by considering the Brownian motion of a particle in a potential $V(x)$ and requiring that ultimately the Maxwell-Boltzmann distribution of velocities of the gas particles should prevail, determined the diffusion coefficient D, obtaining the famous formula:

$$D = \frac{k_B T}{\zeta} \tag{2.6}$$

where ζ is the drag coefficient, and the viscous drag on the particle is assumed to be given by Stokes' Law. Equation (2.5) which connects the mean square fluctuations in the displacement of the Brownian particle with the dissipative coupling to the heat bath is essentially the first fluctuation-dissipation theorem. But let's have a closer look to how the diffusion coefficient D was obtained by Einstein. In a dilute suspension of Brownian

particles, the osmotic pressure force acting on individual particles is $-\nabla V(x)$, where $V(x)$ is the aforementioned thermodynamic potential. Hence, the steady flux of particles driven by this force is $-\phi(x)\mu^{-1}\nabla V(x)$, where $\phi(x)$ is the particle volume concentration and μ is the mobility coefficient of individual particles. At equilibrium, the flux due to the potential force must be balanced by a diffusional flux as:

$$-\phi(x)\mu^{-1}\nabla V(x) = -D\nabla\phi(x). \tag{2.7}$$

Moreover, the concentration should have the form of $\phi(x) \propto e^{-V(x)/k_BT}$ at equilibrium. By substituting the expression of $\phi(x)$ into Eq. (2.7), we obtain Einstein's relation $D = \mu k_B T$. Here, essentially, the particle moves at a terminal drift velocity v_{drift} in the fluid due to the presence of a weak external force given by $F_{ext} = -\partial V(x)/\partial x$, which results in the following relation between a mobility coefficient μ and the friction coefficient ζ such that $\mu = \zeta^{-1} = v_{drift}/F_{ext}$. Finally, by considering Stokes' law, (Batchelor, 2000)[2] for the mobility of a sphere in an incompressible fluid at steady state, and assuming no-slip boundary conditions, as in Stokes work in 1815 we obtain $D = k_BT/4\pi\eta\alpha$ where η is the dynamic viscosity of the fluid and α is the radius of the particle. This connects the mass transport of the particle and momentum transport of the fluid.

Criticism and limitations of the Einstein's diffusion equation Einstein's treatment of the Brownian motion, introduces an external force of potential $V(x)$ only in a virtual sense, just so that he can calculate the diffusion coefficient. In his work, the potential well, which causes a Maxwell-Boltzmann distribution to be set up, only serves to have a stationary solution for the motion of the BP, since otherwise, for a free BP no stationary solution would exist. As Einstein himself later on noted (Einstein, 1906, 1907), the inertia of the particle is neglected. This implies that an infinite force is required to change the velocity of the particle to achieve a random walk at each step. Therefore, its velocity cannot be defined and its trajectories are fractal.

The problem with Einstein's work can be better understood as following. From the Mean Square Displacement (MSD) of the diffusion, we may determine an effective mean velocity over a time interval Δt. However, as $\Delta t \to 0$, this effective velocity diverges and cannot represent the real velocity of the particle. Physically, however, we should be able to find a time scale $t < \tau_b$ for the ballistic regime,(Einstein, 1907) where the velocity does not change significantly, that is, $\Delta x(t) \approx v(0)t$. In Einstein's model, τ_b can be chosen from the time scale for the duration of successive random bombardments. From the equipartition theorem, we have $v^2 = k_BT/m$, where m is the mass of the particle.

[2]Stokes' law is valid for the Knudsen number $Kn = \lambda/\alpha \ll 1$, where λ is the mean free path of fluid particles, and α is the radius of the particle.

Hence, we obtain the MSD expression in the ballistic regime:

$$\left\langle [x(t) - x(t_0)]^2 \right\rangle = \frac{k_B T}{m} t^2. \tag{2.8}$$

In Einstein's model, the time scale τ_b is neglected (i.e., assuming $\tau_b \to 0$) and the MSD is a completely linear function in time. A century ago, Einstein also did not expect that it would be possible to observe the ballistic regime in practice due to the limitation of experimental facilities. Remarkably, such measurements have recently become realistic in rarefield gas,(Blum *et al.*, 2006) normal gas (Li *et al.*, 2010) and liquid, (Huang *et al.*, 2011, Kheifets *et al.*, 2014) with increasing difficulty for fluids with elevated density due to the diminishing of τ_b. However, the experiment on Brownian particles in a liquid is subtle, as it is currently still difficult to resolve time below the sonic scale.(Li and Raizen, 2013) Therefore, the equipartition theorem can only be verified for the total mass of the particle and entrained liquid, but not at the single particle level. (Huang *et al.*, 2011, Kheifets *et al.*, 2014)

In summary, Einstein's pure-diffusion model considers only the independent random bombardments on the particle, but nothing else. Although the resulting MSD expression of Eq. (2.5) is always valid at a large time, the model only has the single time scale of the mass-diffusion process $\tau_D = \alpha^2/D$, which is denoted as the diffusive or Smoluchowski time scale(Dhont, 1996), and ignores the timescale for the transition to the expected ballistic regime. Moreover, the model disallows a definition of velocity, possesses no ballistic regime, and hence its Velocity Auto-Correlation Function (VACF) (which we will introduce later) does not contain any dynamical information. These issues will be resolved in Langevin's model, presented in the next subsection.

Smoluchowski approach to Brownian motion Smoluchowski theory was developed almost in parallel with Einstein's work, but from a quite different perspective. Instead of a purely statistical approach to the problem, where one needs to refer to the central limit theorem, he assumes a specific kinetic microscopic model, namely (in the spirit of Boltzmann) collisions of hard spheres (well described in (Mazo, 2002)). For this reason Smoluchowski approach to Brownian motion is less universal compared to that of Einstein, but offers more physical insights. Just by studying the collisions by means of the conservation of the momentum and energy, and assuming no memory effects, Marian Smoluchowski derived an expression for the mean square displacement. Smoluchowski's approach advantage, is that the inertia of the BP is taken into account. He assumes a Gaussian randomly distributed fluctuating force exerted on each one of these hard spheres upon a collision. Furthermore, by Taylor expanding the probability density $p(x,t)$, and by the homogeneity of the system, he reaches to the Kramers-Moyal expansion (W. T. Coffey

and Waldron, 2004),

$$\begin{aligned}\sum_{n=0}^{\infty}\frac{(\delta t)^n}{n!}\frac{\partial^n p(x;t)}{\partial t^n} &= \sum_{n=0}^{\infty}\left(\frac{\int_{-\infty}^{\infty}L^n\phi(L;\delta t)dL}{n!}\right)\frac{\partial^n p(x;t)}{\partial x^n} \\ &= \sum_{n=0}^{\infty}\frac{\left\langle L^{2n}\right\rangle}{(2n)!}\frac{\partial^{2n}p(x;t)}{\partial x^{2n}}\end{aligned}, \tag{2.9}$$

which can be seen as an equivalent equation to the Smoluchowski integral equation Eq. (2.1). Truncation at the second term in the Kramers-Moyal expansion is possible for a Gaussian randomly distributed fluctuating force because the higher order statistical moments may be all expressed as powers of the second moment (W. T. Coffey and Waldron, 2004). By making use of the Wick's or Isserli's theorem concerning averages of products of Gaussian random variables, which permits a truncation of the Kramers-Moyal expansion, he was finally led to the MSD

$$\left\langle \left[x\left(t\right)-x\left(t_0\right)\right]^2\right\rangle = \frac{k_BTm}{\zeta^2}\left(\frac{\zeta\left|t\right|}{m}-1+e^{-\frac{\zeta}{m}\left|t\right|}\right). \tag{2.10}$$

The equivalence of the two approaches can be understood through the Langevin equation presented in the next section. Note that within this approach indeed one obtains two distinct limits for the behaviour of the MSD with time. One can check that if t is large, namely $t \gg \zeta/m$ then we have normal diffusion, i.e. diffusion as in Eq. (2.5), while for small times, we have ballistic diffusion as in Eq. (2.8).

2.2.2 Langevin equation

The Einstein and Smoluchowski theories look very different on the surface. One employs the dynamics of the particle motion, while the other is a purely statistical theory. A link between the two conceptions was provided in 1908 by P. Langevin (Langevin, 1908). A suspended particle in a fluid is acted upon by forces due to the molecules of the solvent. This force may be expressed as a sum of its average value and a fluctuation around such an average value. Langevin's idea was to treat the mean force dynamically and the residual fluctuating part of the force probabilistically.

Based on Newton's second law of motion, taking into account the inertia of the central particle, the equation of motion for a particle immersed in a medium and under the influence of some external force F should read as

$$\begin{aligned}\tfrac{dx}{dt} &= v \\ M\tfrac{dv}{dt} &= F-\gamma v\end{aligned} \tag{2.11}$$

where, at this level of description, the viscous frictional drag γ is treated as a phenomenological parameter. The frictional drag, i.e. the mean force exerted on a particle in a viscous medium is assumed to be given by $\gamma^{-1} = -v_{drift}\partial V\left(x\right)/\partial x$, treating v_{drift} as a

phenomenological parameter, $V(x)$ is an external potential describing the effect of the medium on the particle. This equation is a good description of the phenomenon only for time intervals much longer than the average time τ_b between molecular collisions.

Since equation Eq. (2.11) is a good first approximation, we assume that it correctly describes the average motion. We now incorporate the effects of the discrete collisions in a stochastic manner by adding a random fluctuating force $\eta(t)$ (with vanishing mean) to the frictional force term:

$$M\frac{dv}{dt} = F - \gamma v + \eta(t) \tag{2.12}$$

which for the type of $\eta(t)$ we will define in what follows, is the famous Langevin equation. So far as the 'fluctuating force' ('noise') $\eta(t)$ is concerned, we assume:

1. $\eta(t)$ is independent of v, and
2. $\eta(t)$ varies extremely rapidly as compared to the variation of v.

Since 'average motion' is still assumed to be governed by Eq. (2.11), we must have $\langle \eta(t) \rangle = 0$, where the average is over the distribution of the noise. This can be implemented practically in two alternative, but equivalent, ways: either averaging over an ensemble of many systems consisting of a single Brownian particle in a surrounding fluid, or averaging over a number of Brownian particles in the same fluid, provided they are sufficiently far apart (possible at low enough density of the particles) so as not to influence each other.

The second assumption above, implies that during small time intervals δt, v and $\eta(t)$ change such that $v(t)$ and $v(t+\delta t)$ differ infinitesimally but $\eta(t)$ and $\eta(t+\delta t)$ have no correlation:

$$\langle \eta(t)\, \eta(t+\delta t) \rangle = 2m^2 B\delta(\delta t), \tag{2.13}$$

where at this level of description, B is a phenomenological parameter. In other word this is the way in which Langevin implemented in his approach Markov approximation. In order that the Brownian particle is in thermal equilibrium with the surrounding fluid, the constant B cannot be arbitrary; only a specific choice $B = \gamma k_B T/m$, guarantees the approach to the appropriate equilibrium Gibbsian distribution. We also assume that the noise is not correlated with the position of the particle, and this together with assumption 1 are expressed as:

$$\langle \eta(t)\, x(s) \rangle = \langle \eta(t)\, v(s) \rangle = 0,\ t > s. \tag{2.14}$$

To be more concrete, we in fact assume that the fluctuating force $\eta(t)$ is a Wiener process (for more details look in (Gardiner, 2009)). As a result, the stochastic differential equation Eq. (2.12) can not be solved, but results can be obtained regarding averages of position and velocity. We aim here to an expression for the mean square displacement of the free Brownian particle, i.e. $F = 0$. We begin by multiplying both sides of Eq. (2.12) for $x(t)$ and then we take the mean value of the result. Recalling the average values from above, we get

$$m\left\langle x\frac{dv}{dt}\right\rangle = -\gamma\left\langle xv\right\rangle . \tag{2.15}$$

Since $v = \dot{x}$, such an equation may be put in the form

$$\frac{m}{2}\frac{\partial^2\left\langle x^2\right\rangle}{\partial t^2} + \frac{\gamma}{2}\frac{\partial\left\langle x^2\right\rangle}{\partial t} = k_BT, \tag{2.16}$$

where we have used the equipartition theorem $\langle v^2\rangle = k_BT/m$. Without loss of generality we assume $\langle x^2(0)\rangle = 0$ which finally leads to the same expression for the average MSD as in Eq. (2.10), replacing $\zeta \to \gamma$.

Comments on the Langevin equation The Langevin equation gives the same behaviour for the MSD of the Brownian motion as treated by Smoluchowski. Hence it is a stochastic dynamical equation that accounts for irreversible processes. On the other hand, in principle, one can write down the Newtonian equations of motion for the Brownian particle as well as that of all the other particles constituting the heat bath; each of these equations of motion will not only be deterministic but will also exhibit time-reversal symmetry. Note that, in the Langevin approach, one writes down only Eq. (2.12) for the Brownian particle and does not explicitly describe the dynamics of the constituents of the heat bath. This raises the question: how do the viscous damping term (responsible for irreversibility) and the random force term (which gives rise to the stochasticity) appear in the equation of motion of the Brownian particle when one 'projects out' the degrees of freedom associated with the bath variables and observes the dynamics in a tiny subspace of the full phase space of the composite system consisting of the Brownian particle + Bath? The answer to this will be given in the next Chapter when the extension of the Langevin theory to the quantum regime will be presented, and a Hamiltonian approach to the problem will be explored.

In Langevin's equation, compared to Einstein's model, $x(t)$ has better regularity, since now $x(t)$ is differentiable. However, $v(t)$ is continuous but not differentiable just as $x(t)$ in Einstein's model. Einstein worked completely in the configuration space of the Brownian particle, without ever introducing the velocity of the particle, hence neglecting the inertia

of the particle and the possibility of the persistence of velocity. In his work, he assumed the short time τ_b , after which the displacements of the particle should be independent, should be longer than γ/m , which in practice it usually is, and for this reason Einstein's model is usually valid. Langevin, on the other hand, worked in the particle's phase space and was able to treat the velocity relaxation. Hence, one can say that Langevin's description is on a finer scale than that of Einstein.

The generalized Langevin equation The simplest derivation of the stochastic Langevin equation for a Brownian particle, starting from the mutually coupled deterministic equations of motion (which are equivalent to Newton's equation) for the Brownian particle and the molecules of the fluid, was given by Robert Zwanzig (Zwanzig, 1961), utilizing his method of projection operators. For the simplicity of analytical calculations, he modeled the heat bath as a collection of harmonic oscillators (of unit mass, for simplicity) each of which is coupled to the Brownian particle. The differential equations satisfied by the position x and the momentum p of the Brownian particle are obtained through the Liouville equations of motion (Mazo, 2002), and have the general form

$$\begin{array}{c} \frac{\partial x}{\partial t} = \frac{p}{m} \\ \frac{\partial p}{\partial t} = F(x) + \sum_j \xi_j \left(q_j - \frac{\xi_j x}{\omega_j^2} \right) \end{array} , \tag{2.17}$$

where $F(x)$ is the external force (not arising from the reservoir), $q_j(t)$ denotes the position, of the j^{th} harmonic oscillator constituent of the reservoir and ω_j is the frequency of this oscillator. Similarly, the equations of motion for the bath variables are

$$\begin{array}{c} \frac{\partial q_j}{\partial t} = p_j \\ \frac{\partial p_j}{\partial t} = -\omega_j^2 \left(q_j - \frac{\xi_j}{\omega_j^2} x \right) \end{array} . \tag{2.18}$$

By solving this set of equations for the bath particles using Green's function techniques and replacing the solution in the equation of motion for the Brownian particle, i.e. projecting out the bath degrees of freedom, a Langevin like equation can be obtained.

$$m \frac{\partial^2 x}{\partial t^2} + m \int_{t_0}^{t} ds \gamma(t-s) \frac{\partial x(s)}{\partial s} + \frac{\partial V(x)}{\partial x} = -m\gamma(t-t_0) x(t_0) + \eta(t) \tag{2.19}$$

where

$$\begin{array}{c} \langle \eta(t) \rangle_{\rho_B} = 0 \\ \langle \eta(t) \eta(s) \rangle_{\rho_B} = m k_B T \gamma(t-s) \end{array} \tag{2.20}$$

with ρ_B the Gibbs state at temperature T. Note that in this case, $\eta(t)$ is a function also of $q_j(t_0), p_j(t_0), \xi_j$ and ω_j, and is not the random variable introduced above. A more detailed expression of it, and an analytic derivation of Eq. (2.19), will be given in the next chapter. Nevertheless in Eq. (2.20), we see that the same statistics are obeyed by this function as that of the random force. Hence, in this equation, both the dissipative viscous drag term and the noise term appear as functions of the bath degrees of freedom. Thus, the molecules in the fluid medium which give the random 'kicks' to the Brownian particle are also responsible for its energy dissipation because of viscous drag. The incessant random motion of the Brownian particle is maintained for ever by the delicate balance of the random kicks it gets. This is mathematically expressed by the fluctuation dissipation theorem, on which we briefly comment in the next section.

2.3 Fluctuation-dissipation theorem, velocity autocorrelation function and diffusion coefficient

Now we turn to the velocity of the Brownian particle, which is the new element in Langevin's model. Furthermore, we may characterize the full dynamics of the particle by the Velocity Auto-Correlation Function (VACF). The Langevin equation, Eq. (2.12), is a first-order inhomogeneous differential equation and has the formal solution: (Uhlenbeck and Ornstein, 1930, Zwanzig, 2001)

$$v(t) = v(0)\, e^{-\gamma t/m} + \frac{1}{m}\int_0^t dt' e^{-\gamma(t-t')/m}\eta(t) \tag{2.21}$$

where the integral in the second term can not be performed, and for this reason earlier was stated that the equation can not be solved. From the above formal solution, we observe that the average of squared velocity $\langle v^2(t)\rangle$ will have three contributions: the first one is $\langle v^2(0)\rangle e^{-2\gamma t/m}$ and the second one is the cross term $\frac{2}{m}e^{-\gamma t/m}\int_0^t dt' e^{-\gamma(t-t')/m}\langle v(0)\eta(t)\rangle$, which becomes zero due to Eq. (2.14). The third contribution is of second order in $\eta(t)$ and, by making use of Eq. (2.14), we have

$$2\int_0^t dt' e^{-\gamma(t-t')/m}\int_0^t dt'' e^{-\gamma(t-t'')/m} B\delta(t-t'') = \frac{mB}{\gamma}\left(1-e^{-2\gamma t/m}\right) \tag{2.22}$$

Therefore, the mean-squared velocity is

$$\left\langle v^2(t)\right\rangle = \left\langle v^2(0)\right\rangle e^{-2\gamma t/m} + \frac{mB}{\gamma}\left(1-e^{-2\gamma t/m}\right) \tag{2.23}$$

At the long-time limit, we expect the equipartition theorem, $\langle v^2(t)\rangle = k_B T/m$ to be valid, such that

$$B = \gamma k_B T/m^2 \tag{2.24}$$

This is yet another form of a Fluctuation-Dissipation Theorem (FDT).(Nyquist, 1928, Callen and Welton, 1951, Kubo, 1966) Roughly speaking, the magnitude of the fluctuation B must be balanced by the strength of the dissipation γ so that temperature is well defined in Langevin's model. Therefore, the pair of friction and random forces in a sense acts as a thermostat for a Langevin system. That such a relation exists between them should not surprise us, since they both come from the same origin, the interactions between the particle and the surrounding fluid molecules.

From the solution of velocity in Eq. (2.21), we can also calculate the VACF of the particle. After multiplying Eq. (2.21) by $v(0)$, and further taking the average, we obtain

$$\langle v(0)\, v(t)\rangle = \left\langle v^2(0)\right\rangle e^{-\gamma t/m} = k_B T/m e^{-\gamma t/m} \tag{2.25}$$

Here, the random force term vanished due to Eq. (2.14) and the equipartition theorem was also used. It is simple to see that $\langle v(0)\, v(t)\rangle$ decays exponentially and the relevant time scale is the Brownian relaxation time, $\tau_b = m/\gamma$. If we take the time integral of the VACF, we find

$$\int_0^\infty \langle v(0)\, v(t)\rangle\, dt = \int_0^\infty k_B T/m e^{-\gamma t/m} dt = k_B T/\gamma = D \tag{2.26}$$

which is just the diffusion coefficient obtained by Einstein. The relation in Eq. (2.26) is not fortuitous, but known as the simplest example of the fundamental Green-Kubo relations.(Green, 1952, 1954, Kubo and Tomita, 1954, Kubo, 1957) These relate the macroscopic transport coefficients to the correlation functions of the variables fluctuating due to microscopic processes(Zwanzig, 1965). Such relations were also postulated by the regression hypothesis of Lars Onsager,(Onsager, 1931) which states that the decay of the correlations between fluctuating variables follows the macroscopic law of relaxation due to small nonequilibrium disturbances. The 1968 Nobel Prize in Chemistry was awarded to Onsager to glorify his reciprocal relations in the irreversible process, which also formed the basis for further development of nonequilibrium thermodynamics by Ilya Prigogine and others(Zwanzig, 2001, de Groot and Mazur, 1962, Prigogine, 1967, Toda *et al.*, 1991).

Limitations and underlying assumptions The Langevin model not only recovers the long-time result of Einstein's model, but also produces the correct ballistic regime at

a short-time limit. An essential ingredient in the model is that the Brownian particle has an inertia, that is a finite mass m. As a result, the velocity and the VACF become well-defined and continuous in time. By considering a very small relaxation time $m/\gamma \to 0$, the Langevin dynamics degenerates to be the overdamped Brownian dynamics of Einstein's model.

Note, that the limitations of the Langevin model can be revealed by considering a microscopic limiting model, the Rayleigh gas,(Kim and Karniadakis, 2013) where one assumes a massive particle in an ideal gas (gas of non-interacting bath particles). Several attempts were made to derive the Langevin equation from this microscopic model in the early 1960s(Lebowitz and Rubin, 1963, Mazur and Oppenheim, 1970). It was realized that the derivation is possible if the interaction between the Brownian particle and any gas particle takes place only for a short microscopic time(Kim and Karniadakis, 2013, Mazur and Oppenheim, 1970). This condition can be rigorously verified under the ideal gas assumption and the infinite mass limit of the Brownian particle (i.e., $m \to \infty$), and thus the microscopic justification of the Langevin equation can be provided through the Rayleigh gas model. We will discuss more on such a microscopic derivation of Langevin theory in the next section. On the other hand, for a Brownian motion in a real gas (of interacting bath particles) or a liquid, a mathematically rigorous justification is intractable. One of the reasons is that if the fluid particles interact among themselves, a collective motion (e.g., correlated collisions) of the fluid particles can occur, which implies that the aforementioned condition (obtained in the Rayleigh gas model) may not hold. The Langevin description is valid only if the Brownian particle is sufficiently denser than the surrounding fluid, where the inertia of the fluid may be neglected. This is one of the main assumption for the application of the so called Hydrodynamic model of Brownian motion. This fact was exploited in a recent experiment,(Li *et al.*, 2010) where a silica bead is trapped by a harmonic potential(Uhlenbeck and Ornstein, 1930) in air and the experimental VACF corroborates well the results of the Langevin model.(Wang and Uhlenbeck, 1945) For a general case of arbitrary density, the collective motion of the fluid particles and their inertia should be reconsidered carefully.

2.4 Anomalous diffusion

Following Einstein's work, extracting information about a system from its diffusive behaviour was heavily popularized, and various modifications and extensions of this work appeared. In particular, with the advancement of technology, it was realized, that in a number of scenarios, the MSD of particles in various types of media, was not growing linearly with time, but rather as a different type of power law

$$MSD \propto t^{\alpha} \tag{2.27}$$

in which case the diffusive behaviour was termed Anomalous Brownian Motion, to indicate the deviation from the normal scenario of Einstein. There are two types of ABM: (i) subdiffusive motion, $0 < \alpha < 1$; (ii) superdiffusive motion, $\alpha > 1$. It was shown that for an ABM, $P(x;t)$ deviates from its Gaussian form. The contrary is not always true: a non-Gaussian does not imply necessarily ABM (Chubynsky and Slater, 2014). This behaviour is captured by the Non-Gaussianity parameter (NG) (Rahman, 1964). There are two reasons why $P(x;t)$ deviates from the Gaussian distribution (Bouchaud and Georges, 1990):

1. A "broad" distribution of the random variables that are summed in order to form $P(x;t)$. This would require a failure of the assumptions related to the Continuous Time Random Walk (CTRW). A possible cause for this is if the Waiting Time Probability Distribution Function (WTPDF) of the CTRW is a power law and the motion is subdiffusive. This implies $\tau \to \infty$ and hence non-stationary increments, which implies ergodicity breaking. However it could also be that the variance of the jump lengths diverges, which would result in superdiffusion (Metzler and Klafter, 2000).

2. The presence of "long range" correlations among the increments in space, i.e. when the random variables that are summed to form $p(x;t)$ are not independent. The motion is superdiffusive if the increments are correlated and subdiffusive if they are anticorrelated. The most prominent example of such an ABM is the fractional BM (fBM) (Mandelbrot and Van Ness, 1968) which usually describes systems in viscoelastic and crowded media. Note that stationarity implies also that fBM is ergodic. Alternatively, fBM can be described as the inertia-less limit of the GLE in the case of a memory kernel with a power law dependence on time with an exponent between -1 and 0 (Goychuk and Hänggi, 2007, Goychuk, 2012).

2.5 Summary

The topics discussed in this chapter that should be particularly emphasized are the following:

- The classical Brownian motion model, is a purely phenomenologically motivated model. The foundational work on it by Einstein in 1905 was undertaken in order to explain the observations of Brown some years earlier. Nevertheless, its contribution in fundamental physics has been enormous since it consolidated the atomistic model of physics, through its prediction on the Avogadro's number.

- The model developed by Einstein was of statistical nature, and gave a prediction on the MSD of a Brownian particle. In particular it predicted it to grow linearly with time, which was later termed as normal diffusion. Einstein's model, predicted

the evolution with time of the probability $p(x,t)$ of finding a particle at position x in time t. The main assumption of Einstein is the existence of a sufficiently small time scale beyond which individual displacements are statistically independent. Smoluchowski reached the same conclusion about the MSD through a kinetic microscopic model of colliding hard spheres. In Smoluchowscki's model, the inertia of the Brownian particle is taking into account.

- Langevin some time later linked the findings of Einstein and Smoluchowski through a very different approach, by giving a stochastic description of a single Brownian particle trajectory. To do so he had to make use of the Wiener process. He essentially made the same set of assumptions as Einstein, except that he did not assume a constant velocity for the BP. This way he could treat velocity correlation function and hence velocity relaxation, making the approach more refined.

- The fluctuation dissipation relation, connects the correlations of this random force in time introduced by Langevin, to a macroscopic measurable quantity, namely the diffusion coefficient.

- By violating the assumptions of Einstein, in particular by either having a "broad" distribution of the random variables appearing in the probability density $p(x,t)$ or by having "long range" correlations among the jumps in space, the normal diffusion is violated, namely the MSD does not grow linearly in time.

CHAPTER 3

QUANTUM BROWNIAN MOTION

In the last Chapter, we defined the classical Brownian motion and presented an overview of the most important developments related to it. This theory is purely classical and rely on phenomenological equations, i.e. equations that are not derived in a Hamiltonian framework, but are proposed starting from experimental results that one aims to interpret. Nevertheless, this study enabled us to develop an intuition regarding the phenomenon of Brownian motion, that will serve to understand the relevant assumptions that go in the works related to its quantum analogue.

In this section we begin with a short presentation of a number of problems related to this classical theory, which will also constitute the main motivation for considering studies of an extension of the theory in the quantum regime. To proceed in studying the quantum version of the phenomenon of BM, and having in mind that the standard procedures of quantization are based on the existence of Hamiltonians (or equivalently Lagrangians), then the first step we make is to look for a Hamiltonian description. Precisely, one has to write a Hamiltonian leading to the phenomenological equations, such as those of Einstein Eq. (2.3) and Langevin Eq. (2.12) . Then, by replacing functional variables with operator ones it is possible to obtain a quantum Hamiltonian for Brownian motion.

With this point of view in mind, Caldeira and Leggett (Caldeira and Leggett, 1981), proceeded in introducing the Hamiltonian of Quantum BM (QBM). This basically describes a quantum particle, usually trapped in a harmonic potential, coupled to a set of non-interacting harmonic oscillators. This Hamiltonian encodes all the information to

study the physics of QBM. There are a number of approaches one can use to study the quantum version of BM, and we present here an overview of a number of them, commenting mainly on the advantages and disadvantages of each one. We pay particular attention to the approach of the Quantum General Langevin equation, a quantum extension of the classical model presented above, and we comment how it compares to the rest of the approaches, and what the limitations of this approach are. Indeed this is the approach used to derive the results of the next sections. Finally, we summarize a number of important applications of the Quantum Brownian motion, which will motivate also the works that we undertook in the sections to come.

3.1 Motivation

3.1.1 Problems with classical Brownian motion

In this subsection we focus on a number of problems one can encounter when studying the classical Brownian motion. These are basically contradictions arising either from ignoring the quantum nature of the system or from the non-physical assumption of stochastic dynamics that while they might be compatible with statistical physics, they contradict classical physics. The three major problems appearing would be:

1. Loschmidt objection or the irreversibility paradox: The diffusion equation, Eq. (2.3) as well as the Langevin equation, Eq. (2.12) are both not invariant under time-reversal. On the other hand, the BP and the fluid molecules, classically obey Newton's reversible laws, clearly leading to a contradiction (Zwanzig, 2001)

2. Zermelo's paradox: Consider a configuration with many BP at the center of the fluid. According to the diffusion equation, these after some time will spread throughout the volume. This means that we will never find them at any later time back in the center, i.e. in the initial configuration. This is at odds with Poincare's theorem, which asserts that the trajectories of a bounded system (in phase space) will pass arbitrarily close to the initial state, after a time called the recurrence time.

3. Quantization problem and the Heisenberg Uncertainty violation: It is not straightforward how one can quantize an irreversible or stochastic equation. Phenomenological quantization schemes exist (say, the counterpart of plugging $-\gamma x$ in Newton equation) but can lead to violations of basic issues (like the very normalization of the state, or commutation relations). (Wallraff, 2001) The question of quantization can not be ignored, since it is well known that at low temperatures of the environment quantum effects in the behaviour of the particle become important. Furthermore, one can check that a classical dissipative equation, like the Langevin equation above, contradicts the uncertainty relation which must be satisfied in the quantum theory (Louisell and Louisell, 1973). One can say that the main difficulty

of any quantum mechanical description of Brownian motion lies in the concept of friction. In classical mechanics the friction force cannot be derived from a Hamiltonian theory. This is obvious from the fact that the friction causes a decrease in the phase space volume, i.e. Liouville's theorem is not valid. This contraction is also what contradicts the Heisenberg uncertainty relations: Any finite volume in phase space will in the course of time fall into a volume smaller than $\hbar/2$. The diffusion term in the Langevin equation increases the volume in phase space of course, the equilibrium state being such that the two tendencies balance.

From all the above, hence, one understands that the quantum description of dissipation must start from reversible dynamics described by some Hermitian Hamiltonian. The irreversibility observed at the end, should then come from additional assumptions made on this description. However, in the classical Langevin equation, the irreversibility is introduced right from the beginning.

Why is a quantum version of BM necessary?

As already stated above, in many cases particularly at low temperatures a theory of dissipation based on the classical Brownian motion may be inadequate because it can not accommodate quantum effects since the Langevin equation can not in principle be quantized. Nevertheless, quantum noise arising from quantum fluctuations is important in many settings, for instance in nanoscale and biological systems (Abbott *et al.*, 2008). We mention as typical examples of processes where quantum effects play an important role, the noise assisted tunneling and transfer of electrons and quasiparticles (Hanggi *et al.*, 2005). The characteristics of such quantum noise vary strongly as a function of temperature. At high temperatures a crossover to Johnson-Nyquist noise which is essentially governed by the classical Brownian motion takes place.

The above considerations are enhanced by recent studies on the quantum mechanics of macroscopic quantum variables, such as the decay of a zero voltage state in a biased Josephson junction, flux quantum transitions in a SQUID (Hänggi *et al.*, 1990) and the possible reversal by quantum tunneling of the magnetization of a single domain ferromagnetic particle, which call for extensive studies in a quantum version of the Langevin equations. One may also remark in the context of macroscopic quantum tunneling (which is a mesoscale quantum phenomenon) that substantial experimental data on magnetic relaxation now exists (Wernsdorfer, 2001) at mK temperatures. The analysis of this phenomenon was severely hampered by the lack of an appropriate theory of quantum dissipation which could predict for example the relaxation behaviour as a function of spin size. All these, necessitated the development of a theory of quantum Brownian motion. With the development of such theory, it has been proven that the Brownian motion can play a vital role in information and communications technology as well as in fundamental

issues of applied mathematics and theoretical physics.

3.1.2 Historical origins

After having motivated the necessity for the development of such a quantum theory of BM, let's have a brief look at the most important historical developments. Even as early as in the birth of quantum mechanics in early 1920's one can encounter references to the so called quantum noise. In the very final paragraph of the 1928 paper by Nyquist (Nyquist, 1928) for the first time the introduction of quantum mechanical noise via the substitution of the energy k_BT from the classical equipartition law [1] by the thermally averaged quantum energy (but leaving out the zero point energy contribution) of the harmonic oscillator. Nyquist's remark thus constitutes a precursor of the celebrated work by Callen and Welton (Callen and Welton, 1951) who generalized the relations by Einstein, Nyquist, and Johnson to include quantum effects. The proof of the associated quantum fluctuation-dissipation theorem was a milestone in the study of quantum Brownian motion (Callen and Welton, 1951, Kubo, 1966).

Soon after, it was shown that, in contrast to the phenomenological way, the quantum Langevin equation can be obtained from the forward-backward path integrals within some concrete quantum model of dissipation (Kleinert, 2004). The physical cause of dissipation is the influence of the environment on the relevant system. Hence a consecutive quantum theory of dissipative systems should be derived using some dissipative Hamiltonian in which the surrounding medium and its influence on the system are taken into account. This lead to the so-called system-plus-bath model where the full system is split into the relevant system consisting of a few degrees of freedom and a thermal bath represented by a large or infinite number of degrees of freedom. In the next subsection, we discuss how using this as a starting point one can study a motion analogous to the classical Brownian motion presented in the previous section.

3.2 Hamiltonian approach to the Brownian motion

There are in general two ways to approach the problem of quantizing Brownian motion: either one looks for new schemes of quantization, beyond the standard ones which require one to have at hand a Hamiltonian of the system, or one uses the system-plus-reservoir approach (Caldeira and Leggett, 1983a). The former approaches always rely on some questionable hypotheses and lead us to results dependent on the method used, besides not being very realistic (Weiss, 2012). We focus on the second case.

In this approach, precisely, one has to write a Hamiltonian leading to the phenomenological equations, such as those of Einstein, Fokker-Planck and Langevin. Then, by re-

[1] It is worthwhile to recall that the "rigorous" validity of the equipartition theorem is restricted to classical statistical mechanics.

placing functional variables with adjoint operators it is possible to obtain a quantum Hamiltonian for BM. There have been several excellent monographs and reviews covering how this can be done such that a quantum Brownian motion (Wang and Uhlenbeck, 1945, Breuer *et al.*, 2002, Leggett *et al.*, 1987, Hanggi *et al.*, 2005, Weiss, 2012) is obtained. In this approach, one considers explicitly the fact that the dissipative system is always coupled to a given thermal environment. The importance of this framework of modeling lies in its generality, since there is no known dissipative system which is not coupled to another system that is responsible for its losses.

To proceed, one needs to consider explicitly the coupling of the system of interest to the environment. This firstly requires knowledge of the type of the environment and secondly how the coupling with the central system, the BP, takes place. This can be a very hard task. Nevertheless, fundamentally different composite systems, by which we mean systems of interest-plus-environment, might have the former obeying Brownian dynamics in the classical limit (e.g. a central system or a bath made of harmonic oscillators or spins). Although this appears to be an additional complication to our approach, it actually gives us a chance to argue in favor of some simplifying hypotheses. For instance, we can assume that quite distinct reservoirs, e.g. a reservoir of harmonic oscillators and a reservoir of spins, may share some common characteristics, such as the behaviour of their spectrum of excitations or the way they respond when acted on by an external input.

Usually, for many complex systems we do not have a clear understanding of the microscopic origin of damping. However, sometimes one might be able to acquire knowledge of the power spectrum of the stochastic force in the classical regime. Therefore, it is interesting to set up phenomenological system-plus-reservoir models which reduce in the appropriate limit to a description of the stochastic process in terms of a quasi-classical Langevin equation (Barik and Ray, 2005). The simplest model of a dissipative quantum mechanical system that one can come up with is a damped quantum mechanical linear oscillator: a central harmonic oscillator coupled linearly via its displacement coordinate x to a fluctuating dynamical reservoir. In the particular case that the bath is only weakly perturbed by the system, it can be considered as linear and therefore be described by harmonic oscillators. Then the statistics is exactly Gaussian. This model has been introduced and discussed in a series of papers by Ullersma (Ullersma, 1966). Zwanzig generalized the model to the case in which the central particle moves in an anharmonic potential and studied the classical regime (Zwanzig, 1973). Caldeira and Leggett (Caldeira and Leggett, 1981) were among the first who applied this model to quantum mechanical tunneling of a macroscopic variable.

To make the system under consideration more concrete, we comment here on the intuitive workings behind the system. We consider a system with one or few degrees

of freedom which is coupled to a huge environment and imagine that the environment is represented by a bath of harmonic excitations above a stable ground state. The interaction of the system with each individual degree of freedom of the reservoir is proportional to the inverse of the volume of the reservoir. Hence, the coupling to an individual bath mode is weak for a geometrically macroscopic environment. Therefore, it is physically reasonable for macroscopic global systems to assume that the system-reservoir coupling is a linear function of the bath coordinates. This property is very convenient, because it allows to eliminate the environment exactly. Most importantly, the weak perturbation of any individual bath mode does not necessarily mean that the dissipative influence of the reservoir on the system is weak as well. This is because the couplings of the bath modes add up and the number of modes can be very large. We note here that a number of variations of this set-up complying with the picture described above, could be considered. For example, one could consider the central system to be discrete, e.g. a two or more state system, i.e. a qubit or a d-bit, or alternatively the system could be considered to be continuous, as e.g. a harmonic oscillator. In our works, we assume the central system to be continuous. Another variation would be that of considering as the bath a set of spins. It can be shown that such a system shares a lot of common properties and behaviors with the scenario where the bath is made out of harmonic oscillators, and this can be seen by the fact that their corresponding spectral densities (a quantity that will be introduced soon) can be related (Weiss, 2012, Schlosshauer, 2007b). Namely, it can be shown that the two types of reservoirs have the same dissipative influences at $T = 0$, but at finite temperatures, the spin bath has a smaller effect on the system because of the possibility for saturation of the populations in the bath. Finally, let us note that the excitations forming the thermal bath of harmonic oscillators, is assumed to obey Bose-Einstein statistics.

The model is defined by the Hamiltonian

$$H = H_S + H_E + H_I \tag{3.1}$$

where the system, bath and interaction terms are respectively

$$\begin{aligned} H_S =& \frac{p^2}{2m} + V(x) + V_c(x) \\ H_E =& \sum_k \left(\frac{p_k^2}{2m_k} + \frac{m_k \omega_k^2 x_k^2}{2} \right) - E_0 = \sum_k \hbar \omega_k b_k^\dagger b_k \\ H_I =& -\sum_k c_k x_k f(x) \end{aligned} \tag{3.2}$$

In the above expressions p is the particle momentum, m its mass, $V(x)$ the trapping potential depending on its position denoted by x. The expression

$$V_c(x) = \sum_k \frac{c_k^2}{2m_k \omega_k^2} f^2(x) \tag{3.3}$$

represents the so-called counter-term, which needed in the following to remove non-physical divergent renormalizations of the trapping potential arising from the coupling to the bath, as showed in (Breuer *et al.*, 2002). In the work that follows, we ignore such a term. This results in a Hamiltonian that is not positively defined for all the parameter space of the system (note that at this point we match the situation described by Canizares and Sols, 1994, (Cañizares and Sols, 1994) where translational symmetry is broken). In practice in the works that will follow, we take this in mind and for this reason we carefully choose the parameters of our system such that this does not lead to any problems. We will comment later on about the consequences of this. The bath bosons have masses m_k and frequencies ω_k, and their momenta and positions are denoted by p_k and x_k, respectively. Alternatively, we describe them with the help of annihilation and creation operators, b_k and $b_k^\dagger$, where the two are related by

$$\begin{aligned} x_k &= \sqrt{\tfrac{\hbar}{2m_k\omega_k}}\left(b_k^\dagger + b_k\right) \\ p_k &= i\sqrt{\tfrac{\hbar m_k\omega_k}{2}}\left(b_k^\dagger - b_k\right) \end{aligned} \quad . \tag{3.4}$$

From the bath Hamiltonian, we have removed the constant zero-point energy E_0. Here we assume that in the interaction Hamiltonian the bath operators are linearly coupled to a nonlinear function of the position of the Brownian particle $f(x)$ to indicate that this general case can also be considered, but in the works presented in this thesis, the interaction is always considered bilinear, i.e. $f(x) = x$. Note also that other variations of the form of the interaction Hamiltonian have also been considered in the past in the literature, as e.g. in (Cohen, 1997). This situation is the conventional one, and corresponds to a quantum system undergoing state-independent damping and diffusion, i.e. damping and diffusion independent on the position (or other observables). Furthermore, we will restrict our studies to the one dimensional (1D) bath case, but generalizations to 2D or 3D are straightforward.

There exist a number of choices regarding the Hamiltonian method we are going to use to treat our composite system. To start with, we should make some connection with the classical approaches in order to establish which one of them will be more useful for our needs. Here, once again, there are two categories of methods. As we have seen earlier in this chapter we can either employ the equation of motion method, through which one must generate a Langevin equation like, or study the time evolution of probability densities using the Fokker-Planck equation. Quantum mechanically there are two equivalent ways corresponding to each of them, and these are tantamount to the two well-known pictures of quantum mechanics, namely Heisenberg and Schrödinger. Within each of these methods then, there are different approaches to obtain the final result, whether that is an equation of motion for the observables or a an evolution equation for the density matrix.

To summarize, the main simplifying assumptions for the Caldeira-Leggett model dis-

cussed above is the following: The environment "feels" only weakly the presence of the system. Loosely speaking, the bath is big, a macroscopic object (but not necessarily classical); the liquid carrier in Brown's set up. The fluid's properties change very little when a pollen grain, or a handful, are suspended on it. This is mathematically expressed by the fact that in the interaction Hamiltonian, the bath interacts only linearly with the degrees of freedom of the central system (which can be nonlinear). Naturally, the converse does not hold. The grain is indeed affected by the bath.

3.3 Overview of approaches to the Quantum Brownian Motion

In this section, we shall present various methods and schemes of modeling quantum Brownian motion from first principles, i.e. by starting from a Hamiltonian approach. In doing so, we guarantee that the thermal noise must at all times obey the quantum version of the fluctuation-dissipation theorem à la Callen-Weltond. This latter property is necessary in order to be consistent with the second law of thermodynamics and the principle of quantum detailed balance. We elaborate on several alternative but equivalent methods to describe quantum noise and quantum Brownian motion per se. In doing so, we call attention to distinct differences to the classical situation and, in addition, we identify a series of delicate pitfalls which must be observed when making even innocent looking approximations. Such pitfalls involve, among others, the rotating-wave approximation, the use of quasiclassical Langevin forces, the quantum regression hypothesis and/or the Markov approximation. (Grabert *et al.*, 1988, Grifoni and Hänggi, 1998, Talkner, 1986)

3.3.1 Density matrix evolution

Master equation

In the ordinary formalism of open quantum systems, the reduced density operator for a system interacting with some environment, $\rho_S(t)$ is computed via

$$\rho_S(t) = Tr_E\left[U(t)\,\rho_{SE}(0)\,U^\dagger(t)\right] \tag{3.5}$$

where $U(t)$ denotes the time-evolution operator for the whole composite system of system and environment described by the state $\rho_{SE}(t)$. As is evident from Eq. (3.5), this approach requires that we first determine the state of the total system at a generic instant, before we can arrive at the reduced description through the trace operation. In general this task is not so easy (sometimes impossible) to carry out in practice for the majority of the systems.

In contrast, in the master equation formalism the reduced density matrix $\rho_S(t)$ is calculated directly from an expression of the form

$$\rho_S(t) = \mathcal{L}(t)\,\rho_S(0) \tag{3.6}$$

where the superoperator $\mathcal{L}(t)$ is the so-called dynamical map, ruling the temporal evolution of the central system, and should satisfy four properties, namely

1. $\mathcal{L}(t+s) = \mathcal{L}(t)\,\mathcal{L}(s)$ semigroup property
2. $\lim_{t\to 0^+} \mathcal{L}(t)\,\sigma = \sigma$ continuity
3. for $\sigma \geq 0$, $\mathcal{L}(t)\,\sigma \geq 0$, positivity
4. for $\sigma \in \mathcal{T}(H)$, $Tr\left[\mathcal{L}(t)\,\sigma\right] = Tr\left[\sigma\right]$, trace preserving

where $\mathcal{T}(H)$ denotes the Banach space. Expression in Eq. (3.6) is called master equation for $\rho_S(t)$, and it represents the most general structure that such an equation can take. Formally, one can employ the projection operator technique to solve the motion of the bath. By doing so, one obtains the Nakajima-Zwanzig equation which represents the most general form of a master equation and contains an extremely complicated retarded time integration over the history of the reduced system (Nakajima, 1958, Zwanzig, 1960). It thus describes completely non-Markovian memory effects of the reduced dynamics. In this case, the two formalisms must be equivalent. The advantage of this second formalism of master equations, lies in the fact that a series of approximations can be easily implemented that can result in a significantly simplified master equation, at the cost of the generality of the systems and the accuracy of the predictions that this approach allows to study.

Here we shall restrict our attention to master equations (valid under particular hypothesis) that may be written as first-order differential equations showing a local in time structure, namely which can be cast in the form

$$\frac{\partial \rho_S(t)}{\partial t} = \mathcal{L}\left[\rho_S(t)\right] = -\frac{i}{\hbar}\left[H_S(t)\,,\rho_S(t)\right] + \mathcal{D}\left[\rho_S(t)\right] \tag{3.7}$$

This equation is local in time in the sense that the change of the state of the central system at time t depends only on the form of such a state evaluated at t, but not at any other times $s \neq t$. The superoperator $\mathcal{L}$ appearing above, acts on $\rho_S(t)$, and typically depends both on the initial state of the environment and on the form of the Hamiltonian. To convey the physical intuition behind $\mathcal{L}$, it has been decomposed into two parts:

- A unitary part. This originates by the usual von Neumann commutator with the self-Hamiltonian H_S. In general, this term is not identical to the unperturbed free Hamiltonian that would otherwise generate the evolution of the BP in the absence of the interaction with the environment. This is because this coupling often perturbs the free Hamiltonian, leading to a renormalization of its spectrum through the introduction of a counterterm, like that in Eq. (3.3). This effect is often termed Lamb-shift, and has nothing to do with the non-unitary evolution induced by the environment. It simply alters the unitary part of the reduced dynamics.

- A non-unitary part $\mathcal{D}[\rho_S(t)]$. This encodes the action of the environment, as for example the effect of decoherence or dissipation. Without this term, the BP would follow a unitary evolution only altered by the presence of a counter-term.

Born-Markov approximation Before proceeding to present the Born-Markov approximation, let us note that the formal interaction part of the Hamiltonian can be expressed as

$$H_I = \sum_k S_k \otimes E_k \tag{3.8}$$

where S_k and E_k are self-adjoint operators acting on the Hilbert spaces of the central system and the environment, respectively. This bilinear coupling implicitly assumes a weak interaction between the system and the environment, and this is the first assumption in order to get the Born-Markov approximation (This is indeed the main assumption of the Caldeira-Leggett model of QBM explained i the previous chapter). For some applications we shall add a time-dependent contribution $V(t)$ to the Hamiltonian H_S in order to take into account external fields used by the observer to control our system (see work on heat current control in BEC in Chapter 8).

The Born-Markov master equation is based on two core approximations that may be stated as below:

- The Born approximation. This approximation assumes that the coupling between the system and the reservoir is weak, such that the influence of the system on the reservoir is small (weak-coupling approximation). Thus, the density matrix of the reservoir ρ_B is only negligibly affected by the interaction and the state of the total system at time t may be approximately characterized by a tensor product

$$\rho(t) \approx \rho_S(t) \otimes \rho_B \tag{3.9}$$

  To understand the condition for this approximation to hold, one needs to introduce the following timescale, namely $\tau_p = \hbar/\delta E$, where δE is an energy resolution of state preparation or measurement. For a quantum system S with a discrete spectrum, δE should be smaller that the typical separation between the energy levels while for systems with continuous spectrum (e.g. quantum Brownian particle) τ_p is directly related to a chosen time-scale of observation. For the above approximation to be valid then, the following should be true

$$t \gg \tau_p \tag{3.10}$$

- The Markov approximation. To introduce this approximation, we first call upon an intuition developed from the classical scenario of the GLE described above, namely

that the interaction of the bath particles with the central system should result in correlations of the noise in different times, as in Eq. (2.20). We assume here then that these correlations decay in a finite time τ_b. We comment here, that in fact, strictly speaking, a decay of the correlations can only be valid for an environment which is infinitely large and involves a continuum of frequencies, but in the systems that we will study this is a safe assumption. If on the other hand, the frequency spectrum of the reservoir modes is discrete, in general, the correlation functions will be quasi-periodic functions. A rapid decay of the reservoir correlations therefore requires a continuum of frequencies: For an infinitely small frequency spacing Poincaré recurrence times become infinite and irreversible dynamics can emerge. With this in mind, then, the basic condition underlying the Markov approximation is that the reservoir correlation functions decay over a time τ_b that is sufficiently fast, namely much smaller compared to the relaxation time τ_r, i.e. the time at which the state of the system varies noticeably,

$$\tau_b \ll \tau_r. \tag{3.11}$$

Note that the above approximation is quite not general, and is only appropriate if the environment is weakly coupled to the central system, and if the temperature of the bath is sufficiently high. Nevertheless, even if the reservoir has no natural decay time scale τ_b, one can include the averaging effect of the Hamiltonian dynamics of S in order to satisfy the above condition.

Restricting to the Born approximation, the corresponding dynamical map $\mathcal{L}(t)$ will not satisfy the semigroup property, namely the following will not hold $\mathcal{L}(t+s) \approx \mathcal{L}(t)\mathcal{L}(s)$. Introducing the Markovian approximation resolves this problem. The idea is that by making the Markovian approximation, we assume that there exists a certain coarse-grained time scale, roughly determined by τ_r, for which the exact state of the system $S+E$ given by $U(t)[\rho_S(0)\otimes\rho_B]U^\dagger(t)$ does not differ locally from the state $\mathcal{L}[\rho_S(t)]\otimes\rho_B$. Here "locality" is determined by the radius of interaction between S and E. Mathematically this condition can be expressed as a sufficiently fast decay of the reservoirs correlation functions

$$E_{kl}(t) = Tr\left(\rho_B E_k(t+s) E_l(s)\right) \tag{3.12}$$

where $E_k(t) = e^{itH_E}E_k e^{-itH_E}$ and we assume that the reservoir's reference state ρ_B is stationary with respect to its evolution, a consequence of the Born approximation.

Then the evolution of $\rho_S(t)$ is given by the Born-Markov master equation

$$\frac{\partial\rho_S(t)}{\partial t} = -\frac{i}{\hbar}[H_S,\rho_S(t)] - \frac{1}{\hbar^2}\sum_k\{[S_k,B_k\rho_S(t)] + [\rho_S(t)C_k,S_k]\} \tag{3.13}$$

with

$$\begin{aligned} B_k &:= \int_0^\infty dt' \sum_j C_{kj}(t') S_j^{(I)}(-t') \\ C_k &:= \int_0^\infty dt' \sum_j C_{kj}(-t') S_j^{(I)}(-t') \end{aligned} \tag{3.14}$$

Here $S_j^{(I)}(-t')$ denotes the system operator S_k in the interaction picture (Schlosshauer, 2007b). The quantity $C_{kj}(t)$ is given by

$$C_{kj}(t) = \left\langle E_k^{(I)}(t) E_j \right\rangle_{\rho_B} \tag{3.15}$$

where the average is taken over the initial environmental state ρ_B (recall that the Born approximation demands that such a state remains approximately constant at all times $[H_B, \rho_B] = 0$). This quantity will be referred to as the environment self-correlation functions in the following. We note here that the form of the self correlation function is such, because we in addition made the assumption that the bath is at a stationary state ρ_B , then one can show that the reservoir correlation functions are homogeneous in time $\langle E_k(t) E_j(t-s)\rangle = \langle E_k(s) E_j(0)\rangle$. This is not the case if one considers for example a squeezed vacuum state for the reservoir, but we ignore such scenarios in our work.

The reason for calling the above function the environment self-correlation function is easy to understand. The operators E_k can be thought of as observables of the environment, such as the position and momentum of the bath particles. Furthermore, the values of these observables are assumed to be "measured" through the interaction of the bath with the BP. Bath self-correlation functions essentially tell us by how much the value of a supposed measurement of such an observable E_k has been affected by another supposed measurement at a previous time. In other words, broadly speaking, these functions quantify to what degree the environment retains information over time about its interaction with the system.

Rotating Wave approximation (RWA) In fact the aforementioned approximations, do not guarantee, that the resulting equation (3.13) defines the generator of a dynamical semigroup (Davies, 1974, Dümcke and Spohn, 1979), as should be the case for a valid master equation. The reason is that these approximations may lead to non-positive density matrices. One therefore performs a further secular approximation which involves an averaging over the rapidly oscillating terms in the master equation and is known as the rotating wave approximation. The RWA is widely used in quantum optics, which neglects the rapidly oscillating counter-rotating terms and the system Hamiltonian becomes time independent or depends slightly on time in the rotating frame. In the rotating wave approximation rapidly oscillating terms proportional to $e^{i(\omega_k - \omega_j)t}$ are neglected. In the particular case of the system being a harmonic oscillator, at the level of the Hamiltonian, RWA implies that terms of the form $a^\dagger b_k^\dagger$ and $a b_k$ are ignored, where a and $a^\dagger$ are the

central harmonic oscillator annihilation and creation operators related to the position and momentum of it as

$$\begin{aligned} x &= \sqrt{\tfrac{\hbar}{2m\omega}}\left(a^\dagger + a\right) \\ p &= i\sqrt{\tfrac{\hbar m\omega}{2}}\left(a^\dagger - a\right) \end{aligned} \quad . \tag{3.16}$$

Generally, this assumption, ensures that the quantum master equation is in the so-called Lindblad form. The corresponding condition is that the inverse frequency differences involved in the problem are small compared to the relaxation time of the system, that is

$$\tau_p \propto |\omega_k - \omega_j|^{-1} \ll \tau_r \tag{3.17}$$

This in practice implies that during preparation or measurement processes the system S is not strongly perturbed.

In conclusion the structure of the Born-Markov master equation of a given system remains fixed by its Hamiltonian and the two approximations discussed above. A clear derivation of equation (3.13) goes widely beyond the purpose of the present thesis. However, it may be found in a number of standard textbooks (Schlosshauer, 2007b)(Breuer *et al.*, 2002). In particular in (Breuer *et al.*, 2002), the authors show that the Born-Markov master equation may be derived even by the Nakajima-Zwanzig equation. Precisely, it follows from an expansion in the bath-system coupling constant at the second order. For the particular case of the Quantum Brownian motion, one can start with the Hamiltonian presented above, and derive then the relevant master equation. This has been a widely used approach to study QBM, nevertheless, there are a number of criticisms as to why the aforementioned approximations might not hold in nowadays relevant experimental set-ups and we examine this in the next section.

Criticism of Born-Markov master equation and the RWA The Born-Markov quantum master equation method provides a reasonable description in many cases, such as in Nuclear Magnetic Resonance, in laser physics, and in a variety of chemical reactions. However, this method turned out to be not useful in most problems of solid state physics at low temperatures for which neither the Born approximation is valid nor the Markov assumption holds. We comment below why this is the case. Furthermore, in recent developments in the area of circuit and cavity QED systems (Niemczyk *et al.*, 2010), ultra- and deep-strong light-matter couplings became experimentally achievable, which makes it necessary to take the counter-rotating terms into account, i.e. casts the RWA invalid. In fact, recent studies show that the counter-rotating terms in system-reservoir coupling play an important role in non- Markovian effects.

As already mentioned, positive Markovian dynamics is only obtained under careful approximations that are valid only from medium to high temperatures of the thermal

bath (Diósi, 1993), an example being RWA. Furthermore, it has been shown that the requirement that the equilibrium state should be the canonical thermal state determined by the standard Hamiltonian of a harmonic oscillator is incompatible with positivity and translational invariance (Lindblad, 1976, Kohen *et al.*, 1997, de Faria and Nemes, 1998). This incompatibility induced some authors to renounce to translational invariance (Săndulescu and Scutaru, 1987, de Faria and Nemes, 1998), or to accept non-positive dynamical equations and to give more relevance to obtaining time evolutions very close to the classical ones (Caldeira and Leggett, 1981, 1983a, Strunz *et al.*, 1999). A non positive dynamics can be satisfactory when the system is near the classical regime, but this approach becomes questionable when quantum effects are searched for (Jacobs *et al.*, 1999, Giovannetti and Vitali, 2001). In any case, all of these approaches do not solve satisfactorily in a general setting the aforementioned problems.

Non-Markovianity Markovianity is often defined with respect to whether the system is reversible or not. Markovian systems are irreversible, while non-Markovian systems allow the flow of information between the system and environment reversibly (Laine *et al.*, 2012). The non-Markovian open systems are important because of their ability in preserving information and their persistence against decoherence caused by interactions with the environment. Furthermore, in (Ferialdi, 2017), the authors showed that if one is careful in taking the Markov limit, the resulting master equation for the Caldeira-Leggett model is non-dissipative, proving that the only way that one can introduce dissipation in the dynamics of the QBM is by allowing non-Markovian evolutions. Because of these reasons, the study of non-Markovianity property in open systems has attracted much attention, recently.

Therefore, various witnesses and measures have been defined to describe the non-Markovianity features qualitatively and quantitatively. To determine the Markovianity or non-Markovianity of a channel, a witness of non-Markovianity is used and then non-Markovianity is quantified by a measure. A non- Markovianity measure is a function that its numerical value is positive or zero; the value of this function is zero if the dynamics is Markovian. On the other hand, the normalized measure which is between zero and one is called the degree of non-Markovianity (Laine *et al.*, 2012). The non-Markovianity measures are generally introduced on the basis of indivisibility and the backflow information.

Besides reversibility, another way to determine if the evolution of a system is Markovian or not is whether this evolution satisfies the semigroup property (Wolf *et al.*, 2008). Furthermore, in (Rivas *et al.*, 2010) the authors defined an evolution as Markovian, whenever it can be represented by a trace preserving divisible map. Another idea based on divisibility, where the latter is quantified however in terms of the negative values of transition maps was presented in (Rajagopal *et al.*, 2010). In (Breuer *et al.*, 2009), the

non-Markovian evolution was defined as that where one observes a back-flow of information from the environment to the system. Other non-Markovianity measures include one based on the quantum Fisher information flow (Lu *et al.*, 2010) another on the Bures distance (Liu *et al.*, 2013), or one based on the non-monotonicity of the decay of the mutual correlations between the open quantum system and an ancilla (Luo *et al.*, 2012). Taking advantage of the fact that the volume of physical states accessible to a system decreases monotonically for Markov evolutions, while non-Markovian evolutions may present some time intervals where it increases, in (Lorenzo *et al.*, 2013) the authors presented an alternative measure of non-Markovianity. By considering a formal analogy with the entanglement theory, where a Markov evolution would correspond to a separable state, while a non-Markovian evolution would be characterized by the Schmidt number of the relevant entangled state, (Chruściński and Maniscalco, 2014) propose another measure of non-Markovianity. More recently, in (Liu *et al.*, 2016), the non-Markovianity of a chromophore-qubit pair in a super-Ohmic bath was quantified, using the distance between an evolved state and the steady state. Finally in our own work, (Lampo *et al.*, 2018), an alternative measure was introduced based on the distance of an element of a Gaussian covariance matrix at the long-time limit to the corresponding one had the spectral density been assumed to be Markovian. For a number of measures for both discrete as well as continuous variables the writer is referred to (Rivas *et al.*, 2010)

Summary of approximations Let us summarize the different approximations used in the above derivation. The first approximation is a consequence of the weak-coupling assumption which allows us to expand the exact equation of motion for the density matrix to second order. Together with the condition $\rho(t) \approx \rho_S(t) \otimes \rho_B$ this leads to the Born approximation to the master equation. The second approximation is the Markov approximation in which the quantum master equation is made local in time by replacing the density matrix $\rho_S(t)$ at the retarded time s with that at the present time $\rho_S(t)$. Furthermore, the integration limit is pushed to infinity to get the Born-Markov approximation of the master equation. The relevant physical condition for the Born-Markov approximation is that the bath correlation time τ_b is small compared to the relaxation time of the system τ_r, that is $\tau_b \ll \tau_r$. Finally, in the rotating wave approximation rapidly oscillating terms proportional to $e^{i(\omega_k-\omega_j)t}$ are neglected, ensuring that the quantum master equation is in Lindblad form. The corresponding condition is that the inverse frequency differences involved in the problem are small compared to the relaxation time of the system, that is $\tau_p \propto |\omega_k - \omega_j|^{-1} \ll \tau_r$.

3.3.2 Quantum Generalized Langevin equation

The first derivation of the quantum generalized Langevin equation (QGLE) dated back to 1965 in (Ford *et al.*, 1965). They consider a set of $2N+1$ interacting harmonic oscillators

and focus their work on studying the dynamics in a particular one due to the effect of the rest of oscillators acting as a heat bath. The resulting operators equation resembles the classical generalized Langevin equation in coordinate space. Another derivation is that of (Ford *et al.*, 1988). Starting from the Heisenberg equation of motion, they provided a purely quantum derivation of the QGLE with a random force operator acting on the Hilbert space of the entire system. We present a detailed derivation for the case of a Hamiltonian in the form of the Caldeira Leggett model discussed above, where however the system couples through a nonlinear function of its operators to a linear operator of the bath, which is the most general case one can treat with this approach. We also note here that we consider harmonic oscillators for the central system as well as for the bath, but both could in principle replaced by spins. We should also mention that one can consider the coupling of a system to a bath of independent fermions with infinitely many excitation energies. A suitable transformation then allows to map the dissipation onto a bosonic environment with an appropriate coupling strength (Hänggi *et al.*, 1990, Camalet *et al.*, 2003, Chang and Chakravarty, 1985).

From a practical point of view, there are a number of cases where such a modeling of the system would be appropriate and we list here a few of them (Hänggi *et al.*, 1990, Weiss, 2012). Examples are the electromagnetic modes in a resonator acting as a reservoir or the dissipation arising from quasi-particle tunneling through Josephson junctions (Eckern *et al.*, 1984). In the case of an electrical circuit containing a resistor one may use the classical equation of motion to obtain the damping kernel and model the environment accordingly. This approach has been used e.g. to model Ohmic dissipation in Josephson junctions in order to study its influence on tunneling processes (Schön and Zaikin, 1990), and to describe the influence of an external impedance in the charge dynamics of ultra-small tunnel junctions (Ingold and Nazarov, 1992).

Derivation of QGLE

The complete Caldeira—Leggett model leads to the following exact Heisenberg equations of motion (eom) for the Brownian particle and the environmental oscillators,

$$\begin{aligned} \dot{x}(t) &= [H, x(t)] = \tfrac{p}{m} \\ \dot{x}_k(t) &= [H, x_k(t)] = \tfrac{p_k}{m_k} \\ \dot{p}(t) &= \tfrac{i}{\hbar}[H, p(t)] = -\partial_x V(x) + \textstyle\sum_k c_k x_k(t) \\ \dot{p}_k(t) &= \tfrac{i}{\hbar}[H, p_k(t)] = -m_k\omega_k^2 x_k(t) + c_k x(t) \end{aligned} \tag{3.18}$$

which can more compactly written as

$$m\ddot{x}(t) + \partial_x V(x) - \sum_k c_k x_k(t) = 0 \tag{3.19}$$

$$m_k\ddot{x}_k(t) + m_k\omega_k^2 x_k(t) - c_k x(t) = 0 \tag{3.20}$$

The last equation shows that the k^{th} bath oscillator is driven by the force $c_k x(t)$ which depends linearly on the coordinate of the Brownian particle. In order to get a closed equation of motion for $x(t)$ one solves the bath eom Eq. (3.20) in terms of $x(t)$ and of the initial conditions for the bath modes and substitutes the result into the eom of $x(t)$, Eq. (3.19). The solution of Eq. (3.20) is then given by

$$\begin{aligned} x_k(t) =& x_k(0)\cos(\omega_k t) + \frac{p_k(0)}{m_k\omega_k}\sin(\omega_k t) + \frac{c_k}{m_k\omega_k^2}\left(x(t) - \cos(\omega_k t)\, x(0)\right) \\ & - \frac{c_k}{m_k\omega_k}\int_0^t ds \sin\left[\omega_k(t-s)\right]\dot{x}(s) \end{aligned} \tag{3.21}$$

Substituting into Eq. (3.19) yields

$$m\ddot{x}(t) + \partial_x V(x) + m\int_0^t ds\gamma(t-s)\,\dot{x}(s) = B(t) - m\gamma(t)\,x(0) \tag{3.22}$$

where $\gamma(t)$ is the damping kernel

$$\gamma(t) = \frac{1}{m}\sum_k \frac{c_k^2}{m_k\omega_k^2}\cos\left[\omega_k(t)\right]. \tag{3.23}$$

and the operator $B(t)$ which appears on the right-hand side is the interaction picture operator

$$B(t) = \sum_k c_k\left(x_k(0)\cos(\omega_k t) + \frac{p_k(0)}{m_k\omega_k}\sin(\omega_k t)\right). \tag{3.24}$$

Spectral density and the Quantum Fluctuation Dissipation Theorem At this point we introduce a function referred to in the literature as the spectral density function,

$$J(\omega) = \frac{\pi}{2}\sum_k \frac{c_k^2}{m_k\omega_k}\delta(\omega - \omega_k) \tag{3.25}$$

which basically assigns a weight on the influence a particular frequency from the frequency spectrum of the bath has on the motion of the Brownian particle. Moreover, we observe that this quantity only depends on bath properties, and hence we conclude that damping does not depend on the state of the system. This property is a consequence of assuming a bilinear coupling between the particle and the bath. This forces us to make use of linear response theory, which we briefly summarize in App. A.1.1. Furthermore, as stated earlier, we will consider the continuous frequency limit for the bath's frequency spectrum, which implies that $J(\omega)$ is a smooth function (For more details look in App. A.1.2). The damping kernel in terms of this function is rewritten as

$$\gamma(t) = \frac{1}{m}\frac{2}{\pi}\int_0^\infty d\omega \frac{J(\omega)}{\omega}\cos(\omega t) \tag{3.26}$$

One can show then that a direct consequence of considering a quadratic Hamiltonian, is that $B(t)$ satisfies the following Gaussian statistics

$$\begin{aligned} \langle B(t)\rangle_E &= 0 \\ \langle B(t)B(0)\rangle_{\rho_B} &= \frac{\hbar m}{\pi}\int_0^\infty d\omega J(\omega)\left(\coth(\omega\hbar\beta/2)\cos(\omega t) - i\sin(\omega t)\right) \end{aligned} \tag{3.27}$$

where $\langle O\rangle_{\rho_B} = Tr_E\left(e^{-\beta H_E}O\right)$. We drop the subscript ρ_B from the averages from now on for sake of notational clarity. The second equation is usually referred to as the Quantum Fluctuation Dissipation theorem, for which you can read more in App. A.1.3. This term also often refers to an equivalent equality (See App. A.1.3)

$$Re\left[\langle\{B(\omega), B(\omega')\}\rangle\right] = -4\pi\hbar\delta(\omega+\omega')\,Im\left[\chi(\omega)\right] \tag{3.28}$$

where $B(\omega)$ ($\chi(\omega)$) is the Fourier transform of $B(t)$ ($\chi(t)$), with $\chi(t)$ being the susceptibility related to the noise kernel $\lambda(t)$ by $\chi(t) = 2\Theta(t)\lambda(t)/\hbar$. The role of this function will be discussed in more detail later on. This quantity $\langle\{B(\omega), B(\omega')\}\rangle$ is often referred to as the noise kernel. From the above Eq. (3.27) one understands why the operator $B(t)$ plays the role of the noise term in the classical Langevin equation. The randomness here then enters from the initial state in which the bath is set, i.e. on the distribution of $x_k(0)$ and $p_k(0)$, while the eom are deterministic. If we further redefine $B(t) \to \widetilde{B}(t) := B(t) - m\gamma(t)x(0)$ then this new noise operator, depends on the initial preparation of the total system, i.e. also on the initial system position $x(0)$. Clearly, in order to qualify as a stochastic force the random force $\widetilde{B}(t)$ should also not be biased; i.e. its average should be zero at all times. To achieve this, a suitable redefinition of the Gibbs state of the bath has to be made (Weiss, 2012). For the consequences of this redefinition look in (Hanggi *et al.*, 2005). This is equivalent also to ignoring the so called spurious term $-m\gamma(t)x(0)$ from Eq. (3.22), which has as a result to give the form of the classical GLE we had in the previous chapter. Moreover, another property this Brownian quantum noise should exhibit, is that it should constitute a stationary process with time homogeneous correlations. This latter property, can be satisfied at the long-time limit, under the correlation free initial state preparation, as is explained below. It is also interesting to observe that, the force correlation function in Eq. (3.27), only vanishes in the classical limit, while it remains finite even at zero temperature. This reflects the fact that at absolute zero temperature the coupling induces a non-vanishing decoherence via the zero-point fluctuations.

Finally, it is important to mention that if the spectral density introduced before is allowed to assign weight to an infinite frequency this would lead to non-physical results, for example it would lead to an ultraviolet divergence of the noise kernel. For this reason, in (Unruh and Zurek, 1989), the authors introduced a cutoff on the noise kernel integral. Nevertheless this would violate the QFDT in Eq. (3.28), hence a cutoff Λ was introduced

on the maximum frequency allowed in the spectral density, considering therefore only the low frequency part of it $J_{lf}(\omega) = J(\omega) F_{cutoff}(\Lambda, \omega)$. Here $J_{lf}(\omega)$ denotes the low frequency part of the spectral density, but the subscript lf will be dropped in the rest of this thesis. This allows a valid study of the system at much shorter timescales. There are a number of common types of cutoff functions $F_{cutoff}(\Lambda, \omega)$ used in the literature,

1. Lorentz-Drude cutoff
$$F_{cutoff}(\Lambda, \omega) = \frac{\Lambda^2}{\Lambda^2 + \omega^2} \tag{3.29}$$

2. Exponential cutoff
$$F_{cutoff}(\Lambda, \omega) = e^{-\omega/\Lambda} \tag{3.30}$$

3. Hard cutoff
$$F_{cutoff}(\Lambda, \omega) = \Theta(\Lambda - \omega) \tag{3.31}$$

where $\Theta(\Lambda - \omega)$ is the Heaviside theta function and $\omega < \Lambda$. In our work we will mostly use this last form of the cutoff.

Note that instead one could have used the creation and annihilation operators $b_k^\dagger$, b_k for which the solution of Eq. (3.20) would read as

$$x_k(t) = \sqrt{\frac{\hbar}{2m_k\omega_k}}\left(e^{-i\omega_k t} b_k + e^{i\omega_k t} b_k^\dagger\right) + \frac{c_k}{m_k\omega_k}\int_0^t ds \sin\left[\omega_k (t-s)\right] x(s) \tag{3.32}$$

and hence the eom for the Brownian particle would be

$$m\ddot{x}(t) + \partial_x V(x) - \int_0^t ds \lambda(t-s) x(s) = B(t) \tag{3.33}$$

where $\lambda(t)$ is the dissipation kernel (or also sometimes referred to as the susceptibility function)

$$\lambda(t) = \hbar \sum_k \frac{c_k^2}{m_k\omega_k} \sin\left[\omega_k(t)\right] \tag{3.34}$$

which is nothing more than $\lambda(t) = -\hbar m\dot{\gamma}(t)$. Finally, we comment that using the Leibniz integral rule

$$-\frac{1}{\hbar m}\int_0^t ds \lambda(t-s) x(s) = \frac{d}{dt}\int_0^t ds \gamma(t-s) x(s) - \gamma(0) x(t) \tag{3.35}$$

we could rewrite the eom Eq. (3.33) such that the term $-\gamma(0) x(t)$ would be introduced. One can show then, that had we allowed for the introduction of the counter term in the Hamiltonian, this would exactly cancel this term. This is the equivalent idea of the redefinition of the Gibbs state mentioned before, but expressed at the level of the Hamiltonian.

Ohmic spectral density / Classical limit In the case of an environment with an Ohmic spectral density with an exponential cutoff,

$$J(\omega) = \gamma\omega e^{-\omega/\Lambda} \tag{3.36}$$

in the limit of an infinite cutoff, $\Lambda \to \infty$, we get the damping kernel

$$\gamma(t) = 4\gamma\delta(t) \tag{3.37}$$

such that the Heisenberg equations of motion take the form

$$m\ddot{x}(t) + \partial_x V(x) + 2m\gamma\dot{x}(t) = B(t) \tag{3.38}$$

which is equivalent to the classical stochastic differential equations. In the long time limit and in the high temperature (classical) limit, this eom describes normal Brownian diffusion. One can also evaluate the fluctuation dissipation relation in Eq. (3.27) which will give in the finite cutoff limit Λ

$$\langle B(t) B(0)\rangle = \frac{1}{\pi}\frac{\hbar\gamma\Lambda^2(1-i\Lambda t)^2}{\left[1+(\Lambda t)^2\right]^2} + 2k_B T\gamma\widehat{\delta}(t) \tag{3.39}$$

where

$$\widehat{\delta}(t) = \frac{1}{2\tau_O}\left[\frac{\tau_O^2}{t^2} - \frac{1}{\sinh^2(t/\tau_O)}\right] \tag{3.40}$$

with $\tau_O = \hbar/(\pi k_B T)$ the characteristic time of thermal quantum fluctuations. Notice the dramatic change of quantum thermal correlations, from a delta function at $\hbar \to 0$, to an algebraic decay $\widehat{\delta}(t) \propto t^{-2}$ for finite τ_O and $t \gg \tau_O$. The total integral of $\widehat{\delta}(t)$ is unity, and the total integral of the real part of the $T = 0$ contribution is zero. In the classical limit, $\hbar \to 0$, $\widehat{\delta}(t)$ becomes a delta function. Notice also that the real part of the first complex-valued term in Eq. (3.39), which corresponds to zero-point quantum fluctuations, starts from a positive singularity at the origin $t = 0$ in the classical, white noise limit, $\Lambda \to \infty$, and becomes negative $-\hbar\gamma/(\pi t^2)$ for $t > 0$. Hence, it lacks a characteristic time scale. However, it cancels precisely the same contribution, but with the opposite sign stemming formally from the thermal part in the limit $t >> \tau_O$ at $T \neq 0$. Thus, quantum correlations, which correspond to the Stokes or ohmic friction, decay nearly exponentially for $\Lambda \gg 1/\tau_O$, except for the physically unachievable condition of $T = 0$. Here, we see two profound quantum mechanical features in the quantum operator-valued version of the classical Langevin equation (Eq. (3.38)) with memoryless Stokes friction: First, thermal quantum noise is correlated. Second, zero-point quantum noise is present. This is the reason why quantum Brownian motion would not stop even at absolute zero of temperature $T = 0$.

Sub- and Super- Ohmic spectral densities Any spectral density that follows a power law but is not linearly dependent on the bath frequencies, i.e.

$$J(\omega) \propto \omega^s \tag{3.41}$$

where $s > 0$ but $s \neq 1$, is called a non-Ohmic spectral density. It can be shown that such spectral density leads to anomalous Brownian motion (Weiss, 2012). More specifically, if $s > 1$ then the spectral density is called super-Ohmic and is known to lead to superdiffusion in the high-T/classical limit, while for $0 < s < 1$ the spectral density is called sub-Ohmic and is known to lead in subdiffusion in the high-T/classical limit. In (Paavola *et al.*, 2009), it was shown that the sub-Ohmic spectral density is related with more long lasting memory effect, and hence more long lasting non-Markovian behavior. On the other hand, both super- and sub-Ohmic environments exhibit faster decoherence effects compared to the Ohmic case as shown in (Paavola and Maniscalco, 2010). In (Hu *et al.*, 1992) was shown that a sub-Ohmic environment is more strongly dissipative.

Mass renormalization Another important observation for the work that we will present in the chapters to come is the following. We split the original spectral density in two parts, $J(\omega) = J_{lf}(\omega) + J_{hf}(\omega)$ the low frequency and the high frequency parts

$$\begin{aligned} J_{lf}(\omega) &= J(\omega)\,\Theta(\Lambda - \omega) \\ J_{lf}(\omega) &= J(\omega)\,[1 - \Theta(\Lambda - \omega)] \end{aligned} \tag{3.42}$$

Consider the case that $J(\omega) \propto \omega^s$ with $s > 0, s \neq 1$ and define $\gamma(\omega) := F_\omega(\gamma(t))$ where $F_\omega(\cdot)$ denotes the Fourier transform. We focus first on the high frequency part. At the limit $\omega \ll \Lambda$ which corresponds to the effect of the bath on the Brownian particle at $t \gg \Lambda^{-1}$, one can show that

$$\begin{aligned} \gamma_{hf}(\omega) &\underset{\omega \ll \Lambda}{\longrightarrow} -i\omega\Delta m_{hf}/m \\ \Delta m_{hf} &= \tfrac{2}{\pi}\int_0^\infty d\omega \tfrac{J_{hf}(\omega)}{\omega^3} \end{aligned} \tag{3.43}$$

such that the resulting Langevin equation of motion Eq. (3.22) in Fourier space, could have been obtained if one had just considered a particle with a renormalized mass Δm_{hf}. This holds for any $s > 0, s \neq 1$. In addition, for the low frequency part, for the particular case, $s > 2$, a similar scenario will be obtained. Therefore, one concludes that for $s > 2$, the contribution of the bath effect to the motion of the Brownian particle, is simply the appearance of a polaronic cloud that adds to the inertia of the particle. If on the other hand, $s \leq 2$ then the low-energy excitations of the reservoir have effects beyond simple mass renormalization.

Solution of QGLE

Now let us focus on solving the eom from above for the special cases that we will consider in our work, namely a free Brownian particle, and a Brownian particle that is harmonically trapped, for an arbitrary spectral density $J(\omega)$. At this level, the former can actually be seen as a special case of the latter, where the trapping frequency is set to zero. For a quadratic potential

$$V(x) = \frac{1}{2} m\Omega^2 x^2 \tag{3.44}$$

the Heisenberg equation becomes

$$\ddot{x}(t) + \Omega^2 x + \frac{d}{dt}\int_0^t ds\gamma(t-s)\, x(s) = \frac{1}{m} B(t) \tag{3.45}$$

To solve this equation we introduce the fundamental solutions $G_1(t)$ and $G_2(t)$ of the homogeneous part of the eom, which is obtained by setting the right-hand side equal to zero. These solutions are defined through the initial conditions

$$\begin{aligned} G_1(0) &= 1\,, \quad \dot{G}_1(0) = 0 \\ G_2(0) &= 0\,, \quad \dot{G}_2(0) = 1 \end{aligned} \tag{3.46}$$

Then one can write the Laplace transforms of the fundamental solutions as follows,

$$\begin{aligned} \widehat{G}_1(z) &= \tfrac{z+\widehat{\gamma}(z)}{z^2+\Omega^2+z\widehat{\gamma}(z)} \\ \widehat{G}_2(z) &= \tfrac{1}{z^2+\Omega^2+z\widehat{\gamma}(z)} \end{aligned} \tag{3.47}$$

where $\widehat{(\cdot)}$ denotes the Laplace transform. In terms of the fundamental solutions one can write the general solution of the Heisenberg equation as

$$x(t) = G_1(t)\, x(0) + G_2(t)\, \dot{x}(0) + \frac{1}{m}\int_0^t ds G_2(t-s)\, B(s) \tag{3.48}$$

With the help of this solution all desired mean values, variances and correlation functions of the Brownian particle may be expressed in terms of averages over the initial distribution $\rho(0)$ of the total system. The second Green function, $G_2(t)$ is understood to play the role of the propagator, since is the function that determines how the effect of the noise from previous times propagates to time t.

Covariance matrix

Having the solution of the QGLE at hand, permits us to study a number of other quantities that either can be studied experimentally, or can be used to check whether our approximations are valid. For example, we are now in a position to construct the equal time covariance matrix of the system at the long time limit, and check whether this satisfies the uncertainty principle. If we define the covariance matrix elements $C_{ab}(t,t') =$

$C_{ab}(t-t') := \frac{1}{2}\langle a(t)\, b(t') + b(t')\, a(t)\rangle_{\rho_B}$, (which is defined in the long time limit, such that $C_{ab}(t,t')$ only depends on the time difference $t-t'$) where $a, b \in \{x, p\}$ then by the Heisenberg equations of motion, these are related as

$$\begin{aligned} C_{xp}(t) &= m\frac{dC_{xx}(t)}{dt} \\ C_{px}(t) &= -m\frac{dC_{xx}(t)}{dt} \\ C_{pp}(t) &= -m^2\frac{d^2C_{xx}(t)}{dt^2} \end{aligned} \tag{3.49}$$

such that is enough to have an expression for $C_{xx}(t) = \langle x(t)\, x(0)\rangle_{\rho_B}$. By the definition of $S(t)$, the power spectrum, given in App. A.1.3 then $C_{xx}(t) = S(t)$. In our work we will be interested in the equilibrium correlations, where the state of the system is assumed to not change significantly, which implies that we will be looking in $C_{xx}(0) = S(0)$. From the expression in Eq. (A.27) then, we see that

$$C_{xx}(0) = \int_{-\infty}^{\infty} \frac{d\omega}{2\pi}\hbar\chi''(\omega)\coth(\omega\hbar\beta/2) \tag{3.50}$$

Given the relation between the susceptibility and the Green's propagator in Eq. (A.16) of App. A.1.1, one can show that

$$\chi''(\omega) = \frac{1}{m}\frac{\omega Re\left[\widehat{\gamma}(-i\omega)\right]}{\left(\Omega^2 - \omega^2 + \omega Im\left[\widehat{\gamma}(-i\omega)\right]\right)^2 + \omega^2\left(Re\left[\widehat{\gamma}(-i\omega)\right]\right)^2}. \tag{3.51}$$

In (Lampo *et al.*, 2017a) it is proven that

$$\chi''(\omega) = \widehat{G}(-i\omega)\, J(\omega)\left(\widehat{G}(-i\omega)\right)^{\dagger}. \tag{3.52}$$

Brief overview of Gaussian Quantum Mechanics (GQM) Here we review the formalism of GQM, paying particular attention on the aspects necessary in our work. For more details, the reader is referred to (Adesso and Illuminati, 2007). The main advantage of this formalism is that, avoiding any reference to perturbation theory (Brown *et al.*, 2013) or in fact any other open-systems techniques, GQM allows for a study of interacting systems via a direct system-plus-bath perspective. This is the case because, within GQM, one has access to the exact evolution of the bath in addition to the system.

Consider one or more quantum systems described by bosonic canonical quadrature operators, satisfying the Canonical Commutation Relations (CCRs), $[x_i, p_j] = i\hbar\delta_{ij}$. Assume this quantum system to be a set of n quantum harmonic oscillators. Furthermore, let $X = (x_1, p_1, ..., x_n, p_n)^T$. Due to the CCRs, the phase space is a symplectic space, endowed with the structure $[X_a, X_b] = i\Omega_{ab}$, where Ω_{ab} are the components of the so-called symplectic form, given by

$$\Omega = \oplus_{i=1}^{n}\begin{pmatrix} 0 & 1 \\ -1 & 0 \end{pmatrix} \tag{3.53}$$

The main characteristic of GQM is that one always deals with Gaussian states, that have a particularly easy form to handle. A state of an N-mode system is Gaussian if and only if it is an exponent of a quadratic form in $\{X_a\}_{a=1}^{n}$. A very common and important type of states that fall within this general class are thermal states of quadratic Hamiltonians. The defining and most important feature of Gaussian states is that they are fully characterized by only the first and second moments of their quadratures, i.e., their mean position and their variances in phase space. Without loss of generality, in our works, we will assume the first moments of all the states to be zero, which simplifies significantly our calculations. The state of our system, will thus be simply characterized via the $2n \times 2n$ covariance matrix σ, the entries of which are given by

$$\sigma_{ab} = \langle X_a X_b + X_b X_a \rangle = Tr\left[\rho \left(X_a X_b + X_b X_a\right)\right] \tag{3.54}$$

Within GQM, one can work exclusively in phase space rather than in Hilbert space. Hence partition functions are represented as direct sums rather than tensor products, which simplifies things a lot, namely it allows to easily create ensembles and perform partial traces. As a result, any combined state of two systems A and B in GMQ takes the form

$$\sigma_{AB} = \begin{pmatrix} \sigma_A & \gamma_{AB} \\ \gamma_{AB}^T & \sigma_B \end{pmatrix} \tag{3.55}$$

where σ_A and σ_B are the reduced states of systems A and B respectively, and the matrix γ_{AB} specifies the correlations between the systems. The superscript T denotes transposition.

Furthermore, if the system and bath are acted by a time-dependent Hamiltonian that only contains terms of up to quadratic order in the system and bath observables, then at any later time, the unitarily evolved state of the system and bath will also be Gaussian (Schumaker, 1986). Any such unitary, U, on the Hilbert space corresponds to a linear symplectic transformation on the phase space of quadratures: $X \to U^\dagger X U = SX$, with S satisfying

$$S\Omega S^T = S^T \Omega S = \Omega \tag{3.56}$$

The symplecticity of S, ensures that the CCRs are preserved throughout the change of basis. On the level of the covariance matrix, it is easy to see that this transformation acts as

$$\sigma \to \sigma' = S\sigma S^T \tag{3.57}$$

Finally, Williamson showed that any symmetric positive-definite matrix can be put into a diagonal form via a symplectic transformation. An important use of this result, which amounts physically to a normal mode decomposition, is in finding the so-called symplectic eigenvalues of an arbitrary Gaussian state characterized by a covariance matrix σ. This statement is formalized in the following theorem (Williamson, 1936): Let σ be a $2n \times 2n$

positive-definite matrix. Then there exists a $S \in Sp(2n, R)$ that diagonalises σ such that

$$\sigma = S \oplus_{i=1}^{n} \begin{pmatrix} \nu_i & 0 \\ 0 & \nu_i \end{pmatrix} S^T \tag{3.58}$$

We will make use of this theorem in our work in order to evaluate a quantity called the logarithmic negativity used in Chapter 5, but most importantly to check whether the Uncertainty principle is satisfied. We comment on this below.

Uncertainty principle As already explained, despite the infinite dimension of the associated Hilbert space, the complete description of an arbitrary Gaussian state ρ (up to local unitary operations) is hence given by the $2n \times 2n$ covariance matrix σ. As the real σ contains the complete locally-invariant information on a Gaussian state, it is natural to expect that some constraints exist which have to be obeyed by any bona fide covariance matrix, reflecting in particular the requirement that the associated density matrix ρ in Hilbert space be positive semidefinite. Indeed, such a condition together with the canonical commutation relations imply

$$\sigma + i\Omega \geq 0 \tag{3.59}$$

Given a Gaussian state, the above inequality is the necessary and sufficient condition the matrix σ has to fulfill to describe a physical density matrix ρ (Simon *et al.*, 1987, 1994). More in general, the previous condition is necessary for the covariance matrix of any, generally non-Gaussian, CV state (characterized in principle by nontrivial moments of any order). We note that such a constraint implies $\sigma > 0$. The above inequality is the expression of the uncertainty principle on the canonical operators in its strong, Robertson–Schrodinger form (Robertson, 1929, Schrodinger, 1930, Serafini, 2006). Gaussian states ρ can, of course, be pure or mixed. We can easily define pure and mixed Gaussian states by

$$\det \sigma = \begin{cases} 1 & \Rightarrow pure \\ > 1 & \Rightarrow mixed \end{cases} \tag{3.60}$$

Mean Square displacement

We now focus on the case of a free particle, with the purpose to study the diffusive dynamics of the Brownian particle. This way we can also study directly analogies between the classical and quantum Brownian motion. The first thing to observe is that sending the trapping frequency $\Omega \to 0$ in Eq. (5.59) will lead to a divergence at the limit of low frequencies. This means that the dispersion of the position of the free Brownian particle in thermal equilibrium is infinite. This is a consequence of the fact that the position of a free particle is not bounded. To deal with this, one needs to study the mean square displacement, i.e. $\left\langle [x(t) - x(0)]^2 \right\rangle_{\rho(t)}$ and hence one needs to subtract the initial position

of the particle $x(0)$. From the solution of the QGLE from the previous subsection, one can obtain an expression for the mean square displacement of the quantum Brownian particle $\left\langle [x(t) - x(0)]^2 \right\rangle_{\rho(t)}$. At this point, we make again the assumption of a factorizing initial state $\rho(t) = \rho_s(0) \otimes \rho_B$, as was the case for the Born approximation. We discuss below consequences related to this assumption. This implies then that averages of the form

$$\langle \dot{x}(0) B(s) \rangle = 0 \tag{3.61}$$

vanish. Hence

$$\left\langle [x(t) - x(0)]^2 \right\rangle = G_2^2(t) \left\langle \dot{x}^2(0) \right\rangle + \int_0^t ds \int_0^t d\sigma G_2(t-s) G_2(t-\sigma) \langle \{B(s), B(\sigma)\} \rangle \tag{3.62}$$

where one can show using the FDT that

$$\langle \{B(s), B(\sigma)\} \rangle = 2\hbar\lambda(s-\sigma) \tag{3.63}$$

There is an alternative way to obtain an expression of the MSD given in terms of the response function $\chi(t)$ which is related to the position of the Brownian particle through the Kubo formula for the position of the Brownian particle

$$\chi_{ji}(t,t') = i\Theta(t-t') \langle [x_i(t), x_j(t')] \rangle . \tag{3.64}$$

For this, one needs first to define the quantities

$$\begin{aligned} C^+(t) &= \langle x(t) x(0) \rangle - \langle x(t) \rangle_{\rho_B} \langle x(0) \rangle \\ C^-(t) &= \langle x(0) x(t) \rangle - \langle x(0) \rangle_{\rho_B} \langle x(t) \rangle \end{aligned} \tag{3.65}$$

where $C^+(t) = (C^-(t))^*$ such that

$$C^{\pm}(t) = S(t) \pm iA(t) \tag{3.66}$$

with $S(t)$ the symmetric part of $C^{\pm}(t)$ i.e. $S(t) = S(-t)$, given explicitly in App. A.1.3 and is related to the imaginary of the response function by

$$\hbar\chi''(\omega) \coth(\beta\hbar\omega/2) = S(\omega) \tag{3.67}$$

while

$$\chi(t) = -\frac{2}{\hbar}\Theta(t) A(t) , \tag{3.68}$$

such that $A(t)$, the antisymmetric part of $C^{\pm}(t)$, i.e. $A(t) = -A(-t)$ is given by the noise kernel $A(t) = -\lambda(t)$.

With these in mind, the MSD is shown to be given by

$$\left\langle [x(t) - x(0)]^2 \right\rangle = 2(S(0) - S(t)) \tag{3.69}$$

where upon using Eq. (3.67), we obtain

$$\left\langle \left[x\left(t\right)-x\left(0\right)\right]^{2}\right\rangle =\frac{\hbar}{\pi}\int_{-\infty}^{\infty}d\omega\chi''\left(\omega\right)\coth\left(\omega\hbar\beta/2\right)\left[1-\cos\left(\omega t\right)\right]. \tag{3.70}$$

One can then proceed further and having in mind that

$$\chi\left(t\right)=\Theta\left(t\right)\frac{1}{\pi}\int_{-\infty}^{\infty}d\omega\chi''\left(\omega\right)\sin\left(\omega t\right), \tag{3.71}$$

one can derive the following relation in the long time limit,

$$\lim_{t\to\infty}\frac{1}{\chi\left(t\right)}\frac{d\left\langle \left[x\left(t\right)-x\left(0\right)\right]^{2}\right\rangle }{dt}=2k_{B}T. \tag{3.72}$$

This relation is a version of the Einstein relation. It is also interesting to note that in the derivation of it no specific assumptions on $\chi\left(t\right)$ were made.

In deriving this second expression for the MSD, one had to make the assumption of time translation invariance of the equilibrium autocorrelations,

$$\left\langle x\left(t\right)x\left(t'\right)\right\rangle =\left\langle x\left(t-t'\right)x\left(0\right)\right\rangle \tag{3.73}$$

which holds in the long time limit, when the system is already independent of the initial conditions. This condition was not made in Eq. (3.62), which in fact can lead to problems in some cases, as we will see later on.

Free Brownian motion with an Ohmic spectral density If we assume that the Brownian particle is untrapped and that the bath is characterized by an Ohmic spectral density $J\left(\omega\right)=\gamma\omega$, then the Green functions read as following

$$G_{1}\left(t\right)=1\ ,\ G_{2}\left(t\right)=\frac{1}{\gamma}\left(1-e^{-\gamma t}\right) \tag{3.74}$$

Then by making use of the relation $\chi\left(t\right)=\Theta\left(t\right)G_{2}\left(t\right)/m$, (see App. A.1.1) then one can perform the integral in Eq. (3.70) (making use of the Matsubara frequency representation of the coth function) and after taking the high temperature limit, one obtains

$$\left\langle \left[x\left(t\right)-x\left(0\right)\right]^{2}\right\rangle =\frac{2}{m\beta\gamma^{2}}\left(\gamma t-1+e^{-\gamma t}\right) \tag{3.75}$$

which is the same expression obtained for the classical BM in Eq. (2.10). This allows us to conclude that the classical results of normal Brownian motion are recovered for an ohmic spectral density and in the high T limit.

Correlation free initial state preparation Let us assume the initial density matrix for system plus bath to be of the factorized form, with the bath initially being at canonical equilibrium at a certain temperature. As discussed in (Anglin *et al.*, 1997) such factorization will not yield a correct description of decoherence, nevertheless it helps us significantly reduce the complexity of the system and allow us in certain cases to obtain analytical results that will be correct even if the decoherence process is not accurately described.

It is essential to remember, that even though the equations themselves are written only for operators of the open system, these operators are still defined in the Hilbert space of the whole system (system + bath). This implies that both classical and quantum noises should coexist in the equation. As a result, the standard way to treat the system, without making the unnatural correlation free approximation, is through the Feynman-Vermon path integral approach. This was first studied in the work of Grabert et al. (Grabert *et al.*, 1988) which indeed included the initial preparation in his studies. Path integral approaches are however much more difficult to treat analytically, and in some cases one can show that resorting to the QGLE approach, where the correlation free initial state preparation assumption is made, can already give experimentally relevant results.

As already stated such assumption is widely accepted and used in the literature for many applications of the QBM and we refer here to some examples. For instance, for harmonic systems, the approach just described, i.e. of a separable initial density matrix, has been used extensively in the past for heat transport (Dhar, 2008), and it was shown to be fully equivalent to the method based on non-equilibrium Green's functions (Ozpineci and Ciraci, 2001, Wang *et al.*, 2006, Galperin *et al.*, 2007), which is assumed to give experimentally relevant results. In this case, the scheme of the QLE is extended to the nonequilibrium case with the system attached to two baths of different temperature (Zürcher and Talkner, 1990). More recent applications address the problem of the thermal conductance through molecular wires that are coupled to leads of different temperature. Then the heat current assumes a form similar to the Landauer formula for electronic transport: The heat current is given in terms of a transmission factor times the difference of corresponding Bose functions (Segal *et al.*, 2003).

Problems with QGLE

Initial slip or spurious term It is important to note that the form of the Generalized Langevin equation derived above, does not comply with the form of an ordinary generalized Langevin equation: it now contains an inhomogeneous term $\gamma(t)x(0)$, the initial slip term (Ingold, 2002, Hänggi, 1997). This term is often neglected in the so-called "Markovian limit", when the friction kernel at times much larger than the relaxation time of the bath, assumes the ohmic form $\gamma(t) \to 4\gamma\delta(t)$. Nevertheless, this will affect the trajectory

of the phase point, in particular it can introduce instabilities in the solution of the system, as if one had considered a non-positive Hamiltonian. This point is important for the work that we will present, and we take particular care to assure that ignoring such a term does not introduce any unphysical consequences. In general, for the purposes of physical applications, this fine detail can be put aside, but not mathematically, since the universality of the Langevin equation would not be guaranteed in the quantum regime (Ford and Kac, 1987). By universal it is meant that many physical problems satisfy an equation whose form shall be equal for all. It is worth noting that such phenomenon also appears in the study of classical random processes as is shown in (Haake and Lewenstein, 1983), and in studies of adiabatic elimination of the fast variables in stochastic processes (Haake, 1982, Haake *et al.*, 1985).

Initial jolts In Eq. (3.75), we derived an expression for the MSD for the Ohmic case, but using as a starting point the MSD in Eq. (3.70). Had we used the MSD in Eq. (3.62), where the assumption of long time is avoided, Eq. (3.73), and hence the dependence of the MSD on the initial condition remains, we would encounter a problem. In particular, in deriving this MSD, we had to resort also to the unphysical condition of a factorized initial state, and since we don't make the long time limit assumption, this has consequences on the range of validity of the results in time. In particular, the MSD in this way can only be studied for times $t \gg \Lambda^{-1}$, where Λ is the cutoff. If then one tries to send $\Lambda \to \infty$ will not resolve the problem. This is because the factorized initial state, results also to the appearance of the so called initial jolts (peaks) of amplitude $\propto \Lambda$ in the mean energy of the system (Hu *et al.*, 1992, Paz *et al.*, 1993), the decaying factor (Lombardo and Villar, 2007), and the normal diffusion coefficient (Fleming *et al.*, 2011), which lead to divergences in the MSD if the cutoff is send to infinity, which is unphysical since the cutoff should play no role in the dynamics of the system. These peaks can produce a fast diagonalization of the reduced density matrix, i.e. decoherence. From the physical point of view this divergence means that the central particle can absorb an arbitrary amount of energy and can travel an arbitrary distance within a finite time interval. To avoid this initial jolts, one should consider more physical initial conditions such as in (Grabert *et al.*, 1988, Hakim and Ambegaokar, 1985). There is assumed that the system and environment are at equilibrium and at a given time $t = 0$ one performs an imperfect measurement of the system retaining part of the pre-existing correlations. In conclusion, if one tries to compute the decoherence time scale for low temperatures or non-Ohmic environments, it is necessary to take into account the existence of initial correlations or to discount the effect produced by the initial jolt caused by the absence of initial correlations.

Further studies on the effect of the effect of the factorized initial state assumption for different forms of the spectral density, have shown that super-Ohmic environments exhibit

much stronger initial jolts, than there subohmic counterparts (Paavola *et al.*, 2009). Not only this, but for the super-Ohmic environment, in the zero temperature limit, the decay rates show a strong initial jolt for all the values of r, and appear at much longer timescales (Hu *et al.*, 1992). Moreover, the decoherence timescale for the subohmic case at strictly zero temperature is shorter than the corresponding Ohmic case. Furthermore, it was also observed in (Lombardo and Villar, 2007), that the subohmic environment is very efficient in inducing decoherence on the quantum test particle not only at high temperature but at strictly zero temperature as well.

Further criticism and limitations of QGLE The application of the QLE bears some subtleties and pitfalls which must be observed when making approximations. For example, an important feature of QLE that one should have in mind is the following: Since the QLE is an operator equation that acts in the full Hilbert space of system and bath, the coupling between system and environment also implies an entanglement upon time evolution even for the case of an initially factorizing full density matrix. Then, together with the commutator property of quantum Brownian motion, one finds that the reduced, dissipative dynamics of the position operator $q(t)$ and momentum operator $p(t)$ should obey the Heisenberg uncertainty relation for all times (Hanggi *et al.*, 2005, Lampo *et al.*, 2017a). This is a condition that should always be satisfied, and has certain consequences on the approximations that we can do to our system.

For example, one should be careful when making usage of a quasiclassical c-number Langevin equation. In this approximation, the non Markovian (colored) Gaussian quantum noise with real valued correlation $S(t) = S(-t)$ is substituted by a classical non-Markovian Gaussian noise force which identically obeys the correlation properties of (Gaussian) quantum noise $B(t)$. An approximation of this type clearly would not satisfy the commutator property for position and conjugate momentum of the system degrees of freedom for all times and all system parameters. Such schemes work at best near a quasiclassical limit (Schmid, 1982, Eckern *et al.*, 1990), but even then care must be exercised. For example, for problems that exhibit an exponential sensitivity, as for instance the dissipative decay of a metastable state, such an approach will not give an exact agreement with the quantum dissipative theory (Hänggi *et al.*, 1990, Weiss, 2012). It is only in the classical high temperature limit, where the commutator structure of quantum mechanics no longer influences the result. Perfect agreement is only achieved in the classical limit.

In our work, we avoid making use of such quasiclassical Langevin equations. However, motivated by the classical intuition from the previous chapter, i.e. that the bath is hardly affected by the motion of the BP, we make the assumption that the state of the bath is not affected by the evolution of the state of the system, i.e. the bath is always at a thermal state. Although this is not shown to result in any violation of the Heisenberg

uncertainty principle for a single Brownian particle, we find that this can be the case for two Brownian particles immersed in a common or different bath of harmonic oscillators. For this reason, we explicitly check in our work that this condition indeed is satisfied for the parameters considered. The reason for this might be attributed to the fact that by assuming that the state of the bath remains unaffected during the evolution of the composite system+bath, one affects the entanglement between the system and the bath, which can result in violations of the Heisenberg uncertainty principle.

A further limitation of QLE, is that the results of this approach are reliable only when the anharmonic part of the potential can be treated as a perturbation. On this level of approximation, the squeezing of thermal and quantum fluctuations by time-dependent external forces has been studied in (Svensmark and Flensberg, 1993). For a discussion of the validity of the QLE for anharmonic potentials we refer to (Schmid, 1982) and (Eckern *et al.*, 1990). Finally, let us mention that another problem of this Langevin approach to the quantum dynamics, has the additional problem of not admitting simple recipes (as those in the classical case), to convert this Langevin equation into an equation for the distribution (Fokker-Planck like), as is the case in the classical regime.

Revisiting the problems of the classical Langevin equation within the QGLE approach

Now we are in a position permitting to address the two objections related to the classical version of BM:

• First, let us tackle the time-reversal objection due to Loschmidt. It is clear that the Heisenberg equations are reversible. However, the quantum generalized Langevin equation is completely equivalent to them, so the evolution of the system described by these is also reversible. What happens is that one thinks of reversing the velocity of the central particle only, and not those of the bath particles. Therefore, we have a "practical" irreversibility, in the sense that although the whole system+bath is reversible, we cannot change the sign of the velocities of all degrees of freedom, because we have in practice little control on the bath degrees of freedom.

• Second, Zermelo's paradox. The fact that both the effective equations (and the experiments) show that the pollen grains are never brought back together, is just a consequence of the total phase space being very large. Again, we cannot overlook the bath. If one estimates the recurrence time, he will find that it diverges with the number of bath oscillators tending to infinity (Schwabl, 2002, Greiner, 2009). However, if finite "baths" are considered this recurrence time will remain finite. However, in practice, this time can be several times the estimated age of the universe, and as a result, for all practical purposes, we can be sure that the central BP will never return to the initial configuration.

Problem of quantization in the QGLE approach We have just seen how to handle the irreversibility problem. Let us move on to the issue of quantizing a system with Langevin dynamics. The idea is to consider the Hamiltonian as the problem to be quantized. Then we would just need to transform the variables (x, p) and (x_k, p_k) into Hilbert operators and replace Poisson brackets $\{,\}$ by commutators $[,]$. This is how one derives quantum Langevin equations (Ford *et al.*, 1988). However, these are not as useful/generic as their classical counterparts; now both x and the force $f(t)$ are operators, and calculations to-the-end exist only in simple cases (Hanggi *et al.*, 2005, Stockburger, 2003).

3.4 Summary

The main content of this Chapter can be summarized in the following:

- Classical Brownian motion faces the problems of irreversibility, is at odds with Poincare's theorem, is not quantizable and contradicts with Heisenberg uncertainty principle. For this reason it fails to describe quantum phenomena such as decoherence and quantum tunneling, very important in describing transport at the nano- and micro-scale. For these reasons a quantum version of Brownian motion was necessary.

- Caldeira and Leggett proposed a Hamiltonian approach to Brownian motion, which directly enables the promotion of the physics to the quantum regime. The main approximation that goes in this approach is that the interaction Hamiltonian depends linearly on the bath's operators.

- We examined various approaches that enable one to study the dynamics of such a quantum Brownian particle emerging from the aforementioned Hamiltonian, which allow the study of phenomena like decoherence and dissipation.

- The first of these approaches, is the quantum master equation approach, in which one studies the evolution of the density matrix, in direct analogy to the study of the evolution of the probability distribution in the classical world. In this case one usually resorts to the so called Born-Markov approximation, namely that the density matrix of the composite remains a tensor product during the whole time of the evolution. This results in density matrices that can become non-positive during their evolution.

- The second approach, in analogy to the classical case again, involves the study of the evolution of the operators of the Brownian particle, such as the position and the momentum. This led to a direct quantum version of the classical Langevin equation, in Eq. 3.22. Since this is the method that will be used in the rest of this thesis,

a good part of this chapter was devoted in the presentation of the analytical tools appearing in this approach, as well as the assumptions and limitations of it. We saw that this eom can be solved in Eq. 3.48. Furthermore, we examined the connection between spectral densities and diffusion behaviour by studying the MSD, in Eq. 3.62, which allowed us to see how the classical Langevin equation can be recovered from this.

- Finally, we reviewed the problems of the classical Brownian motion under the prism of the presented formalism, and saw how these are circumvented in the quantum/Hamiltonian version of it.

CHAPTER 4

ONE-DIMENSIONAL BOSE EINSTEIN CONDENSATES AND THE BOSE POLARON PROBLEM

After the original work of Brown, studying pollen grains in water, Brownian motion was observed in a number of different settings, ranging from biological systems, such as receptors moving on the membrane of a cell, to stock price evolution. In this thesis, taking advantage of the results in (Lampo *et al.*, 2017a, 2018), we study Brownian motion of impurities in ultracold gases, in particular Bose Einstein Condensates (BEC). Hence before proceeding to present our results, a review of the basics of the theory of BEC is presented, and a special emphasis is given on Bose polarons.

We begin with a short historical review of the major developments regarding BEC and we proceed with a presentation of the main characteristics that define interacting BEC. The Hamiltonian of weakly interacting BEC together with the major assumptions that go in it are discussed. Special attention is given to the Bogoliubov transformation, that is a tool extensively used in our work, that permits us to study Bose polarons as Brownian particles. We close this section with the major assumptions and effects that go in considering trapped and 1D BECs.

In Section 3, we motivate the study of Bose polarons, giving a summary of the most important achievements in this direction. We then define Bose polarons more rigorously,

and hence we comment on the distinction between small and large polarons. In our work we focus on the latter. With these concepts in mind we present the Frohlich Hamiltonian, which is the Hamiltonian that describes impurities in a bath of bosons that are weakly interacting. This is the Hamiltonian that will describe the Bose polarons that we will study as well, and which by further making the dipole approximation will lead to the Bose polarons being described as Quantum Brownian particle (QBP). Finally, we explain in more detail the connection of the Frohlich Hamiltonian to the Caldeira-Leggett model.

4.1 Bose Einstein Condensates

4.1.1 Definition, historical development and state of the art

What is a Bose Einstein Condensate?

One of the most important successes of Quantum mechanics, and in fact what initially attracted interest to it, is the fact that it can give an explanation of the phenomenon of the wave-particle duality of matter and electromagnetic radiation. The theoretical explanation of this came only in 1924 thanks to de Broglie (de Broglie, 1925), who showed that a particle with momentum, whose modulus is p, is associated with a wave of wavelength $\lambda_T = 2\pi\hbar/p$, known as de Broglie wavelength. Soon after, the first ideas of Bose Einstein condensation (BEC) appeared in 1925 when A. Einstein expanded the ideas of S.N Bose about the quantum statistics of light quanta (now called photons) (Bose, 1924). Einstein considered a non-interacting system of massive bosons and he established that below a certain critical temperature, a large finite fraction of bosons would occupy the lowest energy single-particle state (Einstein, 1925).

The intuition behind Einstein's ideas goes as following. If one considers a gas at temperature T, by using the Maxwell-Boltzmann distribution, one can calculate the average momentum per particle $\langle p \rangle \sim \sqrt{mk_BT}$, where m is the mass of the particle and k_B is the Boltzmann constant. Therefore, one can rewrite the de Broglie wavelength as a function of temperature $\lambda_T \sim \sqrt{\hbar^2/(mk_BT)}$, also called thermal wavelength. In a quantum many-body system, it will indeed be the case that T will be larger than the average interparticle distance $n\lambda_T^3 \geq 1$ (in 3D), where $n = N/V$ is the density of the many-body system with N particles in a volume V. Therefore the wavepackets that one can associate to each one of these particles, will necessarily overlap. Such condition can be reached in either high-density systems or for large $\lambda_T \sim \sqrt{1/mT}$ corresponding to small particle mass m or at very low temperature. In both cases, particles are very slow, they lose their identity and they move all together as a giant matter wave. In fact, similarly to waves, particles interfere, and in particular, bosons interfere constructively. At a temperature below a critical value, which increases with n and depends on m, one can observe Bose-Einstein condensation in the many-body system. In this case, a non-zero fraction of the total number of bosons would occupy the lowest-energy single-particle state. In practice, this

implies the following. The mean occupation number of a state s of the system, with energy ϵ_s, for a homogeneous and non-interacting Bose gas, is given by the Bose-Einstein distribution function,

$$n_s\left(\epsilon_s\right) = \frac{1}{e^{(\epsilon_s-\mu)/k_BT}-1} \tag{4.1}$$

where μ, is the chemical potential. Furthermore, for the distribution $n_s\left(\epsilon_s\right)$ to be positive for all states, we assume $\mu < \epsilon_0$, where ϵ_0 is the ground state energy. Then when μ approaches ϵ_0 from smaller values, the occupation number n_0 becomes increasingly large, while it acquires a maximum for all the other states. If n_{max} , the maximum number of excited states, is smaller than n, the total number of particles, the occupation number n_0 of the ground state is substantial and thus it is expected the condensate is formed. One can then talk about a critical number of particles n_c that this happens given a temperature T, or a critical temperature T_c that this happens given the number of particles n. This is the physical picture behind Bose-Einstein condensation.

A number of properties of the Bose gas can alter the above simplified picture. For example the dimensionality of the system. It is known that, one does not expect to see condensation in 1D and 2D (we will focus explicitly on the 1D case in the works that will be presented in this thesis). Furthermore, whether the BEC is trapped or not also plays an important role on the critical temperature of the BEC, because this, introduces finite size effects on the BEC, i.e. away from the thermodynamic limit. Finally, one can then also consider extensions of the phenomenon of condensation for the case of interacting gases. This was studied later on, by Bogoliubov, who developed the first microscopic approach in order to describe an interacting Bose gas (Bogolyubov, 1947), which we will review in more detail in the next section.

Brief historical overview The critical temperature predicted at the time of Einstein (for the number of atoms they could isolate), was far beyond the reach of the experiments. Furthermore, this prediction was done for an ideal gas, without considering interactions, and thus without taking into account the rather probable solidification of the gas (Claude and David, 2011). For this reason it was not until after a few decades when the first attempts to experimentally realize a BEC took place. This was because in the next decades new cooling methods became available. The most important ones were laser cooling (also called cooling by magneto-optical traps (Raab *et al.*, 1987)) and evaporative cooling. Nowadays, BECs can be produced in a much more convenient way on the so-called atom chips (Ott *et al.*, 2001, Schneider *et al.*, 2003, Groth *et al.*, 2004). These are micro-fabricated chips with wires that allow the generation and precise control of magnetic fields. With these fields it is possible to trap and cool atoms. The experimental

accuracy and control achieved in these set-ups, allows many interesting experiments and applications.

Current research and applications

One of the most important recent development in the field of BECs, is the condensation of atoms with high magnetic moment, as for example chromium, dysprosium or erbium. Besides the usual contact atom-atom interaction, these atoms interact through considerable magnetic dipole-dipole interactions as well. This interaction has two major differences with respect to the usual contact interactions. Firstly, it is a long range interaction. Secondly, it is anisotropic. That is, two parallel dipoles repel each other whereas two dipoles oriented head-to-tail attract each other. In addition, this interaction can be tuned using rotating polarizing fields (Giovanazzi *et al.*, 2002). For a recent review on dipolar gases the reader is referred to (Lahaye *et al.*, 2009).

Furthermore, with the development of optical traps as a means of trapping atoms, the possibility of trapping different internal states of the same atoms was offered. This allowed studies with spinor condensates (Ho, 1998, Ohmi and Machida, 1998, Stenger *et al.*, 1998), where more than one hyperfine states are condensed. An important property of these systems, is that the number of particles in each component is not necessarily conserved. This can be a consequence of the presence of spin changing collisions or dipole-dipole interactions, which can couple the different internal states. Another relevant development along these lines, was the creation of mixtures of BECs (Pu and Bigelow, 1998), where different species rather than hyperfine states are condensed. In a binary mixture for example, the two species can be two different elements (Modugno *et al.*, 2002), two different isotopes (Bloch *et al.*, 2001) or two different internal states of the same isotope (Myatt *et al.*, 1997).

After the first realization of BEC, the field of cold atom physics, has been steadily expanding, and it has become an interdisciplinary branch of physics, relating statistical mechanics, atomic physics, photonics, solid state physics, nonlinear physics, condensed matter physics, and high energy physics.

4.1.2 Interacting BEC

In our definition of a BEC above, we restricted ourselves to the case of an ideal Bose gas, which even in the absence of interactions exhibits a purely quantum-statistical phase transition to BEC. However, in reality particles will always interact, and even in the weakly interacting limit a real Bose gas behaves qualitatively differently from an ideal Bose gas. Interactions between atoms will modify the equilibrium shape and dynamics of the condensate. In the rest of this thesis, we focus on the weakly interacting limit, which we define in the next subsection.

BEC standard assumptions Here we discuss the assumptions that go in the definition of a weakly interacting BEC. Diluteness and low temperatures are the main features of these cold gases.

Diluteness:

In a dilute gas, the range of the inter-particle forces, r_0, is much smaller than the average distance d between particles:

$$r_0 \ll d = n^{-1/3} = \left(\frac{N}{V}\right)^{-1/3} \tag{4.2}$$

The interaction between particles is non-zero only when the two particles are separated within the characteristic distance r_0. For a two-body scattering potential $Q(r)$ the Fourier transform is written as

$$Q\left(p\right) = \int Q\left(r\right) e^{-ip\cdot r/\hbar} dr \tag{4.3}$$

and the scattering amplitude $Q(p)$ is independent of the momentum p as far as $p \ll \hbar/r_0$. $Q(p)$ rolls off when p becomes large compared to $\hbar/r_0$. The condition in Eq. (4.2) allows one to consider only two-body interaction; configurations with three or more particles interacting simultaneously can be safely neglected. If this approximation is valid, such a system is called a dilute gas. A second important consequence of the condition in Eq. (4.2) is that the use of the asymptotic expression for the wavefunction of their relative motion is justified when the scattering amplitude is evaluated and that all the properties of the system can be expressed in terms of a single parameter, called a scattering length. The scattering amplitude is safely approximated by its low-energy value $Q_0 = \int Q\left(r\right) dr$, where assuming that characteristic radius of interaction is much smaller than the scattering length and the de Broglie wavelength (Born approximation), which is true for most cases, one can approximate the potential by a point-like so-called contact potential $Q\left(r\right) = Q_0 \delta\left(r\right)$, where Q_0 is determined by the s-wave scattering length a_B through (Pitaevskii and Stringari, 2016):

$$Q_0 = \frac{4\pi\hbar^2}{m} a_B \tag{4.4}$$

In conclusion, the s-wave scattering length a_B characterizes all the interaction effects of the dilute and cold gas. The diluteness condition in terms of the scattering length is summarized by

$$\left|a_B\right| n^{1/3} \ll 1 \tag{4.5}$$

which should always be satisfied in order to apply the perturbation theory of Bogoliubov. This assumption is also necessary to be able to use mean-field theories as suitable theoretical descriptions of the BEC. On the contrary, if the diluteness condition is not satisfied, the system is no longer weakly interacting and other tools must be used, e.g beyond mean-field techniques or quantum Monte-Carlo methods. Furthermore, note that a positive scattering length, which implies a repulsive mean field Q_0, limits the density of the BEC, which is crucial for its stability. On the contrary, a negative mean-field energy resulting from a negative scattering length leads to a strong increase in density. Consequently, the BEC collapses above a certain atom number, when the zero-point energy can no longer balance the attractive mean field interaction. In this thesis, we restrict ourselves to considering positive scattering lengths.

Low temperatures:

As explained above, BEC is achieved for temperatures lower than a critical temperature, which for a 3D untrapped ideal gas at the thermodynamic limit reads as $k_B T_c = \frac{2\pi\hbar^2}{m}\left(\frac{n}{2.612}\right)^{2/3}$ (Pitaevskii and Stringari, 2016). Therefore one should determine such a critical temperature depending on the particular case at hand, trapped or untrapped, interacting or ideal BEC studied at the thermodynamic limit or at a finite size. In fact, this critical temperature as was briefly explained at the beginning, comes from the requirement that the thermal de Broglie wavelength λ_T for massive particles must be on the order of the interparticle distance $n\lambda_T^3 \sim 1$.

Feshbach resonances BEC dynamics is strongly affected by atom-atom interactions which make atomic condensates an interesting system for many-body physics and nonlinear atom optics. The effective atom-atom interactions are determined by the scattering properties of atoms. The scattering properties are adjustable with external magnetic field. Since an atom has a magnetic moment and consequently the energy levels of the molecular states of two colliding atoms depend on a magnetic field, a scattering resonance happens when the energy of the bound molecular state crosses zero (Cornish and Cassettari, 2003). At this moment the effective scattering length diverges. This is called Feshbach resonance (Inouye *et al.*, 1998), which gives a substantial freedom to atomic systems with quantum degenerate gases: an experimental knob for tuning atom-atom interactions.

4.1.3 Hamiltonian of the weakly interacting Bose gas

The Hamiltonian of the system is expressed in terms of the field operators $\widehat{\psi}$:

$$H = \int \left(\frac{\hbar^2}{2m} \nabla \widehat{\psi}^\dagger (\mathbf{x}) \nabla \widehat{\psi} (\mathbf{x}) \right) d\mathbf{x} + \frac{1}{2} \int \widehat{\psi}^\dagger (\mathbf{x}) \widehat{\psi}^\dagger (\mathbf{x}') Q (\mathbf{x} - \mathbf{x}') \widehat{\psi} (\mathbf{x}) \widehat{\psi} (\mathbf{x}') d\mathbf{x} d\mathbf{x}' \quad (4.6)$$

where $Q(\mathbf{x}-\mathbf{x}')$ is the two-body scattering potential. For a uniform gas occupying a volume V, the field operator $\widehat{\psi}$ can be expanded by the plane waves:

$$\widehat{\psi}(\mathbf{x}) = \frac{1}{\sqrt{V}} \sum_{\mathbf{p}} \widehat{a}_{\mathbf{p}} e^{i\mathbf{p}\cdot\mathbf{x}/\hbar} \tag{4.7}$$

where $\widehat{a}_{\mathbf{p}}$ is the annihilation operator for a single particle state of a plane wave with momentum $\mathbf{p}$. By substituting (4.7) into (4.6), one obtains

$$H = \sum_{\mathbf{p}} \frac{\mathbf{p}^2}{2m} \widehat{a}^{\dagger}_{\mathbf{p}} \widehat{a}_{\mathbf{p}} + \frac{1}{2V} \sum_{\mathbf{p}_1,\mathbf{p}_2,\mathbf{q}} Q_{\mathbf{q}} \widehat{a}^{\dagger}_{\mathbf{p}_1+\mathbf{q}} \widehat{a}^{\dagger}_{\mathbf{p}_2-\mathbf{q}} \widehat{a}_{\mathbf{p}_1} \widehat{a}_{\mathbf{p}_2} \tag{4.8}$$

Here $Q_{\mathbf{q}} = \int Q(\mathbf{r})\, e^{-i\mathbf{q}\cdot\mathbf{r}} d\mathbf{r}$ is the Fourier transform of the two-body scattering potential. In real systems $Q(\mathbf{r})$ always contains a short-range term, which makes it difficult to solve the Schrödinger equation at the microscopic level. However, in virtue of the above assumptions on the dilute and cold gases, one can conclude that the actual form of $Q(\mathbf{r})$ is not important for describing the macroscopic properties of the gas, as far as the assumed fictitious potential $Q_{eff}(\mathbf{r})$ gives the correct value for the low momentum value of its Fourier transform $Q_{\mathbf{q}\ll\hbar/\mathbf{r}_0}$. It is therefore convenient to replace the actual potential $Q(\mathbf{r})$ with an effective, smooth potential $Q_{eff}(\mathbf{r})$. Since the macroscopic properties of the system depend on $Q_{q=0} = Q_0 = \int Q_{eff}(\mathbf{r})\, d\mathbf{r}$ (or the s-wave scattering length a_B), this procedure will provide the correct answer to this complicated many-body problem as far as the system is dilute and cold.

After rewriting the Hamiltonian taking into account the assumption mentioned above, one can then make the following crucial substitution in order to implement the Bogoliubov approximation, namely $\widehat{a}_0 \to \sqrt{N_0}$. For an ideal Bose gas at zero temperature the occupation number for $\mathbf{p} \neq 0$ vanishes because all the atoms are in the condensed state $N_0 = N_{tot.}$. In a dilute gas the occupation number for states with $\mathbf{p} \neq 0$ is finite but small. To lowest order, it is valid to neglect all the terms in the Hamiltonian containing terms with $\mathbf{p} \neq 0$ and therefore $\widehat{a}_0 \equiv \sqrt{N_0} = \sqrt{N}$. Within these approximations the ground-state energy is given by

$$E_0 = \frac{nN}{2} Q_0 \tag{4.9}$$

By computing the total pressure for the interacting gas one obtains $P \equiv -\partial E_0/\partial V = \frac{n^2}{2} Q_0$, which does not vanish at zero temperature in contrast with the non-interacting Bose gas. By computing the compressibility of the gas one obtains $\kappa = \partial n/\partial P = 1/Q_0 n$. Thermodynamic stability requires that $\kappa > 0$ and therefore a weakly interacting Bose gas is stable if $Q_0 > 0$ (repulsive interactions). The ground-state energy in Eq. (4.9) has been derived within the lowest-order mean-field approach. A higher-order approximation

scheme can be used where quantum fluctuations are included. To achieve this, one should abide to the following changes. First, one should consider splitting the $\widehat{a}_0$ from the $\widehat{a}_{\mathbf{p}}$ terms in the interaction part of the Hamiltonian which after some redefinition of the summation parameters, will result in:

$$H = \sum_{\mathbf{p}} \frac{\mathbf{p}^2}{2m} \widehat{a}_{\mathbf{p}}^{\dagger} \widehat{a}_{\mathbf{p}} + \frac{Q_0}{2V} \widehat{a}_0^{\dagger} \widehat{a}_0^{\dagger} \widehat{a}_0 \widehat{a}_0 + \frac{Q_0}{2V} \sum_{\mathbf{p} \neq 0} 4 \widehat{a}_0^{\dagger} \widehat{a}_{\mathbf{p}}^{\dagger} \widehat{a}_0 \widehat{a}_{\mathbf{p}} + \widehat{a}_{\mathbf{p}}^{\dagger} \widehat{a}_{-\mathbf{p}}^{\dagger} \widehat{a}_0 \widehat{a}_0 + \widehat{a}_0^{\dagger} \widehat{a}_0^{\dagger} \widehat{a}_{\mathbf{p}} \widehat{a}_{-\mathbf{p}} \quad (4.10)$$

One can then replace $\widehat{a}_0 \to \sqrt{N}$ as before, but for the second term of the Hamiltonian, one needs to use the normalization relation

$$\widehat{a}_0^{\dagger} \widehat{a}_0 + \sum_{\mathbf{p} \neq 0} \widehat{a}_{\mathbf{p}}^{\dagger} \widehat{a}_{\mathbf{p}} = N_{tot.} \quad (4.11)$$

which leads to $\widehat{a}_0^{\dagger} \widehat{a}_0^{\dagger} \widehat{a}_0 \widehat{a}_0 = N_{tot.}^2 - 2N_{tot.} \sum_{\mathbf{p} \neq 0} \widehat{a}_{\mathbf{p}}^{\dagger} \widehat{a}_{\mathbf{p}}$ and the Hamiltonian then reads as

$$H = \frac{nN}{2} Q_0 + \sum_{\mathbf{p}} \frac{\mathbf{p}^2}{2m} \widehat{a}_{\mathbf{p}}^{\dagger} \widehat{a}_{\mathbf{p}} + \frac{n}{2} Q_0 \sum_{\mathbf{p} \neq 0} 2 \widehat{a}_{\mathbf{p}}^{\dagger} \widehat{a}_{\mathbf{p}} + \widehat{a}_{\mathbf{p}}^{\dagger} \widehat{a}_{-\mathbf{p}}^{\dagger} + \widehat{a}_{\mathbf{p}} \widehat{a}_{-\mathbf{p}} \quad (4.12)$$

which can be diagonalized by the standard Bogoliubov transformation.

Standard Bogoliubov transformation

The standard Bogoliubov transformation amounts to performing the following linear transformation

$$\widehat{a}_{\mathbf{p}} = u_{\mathbf{p}} \widehat{b}_{\mathbf{p}} + v_{-\mathbf{p}} \widehat{b}_{-\mathbf{p}}^{\dagger} \ , \ \widehat{a}_{\mathbf{p}}^{\dagger} = u_{\mathbf{p}} \widehat{b}_{\mathbf{p}}^{\dagger} + v_{-\mathbf{p}} \widehat{b}_{-\mathbf{p}} \quad (4.13)$$

where we require that the new variables also describe bosons

$$\left[\widehat{b}_{\mathbf{p}}^{\dagger}, \widehat{b}_{\mathbf{p}'} \right] = \delta_{\mathbf{p}\mathbf{p}'} \quad (4.14)$$

where $[\cdot, \cdot]$ denotes a commutator. This commutation relation imposes the constraint for the two parameters $u_{\mathbf{p}}$ and $v_{-\mathbf{p}}$

$$u_{\mathbf{p}} = \cosh(\alpha_{\mathbf{p}}) \ , \ v_{-\mathbf{p}} = \sinh(\alpha_{\mathbf{p}}) \quad (4.15)$$

i.e. the transformation amounts to a rotation. Upon choosing the value of $\alpha_{\mathbf{p}}$ in such a way as to make the coefficients of the non-diagonal terms of the Hamiltonian vanish, the

final form of it reads as

$$H = E_0 + \sum_{\mathbf{p}\neq 0} \varepsilon(\mathbf{p})\, \widehat{b}^{\dagger}_{\mathbf{p}} \widehat{b}_{\mathbf{p}} \tag{4.16}$$

where $E_0 = \frac{Q_0 n^2}{2}$ is a constant and is the ground state energy calculated to the higher-order of approximation, while

$$\varepsilon(\mathbf{p}) = \sqrt{\frac{Q_0 n}{m}\mathbf{p}^2 + \left(\frac{\mathbf{p}^2}{2m}\right)^2} \tag{4.17}$$

The Bogoliubov transformation allow us to map a weakly-interacting system into a system of independent quasiparticles with energy $\varepsilon(\mathbf{p})$. The operators $\widehat{b}_{\mathbf{p}}$ and $\widehat{b}^{\dagger}_{\mathbf{p}}$ are the annihilation and creation operators of these quasiparticles. We comment here that, the true ground-state of the system is a solid and the gas phase can be observed as a metastable phase where thermalization is ensured by two-body collisions and extremely rare events three-body collisions.

Note that we could have considered a higher-order (we assume a second-order) Born approximation for the relation between the potential Q_0 and the scattering length a_B. Then by solving the Lippmann-Schwinger equation up to second order, as in (Landau and Lifshitz, 1965), we would obtain the following expression for the ground state energy E_0,

$$E_0 = \frac{Q_0 n^2}{2}\left(1 + \frac{128}{15\sqrt{\pi}}\left(n_0 a_B^3\right)^{1/2}\right). \tag{4.18}$$

This is the expression for the ground state energy including the so called Lee-Yang-Huang term.

Finally let us comment that a more general transformation exists to diagonalize multi-component BECs developed in (Tommasini *et al.*, 2003), that we made use in order to derive the dispersion relation for a coherently coupled two-component BEC in the work presented in Chapter 6.

Gross-Pitaevskii equation

Another way to describe BECs is the Gross-Pitaevskii equation (Dalfovo *et al.*, 1999, Pitaevskii, 1961, Gross, 1961). It is a mean field approximation that is based on the assumption that all atoms are in the same state and can therefore be described with the same wave function. This assumption is valid for weakly interacting gases, if the gas is diluted enough that there is on average less than one atom in the s-wave scattering length (Dalfovo *et al.*, 1999). The Gross-Pitaevskii equation looks very similar to the Schrödinger

equation, but has an additional, nonlinear term that describes the interaction between the atoms.

After making the diluteness and Born assumptions, the mean-field theory starts with an ansatz for the many-body wave function,

$$\Psi\left(\mathbf{x}_1, ..., \mathbf{x}_{N_{tot.}}\right) = \prod_{i=1}^{N_{tot.}} \phi\left(\mathbf{x}_i\right) \tag{4.19}$$

which basically assumes that the $N_{tot.}$ bosons are non interacting. The total energy of state E, is then

$$E = N_{tot.} \int d\mathbf{x} \left[\frac{\hbar^2}{2m} \left|\nabla\phi\left(\mathbf{x}\right)\right|^2 + \frac{N_{tot.}-1}{2} Q_0 \left|\phi\left(\mathbf{x}\right)\right|^4 \right] \tag{4.20}$$

Minimization of E subject to the constraint of normalization of $\phi\left(\mathbf{x}\right)$ and the introduction of the wave function of the condensate, $\psi\left(\mathbf{x}\right) = \sqrt{N}\phi\left(\mathbf{x}\right)$, would result to the following Heisenberg equation

$$\left[-\frac{\hbar^2}{2m}\nabla^2 + Q_0 \left|\psi\left(\mathbf{x}\right)\right|^2 \right] \psi\left(\mathbf{x}\right) = \mu\psi\left(\mathbf{x}\right) \tag{4.21}$$

where $\mu = \partial E / \partial N_{tot.}$ is the chemical potential of the system. This is referred to as the time-independent Gross-Pitaevskii equation. The generalized time-dependent Gross-Pitaevskii equation $i\hbar\partial\psi\left(\mathbf{x},t\right)/\partial t = \mu\psi\left(\mathbf{x},t\right)$ gives a non-linear Schrödinger equation governing the dynamics of the wave function of the condensate.

The mean-field approach has been very successful in accounting for most of the experimental results. Nevertheless, as being one of simplest approaches for many-body systems, the mean-field theory has some theoretical inconsistencies to be improved. Leggett (Leggett, 2001) pointed out that the mathematical origin of the limitation is the fact that the trial ansatz in Eq. (4.19) does not allow two-particle correlation and restricts the whole description in a reduced Hilbert space. Since the two-particle interaction would cause some correlation between particles especially in a short range separation, a better ansatz should accommodate the possibility of two-particle correlations, which is the essence of the advanced Bogoliubov approach presented above.

4.1.4 Trapped BEC

Even though it is analytically easier to treat homogeneous BEC without a trap, in practice the BEC is always confined by some trapping potential which also affects its

density's spatial distribution. The harmonic potential

$$V_{trap}(\mathbf{r}) = \frac{m}{2}\left(\omega_x^2 x^2 + \omega_y^2 y^2 + \omega_z^2 z^2\right) \tag{4.22}$$

is the easier one to treat analytically as will be explained below. For such a potential, and for a non-interacting BEC, one can make the same trial ansatz as before and the ground state wavefunctions of the single bosons can now be approximated by Gaussians, rather than the plane waves we had before. The spatial extension of the ground state wave function will be independent of $N_{tot.}$ and derives from the width of the Gaussian distribution which can be shown to be given by the so called harmonic oscillator length: $a_{HO} = \sqrt{\hbar/m\omega_{HO}}$ where $\omega_{HO} = (\omega_x\omega_y\omega_z)^{1/3}$ is the geometrical mean of the harmonic trap oscillation frequencies. The size of the ground state wave function is given by a_{HO} and is an important length scale of the system. In addition, for such a non-interacting BEC, the introduction of a harmonic trap, has important implications once one needs to consider the BEC far from the thermodynamic limit. In this case, a shift of the critical temperature is observed as is explained in (Grossmann and Holthaus, 1995a,b, Ketterle and van Druten, 1996, Kirsten and Toms, 1996).

Furthermore, if one allows for interactions in such a harmonically trapped BEC, one can show that the kinetic energy per particle E_{kin} stays constant at $\sim \hbar\omega_{HO}$, while the interaction energy per particle $E_{int.}$ increases as $Q_0 n$, the mean density n being of order $1/a_{HO}^3$. From this, one can show that the ratio of the interaction energy $E_{int.}$ and the kinetic energy E_{kin} is given by $E_{int.}/E_{kin.} \propto Na_B/a_{HO}$. Hence, if one can control the system such that E_{kin} is negligible compared to $E_{int.}$, which would be the case if $Q_0 n \gg \hbar\omega_{HO}$, then one can do the Thomas-Fermi approximation

$$n(\mathbf{r}) = \begin{cases} \frac{\mu - V_{trap}(\mathbf{r})}{Q_0} & \mu > V_{trap}(\mathbf{r}) \\ 0 & otherwise \end{cases} \tag{4.23}$$

which for the harmonic trap above amounts to assuming that the density distribution is an inverted parabola with a maximal density $n(0) = \mu/Q_0$ at the center of the trap (hence the condition from before can also be expressed as $\mu \gg \hbar\omega_{HO}$). This approximation is important, because it allows one to solve analytically the relevant nonlinear Gross-Pitaevskii equation. This allows us to show that the characteristic radius of the size of the system for an isotropic trap is given by the Thomas-Fermi radius

$$R = \sqrt{\frac{2\mu}{m\omega_{HO}^2}} \tag{4.24}$$

and that by taking into account the normalization of the wave function to density, the

chemical potential for a 3D gas reads as

$$\mu = \frac{\hbar\omega_{HO}}{2}\left(\frac{15N_{tot.}Q_0}{a_{HO}}\right)^{2/5} \tag{4.25}$$

This approximation, also allows us to solve the Bogoliubov de Gennes equations (De Gennes, 1966) necessary to diagonalize the relevant Hamiltonian and find hence the energy spectrum of the BEC. Finally, contrary to the non-interacting case, the introduction of a trap does not affect the critical temperature. It is important to note here that the ultimate control in quantum gas experiments allows to create almost arbitrary trapping potentials and thus to reduce the dimensionality of a system. This implies a very strong trapping in some of the dimensions of the system, which in the case that one wants to make the Thomas-Fermi assumption, one should make sure that the required trapping strength in order to reduce the dimensions of the system does not violate the condition above. In our work we will focus on 1D ultracold gases the particularities of which we discuss in the next subsection. For this 1D gases, the resulting chemical potential under the Thomas-Fermi approximation reads as

$$\mu = \left(\frac{3\omega_{HO}N_{tot.}Q_0\sqrt{m}}{4\sqrt{2}}\right)^{2/3} \tag{4.26}$$

However, the regimes of quantum degeneracy in 1D trapped gases, are drastically different from those in 3D, and therefore particular attention needs to be paid as to what parameter regimes one should consider in realistic experimental set-ups in order to obtain a 1D ultracold gas at the Thomas-Fermi approximation. In the spirit of this thesis, which is to propose experiments at realistic parameter regimes, in the next section, we discuss in more detail what assumptions go in the 1D gases that we will consider in all of our works.

4.1.5 1D BEC

3D elongated Bose gases as quasi-1D Bose gases

We now examine the scenario where the 1D gas is obtained from a 3D, as is the case in practice in an experiment. A condition for a 3D ultracold gas to be considered 1D, is that its transverse degrees of freedom are frozen out, but not the longitudinal motion of the particles: $k_BT \ll \hbar\omega_\perp$ and $k_BT \gg \hbar\omega_\parallel$. Here we assumed a cylindrical trap. It is important to point out here that the transition to 1D we discuss in this case is not solely from a geometrical point of view, but we deal with a true 1D system whose quantum and thermal motion is frozen in two of the three directions. This implies tightly confining the motion of trapped particles in two directions to zero point oscillations. The particles are in the transverse (single particle) ground state, but populate many longitudinal modes. This regime could be named thermodynamic 1D regime. In this way, kinematically the

gas is 1D, and the difference from purely 1D gases is only related to the value of the interparticle interaction $\widetilde{Q}_0$ which now depends on the tight confinement:

$$\widetilde{Q}_0 = \frac{2\hbar^2}{m} \frac{a_B}{a_{HO,\perp}\left(a_{HO,\perp} - 1.03a_B\right)} \tag{4.27}$$

where $a_{HO,\perp} = \sqrt{\hbar/m\omega_\perp}$ is the radial extension of the wavefunction. Note that, in our work we assume that $a_{HO,\perp}$ is much larger than the radius of the interatomic potential R, such that the interaction between particles acquires a 3D character and will be characterized by the 3D scattering length a_B. Furthermore, for sufficiently large $a_{HO,\perp}$, the sample can be treated as a 3D gas with a sharp (harmonic oscillator) radial density profile, and the coupling constant $\widetilde{Q}_0 \propto a_B$. This is an assumption we also abide to. Note that for $a_B > 0$, the repulsion changes to attraction at $a_{HO,\perp} < a_B$. We assume that this is not the case, i.e. we take $a_{HO,\perp} > a_B$.

Under the above conditions, the statistical properties of the sample are the same as those of a purely 1D (trapped) system. This 1D gas, exhibits a number of different behaviors, depending on the interparticle interactions which now depend on the tight confinement characteristics. Furthermore, the trapping potential introduces a finite size of the sample and changes the picture of long-wave fluctuations of the phase compared to the uniform case. Note that in experimentally relevant scenarios, one can not have a free gas, since some kind of potential has to be implemented in order to maintain the gas within certain limits. The type of trap that is easier to implement is that of a harmonic trap, which is the one we consider in our work as well.

Harmonically trapped weakly interacting quasi-1D gas It is interesting to see how the above results change in the more realistic scenario of allowing for interactions.

Identifying 1D interaction regime of interest First of all we remind that we avoid the Tonks gas regime, i.e. we focus on weak interactions. For the trapped case considered here, this is described by the condition $\widetilde{\xi} \gg 1/n$ where $\widetilde{\xi} = \hbar/\sqrt{mn\widetilde{Q}_0}$ i.e. the correlation for this new interparticle interaction term, and can be cast in the following:

$$\gamma = \frac{1}{\left(\widetilde{\xi}n\right)^2} = \frac{m\widetilde{Q}_0}{\hbar^2 n} \ll 1 \tag{4.28}$$

The only two cases that can be treated analytically, and hence allow us to identify the various regimes of behaviour of the gas, is if we leave the gas untrapped in the unconfined dimension, or if we trap it harmonically in this dimension as well, in a trap of frequency Ω. These are also the cases that we will consider in this thesis as well. In the first case, the

description of the gas then falls in the category discussed in the previous subsection, only the interparticle interaction is given by $\widetilde{Q}_0$. The second case is slightly more involved. To study it properly it is convenient for one to introduce the quantity $\alpha = m\widetilde{Q}_0\widehat{\xi}/\hbar^2$, where $\widehat{\xi} = \sqrt{\hbar/m\Omega}$ is the amplitude of axial zero point oscillations. This encodes the relation between the interaction strength $\widetilde{Q}_0$ and the trap frequency Ω.

Notice that the case of harmonically trapping the gas in the longitudinal direction as well can be treated by considering the Thomas Fermi (TF) approximation ($\mu \gg \hbar\Omega$) mentioned in the previous section. However, now we are in a position to identify the conditions that should hold in order to be able to do this approximation in an experimentally relevant scenario. As mentioned above, the trapping in the transverse directions introduces finite size effects that should be taken into account. There are two regimes to consider. Firstly, the case of $\alpha \gg 1$, i.e. when the interaction strength $\widetilde{Q}_0$ is much larger than the trap frequency Ω. In this case one can show that the TF condition is always satisfied, i.e. $\mu \gg \hbar\Omega$, but in this case it might be that the interactions can become strong. For this reason, a sufficiently large number of particles is required which can be shown to correspond to

$$N \gg \alpha^2 \tag{4.29}$$

On the other hand, if $\alpha \ll 1$, then weakness of interactions is guaranteed, but in order to have a TF regime, one needs to make sure that $N \gg \alpha^{-1}$. Under these conditions, for which the TF assumption is valid, one can show that at $T = 0$, one has a true BEC. It is interesting to comment on the two remaining complementary scenarios. First, the case where $\alpha \ll 1$ and $N \ll \alpha^{-1}$, for which one can show that the gas behaves as an ideal gas, since the mean-field interactions are much smaller than the level spacing in the trap $\hbar\omega$ and a macroscopic occupation of the ground state takes place. The second case is the scenario of $\alpha \gg 1$ and $\gamma \gg 1$. In this case as explained before one will get the Tonks gas. In our work we assume that the conditions for the TF approximation hold true. The decrease of temperature to below the temperature of quantum degeneracy, which reads in this case as $T_d = N\hbar\Omega$ continuously transforms a classical 1D gas to the regime of quantum degeneracy. At $T = 0$ this weakly interacting gas turns to the true TF condensate, but what is of more interest, is to understand how the correlation properties change with temperature at $T < T_d$.

Quantum fluctuations and the single-particle correlation function

A BEC can be identified in practice by studying the single-particle correlation function (or one-particle density matrix or first order coherence function) defined by (D.S. Petrov

et al., 2004)

$$G^{(1)}\left(r,t;r',t'\right)=\left\langle \Psi^{\dagger}\left(r,t\right)\Psi\left(r',t'\right)\right\rangle \tag{4.30}$$

with $\Psi\left(r,t\right)$ being the field operator that annihilates a particle at the position r at time t. In fact in our work we will only deal with BECs at equilibrium so we will ignore time dependence. Such a field operator would then be expressed as

$$\Psi\left(r\right)=\sum_{i}\varphi_{i}\left(r\right)a_{i} \tag{4.31}$$

with a_i the annihilation operator of a particle in the single particle state $\varphi_i\left(r\right)$, for which it holds that $\left\langle a_i^{\dagger}a_j\right\rangle=\delta_{ij}n_i$ with n_i the occupation number of the i^{th} state. The time-independent coherence function then reads as

$$G^{(1)}\left(r;r'\right)=\frac{1}{V}\int dpn\left(p\right)e^{ip(r-r')/\hbar} \tag{4.32}$$

where V is the volume of the gas and $n\left(p\right)=\left\langle \Psi^{\dagger}\left(p\right)\Psi\left(p\right)\right\rangle$ is the particle distribution over the momentum eigenstates, with $\Psi\left(p\right)$ the Fourier transform of $\Psi\left(r\right)$. Furthermore, for the systems that we will be interested in this thesis, the BECs will be assumed to be uniform and isotropic or controllably approximated as such up to a certain length scale (on which we will comment later on how to exactly describe). In this case, it is safe to assume that $G^{(1)}\left(r;r'\right)=G^{(1)}\left(|r-r'|\right)$ i.e. that the first order coherence function only depends on the distance between two bosons in the gas. If the gas is not condensated, then $n\left(p\right)$ varies smoothly at arbitrarily low momenta which implies that for long distances $|r-r'|\rightarrow\infty$ the coherence function $G^{(1)}\left(|r-r'|\right)\rightarrow 0$. On the contrary, as explained above, if a gas at sufficiently low temperature forms a BEC, the ground state, corresponding to $p=0$, is macroscopically occupied, which implies

$$n\left(p\right)=N_0\delta\left(p\right)+\delta n\left(p\right) \tag{4.33}$$

with N_0 being the ground state occupation number and $\delta n\left(p\right)\ll N_0$ the occupation number of the rest of the states. Note that this assumption is only valid at very low temperatures, where the exact condition would be discussed later on for each one of the cases of the setups that we will consider. Assuming this condition for the moment to be true, then the single-particle correlation function $G^{(1)}\left(|r-r'|\right)$ at long distances $|r-r'|\rightarrow\infty$ goes to a constant. This phenomenon is often referred to as off-diagonal long-range order.

An equivalent assumption to Eq. (4.33), often referred to as the Bogoliubov ansatz,

would be to assume right from the beginning a macroscopic wavefunction for the field operator, i.e.

$$\Psi = \Psi_0 + \delta\Psi \tag{4.34}$$

where Ψ_0 is the ground states wavefunction (assumed to be classical since we deal with a macroscopically occupied state) and in the density-phase representation of a field reads as $\Psi_0 = \sqrt{\widetilde{n}}e^{i\phi}$, where $\widetilde{n}$ would be the density of the ground state and ϕ its coherent phase. $\delta\Psi$ would represent the wave function of the single particle excitations above the ground state, for which for a BEC assuming it to be at low energies, it holds $\delta\Psi \ll \Psi_0$. The condition to be able to write the wavefunction in this form is again that the ground state is heavily populated i.e. that the total density would read as $n = \widetilde{n} + \delta n$ with $\delta n \ll \widetilde{n}$ the density of the excited states. The results for $G^{(1)}(|r - r'|)$ would have been the same. Note that in any realistic setting, the gas can not be uniform and isotropic over the whole space, since for example boundary effects would kick in. Assuming that we have a BEC, its state would then be described as $\Psi(r) = \Psi_0(r) + \delta\Psi(r)$ where $\Psi_0(r) = \sqrt{\widetilde{n}(r)}e^{i\phi(r)}$[1], which is what we will use in the rest of this subsection. We will consider two cases, uniform BEC where the density $\widetilde{n}(r) \to \widetilde{n}$ is constant in space and a harmonically trapped case as in the previous sections.

In both cases, uniform or not, there can be two reasons that can breakdown the BEC assumption, ground state density fluctuations $\left\langle |\delta n(r)|^2 \right\rangle$ and ground state coherent phase fluctuations $\left\langle |\delta\phi(r)|^2 \right\rangle$ where $\delta\phi(r) = \phi(r) - \phi(0)$. In the first case we lose the assumption of macroscopic occupancy, and in the second the coherency of the BEC. This would also have effects on the single-particle correlation function $G^{(1)}(r; r')$, which taking into account the fluctuations reads as $G^{(1)}(r; r') = \left\langle \Psi^\dagger(r)\Psi(r') \right\rangle = \Psi_0^\dagger(r)\Psi_0(r') + \left\langle \delta\Psi^\dagger(r)\delta\Psi(r') \right\rangle$. In particular conditions can be identified on the distances for which one would obtain again a non-vanishing $G^{(1)}(r; r')$, a sign of the formation of a macroscopic occupation and hence of a BEC.

The uniform "strictly" 1D weakly interacting gas For the density fluctuations, for the uniform 1D case in the regime of a weakly interacting gas ($n\widetilde{\xi} \gg 1$) it was found that the density fluctuations are small for sufficiently low temperature (Kane and Kadanoff, 1967), but this is not the case for the phase fluctuations. Assuming that only the phase fluctuations play a role, the single-particle correlation function can be shown to read as

$$G^{(1)}(r; r') = \widetilde{n}\left\langle e^{-i(\phi(r)-\phi(r'))} \right\rangle = \widetilde{n}e^{-\left\langle (\phi(r)-\phi(r'))^2 \right\rangle/2} \tag{4.35}$$

[1] We remind that for the density-phase representation, holds that $[\widetilde{n}(r), \phi(r')] = i\delta(r - r')$.

where the second equality is a consequence of a Gaussian distribution for the phase fluctuations. This can be further written in the uniform and isotropic limit as

$$G^{(1)}\left(r-r'\right)=\widetilde{n}e^{(\vartheta(r-r')-\vartheta(0))}$$

where $\vartheta\left(r-r'\right)=\left\langle\phi\left(r\right)\phi\left(r'\right)\right\rangle$ is the phase coherence function. Since the density fluctuations are small one can make use of Bogoliubov-de Genes theory. After solving the relevant Gross-Pitaevskii equations (D.S. Petrov *et al.*, 2004) for the density fluctuations δn and the phase $\phi\left(r\right)$, one then can obtain an expression for $\vartheta\left(r-r'\right)$ and from that evaluate $G^{(1)}\left(r-r'\right)$. For the case of a finite temperature $T>0$, one obtains (Reatto and Chester, 1967)

$$G^{(1)}\left(r-r'\right)=e^{-mk_BT(r-r')/2\widetilde{n}\hbar}$$

which implies that at large distances $G^{(1)}\left(r-r'\right)\to 0$ and hence there is no BEC. At $T=0$ a similar scenario appears (Schwartz, 1977) where

$$G^{(1)}\left(r-r'\right)=\left(\frac{\xi}{r-r'}\right)^{\nu}$$

with $\nu=mc/2\pi\hbar\widetilde{n}$ and $\xi=\hbar/\sqrt{mnQ_0}$ the uniform 1D BEC correlation length, such that again at large distances there is no BEC. In this sense, for the strictly uniform 1D BEC, there is no condensation even at $T=0$, but of course, as long as we are dealing with temperatures close to $T=0$ and distances smaller than ξ (or at finite temperatures but at distances less than $2\widetilde{n}\hbar/mk_BT$) one can safely assume that is dealing with a true BEC.One usually refers to this scenario as quasi-condensation.

The harmonically trapped 1D weakly interacting gas Once again one can show that the density fluctuations are negligible at low enough temperatures. In particular, one can show for distances much larger than the de-Broglie wavelength where one expects the density to vary more, and for thermal fluctuations i.e. $T\gg\hbar\Omega$ (which are larger than the vacuum $T=0$ fluctuations), the density fluctuations are given by (D.S. Petrov *et al.*, 2004)

$$\frac{\left\langle\left|\delta n\right|^2\right\rangle}{\widetilde{n}^2}=\frac{T}{T_d}\min\left\{\frac{T}{\mu},1\right\} \tag{4.36}$$

with μ being the chemical potential and $T_d=N\hbar\Omega$ the degeneracy temperature. Hence for $T\ll T_d$ the fluctuations are small even for the thermal fluctuations.

Furthermore, the single-particle correlation function $G^{(1)}\left(r;r'\right)$ will again be given by Eq.(4.35). For the vacuum fluctuations, the fluctuations read as

$$\left\langle\left|\delta\phi\left(r\right)\right|^2\right\rangle\propto\ln\left[r/\xi\right] \tag{4.37}$$

such that for any realistic size of the gas cloud, r is larger than ξ and hence this quantity is small. Hence a BEC is obtained if one is strictly at $T = 0$. If the thermal phase fluctuations are considered (i.e. at $T \gg \hbar\Omega$), one finds

$$\left\langle \left|\delta\phi\left(r\right)\right|^2 \right\rangle = \frac{4T\mu}{3T_d\hbar\Omega} \left| \log\left[\frac{\left(1 - r/R\right)}{\left(1 + r/R\right)} \right] \right| \tag{4.38}$$

which results in the following single-particle correlation function $G^{(1)}\left(r; r'\right)$ near the center of the trap (Kadio *et al.*, 2005), i.e. $r/R \ll 1$

$$G^{(1)}\left(r; r'\right) \sim e^{-r/2R_\phi} \tag{4.39}$$

where $R_\phi = RT_d\hbar\Omega/\mu T$ is the phase coherence length, such that for sufficiently low temperature and for distances smaller than $2R_\phi$ one can assume that is dealing with a BEC. Hence once again we have quasi-condensation. Finally, we comment that very similar results were obtained for the more realistic scenario of elongated 3D BECs mentioned above (Petrov *et al.*, 2001).

4.2 Bose polaron problem

4.2.1 Historical overview and motivation

The polaron problem, in its original formulation, considers the motion of an electron in an ionic crystal or polar semiconductors. The history of the polaron begins in parallel with the advent of modern, solid state physics. During the first years of its conception, the polaron problem attracted major interest by some of the greatest names of the time in physics, but even till today remains a highly relevant topic of study. The reasons are mainly two-fold. Firstly and most importantly, polarons have potential applications in semiconductors and therefore, have been of interest from the point of view of semiconductor technology. Secondly but of equal importance, they cast the simplest possible model of a particle interacting with a non-relativistic, quantum field and therefore, serve as a simple test-bed for developments in quantum field theory.

In recent years, with the discovery of high-temperature superconductivity, the polaron problem has received a renewed boost. One of the main reasons for this is that it is believed that polaronic interaction may play an important role in inducing pairing in Cu-based, ceramic, high-temperature superconductors. Polaron physics has also found applications in several other areas like organic polymers and biological physics. A prominent example of a polaronic system would be the BEC polaron consisting of an impurity atom interacting with the Bogoliubov excitations of an atomic Bose–Einstein condensate (BEC) (Cucchietti and Timmermans, 2006b, Sacha and Timmermans, 2006, Tempere *et al.*, 2009), on which we will focus in this thesis.

4.2.2 Quasi-particles

Before introducing the concept of a polaron, one needs to have in mind the definition of the concept of a quasiparticle. This is a pseudo particle, result of an emerging phenomenon, where a complicated many-body system of interacting particles is modeled by a simpler problem in free space. The typical scenario where one can employ such a description of a system in terms of quasiparticles, is that of a real particle moving through the system, pushing or pulling on its neighbors and thus becoming surrounded/dressed by a cloud of agitated particles (excitations) (Mattuck, 1992). A special example of this is the polaron which is described in more detail in the next subsection. The real particle plus its cloud is then treated as an elementary excitation (quasi-particle) of the many-body system. Since the quasi-particle behaves like an individual particle, its concept may be assigned to the microscopic description of the many-body system.

The quasi-particle properties are quite distinct from those of the bare particle. The quasi-particle has an effective mass which is generally larger than the real particle mass. It has also a finite lifetime. Furthermore, The cloud screens the real particles, hence quasi-particles interact with an effective interaction which is weaker than the particle-particle interaction. It is important to note that all quasi-particle properties are experimentally observable.

Bogoliubov quasiparticles An important example of a different type of quasiparticles are the Bogoliubov quasi-particles, which are the elementary excitations in a superconductor. Even if they are called quasi-particles, their structure is quite different from the "particle plus cloud" picture described above. Usually, they consist of a linear combination of an electron in state $(+k, \uparrow)$ and a hole in $(-k, \downarrow)$. However, in our work, we will consider the simpler case of such Bogoliubov quasi-particles in spinless weakly interacting Bose atomic gases at zero temperature. The bath particles in our studies will be of this form of quasiparticles.

4.2.3 What is a Polaron?

Consider an additional electron introduced in an ionic crystal or a polar semiconductor. Naturally, the electron will attract the positive ions, but on the other hand, it will repel the negative ions in its vicinity. The result, will be that the lattice in the immediate neighborhood of the electron, will be distorted. However, the electron is not static, it's mobile. As it moves away from its previous position to a new position, the lattice in the previous position will try to relax towards its original configuration. However, the part of the lattice surrounding the electron in the new position will then become distorted. So the overall picture looks as if the electron as it propagates through the crystal, it carries together with it the lattice distortion. This complex, that is, the electron together with

the lattice distortion, constitutes what may be called a quasiparticle, introduced in the previous subsection. This particular quasi-particle however, is called a polaron. This name was coined by Pekar (Landau and Pekar, 1948a).

Dielectric theory describes the aforementioned distortion by the induction of a polarization for the distorted lattice around the charge carrier, which follows the charge carrier when it is moving through the medium. The charge of the electron in this case is also modified, a consequence of the aforementioned screening. If characteristic phonon frequencies are sufficiently low, the local deformation of ions, caused by the electron, creates a potential well, which can trap the electron even in a perfect crystal lattice. The idea of the auto-localization of an electron due to the induced lattice polarization was first proposed by L. D. Landau (Landau, 1933). This is essentially what the name "polaron" refers to. It was studied in greater detail (Devreese, 1996, Feynman, 1955, Fröhlich, 1954, Pekar, 1946, Rashba, 1957) in the effective mass approximation for the electron placed in a continuum polarizable (or deformable) medium, which leads to a so-called large or continuum polaron which we describe in more detail in the next section. In a perfect lattice, the self-trapping is never complete and hence the electron plus its surrounding polarization can move through the medium. The electron has to move slowly, i.e. with low kinetic energy, so that the ionic polarization can follow the electron. This is a requirement imposed by the finiteness of the bath phonon frequencies.

A polaron behaves as a free electron but with an enhanced effective mass (Alexandrov and Devreese, 2010). Landau and Pekar were the first to calculate the effective mass of a polaron (Landau and Pekar, 1948a). Fröhlich later showed that the results obtained by Pekar and Landau can be obtained with a variational method in the strong-coupling limit of the Fröhlich model (Fröhlich, 1954). We will discuss this in the next section. The physical properties of a polaron differ from those of a band-carrier. A polaron is characterized by its binding (or self-) energy E_p, an effective mass m_p and by its characteristic response to external electric and magnetic fields (e. g. dc mobility and optical absorption coefficient). A similar setting can be imagined for an impurity immersed in a BEC where the impurity is screened by a cloud of atoms of the BEC. This is the setting we consider in this thesis.

4.2.4 Large polarons vs small polarons

In the context of field theory, distortion of lattice is translated as excitation of phonons. Therefore in this language of field theory (in which the electron is supposed to be the source of phonons) a polaron is an electron dressed with a cloud of virtual phonons. If the lattice distortion extends over a few lattice points, we call it a large polaron. On the other hand, if the distortion is confined within one lattice spacing, the corresponding polaron is called a small polaron. In other words, small polarons contrary to large ones,

are governed by short-range interactions.

The large polaron, or also called the continuum polaron, i.e. the definition of a polaron ignoring the discreteness of the lattice, is valid if coupling to long-wavelength optical (LO) phonons dominates the interaction. To define the concept of a large (also called continuum) polaron, one needs to assume space as discretized in a lattice structure as mentioned above. Then consider as an example, the Longitudinal Optical (LO) phonon field with frequency ω_{LO} interacting with an electron. Denote by $\Delta\nu$ the quadratic mean square deviation of the electron velocity. If the electron-phonon interaction is weak, the electron can travel a distance $\Delta x \approx \Delta\nu/\omega_{LO}$ during a time ω_{LO}^{-1} , characteristic for the lattice period. This is the distance within which the electron can be localized using the phonon field as measuring device. From the uncertainty relations it follows

$$\Delta p \Delta x = \frac{m}{\omega_{LO}} (\Delta\nu)^2 \approx \hbar \tag{4.40}$$

where $\Delta\nu \sim \sqrt{\hbar\omega_{LO}/m}$. At weak coupling Δx is a measure of the polaron radius r_p. In other words, the polaron radius is measured by the extension of the lattice distortion induced by the excess electron (Appel, 1968). To be consistent, the polaron radius r_p must be considerably larger than the lattice parameter a. (this is a criterion of a "large polaron"). Large polarons have $r_P \gg a$, so that the continuum approximation becomes valid, as e.g. for the Fröhlich Hamiltonian (Fröhlich, 1963).

Weak- and Strong- coupling polarons Polarons can also be classified according to the coupling strength between the electron and the phonon field. The stronger the coupling the more phonons will be in the cloud surrounding the electron. If the average number $\bar{N}$ of phonons in the cloud is $\bar{N} \ll 1$, it is called a weak-coupling polaron. If on the other hand $\bar{N} \gg 1$, the polaron will be regarded as a strong-coupling polaron (Rashba, 1957).

4.2.5 Frohlich Hamiltonian

Landau was the first to introduce the concept of polaron, which was later studied in more detail by Pekar who introduced a semiclassical model with the lattice properties incorporated into a classical macroscopic polarization (Gerlach and Löwen, 1991). However, the real interest in this area was boosted by the pioneering work of Frohlich (Fröhlich *et al.*, 1950) who provided the microscopic quantum mechanical model Hamiltonian, on which the modern polaron theory has been built. The picture of the polaron conceived by Frohlich is again that of a complex (quasi-particle) consisting of an electron and the lattice distortion (polarization) induced by it, but unlike the case of Landau-Pekar polaron, the above complex can be found anywhere in the lattice. In his picture of the polaron, if the lattice is static and the distortion in the lattice is neglected, the

electron would be just a Bloch electron. The Frohlich model (Fröhlich, 1963, Austin and Mott, 1969, Fröhlich *et al.*, 1950, Fröhlich, 1954) considers a low-lying or a slow electron so that the de Broglie's wavelength is much larger than the lattice constant, and in this limit, the structure of the lattice becomes unimportant and lattice can be considered to be a continuum. Application of standard classical electrodynamics followed by canonical quantization then leads to a Hamiltonian which consists of three parts. These are the Bloch (free) electron, the free phonon field, and the interaction between the two described only by a single dimensionless coupling constant. This Hamiltonian introduced in solid state physics, maybe for the first time, the field theoretic concept of the interaction of a particle (electron) with a scalar boson field (phonons) and the concept that an electron can be considered to be a source of phonons. Apart from its importance in demonstrating the properties of an electron in ionic crystals or polar semiconductors which is of practical interest, this model Hamiltonian was very simple, but still at the same time sufficiently sophisticated, from the point of view of theoretical physics.

Our starting point is a single free impurity interacting with a gas of interacting Bosons in one dimension. Note that we neglect any spin and relativistic effects in our studies. This situation can be described by the following microscopic Hamiltonian,

$$\begin{aligned} H = & \int dx \phi^{\dagger}(x) \left[-\frac{\partial^2}{2m_B \partial x^2} + \frac{g_{BB}}{2} \phi^{\dagger 2}(x) \phi(x) \right] \phi(x) \\ & + \int dx \psi^{\dagger}(x) \left[-\frac{\partial}{2m \partial x^2} + g_{IB} \phi^{\dagger}(x) \phi(x) \right] \psi(x) \end{aligned} \tag{4.41}$$

where $\phi(x)$ stands for the Bose field operator, $\psi(x)$ is the impurity field and $\hbar = 1$. The boson (impurity) mass is m_B (m) and g_{BB} (g_{IB}) denote the boson–boson and impurity–boson coupling constants respectively.We assume that only a single impurity is present in the homogeneous Bose gas with density n_0. Experimentally this corresponds to a situation with sufficiently low impurity concentration, ideally with less than one impurity per healing length ξ. To arrive at a polaron description of the impurity problem described above, one needs to do a Bogoliubov transformation as in (Tempere *et al.*, 2009, Devreese, 2016, Grusdt and Demler, 2015, Mathey *et al.*, 2004) that brings the Hamiltonian in the form

$$H = H_F + H_{2ph} + H_{ph-ph} \tag{4.42}$$

where up to constant terms,

$$H_F = H_{BEC} + H_{Imp.} + H_{Int.} \tag{4.43}$$

with

$$\begin{aligned} H_{BEC} &= \int dk \omega_k a_k^\dagger a_k \\ H_{Imp.} &= \tfrac{p^2}{2m} \\ H_{Int.} &= \int dk V_k e^{ikx} \left(a_k^\dagger + a_{-k} \right) \end{aligned} \tag{4.44}$$

the Bogoliubov diagonalized BEC Hamiltonian, the free impurity Hamiltonian and the impurity-BEC interacting Hamiltonian respectively, where

$$\omega_k = ck \left(1 + \frac{1}{2} k^2 \xi^2 \right)^{-1/2} \tag{4.45}$$

is the Bogoliubov dispersion relation (that can be interpreted as the constant frequency of a longitudinal optical phonon) and $c = \sqrt{g_{BB} n_0 / m_B}$ and $\xi = 1/\sqrt{2 m_B g_{BB} n_0}$ are the speed of sound in the BEC and correlation length respectively. The scattering amplitude V_k is given by $V_k = \sqrt{n_0} (2\pi)^{-1/2} g_{IB} \left((\xi k)^2 / \left(2 + (\xi k)^2 \right) \right)^{1/4}$. In the above, p and x denote the momentum and position operators in first quantization. H_F is referred to as the standard Frohlich Hamiltonian. The second term of Eq. (4.42), H_{2ph} describes two-phonon scattering processes (Rath and Schmidt, 2013, Shchadilova *et al.*, 2016d). H_{ph-ph} term summarizes all the additional interactions between the Bogoliubov phonons beyond two-phonon.

Weak bosons interactions regime The two terms above, H_F and H_{2ph}, provide an accurate model for the polaron problem when the Bose gas can be treated within Bogoliubov theory. This Mean Field (MF) description of the interacting bosons assumes a macroscopic occupation of the condensate which is absent in one dimension (Hohenberg, 1967, Mermin and Wagner, 1966). As pointed out by Lieb and Liniger (Lieb and Liniger, 1963), some quantities including the total energy can nevertheless be calculated accurately using Bogoliubov theory in the regime of weak interactions. This is the case when the dimensionless coupling strength γ is sufficiently small (Lieb and Liniger, 1963, Grusdt *et al.*, 2017a), where $\gamma = m_B g_{BB} / n_0$, namely

$$\gamma \ll 1 \tag{4.46}$$

since then this can be used as a small expansion parameter, and hence ignore phonon interactions that are higher than two phonon interactions.

Validity of the Frohlich Hamiltonian/ weak impurity-BEC coupling regime

Beyond the approximation mentioned above, a condition can also be provided for which neglecting H_{2ph} in comparison to H_F is valid, which casts a condition for the validity of the Frohlich Hamiltonian. This is the case when the depletion of the quasi-1D condensate is

small, justifying also the assumption that phonon–phonon interactions cannot modify the polaron cloud substantially in this regime. To do so, one needs to consider the phonon number in the polaron cloud for the two cases, for $H \approx H_F$ and $H \approx H_F + H_{2ph}$, by employing mean field theory (Grusdt *et al.*, 2017a). By comparing the two results one can show that the condition for the Frohlich Hamiltonian to be valid is

$$g_{IB} \ll \sqrt{2}\pi c. \tag{4.47}$$

The Fröhlich Hamiltonian has been of great interest to various branches of solid-state physics ever since its introduction to the physics community. Besides its physical importance, i.e. properties of electrons in polar materials and ionic crystals, it is also often used as a pure mathematical problem. The Fröhlich Hamiltonian is one of the simplest quantum field theoretical models in solid-state physics. In its most general form, it describes a particle coupled to its environment. We note that for experimentally feasible parameters, in particular the ones used in the experiment of Catani et al. in (Catani *et al.*, 2012a), which are also similar to the ones we consider in our work, the critical coupling strength where the Fröhlich model breaks down is given by $\eta_c \equiv g_{IB}/g_{BB} \approx 6$.

4.2.6 Bose Polaron as a Quantum Brownian particle

An alternative approach to the Bose polaron problem was proposed in (Lampo *et al.*, 2017a), and this is the line of thought that we follow in our work as well. In this work, the authors study the physics of the impurity as an open system in the framework of quantum Brownian motion (QBM) model. In general, the QBM describes a Brownian particle moving in a thermal bath consisting of a collection of non-interacting harmonic oscillators satisfying the Bose-Einstein statistics (Gardiner and Zoller, 2004, Breuer and Petruccione, 2007a, Schlosshauer, 2007b, 2005, Zurek, 2003, Caldeira and Leggett, 1983a,b), as was explained in the previous section. In the context of (Lampo *et al.*, 2017a), the impurity plays the role of the Brownian particle, while the bath consists of the Bogoliubov modes of the BEC. The bath in (Lampo *et al.*, 2017a) was assumed to be homogeneous, i.e. the density of the BEC is space-independent, but in a subsequent work (Lampo *et al.*, 2018), the equivalent problem but with the BEC being harmonically trapped, was treated. Note that in the literature a number of works applied open quantum system techniques to study problems in the context of ultracold quantum gases. For instance, the system of a bright soliton in a superfluid in one dimension in (Efimkin *et al.*, 2016a), the system of a dark soliton in a one-dimensional BEC coupled to a non-interacting Fermi gas in (Hurst *et al.*, 2017b), the system of the component of a moving superfluid (Keser and Galitski, 2018), and the system of an impurity in a Luttinger liquid in (Bonart and Cugliandolo, 2012a, 2013). In particular, in this work, the formalism of Quantum Langevin equations is employed, for the advantages that have been presented in the previous Chapter.

The first step in this work, was to show that the Hamiltonian of an impurity in an ultracold gas can be expressed as that of the Frohlich Hamiltonian, as presented above. The coupling between the system and the environment in the resulting Hamiltonian is nonlinear due to the interacting term. To proceed to the next step, which is to cast the Hamiltonian into the form of the Hamiltonian describing the QBM model, also referred to as the Caldeira-Leggett model, one needs to linearize this Hamiltonian, and the authors find under what conditions it is valid to approximate the nonlinear interaction by a linear one. A detailed study of the regimes of parameters in which this assumption is valid is presented, and these are evaluated in view of current experimental feasibility for this system. In particular, they find the regimes of temperatures, interaction strength, experimental time and trapping frequency for the impurity in which the model is valid. The spectral density (SD) of the system is derived, which encapsulates the effect of the bath on the central system. The spectral density is found to be super-ohmic, corresponding to the presence of memory effects in the dynamics of the system. The quantum Langevin equations to describe the evolution of relevant observables associated to the impurity are obtained, and solved either numerically or analytically for both a free impurity and a harmonically trapped impurity. For the untrapped impurity, the mean square displacement, a measurable quantity in experiments (Catani *et al.*, 2012a), is studied, and found to behave superdiffusively, while for the trapped impurity a genuine position squeezing effect is identified, which increases with increasing coupling strength between the impurity and the bath.

In practice, what allows for the Hamiltonian to be cast into that of QBM is taking the limit

$$kx \ll 1 \tag{4.48}$$

which turns the interacting part of the Hamiltonian in Eq. (4.44) into

$$H_{Int.} = \int dk V_k \left(I + ikx\right) \left(a_k^\dagger + a_{-k}\right). \tag{4.49}$$

A similar assumption to Eq. (4.48) is considered in (Efimkin *et al.*, 2016a) to study the physics of a bright soliton in a superfluid, and in (Bonart and Cugliandolo, 2012a) where QBM has been employed to treat the dynamics of an impurity in a Luttinger Liquid. The resulting Hamiltonian of the impurity in a BEC is

$$H = H_{Imp.} + H_{BEC} + \int dk g_k x \pi_k \tag{4.50}$$

where $\pi_k = i\left(a_k^\dagger - a_{-k}\right)$ is the (dimensionless) momenta of the bath particles. To get

Eq. (4.50) the redefinition of the Bogoliubov modes operators as $a_k \to a_k - V_k/\omega_k I$ was implemented, and a non-operator term was neglected. The Hamiltonian in Eq. (4.50), resembles the Hamiltonian of QBM in (3.2), only the coupling of the impurity is to the (dimensionless) momenta, π_k of the bath particles, which however does not changes anything regarding the methods one would employ to approach the problem. Unfortunately, the Hamiltonian now, is not positively defined (note that at this point we match the situation described in (Cañizares and Sols, 1994), where translational symmetry is broken). One could repair this by taking into account bilinear terms in a_k and $a_k^\dagger$, as in (Rath and Schmidt, 2013, Shchadilova *et al.*, 2016d,b, Bruderer *et al.*, 2007, Christensen *et al.*, 2015a), and including them in the theory in an exact manner, that would lead to an extension similar to the Lee-Yang-Huang term from above. This is possible, but technically complex. However, the authors in (Lampo *et al.*, 2017a) use a much simpler method, which was first used in the work of Caldeira and Leggett in their seminal paper – i.e. complete the Hamiltonian to a positively defined one by writing

$$H = H_{Imp.} + \int dk\omega_k \left(a_k^\dagger + ig_k x/\omega_k\right)\left(a_k - ig_k x/\omega_k\right). \tag{4.51}$$

Clearly, Caldeira-Leggett remedy leads directly to the trapping harmonic potential for the impurity that cancels the negative harmonic frequency shift that appears in the absence of the compensation term. However, this required the introduction of what is referred to as the renormalization term in the Hamiltonian, and since this term does not arise from any physical ground, what the authors did in (Lampo *et al.*, 2017a) was to use the original Hamiltonian in the QBM form in Eq. (4.50), but evaluate explicitly for which set of parameters this would be positive.

This work is based on the common assumption (Shashi *et al.*, 2014b, Tempere *et al.*, 2009, Casteels *et al.*, 2012) that the interaction between the impurity and the BEC can be approximated by a contact interaction, i.e. again the Bohr approximation was employed. This leads to the Frohlich Hamiltonian, which in general, there is still an open debate concerning the validity regime of it, i.e. for which values of the system parameters the quadratic Bogoliubov operators terms can be dropped out. However, if we stick to the assumptions mentioned above, one could safely expect that the Frohlich approximation is valid. In particular this results on a maximum allowed value for the coupling strength between the impurity and the BEC as explained above, and in this work the authors constrain themselves in this limit.

4.3 Summary

The main points studied in this chapter are the following:

- Diluteness and low temperature of a gas of weakly interacting bosons or fermions

are the main assumptions to obtain a BEC. In the Hamiltonian that describes such an ultracold gas, the boson-boson coupling is the only parameter (apart from the free boson parameters such as the mass) that controls the interactions and hence the energy of the system.

- The Bogoliubov transformation, allows one to diagonalize a Hamiltonian of weakly interacting Bosons. Within mean-field theory, i.e. under the many-body ansantz that assumes non-interacting bosons, the Heisenberg equation for bosons of a BEC is called the (time dependent/independent) Gross-Pitaevskii equation and can be analytically solved in many cases. It ignores however two-particle correlations.

- The nonlinear Gross -Pitaevskii equation can be analytically solved for harmonically trapped BEC under the Thomas-Fermi approximation, i.e. assuming that the kinetic energy of the bosons is much smaller than their interaction energy.

- For 1D BECs, which are essentially elongated 3D BECs, the interaction between bosons can also be controlled by the trapping frequency in the confined dimension.

- A Bose polaron is a quasiparticle, in particular the composite of an impurity and the distortion that this causes to the lattice on which is moving. The quasiparticle behaves as a free particle but with enhanced mass.

- A Bogoliubov quasiparticle on the other hand is the composite of a particle of a given momentum k and its antiparticle of momentum $-k$. Alternatively this can also be composed by phonons of opposite frequencies, which is how will treat them in our work.

- An impurity interacting with a weakly interacting gas of bosons, is described by the Frohlich Hamiltonian. Rigorous conditions determine up to what strength of the impurity-BEC coupling constant g_{IB} this Hamiltonian is valid. We also reviewed in this chapter approaches that go beyond the validity of this Hamiltonian, but in our work we restrict to the regime of validity of the Frohlich Hamiltonian.

- The necessary conditions for an impurity immersed in a BEC described by the Frohlich Hamiltonian to be treated as a QBP were presented. Namely, the range of validity of the relevant dipole approximation was discussed.

CHAPTER 5

TWO DISTINGUISHABLE IMPURITIES IN A BEC: SQUEEZING AND ENTANGLEMENT OF TWO BOSE POLARONS

In this Chapter, we study the emergence of entanglement between two Bose polarons immersed in a common BEC bath. The major motivation for us to undertake this work is the contemporary progress in the manipulation and control of ultracold atoms and ions, that paves the way to new possible experiments. The behaviour of an impurity in a Bose gas has recently attracted a lot of attention, both on the theoretical and experimental side (Schirotzek *et al.*, 2009a, Massignan *et al.*, 2014b, Lan and Lobo, 2014, Levinsen and Parish, 2014, Schmidt *et al.*, 2012, Côté *et al.*, 2002, Catani *et al.*, 2012b, Shashi *et al.*, 2014a, Christensen *et al.*, 2015b, Levinsen *et al.*, 2015, Grusdt and Demler, 2015, Shchadilova *et al.*, 2016c, Ardila and Giorgini, 2016, Jørgensen *et al.*, 2016, Rentrop *et al.*, 2016, Lampo *et al.*, 2017b, Yoshida *et al.*, 2018, Guenther *et al.*, 2018a). The main feature of such a system lies in the creation of excitation modes (Bogoliubov quasiparticles) associated to the motion of the atoms of the gas, that dress the impurity, leading to the formation of a compound system named Bose polaron. For two such impurities within a BEC, studies have focused in the past Camacho-Guardian *et al.* (2018), Dehkharghani *et al.* (2018) on the possibility to form bound states (bipolarons) for sufficiently strong

interactions between the impurities and the condensate atoms. Furthermore, the Bose polaron problem was recently studied within the quantum Brownian motion (QBM) model (Lampo *et al.*, 2017b, 2018), which describes the dynamics of a quantum particle interacting with a bath made up of a huge number of harmonic oscillators obeying the Bose-Einstein statistics (Breuer and Petruccione, 2007b, Schlosshauer, 2007a, Caldeira and Leggett, 1983a, de Vega and Alonso, 2017a). In this analogy, the impurity plays the role of the Brownian particle and the Bogoliubov excitations of the BEC are the bath-oscillators. Here, by extending this view, we study the creation of entanglement between two different impurities in a Bose gas, as a consequence of the coupling induced by the presence of the Bogoliubov modes, which play the role of the bath.

Note that the QBM model for the motion of the two kinds of impurities in a BEC is a continuous-variable description i.e. it is expressed in terms of position and momentum operators. Thus, entanglement measures based on the density matrices are not conveniently calculable because the density matrix in this case is infinite-dimensional. We therefore use the logarithmic negativity (Vidal and Werner, 2002) as a more fitting choice in this context. This measure is expressed in terms of the covariance matrix, namely a matrix, whose elements are all of the position and momentum related correlation functions.

To compute these correlation functions, we solve the Heisenberg equations of the system, which can be reduced to a quantum stochastic Langevin equation for each particle. This set of two coupled equations are non-local in time, namely the dynamics of both impurities in a BEC carry certain amount of memory. In this context, such a feature is often related to the superOhmic character of the spectral density, constituting the main quantity that embodies the properties of the bath. The presence of memory effects (non-Markovianity) can also be shown to lead to the appearance of entanglement (Hörhammer and Büttner, 2008, Zell *et al.*, 2009, Vasile *et al.*, 2010b, Fleming *et al.*, 2012, Correa *et al.*, 2012). The role of the memory effects in the works above is to preserve entanglement in the long-time regime (de Vega and Alonso, 2017b) and in the high temperature regime (Doll, R. *et al.*, 2006). Nevertheless, in these works the spectral density was assumed to be Ohmic, such that the non-Markovianity is purely attributed to the influence of one particle on the other. Indeed, the disturbances caused by particles to one another is mediated through the common bath, which take a finite time to propagate through the medium, making the evolution of each particle history-dependent. This results on a decay of entanglement in several stages (Doll, R. *et al.*, 2006, Doll *et al.*, 2007) or to a limiting distance for bath induced two-mode entanglement (Zell *et al.*, 2009). In (Valido *et al.*, 2013a), the scenario of an additional source of non-Markovianity, emerging from a non-Ohmic spectral density was considered. The non-ohmic spectral density resulted in more robust entanglement among the two impurities.

In this work we study entanglement as a function of the physical quantities of the system, such as temperature, impurity-gas coupling, gas interatomic interaction and density. These parameters may be tuned in experiments allowing to control the amount of entanglement between the impurities. We distinguish the situation in which the impurity is trapped in a harmonic potential and that where it is free of any trap. In the trapped case, we also study squeezing which is a resource for quantum sensing.

The manuscript is organized as follows. In Sec. 5.1 we present the Hamiltonian of the system, showing that it can be reduced to that of two quantum Brownian particles interacting with a common bath of Bogoliubov modes. We also write the quantum Langevin equations, find the expression for the spectral density showing that it presents a super-ohmic form, and solve the equations in order to evaluate the position and momentum variances. Finally, we review and discuss the logarithmic negativity as an entanglement quantifier and a criterion which we use to detect two-mode squeezing. In Sec. 5.2.1 we study the out-of-equilibrium dynamics of untrapped impurities, while in Sec. 5.2.2 we study entanglement and squeezing of the two impurities as a function of the system parameters for the trapped case. In Sec. 5.3 we offer the conclusions and outlook. We discuss details on the derivations of the spectral density and susceptibility in appendices B.1 and B.2. In App. B.3, we comment on the difficulty of finding an analytic solution for the trapped case even when the centers for the particles potentials coincide, and in App. B.4 we study, for the trapped case, the effective equilibrium Hamiltonian of the system reached at long-times. All the material presented in this chapter was published in (Charalambous *et al.*, 2019a).

5.1 The model system

5.1.1 Hamiltonian

We consider two kinds of distinguishable impurities of mass m_1 and m_2, immersed in a bath of interacting bosons of mass m_{B} enclosed in a box of volume V. This system is described by the Hamiltonian

$$H = H_{\mathrm{I}}^{(1)} + H_{\mathrm{I}}^{(2)} + H_{\mathrm{B}} + H_{\mathrm{BB}} + H_{\mathrm{IB}}^{(1)} + H_{\mathrm{IB}}^{(2)}, \tag{5.1}$$

with

$$H_{\mathrm{I}}^{(j)} = \frac{\mathbf{p}_j^2}{2m_j} + T_j\left(\mathbf{x}_j, \mathbf{d}_j\right), \tag{5.2a}$$

$$H_{\mathrm{B}} = \int d^d\mathbf{x}\Psi^\dagger\left(\mathbf{x}\right)\left(\frac{\mathbf{p}_{\mathrm{B}}^2}{2m_{\mathrm{B}}} + U\left(\mathbf{x}\right)\right)\Psi\left(\mathbf{x}\right) = \sum_k \epsilon_k a_k^\dagger a_k, \tag{5.2b}$$

$$H_{\mathrm{BB}} = g_{\mathrm{B}}\int d^d\mathbf{x}\Psi^\dagger\left(\mathbf{x}\right)\Psi^\dagger\left(\mathbf{x}\right)\Psi\left(\mathbf{x}\right)\Psi\left(\mathbf{x}\right) = \frac{1}{2V}\sum_{q,k',k} C_{\mathrm{B}}\left(q\right) a_{k'-q}^\dagger a_{k+q}^\dagger a_{k'} a_k, \tag{5.2c}$$

$$H_{\mathrm{IB}}^{(j)} = \frac{1}{V}\sum_{q,k} C_{\mathrm{IB}}^{(j)}\left(k\right)\rho_{\mathrm{I}}^{(j)}\left(q\right) a_{k-q}^\dagger a_k, \tag{5.2d}$$

with $a^\dagger$ and a being the bath creation and annihilation operators respectively, $\mathbf{x}_j$ and $\mathbf{p}_j$ the position and momentum operators of particle $j = 1, 2$, where they satisfy the commutation relations $[a^\dagger, a] = 1$ and $[\mathbf{x}_j, \mathbf{p}_k] = i\hbar\delta_{jk}$. Here, we consider the bosons to be in a homogeneous medium, i.e. $U\left(\mathbf{x}\right) = \text{const}$, and the external potential experienced by the impurities is

$$T_j\left(\mathbf{x}_j, \mathbf{d}_j\right) = \sum_{i=1}^{3}\frac{m_j\mathbf{\Omega}_j^2(\mathbf{x}_j + \mathbf{d}_j)^2}{2}, \tag{5.3}$$

that is a 3D parabolic potential centered at $\mathbf{d}_j = (d_{j,x}, d_{j,y}, d_{j,z})$ and with frequency $\mathbf{\Omega}_j = (\Omega_{j,x}, \Omega_{j,y}, \Omega_{j,z})$. We will consider both the trapped $\mathbf{\Omega}_j > 0$ and untrapped cases $\mathbf{\Omega}_j = 0$. The densities of the impurities in the momentum domain $\rho_{\mathrm{I}}^{(j)}\left(q\right)$ are

$$\rho_{\mathrm{I}}^{(j)}\left(q\right) = \int_{-\infty}^{\infty} e^{-iq\mathbf{x}}\delta\left(\mathbf{x} - \left(\mathbf{x}_j + \mathbf{d}_j\right)\right) d^d\mathbf{x}. \tag{5.4}$$

The Fourier transforms of the interactions among the j^{th} impurity and the bath and among bath particles themselves are, respectively

$$C_{\mathrm{IB}}^{(j)}\left(k\right) = \mathcal{F}_{\mathrm{IB}}\left[g_{\mathrm{IB}}^{(j)}\delta\left(\mathbf{x} - \mathbf{x}'\right)\right], \tag{5.5a}$$

$$C_{\mathrm{B}}\left(q\right) = \mathcal{F}_{\mathrm{B}}\left[g_{\mathrm{B}}\delta\left(\mathbf{x} - \mathbf{x}'\right)\right]. \tag{5.5b}$$

The coupling constants in Eq. (5.5) are

$$g_{\mathrm{IB}}^{(j)} = 2\pi\hbar^2\frac{a_{\mathrm{IB}}^{(j)}}{m_{\mathrm{R}}^{(j)}}, \tag{5.6a}$$

$$g_{\mathrm{B}} = 4\pi\hbar^2\frac{a_{\mathrm{B}}}{m_{\mathrm{B}}}, \tag{5.6b}$$

where $m_{\mathrm{R}}^{(j)} = \frac{m_{\mathrm{B}}m_j}{(m_{\mathrm{B}}+m_j)}$, is the reduced mass, and $a_{\mathrm{IB}}^{(j)}$ and a_{B} are the scattering lengths between the impurities and the bath particles and between the bath particles themselves, respectively.

By performing a Bogoliubov transformation,

$$a_{\mathbf{k}} = u_{\mathbf{k}}b_{\mathbf{k}} - w_{\mathbf{k}}b_{-\mathbf{k}}^\dagger\ ,\ a_{\mathbf{k}}^\dagger = u_{\mathbf{k}}b_{-\mathbf{k}} - w_{\mathbf{k}}b_{\mathbf{k}}^\dagger, \tag{5.7}$$

with

$$u_{\mathbf{k}}^2 = \frac{1}{2}\left(\frac{\epsilon_{\mathbf{k}} + n_0 C_{\mathrm{B}}}{E_{\mathbf{k}}} + 1\right),$$

and

$$w_{\mathbf{k}}^2 = \frac{1}{2}\left(\frac{\epsilon_{\mathbf{k}} + n_0 C_{\mathrm{B}}}{E_{\mathbf{k}}} - 1\right),$$

the terms related purely with the bath particles transform to the following non-interacting term

$$H_{\mathrm{B}} + H_{\mathrm{BB}} = \sum_{\mathbf{k}\neq 0} E_{\mathbf{k}} b_{\mathbf{k}}^\dagger b_{\mathbf{k}}, \tag{5.8}$$

where we neglected some constant terms, such that the diagonal form of the Hamiltonian is only valid up to quadratic order in the bath operators. In the above expression, $E_{\mathbf{k}} = \hbar c\,|\mathbf{k}|\sqrt{1+\frac{1}{2}(\xi\mathbf{k})^2} \equiv \hbar\omega_{\mathbf{k}}$ is the Bogoliubov spectrum, where

$$\xi = \frac{\hbar}{\sqrt{2 g_{\mathrm{B}} m_{\mathrm{B}} n_0}}, \tag{5.9}$$

is the coherence length for the BEC and

$$c = \sqrt{\frac{g_{\mathrm{B}} n_0}{m_{\mathrm{B}}}}, \tag{5.10}$$

is the speed of sound in the BEC. Finally, n_0 is the density of the bath particles in the ground state, which turns out to be constant as a result of the homogeneity of the BEC. For a macroscopically occupied condensate, i.e. $N_{j\neq 0} \ll N_0$ where N_j is the occupation number of the j^{th} state, we obtain the following expression for the interaction part of the Hamiltonian

$$H_{\mathrm{IB}}^{(j)} = n_0 C_{\mathrm{IB}}^{(j)} + \sqrt{\frac{n_0}{V}} \sum_{\mathbf{k}\neq 0} \rho_{\mathrm{I}}^{(j)}(\mathbf{k})\, C_{\mathrm{IB}}^{(j)} \left(a_{\mathbf{k}} + a_{-\mathbf{k}}^\dagger\right), \tag{5.11}$$

which after the Bogoliubov transformation, becomes

$$H_{\mathrm{IB}}^{(j)} = \sum_{\mathbf{k}\neq 0} V_{\mathbf{k}}^{(j)} e^{i\mathbf{k}\cdot(\mathbf{x}_j+\mathbf{d}_j)} \left(b_{\mathbf{k}} + b_{-\mathbf{k}}^\dagger\right). \tag{5.12}$$

Here, the couplings are

$$V_{\mathbf{k}}^{(j)} = g_{\mathrm{IB}}^{(j)} \sqrt{\frac{n_0}{V}} \left[\frac{(\xi\mathbf{k})^2}{(\xi\mathbf{k})^2 + 2}\right]^{\frac{1}{4}}. \tag{5.13}$$

After this procedure the Hamiltonian is transformed into

$$H = H_{\mathrm{I}}^{(1)} + H_{\mathrm{I}}^{(2)} + \sum_{\mathbf{k}\neq 0} E_{\mathbf{k}} b_{\mathbf{k}}^\dagger b_{\mathbf{k}} + \sum_{\mathbf{k}\neq 0} \left[V_{\mathbf{k}}^{(1)} e^{i\mathbf{k}\cdot(\mathbf{x}_1+\mathbf{d}_1)} + V_{\mathbf{k}}^{(2)} e^{i\mathbf{k}\cdot(\mathbf{x}_2+\mathbf{d}_2)}\right] \left(b_{\mathbf{k}} + b_{-\mathbf{k}}^\dagger\right). \tag{5.14}$$

The above Hamiltonian with a non-linear interacting part is in general difficult to treat, and requires the usage of influence functional techniques (Duarte and Caldeira, 2009). To

simplify the situation we will resort to the so called long-wave or dipole approximation. This is expressed by the assumption

$$\mathbf{k}\cdot\mathbf{x}_1 \ll 1, \quad \mathbf{k}\cdot\mathbf{x}_2 \ll 1, \tag{5.15}$$

such that we can approximate the exponentials by a linear function. The validity of the linear approximation was studied in (Lampo *et al.*, 2017b). For the untrapped impurities, it turned into a condition of a maximum time as a function of T for which the linear approximation holds. For the trapped case, the condition was over the trapping frequency as a function of T. The results we present here fulfill these conditions. With this, the Hamiltonian reads

$$H_{\text{Lin}} = H_{\text{I}}^{(1)} + H_{\text{I}}^{(2)} + \sum_{\mathbf{k}\neq 0} E_{\mathbf{k}} b_{\mathbf{k}}^{\dagger} b_{\mathbf{k}} + \sum_{\mathbf{k}\neq 0} \widetilde{V}_{\mathbf{k}} \left[\mathbb{I} + i\mathbf{k} f_{\mathbf{k}}\left(\mathbf{x}_1, \mathbf{x}_2, \mathbf{d}_1, \mathbf{d}_2\right)\right] \left(b_{\mathbf{k}} + b_{-\mathbf{k}}^{\dagger}\right),$$

with $\mathbb{I}$ the identity and where

$$\widetilde{V}_{\mathbf{k}}\left(\mathbf{d}_1, \mathbf{d}_2\right) := V_{\mathbf{k}}^{(1)} e^{i\mathbf{k}\cdot\mathbf{d}_1} + V_{\mathbf{k}}^{(2)} e^{i\mathbf{k}\cdot\mathbf{d}_2}, \tag{5.16}$$

and

$$f_{\mathbf{k}}\left(\mathbf{x}_1, \mathbf{x}_2, \mathbf{d}_1, \mathbf{d}_2\right) := \frac{V_{\mathbf{k}}^{(1)} \mathbf{x}_1 e^{i\mathbf{k}\cdot\mathbf{d}_1} + V_{\mathbf{k}}^{(2)} \mathbf{x}_2 e^{i\mathbf{k}\cdot\mathbf{d}_2}}{V_{\mathbf{k}}^{(1)} e^{i\mathbf{k}\cdot\mathbf{d}_1} + V_{\mathbf{k}}^{(2)} e^{i\mathbf{k}\cdot\mathbf{d}_2}}. \tag{5.17}$$

Performing the transformation $b_{\mathbf{k}} \to b_{\mathbf{k}} - \frac{\widetilde{V}_{-\mathbf{k}}(\mathbf{d}_1, \mathbf{d}_2)}{E_{\mathbf{k}}}\mathbb{I}$, one obtains the following Hamiltonian

$$H_{\text{Lin}} = \sum_{j=1,2} H_{\text{I}}^{(j)} + i \sum_{\substack{j=1,2 \\ \mathbf{k}\neq 0}} \hbar g_{\mathbf{k}}^{(j)} \left(e^{i\mathbf{k}\cdot\mathbf{d}_j} b_{\mathbf{k}} - e^{-i\mathbf{k}\cdot\mathbf{d}_j} b_{\mathbf{k}}^{\dagger}\right) \mathbf{x}_j + \sum_{\mathbf{k}\neq 0} E_{\mathbf{k}} b_{\mathbf{k}}^{\dagger} b_{\mathbf{k}} + W\left(\mathbf{d}_1, \mathbf{d}_2\right)\left[\mathbf{x}_1 + \mathbf{x}_2\right], \tag{5.18}$$

with

$$W\left(\mathbf{d}_1, \mathbf{d}_2\right) = 2i \sum_{\mathbf{k}\neq 0} \frac{\mathbf{k} V_{\mathbf{k}}^{(1)} V_{\mathbf{k}}^{(2)} \cos\left(\mathbf{k}\cdot\mathbf{R}_{12}\right)}{\hbar\omega_{\mathbf{k}}}, \tag{5.19}$$

where $\mathbf{R}_{jq} = |\mathbf{d}_j - \mathbf{d}_q|$, and $g_{\mathbf{k}}^{(j)} = \frac{\mathbf{k}\mathbf{V}_{\mathbf{k}}^{(\mathbf{j})}}{\hbar}$. At this point we note that, to preserve the bare oscillator potential in Eq. (5.8) and hence ensure a positively defined Hamiltonian, it is conventional to introduce a counter term to the Hamiltonian. In this way the Hamiltonian at hand can be interpreted as a minimal coupling theory with $U(1)$ gauge symmetry Kohler and Sols (2013). This term is important because its introduction guarantees that no "runaway" solutions appear in the system, as shown in (Coleman and Norton, 1962a). Nevertheless, we are committed not to introduce any artificial terms in the Hamiltonian and maintaining the fact that we are considering a Hamiltonian that describes a physical system. We will however identify a condition under which the problem of "runaway" solutions will not appear.

For the trapped impurities case, Hamiltonian (5.18) shows similarities to the Hamiltonian that describes the interaction of three harmonic oscillators in a common heat bath (Valido *et al.*, 2013a). However, the two Hamiltonians differ in the following three aspects: First, our Hamiltonian describes the interaction as a coupling between the position of the particle and a modified expression of the momentum of the bath particles while (Valido *et al.*, 2013a) describes a position-position interaction. Second, the term $W\left(\mathbf{d}_1,\mathbf{d}_2\right)\left[\mathbf{x}_1+\mathbf{x}_2\right]$ is absent in the Hamiltonian in (Valido *et al.*, 2013a); Finally, our Hamiltonian lacks the counter term which is artificially introduced in (Valido *et al.*, 2013a) that results in a renormalization of the potential of the harmonic oscillator.

5.1.2 Heisenberg equations

From here on we treat only the one dimensional case, i.e. we assume that the BEC and the impurities are so tightly trapped in two directions as to effectively freeze the dynamics in those directions. In practice, the one dimensional coupling constant has to be treated appropriately, as discussed in (Olshanii, 1998). To study the out-of-equilibrium dynamics of the system, we first obtain the Heisenberg equations, which read as

$$\frac{dx_j}{dt}=\frac{i}{\hbar}\left[H,x_j\right]=\frac{p_j}{m_j}, \tag{5.20a}$$

$$\frac{dp_j}{dt}=\frac{i}{\hbar}\left[H,p_j\right]=-m_j\Omega_j^2x_j\left(t\right)-i\sum_{k\neq0}\hbar g_k^{(j)}\left(b_ke^{ikd_j}-b_k^{\dagger}e^{-ikd_j}\right), \tag{5.20b}$$

$$\frac{db_k}{dt}=\frac{i}{\hbar}\left[H,b_k\right]=-i\omega_kb_k-\sum_{j=1}^{2}g_k^{(j)}e^{-ikd_j}x_j, \tag{5.20c}$$

$$\frac{db_k^{\dagger}}{dt}=\frac{i}{\hbar}\left[H,b_k^{\dagger}\right]=i\omega_kb_k^{\dagger}-\sum_{j=1}^{2}g_k^{(j)}e^{ikd_j}x_j. \tag{5.20d}$$

Next we solve the equations of motion for the bath particles (5.20c) and (5.20d),

$$b_k\left(t\right)=b_k\left(0\right)e^{-i\omega_kt}-\int_0^t\sum_{j=1}^{2}g_k^{(j)}e^{-ikd_j}x_j\left(s\right)e^{-i\omega_k(t-s)}ds, \tag{5.21}$$

$$b_k^{\dagger}\left(t\right)=b_k^{\dagger}\left(0\right)e^{i\omega_kt}-\int_0^t\sum_{j=1}^{2}g_k^{(j)}e^{ikd_j}x_j\left(s\right)e^{i\omega_k(t-s)}ds. \tag{5.22}$$

Replacing these in Eqs.(5.20a)-(5.20b) yields the following equations of motion for the two particles

$$m_j\ddot{x}_j+m_j\Omega_j^2x_j+m_jW\left(d_1,d_2\right)-\int_0^t\sum_{q=1}^{2}\lambda_{jq}\left(t-s\right)x_q\left(s\right)ds=B_j\left(t,d_j\right), \tag{5.23}$$

where $B_j\left(t,d_j\right)$ plays the role of the stochastic fluctuating forces, given by

$$B_j\left(t,d_j\right)=\sum_{k\neq0}i\hbar g_k^{(j)}\left[e^{i(\omega_kt-kd_j)}b_k^{\dagger}\left(0\right)-e^{-i(\omega_kt-kd_j)}b_k\left(0\right)\right], \tag{5.24}$$

and the memory friction kernel $\lambda_{jq}(t-s)$ reads as

$$\lambda_{jq}(t) = \sum_{k\neq 0} \Theta\left(t - \left|\frac{kR_{jq}}{\omega_k}\right|\right) \tilde{g}_k^{(jq)} \sin\left(kR_{jq} + \omega_k (t-s)\right), \tag{5.25}$$

with, $\tilde{g}_k^{(jq)} = 2\hbar g_k^{(j)} g_k^{(q)}$. In the literature, $\lambda_{jq}(t)$, is also referred to as the dissipation kernel, or also the susceptibility. The Heaviside function guarantees causality by introducing the corresponding retardation due to the finite distance $d_j - d_q$ between the centers of the two harmonic oscillators. The two are related by the Kubo formula as

$$\lambda_{jq}(t-s) = -i\Theta\left(t - \left|\frac{kR_{jq}}{\omega_k}\right|\right) \langle [B_j(t,d_j), B_q(s,d_q)] \rangle_{\rho_B}. \tag{5.26}$$

Hence, we understand that the reason the Heaviside step function arises is due to the fact that the forces commute for time-like separations. On the left hand side of Eq. (5.23) appears a restoring force which is originated by the fact that the impurities are similar to two harmonic oscillators. Furthermore, also non-local terms appear due to the interaction of the impurities with the environment, in particular a dissipative self-force and a history-dependent non-Markovian interaction between the two impurities. Both of these non-linear terms are a consequence of the coupling of the impurities to the bath. On the right hand side, the stochastic fluctuating force appears with Gaussian statistics, i.e. the first moment, which is assumed to be $\langle B_j(t,d_j)\rangle = 0$ for $j = 1, 2$, and the second moment of the probability distribution related to the state of the stochastic driving force $B_j(t,d_j)$ is enough to describe the state of the bath.

There is another equivalent way of writing the equations of motion for the particles, in terms of the damping kernel $\Gamma_{jq}(t-s)$, related to the susceptibility as $\frac{1}{m_j}\lambda_{jq}(t-s) := -\frac{\partial}{\partial t}\Gamma_{jq}(t-s)$, which will enable us to identify a condition on the range of parameters for which our system is valid. Making use of the Leibniz integral rule, one can show that

$$-\frac{1}{m_j}\int_0^t \lambda_{jq}(t-s)\, x_q(s)\, ds = -\Gamma_{jq}(0)\, x_q(t) + \frac{\partial}{\partial t}\int_0^t \Gamma_{jq}(t-s)\, x_q(s)\, ds. \tag{5.27}$$

With this, one can rewrite the equations of motion for each particle position in terms of the damping kernel

$$\ddot{x_j} + \Omega_j^2 x_j - \sum_{q=1}^{2} \Gamma_{jq}(0)\, x_q(t) + \frac{1}{m_j} W(d_1, d_2) + \frac{\partial}{\partial t}\left[\int_0^t \sum_{q=1}^{2} \Gamma_{jq}(t-s)\, x_q(s)\, ds\right] = \frac{1}{m_j} B_j(t,d_j). \tag{5.28}$$

One can identify that $\Gamma_{jq}(0)\, x_q(t)$ in equations of motion (5.28) play the role of renormalization terms of the harmonic potential. Most importantly, these terms will not be present in case one includes a counter term in the initial Hamiltonian, Eq. (5.18). Under

the assumption of weak coupling, one expects that these terms will not affect the long-time behaviour of the system, as explained in (Breuer and Petruccione, 2007b). At the end of this section we obtain the necessary condition that ensures the positivity of the Hamiltonian.

It is useful to write Eqs. (5.23) as a single vectorial equation,

$$\underline{\ddot{X}}\left(t\right)+\underline{\underline{\Omega}}^{2}\underline{X}\left(t\right)-\underline{\underline{M}}^{-1}\int_{0}^{t}\underline{\underline{\lambda}}\left(t-s\right)\underline{X}\left(s\right)ds=\underline{\underline{M}}^{-1}\left(\underline{B}^{T}\left(t,d_{1},d_{2}\right)-\underline{W}\left(d_{1},d_{2}\right)\mathbb{I}\right)\mathbb{I}, \tag{5.29}$$

where

$$\underline{X}\left(t\right)=\begin{pmatrix}x_{1}\left(t\right)\\x_{2}\left(t\right)\end{pmatrix},\quad\underline{\underline{M}}=\begin{pmatrix}m_{1}&0\\0&m_{2}\end{pmatrix},\quad\underline{\underline{\Omega}}^{2}=\begin{pmatrix}\Omega_{1}^{2}&0\\0&\Omega_{2}^{2}\end{pmatrix}, \tag{5.30}$$

$$\underline{W}\left(d_{1},d_{2}\right)=\begin{pmatrix}W_{1}\left(d_{1},d_{2}\right)\\W_{2}\left(d_{1},d_{2}\right)\end{pmatrix}, \tag{5.31}$$

$$\underline{\underline{\lambda}}\left(t-s\right)=\begin{pmatrix}\lambda_{11}\left(t-s\right)&\lambda_{12}\left(t-s\right)\\\lambda_{21}\left(t-s\right)&\lambda_{22}\left(t-s\right)\end{pmatrix}, \tag{5.32}$$

$$\underline{B}\left(t,d_{1},d_{2}\right)=\begin{pmatrix}B_{1}\left(t,d_{1}\right)\\B_{2}\left(t,d_{2}\right)\end{pmatrix}. \tag{5.33}$$

Equivalently, the vectorial equation that corresponds to Eqs. (5.28) (i.e. in terms of the damping kernel), is

$$\underline{\ddot{X}}\left(t\right)+\underline{\underline{\tilde{\Omega}}}^{2}\underline{X}\left(t\right)+\frac{\partial}{\partial t}\int_{0}^{t}\underline{\underline{\Gamma}}\left(t-s\right)\underline{X}\left(s\right)ds=\underline{\underline{M}}^{-1}\left(\underline{B}^{T}\left(t,d_{1},d_{2}\right)-\underline{W}\left(d_{1},d_{2}\right)\right)\mathbb{I}, \tag{5.34}$$

where

$$\underline{\underline{\Gamma}}\left(t-s\right)=\begin{pmatrix}\Gamma_{11}\left(t-s\right)&\Gamma_{12}\left(t-s\right)\\\Gamma_{21}\left(t-s\right)&\Gamma_{22}\left(t-s\right)\end{pmatrix}, \tag{5.35}$$

$$\underline{\underline{\tilde{\Omega}}}^{2}=\begin{pmatrix}\Omega_{1}^{2}-\Gamma_{11}\left(0\right)&-\Gamma_{12}\left(0\right)\\-\Gamma_{21}\left(0\right)&\Omega_{2}^{2}-\Gamma_{22}\left(0\right)\end{pmatrix}. \tag{5.36}$$

We then introduce the transformation matrix $\underline{Q}=\underline{\underline{O}}\,\underline{X}$ such that Eq. (5.34) transforms into

$$\underline{\ddot{Q}}\left(t\right)+\underline{\underline{\tilde{\Omega}_{\mathrm{D}}}}^{2}\underline{Q}\left(t\right)+\frac{\partial}{\partial t}\int_{0}^{t}\underline{\underline{\Xi}}\left(t-s\right)\underline{Q}\left(s\right)ds=\underline{\underline{M}}^{-1}\left(\underline{D}^{T}\left(t,d_{1},d_{2}\right)-\underline{\underline{O}}W\left(d_{1},d_{2}\right)\right)\mathbb{I}, \tag{5.37}$$

where $\underline{\underline{\Xi}}\left(t-s\right)=\underline{\underline{O}}\,\underline{\underline{\Gamma}}\left(t-s\right)\underline{\underline{O}}^{T}$, $\underline{D}^{T}\left(t,d_{1},d_{2}\right)=\underline{\underline{O}}\,\underline{B}^{T}\left(t,d_{1},d_{2}\right)$ and

$$\underline{\underline{\tilde{\Omega}_{\mathrm{D}}}}=\underline{\underline{O}}\,\underline{\underline{\tilde{\Omega}}}^{2}\underline{\underline{O}}^{T}=\begin{pmatrix}\tilde{\Omega}_{\mathrm{D}}^{1}&0\\0&\tilde{\Omega}_{\mathrm{D}}^{2}\end{pmatrix}, \tag{5.38}$$

i.e. it is diagonal. In the following sections we solve Eqs (5.29) and (5.34) for the cases under study, by considering the Laplace or Fourier transforms as is presented in section 5.1.4.

We now identify from Equation (5.29) the condition under which even though the Hamiltonian lacks an *ad hoc* introduced renormalization term, this does not affect the long-time dynamics of the particles. This condition is that both $\tilde{\Omega}_{\mathrm{D}}^{1}\,,\,\tilde{\Omega}_{\mathrm{D}}^{2}>0$, because this way the Hamiltonian remains positive–definite and diverging solutions are avoided. In particular, it is required that

$$\frac{1}{2}\Big[\Gamma_{11}\left(0\right)+\Gamma_{22}\left(0\right)-\Omega_{1}^{2}-\Omega_{2}^{2}+\Big[4\Gamma_{12}\left(0\right)\Gamma_{21}\left(0\right)+\left(\Gamma_{11}\left(0\right)-\Gamma_{22}\left(0\right)-\Omega_{1}^{2}+\Omega_{2}^{2}\right)^{2}\Big]^{1/2}\Big]<0. \tag{5.39}$$

This imposes a restriction on the coupling constants range. Note that if we decouple the second particle i.e. if $g_{k}^{(2)}=0$ for all k, then we obtain the same condition as for the one particle, $\Omega_{1}^{2}>\Gamma_{11}\left(0\right)$ (Lampo *et al.*, 2017b).

5.1.3 Spectral density

Let us write the dissipation kernel in Eq. (5.25) as

$$\lambda_{jq}\left(t-s\right)=\int_{0}^{\infty}\Big[J_{jq}^{\text{antisym.}}\left(\omega\right)\cos\left(\omega\left(t-s\right)\right)+J_{jq}^{\text{sym.}}\left(\omega\right)\sin\left(\omega\left(t-s\right)\right)\Big]\,d\omega, \tag{5.40}$$

where we identify the spectral densities as

$$J_{jq}^{\text{antisym.}}\left(\omega,t-s\right)=\sum_{k\neq0}\Theta\left(t-s-\left|\frac{kR_{jq}}{\omega_{k}}\right|\right)\tilde{g}_{k}^{(jq)}\delta\left(\omega-\omega_{k}\right)\sin\left(kR_{jq}\right), \tag{5.41}$$

and

$$J_{jq}^{\text{sym.}}\left(\omega,t-s\right)=\sum_{k\neq0}\Theta\left(t-s-\left|\frac{kR_{jq}}{\omega_{k}}\right|\right)\tilde{g}_{k}^{(jq)}\delta\left(\omega-\omega_{k}\right)\cos\left(kR_{jq}\right). \tag{5.42}$$

We note that $g_{k}^{(j)}g_{k}^{(q)}$ is an even function of k, which implies that $J_{jq}^{\text{antisym.}}\left(\omega\right)=0$. Then, in App. B.1 we show that in the continuum limit of the spectrum, Eq. (5.40) takes the following integral form for a system with 1D environment

$$\lambda_{jq}\left(t-s\right)=\int_{0}^{\infty}\Theta\left(t-s-\left|\frac{k_{\omega}R_{jq}}{\omega}\right|\right)J_{jq}\left(\omega\right)\sin\left(\omega\left(t-s\right)\right)d\omega, \tag{5.43}$$

with

$$J_{jq}\left(\omega\right)=\widetilde{\tau}_{jq}\omega^{3}\cos\left(k_{\omega}R_{jq}\right)\chi_{1D}\left(\omega\right), \tag{5.44}$$

where

$$\widetilde{\tau}_{jq}=2\tilde{m}\tau\eta_{j}\eta_{q}, \tag{5.45}$$

with

$$\eta_j = \frac{g_{\mathrm{IB}}^{(j)}}{g_{\mathrm{B}}}, \tag{5.46}$$

and

$$\tau = \frac{1}{2\pi\tilde{m}} \left(\frac{m_{\mathrm{B}}}{n_0 g_{\mathrm{B}}^{1/3}} \right)^{3/2}, \tag{5.47}$$

represents the relaxation time, with $\tilde{m} = \frac{m_1 m_2}{m_1+m_2}$. For the single impurity case, $R_{12} = 0$ and $\eta_2 = 0$, we obtain a cubic dependence of the spectral density on ω, in accordance with the results obtained in (Lampo *et al.*, 2017b). It is worth noting here that the validity of the Fröhlich type Hamiltonian we have here imposes a restriction on η_j (Grusdt and Demler, 2015, Grusdt *et al.*, 2017a), namely

$$\eta_j \leqslant \pi \sqrt{\frac{2n_0}{g_{\mathrm{B}} m_{\mathrm{B}}}}. \tag{5.48}$$

Therefore, we restrict ourselves within this limit, which for typical values of the related parameters, such as for example $g_{\mathrm{B}} = 2.36 \times 10^{-37} J \cdot m$ and $n_0 = 7\,(\mu m)^{-1}$ which are values that were experimentally considered in (Catani *et al.*, 2012b), becomes $\eta^{(cr)} \approx 7$. This condition is satisfied for all the values of η_j, g_{B} and n_0 considered here. Note also that within the range of coupling strengths that we will consider, we assume that we also avoid the scenario of the two impurities forming a bipolaron (Casteels *et al.*, 2013), i.e. that $\left(g_{IB}^{(j)}\right)^2 / \xi g_B < 1.22$ for $j = 1, 2$. Finally, k_ω in Eq. (5.44) is the inverse of the Bogoliubov spectrum

$$k_\omega = \frac{1}{\xi} \sqrt{\sqrt{1 + 2\left(\frac{\xi\omega}{c}\right)^2} - 1},$$

and the susceptibility is

$$\chi_{1\mathrm{D}}(\omega) = 2\sqrt{2} \left(\frac{\Lambda}{\omega}\right)^3 \frac{\left[\sqrt{1 + \frac{\omega^2}{\Lambda^2}} - 1\right]^{\frac{3}{2}}}{\sqrt{1 + \frac{\omega^2}{\Lambda^2}}}, \tag{5.49}$$

where c is the speed of sound, ξ the coherence length, and

$$\Lambda = \frac{g_{\mathrm{B}} n_0}{\hbar}. \tag{5.50}$$

One identifies two opposite limits for $\chi_{1D}(\omega)$, i.e. $\omega \ll \Lambda$ and $\omega \gg \Lambda$. Hence Λ appears naturally as the characteristic cutoff frequency to distinguish between low and high frequencies. Note that the spectral density exhibits a super-ohmic behaviour given by the third power of the bath frequency in the continuous limit. Same behaviour was found in (Efimkin *et al.*, 2016b, Bonart and Cugliandolo, 2012b, Peotta *et al.*, 2013) for analogous problems, and it is attributed to the linear part of the Bogoliubov spectrum. With such

a spectral density, it can be shown that certain quantities, e.g. the momentum dispersion would be divergent, unless the high frequencies are somehow removed from the spectrum. This can be achieved by introducing an ultraviolet cutoff given by Λ such that only the part of the spectrum where $\omega < \Lambda$ remains. Upon doing so, $\chi_{1D}(\omega) \to 1$, and the Bogoliubov spectrum takes the linear form $\omega = c|k|$ such that the spectral density becomes

$$J_{jq}(\omega) = \widetilde{\tau}_{jq}\omega^3 \cos\left(\frac{\omega}{c}R_{jq}\right). \tag{5.51}$$

We consider two different possible analytical forms of the cut-off, the sharp one

$$J_{jq}(\omega) = \widetilde{\tau}_{jq}\omega^3 \cos\left(\frac{\omega}{c}R_{jq}\right)\Theta(\omega - \Lambda), \tag{5.52}$$

provided by an Heaviside function, and the exponential cutoff

$$J_{jq}(\omega) = \widetilde{\tau}_{jq}\omega^3 \cos\left(\frac{\omega}{c}R_{jq}\right)e^{-\frac{\omega}{\Lambda}}. \tag{5.53}$$

In (Lampo *et al.*, 2017b), it is shown that the physics of the system in the long-time limit, *i.e.* associated to frequency regime $\omega \ll \Lambda$, does not depend on the existence, nor the form, of the cutoff. In this paper we will use both types of cutoffs depending on the problem at hand, namely we will use the exponential cutoff whenever we study the problem for distances between the traps of each kind of impurity different than 0 and the sharp cutoff otherwise. Finally, note that in comparison to the equations of motion obtained in (Valido *et al.*, 2013a), in our case the couplings of the two particles can be different, adding an extra parameter.

5.1.4 Solution of Heisenberg equations and covariance matrix

To evaluate the covariances one needs to solve the above equations of motion. In particular, we solve Eq. (5.34) by first obtaining the solution for the homogeneous equation, and then adding to that the particular solution (Breuer and Petruccione, 2007b, Lampo *et al.*, 2017b),

$$\underline{X}(t) = \underline{\underline{G_1}}(t)\,\underline{X}(0) + \underline{\underline{G_2}}(t)\,\dot{\underline{X}}(0) + \int_0^t ds\,\underline{\underline{G_2}}(t-s)\left[\left(\underline{B}^T(s,d_1,d_2) - \underline{W}(d_1,d_2)\right)\mathbb{I}\right], \tag{5.54}$$

where

$$\mathcal{L}_z\left[\underline{\underline{G_1}}(t)\right] = \frac{z\mathbb{I}}{z^2\mathbb{I} + \mathbb{I}\underline{\underline{\tilde{\Omega}}}^2 + z\mathcal{L}_z\left[\underline{\Gamma}(t)\right]}, \tag{5.55}$$

and

$$\mathcal{L}_z\left[\underline{\underline{G_2}}(t)\right] = \frac{1}{z^2\mathbb{I} + \mathbb{I}\underline{\underline{\tilde{\Omega}}}^2 + z\mathcal{L}_z\left[\underline{\Gamma}(t)\right]}, \tag{5.56}$$

with $\mathcal{L}_z[\cdot]$ denoting the Laplace transform. Notice that the second function is often referred to as the susceptibility, in analogy with the harmonic oscillator. It basically

carries the same information as $\frac{\partial}{\partial t}\underline{\underline{\Gamma}}(t-s)$, which is what we refer to as susceptibility in this paper. We now need to evaluate the covariance matrix

$$C(0)=\begin{pmatrix} C_{\underline{\mathrm{X}}\underline{\mathrm{X}}}(0) & C_{\underline{\mathrm{X}}\underline{\mathrm{P}}}(0) \\ C_{\underline{\mathrm{P}}\underline{\mathrm{X}}}(0) & C_{\underline{\mathrm{P}}\underline{\mathrm{P}}}(0) \end{pmatrix}, \tag{5.57}$$

with $\underline{P}(t)=(p_1(t),p_2(t))^T$ the momentum vector and

$$C_{\mathrm{AB}}(t-t')=\frac{1}{2}\left\langle A(t)B^T(t')+B(t')A^T(t)\right\rangle. \tag{5.58}$$

Hence, matrix (5.57) is constructed from the vector $Y(t)=(x_1(t),x_2(t),p_1(t),p_2(t))$ as the product $\frac{1}{2}\langle\{\underline{Y}^T(t)\cdot\underline{Y}(t),(\underline{Y}^T(t)\cdot\underline{Y}(t))^T\}\rangle_{\rho_{\mathrm{B}}}$. Furthermore, if we assume the initial state of the system to be of the Feynman-Vernon type, i.e. $\rho(0)=\rho_{12}(0)\otimes\rho_{\mathrm{B}}$, then quantities like $\left\langle\underline{X}(0)\underline{B}^T(t,d_1,d_2)\right\rangle$ will vanish. We note that the appearance of the extra term $W(d_1,d_2)$ in the dynamics, absent in (Valido *et al.*, 2013a), indeed does not affect the evaluation of the covariance matrix since we are only interested in averages with respect to the state of the bath. In addition, the bath is assumed to be large enough such that the effects of the impurity dynamics on the state of the bath are assumed to be negligible. Proceeding in a similar manner as in (Lampo *et al.*, 2017b) for a thermal equilibrium bath at temperature T we conclude that the equal time correlation function of position reads as

$$C_{x_jx_q}(0)=\hbar\int_0^\infty d\omega\coth\left[\frac{\hbar\omega}{2k_{\mathrm{B}}T}\right]K_{jq}(\omega), \tag{5.59}$$

where

$$K_{jq}(\omega)=\sum_{k,s=1}^{2}\left(\mathcal{L}_{-i\omega}\left[\underline{\underline{G_2}}(t)\right]\right)_{jk}J_{ks}(\omega)\left(\mathcal{L}_{i\omega}\left[\underline{\underline{G_2}}(t)\right]\right)_{sq}. \tag{5.60}$$

Similarly, one can obtain the position-momentum and momentum-momentum blocks of the covariance matrix,

$$C_{x_jp_q}(0)=\hbar\int_0^\infty d\omega\,(im_q\omega)\coth\left[\frac{\hbar\omega}{2k_{\mathrm{B}}T}\right]K_{jq}(\omega), \tag{5.61}$$

and

$$C_{p_jp_q}(0)=\hbar\int_0^\infty d\omega m_jm_q\omega^2\coth\left[\frac{\hbar\omega}{2k_{\mathrm{B}}T}\right]K_{jq}(\omega). \tag{5.62}$$

Notice that for $g_k^2=0\;\forall k$, i.e. by removing the second particle from the system, one reproduces the expressions provided in (Lampo *et al.*, 2017b) for the single particle case, by considering the Laplace transform of the damping kernel $\mathcal{L}_z\left[\underline{\underline{\Gamma}}(t)\right]$. Importantly, in the presence of the second particle, the expressions for (5.59), (5.61) and (5.62) can still be obtained with the method described in (Lampo *et al.*, 2017b), but only when $d_j-d_q=0$,

i.e. when the centers of the particle potentials are in the same position. Indeed, for $d_j - d_q = 0$, the Laplace transform of the damping kernel can be computed as

$$\mathcal{L}_z\left[\Gamma_{jq}(t)\right] = z\widetilde{\tau}_{jq}\left[\Lambda - z\arctan\left(\frac{\Lambda}{z}\right)\right]. \tag{5.63}$$

However, if $d_j - d_q \neq 0$, $\mathcal{L}_z\left[\underline{\underline{\Gamma}}(t)\right]$ cannot be obtained as the integral does not converge. In such case, we use the method presented in (Valido *et al.*, 2013a), where the Fourier transform of the susceptibility is evaluated instead, through the usage of the Hilbert transform to solve Eq. (5.29). In the following, we find that we circumvent the aforementioned problem by using the Fourier method. By doing so, we are avoiding the integral on the imaginary axis, since the following relation is known between the Fourier and Laplace transforms

$$\tilde{f}_{\pm}(\omega) = lim_{\epsilon\to 0}[\hat{f}(\epsilon + i\omega) \pm \hat{f}(\epsilon - i\omega)], \tag{5.64}$$

for even (+) and odd (-) functions respectively, for the functions $J(\omega)$, i.e. the spectral density, and $\lambda(\omega)$, i.e. the susceptibility, where the definition of the Fourier transform is (Fleming and Cummings, 2011)

$$\tilde{f}(\omega) = \int_{-\infty}^{+\infty} dt e^{-i\omega t} f(t)[\theta(t) + \theta(-t)]. \tag{5.65}$$

The correlation functions take the following form

$$C_{\mathrm{x_j x_q}}(0) = \frac{\hbar}{2\pi}\int_{-\infty}^{\infty} d\omega \coth\left[\frac{\hbar\omega}{2k_{\mathrm{B}}T}\right] Q_{jq}(\omega), \tag{5.66}$$

where

$$Q_{jq}(\omega) = \sum_{k,s=1}^{2} \left(\underline{\underline{\alpha}}(\omega)\right)_{js} \cdot \mathrm{Im}\left[\underline{\underline{\lambda}}(\omega)\right]_{sk} \cdot \left(\underline{\underline{\alpha}}(-\omega)\right)_{kq}, \tag{5.67}$$

and Im[.] is the imaginary part. Here,

$$\underline{\underline{\alpha}}(\omega) = \frac{1}{-\omega^2\mathbb{I} + \underline{\underline{\Omega}}^2\mathbb{I} + \frac{1}{\underline{\underline{M}}}\mathcal{F}_\omega\left[\underline{\underline{\lambda}}(t)\right]}. \tag{5.68}$$

From (Valido *et al.*, 2013a) we have

$$\mathrm{Im}[\underline{\underline{\lambda}}(\omega)] = -\hbar\left(\Theta(\omega) - \Theta(-\omega)\right)\underline{\underline{J}}(\omega), \tag{5.69}$$

where $\underline{\underline{\lambda}}(\omega)$ is the Fourier transform of the susceptibility $\underline{\underline{\lambda}}(t)$. We remind that the bath is assumed to be at thermal equilibrium. Equation (5.66) was proven in (Ludwig *et al.*, 2010). The other autocorrelation functions can be obtained in a similar way once we relate the momentum to the time derivative of the position as

$$C_{x_j p_q}(0) = \frac{\hbar}{2\pi}\int_{-\infty}^{\infty} d\omega\, (im_q\omega) \coth\left[\frac{\hbar\omega}{2k_{\mathrm{B}}T}\right] Q_{jq}(\omega), \tag{5.70}$$

and

$$C_{p_j p_q}(0) = \frac{\hbar}{2\pi}\int_{-\infty}^{\infty} d\omega m_j m_q \omega^2 \coth\left[\frac{\hbar\omega}{2k_{\mathrm{B}}T}\right] Q_{jq}(\omega)\,. \tag{5.71}$$

To proceed further, one needs to evaluate $\mathcal{F}_\omega\left[\underline{\underline{\lambda}}(t)\right]$ that appears in Eq. (5.68). We already know the imaginary part of the susceptibility from Eq. (5.69). The real part of the susceptibility can be obtained by making use of the Kramers-Kronig relations, which mathematically means that one has to take the Hilbert transform $\mathcal{H}$ of the imaginary part of the susceptibility

$$\begin{aligned}\mathrm{Re}\left[\lambda_{jq}(\omega')\right] &= \mathcal{H}\left[\mathrm{Im}[\lambda_{jq}(\omega)]\right](\omega') \\ &= \frac{1}{\pi}\mathcal{P}\int_{-\infty}^{\infty}\frac{\mathrm{Im}[\lambda_{jq}(\omega)]}{\omega-\omega'}d\omega,\end{aligned} \tag{5.72}$$

where Re is the real part and P denotes the Cauchy principal value.

For the particular form of the spectral density in Eq. (5.53), the susceptibility takes the following form:

$$\begin{aligned}\lambda_{jq}(\omega) = -\frac{\hbar\widetilde{\tau}_{jq}}{\pi}\Bigg\{&\omega^3\mathrm{Re}\left[g(\omega)-g(-\omega)\right] + \pi\omega^3\mathrm{Im}\left[\Theta(\omega)\,e^{-\frac{\omega}{\Lambda}+i\frac{\omega}{c}R_{jq}} + \Theta(-\omega)\,e^{\frac{\omega}{\Lambda}-i\frac{\omega}{c}R_{jq}}\right] \\ &+ 2\omega^2\frac{\Lambda}{1+\left(\Lambda\frac{R_{jq}}{c}\right)^2} + 4\frac{\left(\frac{1}{\Lambda^3}-3\frac{R_{jq}^2}{\Lambda c^2}\right)}{\left(\frac{1}{\Lambda^2}+\frac{R_{jq}^2}{c^2}\right)^3}\Bigg\} - i\hbar\Theta(\omega)\,\widetilde{\tau}_{jq}\omega^3\cos\left(\frac{\omega}{c}R_{jq}\right)e^{-\frac{\omega}{\Lambda}},\end{aligned} \tag{5.73}$$

with

$$g(\omega) = e^{-\frac{\omega}{\Lambda}+i\frac{\omega}{c}R_{jq}}\Gamma\left[0, -\frac{\omega}{\Lambda}+i\frac{\omega}{c}R_{jq}\right], \tag{5.74}$$

where $\Gamma[\alpha,z] = \int_{-\infty}^{z} t^{\alpha-1}e^{-t}dt$ denotes the incomplete gamma function.

Finally, we remark here that for the case $R_{12} = 0$, one could proceed by using the Laplace transform as initially intended. With the work in (Correa *et al.*, 2012) in mind, one could think that an analytic expression could be obtained, but we explain Appendix B.3, that this method is not applicable for a super-ohmic spectral density, and hence numerical integration should be applied instead, as is the case for the method using the Fourier transform.

Entanglement measure

We will address the existence and dependence of entanglement between the two impurities on the parameters of the model, both for trapped and untrapped impurities. For continuous-variable systems, an entanglement measure based on the density matrix is not conveniently calculable because the density matrix in this case is infinite-dimensional. For Gaussian bipartite states however, there are a number of ways to circumvent this problem (Weedbrook *et al.*, 2012). In general, a state that is not separable is considered

entangled. The well known Peres-Horodecki separability criterion (Peres, 1996, Horodecki *et al.*, 1996), which poses a necessary condition for separability, was shown to be easily formulated for a Gaussian quantum bipartite state through the usage of the symplectic eigenvalues of the covariance matrix of the bipartite system. However, this criterion alone does not allow for a quantification of the entanglement in the system, because it does not offer a way to quantify entanglement that is a monotonic function of the aforementioned symplectic eigenvalues (Hsiang and Hu, 2015). For pure states a unique quantification measure exists, which is the entropy of entanglement (Bennett *et al.*, 1996a). This is defined as the von Neumann entropy of the reduced states of the bipartite system. For mixed states however this is not the case. In this case, there are a number of possible measures of entanglement, such as the entanglement of formation (Bennett *et al.*, 1996b), the distillable entanglement (Horodecki *et al.*, 2009b) and the logarithmic negativity (Vidal and Werner, 2002). The first two are notoriously hard to calculate in general. For this reason we resort to the usage of logarithmic negativity as the most convenient measure to quantify entanglement. The logarithmic negativity is defined as

$$E_{\mathrm{LN}}\left(\rho_{12}\right)=\max\left[0,-\ln\left(2\nu_{-}\right)\right], \tag{5.75}$$

where ρ_{12} is the density matrix of the two impurities and ν_{-} is the smallest symplectic eigenvalue of the partial transpose covariance matrix $C^{T_2}\left(0\right)$, where the partial transpose is taken with respect to the basis of only one of the impurities. Here, we briefly present the method to obtain the symplectic eigenvalues of $C^{T_2}\left(0\right)$. To do so, it will be more convenient to reconstruct the covariance matrix in Eq. (5.57) using the rearranged vector $\hat{Y}\left(t\right)=\left(x_1\left(t\right),p_1\left(t\right),x_2\left(t\right),p_2\left(t\right)\right)$ such that the matrix becomes

$$C\left(0\right)=\begin{pmatrix} C_{11}\left(0\right) & C_{12}\left(0\right) \\ C_{21}\left(0\right) & C_{22}\left(0\right) \end{pmatrix}.$$

Thus, the diagonal matrices $C_{11}\left(0\right)$, $C_{22}\left(0\right)$ represent the covariance matrices of the first and second particle respectively, and $C_{21}\left(0\right)=C_{12}^{T}\left(0\right)$ represent the correlations between the two particles. It can be shown that, for such Gaussian quantum bipartite systems, partial transposition corresponds to time reversal (Horodecki *et al.*, 1998). Therefore the partial transpose of $C\left(0\right)$ with respect to the second particle degrees of freedom is obtained by assigning a minus sign to all the entries of the matrix where $p_2\left(t\right)$ appears. The symplectic spectrum then is obtained as the standard eigenspectrum of $\left|iQC^{T_2}\left(0\right)\right|$ where Q is the symplectic form and $|.|$ represents taking the absolute value. The 4×4 symplectic matrix is defined as

$$\left[\hat{Y}_j\left(t\right),\hat{Y}_q\left(t\right)\right]=i\hbar Q_{jq}, \tag{5.76}$$

which in our case it reads as

$$Q = \begin{pmatrix} 0 & 1 & 0 & 0 \\ -1 & 0 & 0 & 0 \\ 0 & 0 & 0 & 1 \\ 0 & 0 & -1 & 0 \end{pmatrix}.$$

The final result is a diagonal matrix $C^{T_2}_{\text{diag.}}(0)$ with diagonal entries diag $(\nu_1, \nu_1, \nu_2, \nu_2)$ from which the smallest one is selected and introduced in Eq. (5.75) to obtain a quantification of entanglement. At the Hilbert space level, this symplectic diagonalization transforms the state into a tensor product of independent harmonic oscillators (Vidal and Werner, 2002), each of which is in a thermal state, the temperature of which is a function of ν_j. We recall that the Peres-Horodecki criterion states that if a density matrix ρ_{12} of a bipartite system is separable, then $\rho_{12}^{T_2} \geq 0$. The logarithmic negativity quantifies how much this condition is not satisfied (Weedbrook *et al.*, 2012).

In (Adesso *et al.*, 2004, Adesso and Illuminati, 2005) it was shown that logarithmic negativity quantifies the greatest amount of EPR correlations which can be created in a Gaussian state by means of local operations, and in (Plenio, 2005) it was shown that logarithmic negativity provides an upper bound to distillable entanglement. The form of the symplectic eigenvalues can be explicitly given for the bipartite Gaussian system above using symplectic invariants constructed from determinants of the covariance matrix as (Hörhammer and Büttner, 2008, Simon, 2000)

$$\nu_{\pm} = \sqrt{\frac{\Delta \pm \sqrt{\Delta^2 - 4 \det\left[C^{T_2}(0)\right]}}{2}}, \tag{5.77}$$

where $\Delta = \det\left[C_{11}(0)\right] + \det\left[C_{22}(0)\right] - 2\det\left[C_{12}(0)\right]$. In this scenario, the uncertainty relation can also be conveniently expressed in terms of the symplectic invariants constructed from determinants of the covariance matrix. In particular, it becomes equivalent to the following three conditions

$$C^{T_2}(0) > 0, \tag{5.78a}$$

$$\det\left[C^{T_2}(0)\right] \geq \frac{1}{2}, \tag{5.78b}$$

$$\Delta \leq 1 + \det\left[C^{T_2}(0)\right]. \tag{5.78c}$$

This can also be proven to be equivalent to the condition that the lowest eigenvalue of the symplectic matrix of $C(0)$, is larger than $\frac{1}{2}$, i.e.

$$\tilde{\nu}_{-} \geq \frac{1}{2}. \tag{5.79}$$

We notice here that the logarithmic negativity can take arbitrarily large values as ν_{-} can in principle go to 0, with the uncertainty principle still being satisfied. To attain

maximal, finite entanglement, one has to fix the values of both local and global purities of the state of the two-impurity system (Adesso *et al.*, 2004, Adesso and Illuminati, 2005). Note also that one can construct an estimate of entanglement, the average logarithmic negativity, that is a function of these purities, which are easier to measure in an experiment (Adesso *et al.*, 2004, Adesso and Illuminati, 2005). However, in this work we focus on the study of the logarithmic negativity itself, because for the amount of entanglement that we find in our numerical results, average logarithmic negativity is not a good estimate, i.e. the error as defined in (Adesso *et al.*, 2004, Adesso and Illuminati, 2005) is large.

We comment here on the experimental feasibility of our studies. From a practical point of view, there are two kind of terms that appear in the covariance matrix that one should evaluate, single particle expectation values, such as $\langle x_j^2 \rangle, \langle p_j^2 \rangle$, and crossterms such as $\langle x_1 x_2 \rangle, \langle p_1 p_2 \rangle$. For the former, there are already experiments in which one is able to evaluate them (Catani *et al.*, 2012b). The idea is that one measures the position (or momentum) of the particle using a time of flight experiment in a system with a two species ultracold gas, in which one of the species is much more dilute - dilute enough as to consider its atoms as impurities immersed in a much bigger BEC. The position variance is obtained from the time-of-flight experiments, by releasing the atoms into free space initially and after allowing for the free expansion of their wavefunction for some time, measuring their position by irradiating them with a laser. Nevertheless, this method is not ideal for obtaining the real space information of a trapped sample, since during the free expansion process, signals from other atoms can easily be mixed with the signal of the atoms of interest. Furthermore, the current status of time-of-flight experiments does not allow for the measurement of the cross-term covariances, which as of now there are no experiments to measure them, but we believe that one should be able in principle to do so.

In particular, a quantum gas microscope (Sherson *et al.*, 2010, Bakr *et al.*, 2009) might be an option. This technique uses optical imaging systems to collect the fluorescence light of atoms, and has been used in the study of atoms in optical lattices, achieving much better spatial resolution (Sherson *et al.*, 2010, Bakr *et al.*, 2009), and avoiding the aforementioned problem with time-of-flight experiments. With this technique, in principle, one should be able to measure all elements of the covariance matrix.

In the past quantum gas microscopes have been used to study spatial entanglement between itinerant particles, by means of quantum interference of many body twins, which enables the direct measurement of quantum purity (Islam *et al.*, 2015). In addition, there is an alternative way to study entanglement in continuous variable system, and that is by means of the average logarithmic negativity (Adesso *et al.*, 2004). This quantity, can be

related to the global and local purities of our system, which are measurable quantities. Nevertheless this is a more brute measure, since it is not estimated directly from the state of our system, and hence it may miss to detect entanglement for the actual state of our system.

Even if this is the case for average logarithmic negativity, with the knowledge of the existence of this measure and the technique of quantum gas microscopes, one could still consider this way of measuring entanglement as the worst case scenario. In general, it is known that to measure entanglement in a system of continuous variables is a difficult task, which is a problem that is not restricted to our case.

Squeezing

Once the covariance matrix is obtained, *squeezing* in the long time limit state of the system can also be rigorously studied. To this end one can use a set of criteria identified in (Simon, 2000). As is noted in this work, squeezing in phase space in a system is a consequence of the appearance of non-compact terms in the Hamiltonian, i.e. terms that do not preserve the particle number, of the form

$$H \sim a_j^\dagger a_q^\dagger \pm a_j a_q. \tag{5.80}$$

This is indeed the form of the interacting part of the Hamiltonian in Eq. (5.18) once we write it in terms of creation and annihilation operators of the harmonic oscillators

$$x_j \sim \left(a_j^\dagger + a_j\right)$$
$$p_j \sim \left(a_j^\dagger - a_j\right)$$

and observe that in the Hamiltonian, terms of the form

$$a_j^\dagger b_q^\dagger \pm a_j b_q$$

appear. The criterion derived in (Simon, 2000) states that if

$$\nu_{min} \leq \frac{1}{2}, \tag{5.81}$$

where ν_{min} is the smallest normal eigenvalue of the covariance matrix (not to be mistaken with the symplectic eigenvalue), then the state is said to be squeezed.

5.2 Results

Before presenting any results, we note that the following checks are made in order to guarantee that the assumptions presented in the previous section are valid. For all the parameters for which we present results here we check:

1. that the constraints for the validity of the linear approximation described in (Lampo *et al.*, 2017b) hold; In particular, for the case of untrapped particles we check that the condition

$$\chi^{(Un)} := \frac{k_B T}{\hbar c}\sqrt{\frac{\hbar\tau \underline{\underline{M}}^{-1}}{2}}\frac{t\Lambda}{\alpha(\eta)} < 1, \tag{5.82}$$

is fulfilled. This implies an upper bound on the time we can study the impurities. For the case of trapped particles the condition reads as

$$\chi^{(Tr)} := \frac{k_B T}{\hbar c}\sqrt{\frac{2\underline{\underline{M}}\ \underline{\underline{\Omega}}\ C_{XX}(0)}{\hbar}} < 1; \tag{5.83}$$

2. that the condition Eq. (5.39) for the positivity of the Hamiltonian holds;

3. that the interactions are not so strong as to make invalid the initial Hamiltonian, as discussed in (Grusdt and Demler, 2015, Grusdt *et al.*, 2017a) (see also discussion in (Lampo *et al.*, 2017b)); In particular the interaction strengths η_j for $j \in 1, 2$ have to satisfy

$$\eta_j < \eta_{crit} := \pi\sqrt{\frac{2n_0}{m_B g_B}}; \tag{5.84}$$

4. that the Heisenberg uncertainty principle condition Eq. (5.79) holds;

5. that the high temperature limit obeys equipartition theorem, meaning that at the limit of $T \to \infty$

$$\left\langle x_j^2 \right\rangle \ , \ \left\langle p_j^2 \right\rangle \propto T^{\frac{1}{2}}$$

for $j \in 1, 2$. We used the fact that this latter condition was violated as an indication of problems with the numerical integrations that we performed.

5.2.1 Out-of-equilibrium dynamics and entanglement of the untrapped impurities

In this section, we study the case of untrapped impurities, $\Omega_1 = \Omega_2 = 0$. We restrict our studies to the low temperature regime, which is given by the condition $k_B T \ll \hbar\Lambda$. In the untrapped impurities case, the time dependent expressions for the Mean Square Displacement (MSD), defined in Eq. (6.80), the average energy and the entanglement can be obtained analytically. We emphasize that some of these quantities, such as the MSD, can be measured in the lab for ultracold gases (Catani *et al.*, 2012b). Our first aim, is to solve the equation of motion (5.54). To obtain analytic expressions for $G_1(t)$, $G_2(t)$, we first consider the particular form of their Laplace transforms, Eqs. (5.55) and (5.56).

They now read as

$$\mathcal{L}_z\left[\underline{\underline{G_1}}\left(t\right)\right] = \frac{z\mathbb{I}}{z^2\mathbb{I} + z\mathcal{L}_z\left[\underline{\underline{\Gamma}}\left(t\right)\right]} = \frac{1}{z + \mathcal{L}_z\left[\underline{\underline{\Gamma}}\left(t\right)\right]}\mathbb{I}, \tag{5.85a}$$

$$\mathcal{L}_z\left[\underline{\underline{G_2}}\left(t\right)\right] = \frac{1}{z^2\mathbb{I} + z\mathcal{L}_z\left[\underline{\underline{\Gamma}}\left(t\right)\right]}. \tag{5.85b}$$

The above equations depend on the form of the damping kernel. Thus, to get $G_1\left(t\right)$ and $G_2\left(t\right)$, one needs to compute the Laplace transform of the damping kernel, Eq. (5.63). In the long time limit, i.e. when $\mathrm{Re}[z] \ll \Lambda$, the Laplace transform of the damping kernel reads

$$\mathcal{L}_z\left[\Gamma_{jq}\left(t\right)\right] = z\widetilde{\tau}_{jq}\Lambda + O\left(z^2\right). \tag{5.86}$$

Hence equation (5.85a) can be easily inverted to get

$$G_1\left(t\right) = \frac{1}{1 + \widetilde{\tau}_{jq}\Lambda}\mathbb{I}. \tag{5.87}$$

while

$$\mathcal{L}_z\left[\underline{\underline{G_2}}\left(t\right)\right] = \frac{1}{\left(\mathbb{I} + \Lambda\underline{\underline{\widetilde{\tau}}}\right)z^2}, \tag{5.88}$$

where

$$\underline{\underline{\widetilde{\tau}}} = \begin{pmatrix} \tilde{\tau}_{11} & \tilde{\tau}_{12} \\ \tilde{\tau}_{21} & \tilde{\tau}_{22} \end{pmatrix}.$$

This can be inverted as

$$\underline{\underline{G_2}}\left(t\right) = \frac{t}{\left(\mathbb{I} + \Lambda\underline{\underline{\widetilde{\tau}}}\right)} = \frac{\left(\mathbb{I} + \Lambda\begin{pmatrix} \tilde{\tau}_{22} & -\tilde{\tau}_{12} \\ -\tilde{\tau}_{21} & \tilde{\tau}_{11} \end{pmatrix}\right)t}{\left(1 + \Lambda\tilde{\tau}_{11}\right)\left(1 + \Lambda\tilde{\tau}_{22}\right) - \Lambda^2\tilde{\tau}_{12}\tilde{\tau}_{21}},$$

which we rewrite as

$$\underline{\underline{G_2}}\left(t\right) = \underline{\underline{\alpha}}t \;\text{ with }\; \underline{\underline{\alpha}} = \begin{pmatrix} \alpha_{11} & \alpha_{12} \\ \alpha_{21} & \alpha_{22} \end{pmatrix}, \tag{5.89}$$

with

$$\alpha_{jq} = \frac{\left(I_{jq} + (-1)^{j+q}\Lambda\tilde{\tau}_{jq}\right)}{\left(1 + \Lambda\tilde{\tau}_{11}\right)\left(1 + \Lambda\tilde{\tau}_{22}\right) - \Lambda^2\tilde{\tau}_{12}\tilde{\tau}_{21}}. \tag{5.90}$$

Finally, the solutions of the equations of motion for the two impurities, written in the form of Eqs. (5.54), read as

$$x_j(t) = \sum_{q=1}^{2}\frac{1}{1+\widetilde{\tau}_{jq}\Lambda}x_j\left(0\right) + \alpha_{jq}\dot{x}_q\left(0\right)t + \int_0^t(t-s)\,\alpha_{jq}B_q\left(s\right)ds, \tag{5.91}$$

where

$$B_j\left(t\right) = \sum_{k\neq 0} i\hbar g_k^j\left[e^{i\omega_k t}b_k^\dagger\left(0\right) - e^{-i\omega_k t}b_k\left(0\right)\right].$$

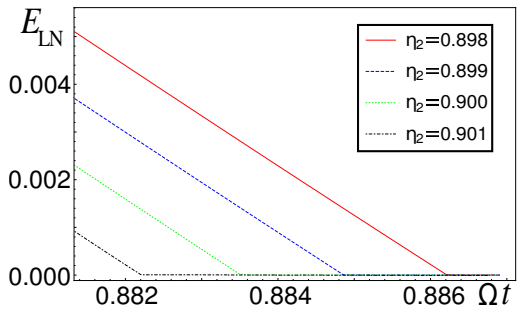

Fig. 5.1 *Time dependence of the entanglement between the two kinds of untrapped impurities.* Entanglement, as evaluated using Eq. 5.75, is observed at the long but not infinite time limit, for the case of untrapped impurities of potassium K in a bath of particles of Rubidium Rb, at the low temperature limit. The initial variances of position and velocity for the two particles, as well as their covariances, are assumed to be 0, i.e. $\langle x_j^2(0)\rangle = \langle \dot{x}_j^2(0)\rangle = \langle \dot{x}_j(0)\, x_q(0)\rangle = \langle \dot{x}_j(0)\, \dot{x}_q(0)\rangle = 0$ for $j \in \{1,2\}$, however the qualitative behavior was the same for other initial conditions as well, namely for setting all quantities equal to a finite value (in particular equal to 1). Entanglement, decreases to zero as time passes. It is studied for a number of different coupling constants η_2 of the second impurity. The rest of the parameters are $\Omega = 2\pi \cdot 500Hz$, $\eta_1 = 1$, $g_{\mathrm{B}} = 3 \cdot 10^{-37} J \cdot m$ and $n_0 = 7(\mu m)^{-1}$. It is observed that increasing η_2 decreases both the value of the entanglement and the time at which it reaches zero.

Now, we can evaluate, first, the MSD for each one of the particles. The MSD is defined as

$$\left\langle [x_j(t) - x_j(0)]^2 \right\rangle . \tag{5.92}$$

For the sake of simplicity, and to study the dynamical evolution of the MSD of the impurities purely due to their interaction with the bath, we assume that the initial states of the impurities and the bath are uncorrelated, $\rho(0) = \rho_I(0) \otimes \rho_{\mathrm{B}}$, such that averages of the form $\langle \dot{x}_j(0)\, B_q(s)\rangle$, that would otherwise appear in the expression, vanish. In the results presented in Fig. 5.1, we assumed that there are no initial correlations between the two impurities such that the terms $\langle \dot{x}_j(0)\, x_q(0)\rangle$ and $\langle \dot{x}_j(0)\, \dot{x}_q(0)\rangle$ for $j \neq q$ also vanish. Nevertheless, the case of finite values for these expectation values, in particular all of them being equal to 1, was also considered without seeing a qualitative difference in the results. Furthermore, to evaluate the MSD one needs to evaluate

$$\langle \{B_j(t), B_q(s)\}\rangle = 2\hbar \nu_{jq}(t-s), \tag{5.93}$$

where

$$\nu_{jq}(t-s) = \Theta(t-s) \int_0^\infty J_{jq}(\omega) \coth\left(\frac{\hbar\omega}{2k_{\mathrm{B}}T}\right) \cos(\omega(t-s))\, d\omega,$$

is the noise kernel. To prove this, we used the fact that for a bath mode at thermal equilibrium at a temperature T,

$$\left\langle b_k^\dagger b_k \right\rangle = \frac{1}{e^{\frac{\hbar\omega}{k_B T}} - 1}.$$

Then the expression for the MSD of one of the particles, in the long time limit, takes the form

$$\begin{aligned}\left\langle [x_j(t) - x_j(0)]^2 \right\rangle_{\rho(t)} &= \alpha_{jj}^2 \left\langle \dot{x}_j^2(0) \right\rangle t^2 \\ &+ \frac{1}{2}\sum_{y,k=1}^{2} \frac{\alpha_{jk}\alpha_{jy}}{m_k m_y} \int_0^t ds \int_0^t d\sigma\, (t-s)(t-\sigma) \langle \{B_k(t), B_y(s)\} \rangle . \end{aligned} \tag{5.94}$$

In the regime of low temperatures, where $\coth\left(\frac{\hbar\omega}{2k_B T}\right) \approx 1$, the MSD becomes

$$\left\langle [x_j(t) - x_j(0)]^2 \right\rangle_{\rho(t)} = \left(\alpha_{jj}^2 \left\langle \dot{x}_j^2(0) \right\rangle + \frac{1}{2}\sum_{y,k=1}^{2} \frac{\hbar \alpha_{jk}\alpha_{jy}\tilde{\tau}_{ky}\Lambda^2}{m_y m_k} \right) t^2. \tag{5.95}$$

Therefore, we find that the particles motion is superdiffusive. We note here that the same result was found for the single particle case (Lampo *et al.*, 2017b), where this effect was attributed to the memory effects present in the system. In this context the result in Eq. (6.80) represents a witness of memory effects on a measurable quantity.

In (Guarnieri *et al.*, 2016, Haikka *et al.*, 2011) the presence of memory effects is associated to backflow of energy. To examine whether such backflow of energy appears in our system as well, we derive an expression for the average energy of the system as a function of time. To do so, we need an expression for the time evolution of the momentum, which reads as

$$p_j(t) = m_j \dot{x}_j(t) = m_j \left(\sum_{q=1}^{2} \alpha_{jq} \dot{x}_q(0) + \int_0^t \alpha_{jq} B_q(s)\, ds \right). \tag{5.96}$$

Thus, in the low temperature limit, the average energy as a function of time, reads as

$$\begin{aligned} E_j(t) = \frac{\langle p_j^2 \rangle}{2m_j} = &\sum_{q,y=1}^{2} g_{\mathrm{IB}}^q n_0 + \alpha_{jq} E_q(0) + \frac{\hbar}{2}\alpha_{jq}\alpha_{jy} m_q \tilde{\tau}_{qy}\Lambda^2 \\ &- \hbar \alpha_{jq}\alpha_{jy}\tilde{\tau}_{qy} \frac{1}{t^2} \left[\cos(\Lambda t) + \Lambda t \sin(\Lambda t) - 1\right]. \end{aligned} \tag{5.97}$$

The oscillatory behaviour of the energy suggests that, in addition to the traditional dissipation process where the impurity loses energy, also the environment provides energy to the impurity, *i.e.* we detect a backflow of energy from the environment to the impurity. We note that, in the two particles case, the diffusion coefficient in Eq. (6.80) is different

for each particle [see expression for α_{jq}, Eq. (5.90)]. Thus, it depends on the interactions of each kind of particle with the BEC and the mass of each particle, together with the density and coupling constant of the BEC [see expression for the cutoff frequency, Λ, Eq. (5.50)].

As explained in Sec. 5.1.4, we will use the logarithmic negativity to study entanglement and hence the covariance matrix of the two impurities is needed. To this end, we find for the low temperature case, $\coth(\hbar\omega/2k_{\mathrm{B}}T) \approx 1$ and in the long-time limit, $\mathrm{Re}[z] \ll \Lambda$

$$\langle x_j x_q\rangle = \sum_{k,y=1}^{2} \delta_{ky}\langle x_k(0)x_y(0)\rangle + \delta_{ky}\alpha_{jk}\alpha_{qy}\langle \dot{x}_k(0)\,\dot{x}_y(0)\rangle\, t^2 \tag{5.98a}$$
$$+ \frac{2\hbar m_j m_q \tilde{\tau}_{ky}\alpha_{jk}\alpha_{qy}(1+\mathrm{mod}_2(i+j))}{m_k m_y}\Big[2\gamma - 2 + \frac{(\Lambda t)^2}{2} + 2\cos(\Lambda t) - 2Ci(\Lambda t) + 2\log(\Lambda t)\Big],$$

$$\langle x_j p_q\rangle = \tag{5.98b}$$
$$\sum_{k,y=1}^{2} \delta_{ky} m_q \alpha_{jk}\alpha_{qy}\langle \dot{x}_k(0)\,\dot{x}_y(0)\rangle\, t + \frac{\hbar m_j m_q \tilde{\tau}_{ky}\alpha_{jk}\alpha_{qy}}{m_y m_k t}\left(\frac{(\Lambda t)^2}{2} - [\cos(\Lambda t) + \Lambda t\sin(\Lambda t) - 1]\right),$$

$$\langle p_j p_q\rangle = \sum_{k,y=1}^{2} \delta_{ky} m_j m_q \alpha_{jk}\alpha_{qy}\langle \dot{x}_k(0)\,\dot{x}_y(0)\rangle \tag{5.98c}$$
$$+ 2m_j g^j_{\mathrm{IB}} n_0 \delta_{jq} + \frac{\hbar m_j m_q \tilde{\tau}_{ky}\alpha_{jk}\alpha_{qy}}{m_y m_k t^2}\left(\frac{(\Lambda t)^2}{2} - [\cos(\Lambda t) + \Lambda t\sin(\Lambda t) - 1]\right),$$

where in Eq. (5.98a) $Ci(x) = -\int_x^\infty \frac{\cos(t)}{t}dt$ is the cosine integral function.

In Fig. 5.1 we depict the entanglement as a function of time for the low temperature scenario and for different coupling constants η_2. We find entanglement in the long-time limit, which vanishes linearly. The maximum time at which entanglement reaches zero is increased by decreasing the interactions of the second kind of impurities. For a given time, entanglement increases with decreasing η_2. Also, for a given time we found that increasing η_1 while keeping the ratio η_1/η_2 constant, increases entanglement. We also studied the dependence of entanglement on density (not shown), finding that for large enough densities, the higher the density, the less entanglement was found and the faster it disappears. However, for low densities, increasing density increases entanglement. Since it is the presence of the bath that entangles the particles, small density is necessary to induce entanglement. This is in accordance with the results for the trapped impurities, presented in next section. Quantitatively, entanglement of an order of magnitude larger was found for a density of an order of magnitude smaller than the one presented in Fig. 5.1. We note that, for each curve, there is a minimum time at which equipartition is fulfilled according

to Eqs. (5.79). The form of ν_- can be analytically obtained from the expressions (5.98). We do not present it here explicitly to avoid long expressions.

Finally, the MSD for the relative motion $r = x_1 - x_2$ and center of mass $R = (x_1 + x_2)/2$ coordinates can also be obtained. We find that they equally perform superdiffusive motions. This means that both the variance of the distance between the two particles and the center of mass increases ballisticaly on average. For the particular case where the impurities are of the same mass and interact with the same strength with the BEC, the relative distance variance is constant in time. This is showing that it decouples from the bath. The center of mass position variance instead still grows ballisticaly with time. Instead, we find that for this case still one can find entanglement. This indicates that the vanishing of the entanglement at large times is not explained solely but the increase of the relative distance variance.

5.2.2 Squeezing and Entanglement for Trapped impurities

We conjecture to find squeezing and entanglement between the two particles in the regime where quantum effects play an important role. Thus, we consider the low temperature regime for the case of harmonically trapped particles, namely the regime where $k_{\mathrm{B}}T \ll \hbar\Omega_j$ with $j = 1, 2$. The parameters that we use are such that the condition (5.39) that guarantees that no runaway solutions are encountered, is satisfied. At the same time the coupling constants used are relatively strong such that the non-Markovian effects are manifested. We find that for entanglement, one has to consider coupling constants in the range that satisfies: $g_{\mathrm{IB}}^{(j)}/\Omega_j \in [0.01, 1]$, as below this range the bath effect is not enough to create entanglement, while above this the effect of the bath destroys entanglement. In the trapped case we make use of the covariance matrix whose elements are constructed by numerical integration from Eq. (5.66), (5.70) and (5.71). In general, and unless stated otherwise, we make the assumption that the centers of the harmonic traps are equal, $d_1 = d_2$, as entanglement is maximized in such case.

5.2.3 Squeezing

In this section we study squeezing as a function of the parameters of the system and the bath. To detect squeezing we make use of the condition (5.81). However, note that the value of ν_{min} is not a measure of the level of squeezing in the system, but a criterion that squeezing occurs. In the numerical computations presented in Fig. 5.2, we take $\Omega_1 = 600\pi Hz$, $\Omega_2 = 450\pi Hz$, $n_0 = 90(\mu m)^{-1}$, $\eta_1 = 0.325$ and $R_{12}/a_{\mathrm{HO}} = 0$, where distance was measured in units of a fixed harmonic oscillator length for both impurities equal to $\alpha_{\mathrm{HO}} = \sqrt{\hbar/(m\Omega)}$, with $m = m_1 = m_2$ and $\Omega = \pi kHz$ a typical frequency of the same order of magnitude as the frequencies considered throughout all of our studies. Without loss of generality, we assumed $d_1 \geq d_2$ such that $R_{12} \geq 0$. In our studies, we varied the temperature T, η_2 and g_{B}. The qualitative behaviour for a varying n_0 was

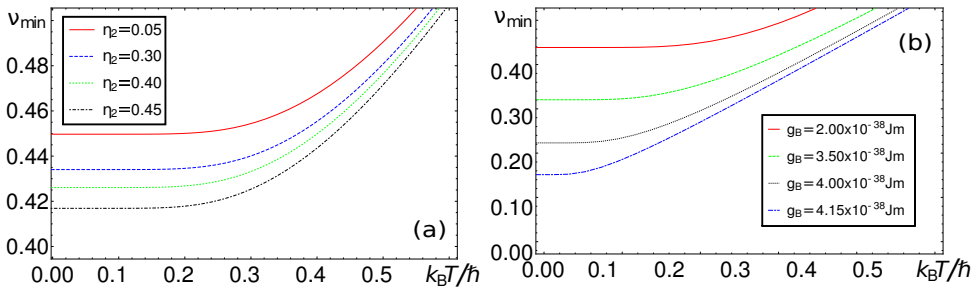

Fig. 5.2 *Temperature dependence of the squeezing between the two kinds of trapped impurities.* In (a) we study the temperature dependence of squeezing for different values of η_2 with $g_{\mathrm{B}} = 2.36 \cdot 10^{-38} J \cdot m$ and in (b) for different values of g_{B} with $\eta_2 = 0.295$. In both cases we use impurities of potassium K in a bath of particles of Rubidium Rb and we set: $\Omega_1 = 600\pi Hz$, $\Omega_2 = 450\pi Hz$, $n_0 = 90(\mu m)^{-1}$, $\eta_1 = 0.325$ and $R_{12}/a_{\mathrm{HO}} = 0$.

found to analogous to that of g_{B}, so the results with respect to this variable are not shown. The parameters used are within current experimental feasibility (Catani *et al.*, 2012b). In Fig. 5.2(a) we studied squeezing as a function of temperature for a number of different η_2 and, in panel (b), squeezing as a function of the temperature for various g_{B}. First, we find squeezing at low temperatures, in the nK regime, that vanishes at higher temperatures. Second, we observe that the temperature at which squeezing vanishes increases with the coupling constant η_2 or g_{B}. Furthermore, as we will show in next section, squeezing appears in the range of temperatures where entanglement appears as well, as can be seen in Fig. 5.3, but the range is slightly larger than that for entanglement. The existence of a relation of squeezing and entanglement is in agreement for example with the work in (Paz and Roncaglia, 2008), where an ohmic spectral density was considered, such that analytic results could be obtained, and they find in the long-time limit that the logarithmic negativity was given by $\mathcal{E}_{\mathrm{LN}}(\rho_{12}) = 2r$ with r being the two-mode squeezed state squeezing parameter.

We also studied the position and momentum variances,

$$\delta_{x_j} = \sqrt{\frac{2m_j\Omega_j \langle x_j^2 \rangle}{\hbar}}, \quad \delta_{p_j} = \sqrt{\frac{2\langle p_j^2 \rangle}{m_j\Omega_j\hbar}}, \tag{5.99}$$

observing that indeed in the large temperature limit they approach the equipartition theorem. This means that, in this limit, the system is formally analogous to two independent harmonic oscillators as expected. We used this as a test to verify the validity of our numerical results. In appendix B.4 we study the equilibrium Hamiltonian in detail. This allows us to find a prediction for the large temperature limit of, e.g., $\langle x_1 x_2 \rangle$ or $\langle p_1 p_2 \rangle$. We found that these correlation functions do not vanish at large T, not implying the presence of quantum correlations but only classical correlations in this limit. This is in agreement

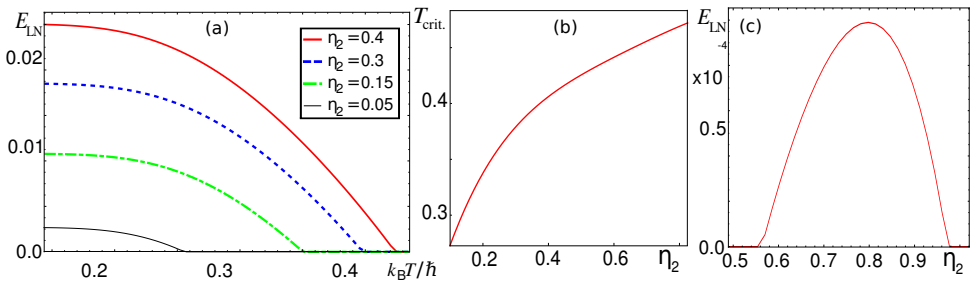

Fig. 5.3 *Coupling strength dependence of the entanglement between the two kinds of trapped impurities.* (a) Entanglement as a function of T for various couplings. As shown, for the values of η_2 considered here, increasing the interactions of the second type of impurities, η_2, enhances entanglement, at fixed T. For increasing T, entanglement decreases and eventually vanishes at certain T_{crit}. (b) The T_{crit} at which the entanglement goes to zero increases with η_2 and seems to saturate at large η_2. (c) the entanglement at fixed $T = 4.35nK$ increases for a range of η_2 and then decreases to zero. In this case we considered $n_0 = 350(\mu m)^{-1}$ and $g_{\text{B}} = 9.75 \cdot 10^{-39} J \cdot m$. In all of the graphs, we are considering impurities of potassium K in a bath of particles of Rubidium Rb. The parameters used in these plots are: $\Omega_1 = 600\pi Hz$, $\Omega_2 = 450\pi Hz$, $\eta_1 = 0.325$, $n_0 = 90(\mu m)^{-1}$, $g_{\text{B}} = 2.36 \cdot 10^{-38} J \cdot m$ and $R_{12}/a_{\text{HO}} = 0$

with the fact that one only finds entanglement for very low T.

In addition, we calculated the uncertainty δ_{x_1} when compared to δ_{p_1}, restricting only to the regime where Heisenberg uncertainty principle was fulfilled. This amounts to studying squeezing for the partially traced state of the system, tracing out the other kind of impurities. This way we were able study how the introduction of a second kind of impurities modified the squeezing found when defined as that of only one impurity (as is done in (Lampo *et al.*, 2017b)). We found that the squeezing observed for one particle reduces as η_2 increases.

5.2.4 Thermal entanglement induced by isotropic substrates

Here we study the appearance of thermal entanglement, i.e. assuming that the entangled resource, the bath, connecting the two impurities is in a canonical Gibbs ensemble density matrix at certain T. In general the following parameters were used: $\Omega_1 = 600\pi Hz$, $\Omega_2 = 450\pi Hz$, $\eta_1 = 0.325$, $\eta_2 = 0.295$, $n_0 = 90(\mu m)^{-1}$, $T = 4.35nK$, $g_{\text{B}} = 2.36 \cdot 10^{-38} J \cdot m$ and $R_{12}/a_{\text{HO}} = 0$. In certain cases we consider other values of n_0 and g_{B} to study the appearance of the phenomenon of the bath causing a decrease of the entanglement. Also, some general comments about the results that will be presented below, are the following. First, it was observed that parameter regimes existed in which the uncertainty principle, translated into the condition Eq. (5.79), was not satisfied. We only present results when

this condition is fulfilled. In the results presented here, entanglement is normalized based on the instance of maximum entanglement found in the system, which was obtained for the following parameters: $\Omega_1 = 600\pi Hz$, $\Omega_2 = 450\pi Hz$, $\eta_1 = 0.325$, $\eta_2 = 0.295$, $n_0 = 90(\mu m)^{-1}$, $T = 0.0435nK$, $g_B = 4.25 \cdot 10^{-38} J \cdot m$ and $R_{12}/a_{HO} = 0$, and the maximum value of entanglement obtained was $\mathcal{E}_{LN} = 1.025$.

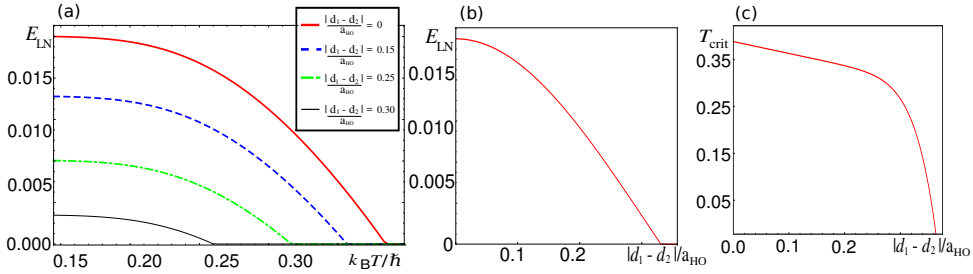

Fig. 5.4 *Distance dependence of the entanglement between the two kinds of impurities.* In (a) we study entanglement as a function of T for various distances between the trap of each kind of impurity. As expected the entanglement is reduced as the distance is increased. This is shown in figure (b). For each distance, at certain T the entanglement vanishes. The dependence of this critical temperature as a function of distance is shown in (c). In all of the graphs, we are considering impurities of potassium K in a bath of particles of Rubidium Rb. The parameters used in these plots are: $\Omega_1 = 600\pi Hz$, $\Omega_2 = 450\pi Hz$, $\eta_1 = 0.325$, $\eta_2 = 0.295$, $n_0 = 90(\mu m)^{-1}$, $T = 4.35nK$ and $g_B = 2.36 \cdot 10^{-38} J \cdot m$.

For all figures where we show the dependence of entanglement on temperature, we emphasize that below a certain temperature, the uncertainty principle was not satisfied. This minimum temperature depends on the other parameters of the system. For example, the larger the distance considered was, the lower temperatures that one can reach under the requirement that the uncertainty principle holds. We also note that for low enough temperatures, we find numerically a saturation of entanglement in all cases. Finally, the general behaviour of entanglement with temperature is to decrease, as expected, and beyond a certain temperature it vanishes. We term this as critical temperature, T_{crit}

In Fig. 5.3 (a), the temperature dependence of entanglement was studied for a number of coupling constants η_2, and it was observed that increasing η_2 implied an increase in entanglement, as well as an increase in T_{crit}. Information about this temperature is particularly important experimentally, and for this reason we studied the dependence of T_{crit} on η_2 in Fig. 5.3 (b). We see that the increase of T_{crit} with η_2 is decreasing for larger η_2. The dependence of entanglement was studied also as a function of η_2. In this case we considered $n_0 = 350(\mu m)^{-1}$ and $g_B = 9.75 \cdot 10^{-39} J \cdot m$ which allowed us to see the diminishing effect of the bath, meaning that entanglement reached a peak value for some

η_2 and was later then decreases with increasing values of η_2.

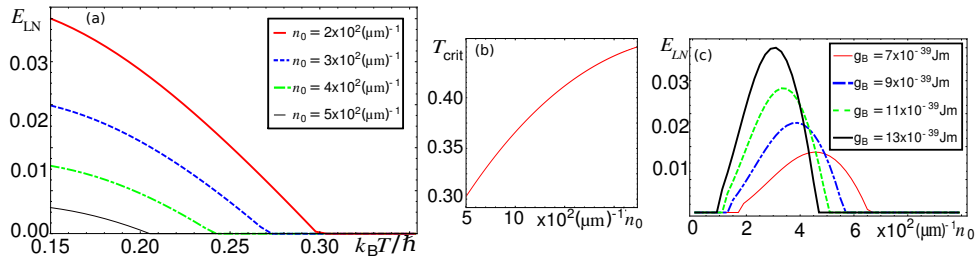

Fig. 5.5 *Dependence of the entanglement between the two kinds of impurities on the density of the bosons in the bath.* In (a) we study entanglement as a function of T for various densities of bosons. As shown, in this range of densities, increasing the density of bosons enhances entanglement. For each density, at certain $T_{\rm crit}$, the entanglement vanishes. The dependence of $T_{\rm crit}$ as a function of density is shown in (b). In (c) we illustrate that the entanglement at fixed T increases for a range of n_0 and then decreases to zero, as it was the case with η_2 in Fig. 5.1. We show this dependence for various values of the coupling constant among the bosons. As shown, increasing $g_{\rm B}$ increases the maximum value of the entanglement reached, but also entanglement vanishes at a smaller value of the density. In all of the graphs, we are considering impurities of potassium K in a bath of particles of Rubidium Rb. The parameters are: $\Omega_1 = 600\pi Hz$, $\Omega_2 = 450\pi Hz$, $\eta_1 = 0.325$, $\eta_2 = 0.295$, $T = 4.35nK$, $g_{\rm B} = 2.36 \cdot 10^{-38} J \cdot m$ and $R_{12}/a_{\rm HO} = 0$.

In Fig. 5.4 (a), we study entanglement as a function of the temperature for various distances between the two impurities. As expected, entanglement decreases with increasing distance. Furthermore, in Fig. 5.4 (c) the $T_{\rm crit}$ also decreases with distance and it acquires a maximum for distance equal to 0. In Fig. 5.4 (b) we see that entanglement drops to 0 beyond a certain distance which is $R_{12} \sim 0.35 a_{\rm HO}$, which for the parameters that we have chosen results in $0.2\mu m$. The distance at which entanglement drops to 0 depends on the other parameters of the system as well, e.g. it increases with decreasing temperature, but remains at the same order of magnitude. Furthermore, note that uncertainty principle is not satisfied for very short distances, since it is known that for distances from any of the two impurities smaller than their corresponding coherence lengths, the Frohlich Hamiltonian description does not apply (Grusdt *et al.*, 2015).

In Fig. 5.5 (a), we show the dependence of entanglement with T for various densities. The dependence of $T_{\rm crit}$ on the density in Fig. 5.5 (b) again shows that it increases with n_0 for small densities. However, in Fig. 5.5 (c) we show that while for small densities entanglement grows with the density, for larger values of the density it starts to decrease toward zero. We plot this figure for various values of $g_{\rm B}$ showing that the larger the bosons

interactions the smaller the value of n_0 at which the entanglement starts to decrease to zero.

Similar studies with similar results were undertaken for the dependence of the system on g_{B} and are presented in Fig. 5.6. There, for $g_{\mathrm{B}} = 4.2 \cdot 10^{-38} J \cdot m$ we see the qualitative behaviour of entanglement with a varying temperature. These results, together with the fact that we do not assume a particular form for the state of the two impurities initially, are clear indications that the induced entanglement between the two impurities is an effect of their interaction with the common bath.

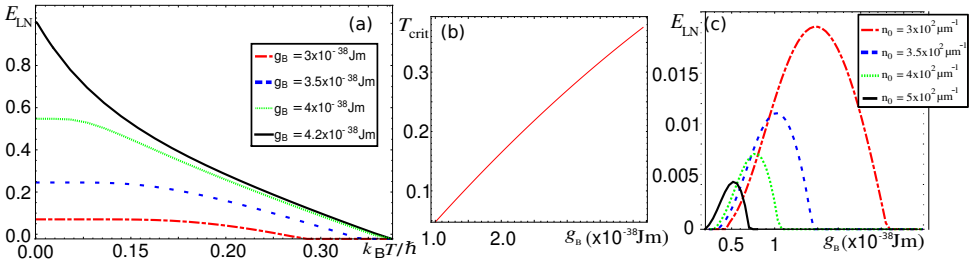

Fig. 5.6 *Dependence of the entanglement between the two kinds of impurities on the coupling constant between the bosons* g_{B}. In (a) we study entanglement as a function of T for various g_{B}. As can be seen for the largest considered value of g_{B}, namely $g_{\mathrm{B}} = 4.2 \cdot 10^{-38} J \cdot m$, the qualitative behaviour of entanglement with temperature, changes. For each density, at certain T_{crit}, the entanglement vanishes. The dependence of T_{crit} as a function of density is shown in (b). In (c) we illustrate that the entanglement at fixed T increases for a range of g_{B} and then decreases to zero, as it was the case with η_2 in Fig. 5.1. We show this dependence for various values of the density of the bosons. As shown, in this range of parameters, decreasing n_0 increases the maximum value of the entanglement reached, but also entanglement vanishes at larger values of g_{B}. In all of the graphs, we are considering impurities of potassium K in a bath of particles of Rubidium Rb. The parameters used in these plots are: $\Omega_1 = 600\pi Hz$, $\Omega_2 = 450\pi Hz$, $\eta_1 = 0.325$, $\eta_2 = 0.295$, $n_0 = 90(\mu m)^{-1}$, $T = 4.35nK$ and $R_{12}/a_{\mathrm{HO}} = 0$.

In Fig. 5.7 (a) we present the results of the dependence of entanglement with T for various ratios Ω_2/Ω_1. In Fig. 5.7 (b) we observe is that T_{crit} is not monotonically dependent on the ratio of trapping frequencies. This implies that there is a regime where, even though one keeps the temperature constant at a value where there is no entanglement, by increasing the trapping potential, such that the second impurity is more confined, entanglement appears for this given temperature. In Fig. 5.7 (c) we see that at resonance ($\Omega_2/\Omega_1 = 1$), entanglement achieves its maximum. This was also observed in Ref. (Correa *et al.*, 2012). The reason is that, since the values of the entries of the matrix $\underline{\underline{\Gamma}}(t)$ we use are so small, what guarantees that the equations of motion for the two harmonic oscillators

cannot be decoupled into two equations of motion for the center of mass and relative distance degrees of freedom, is the fact that the two trapping frequencies are different. To clarify this point, and draw the parallel with the results in (Correa *et al.*, 2012), we note that at relatively high temperatures, in which however entanglement can still be observed, one could assume that the system is described by the effective Hamiltonian Eq. (B.11) in Appendix B.4, where the effect of the bath degrees of freedom is represented by an effective coupling between the two particles. In the limit $K/\Omega_j \to 0$ with $j \in 1, 2$, for $\Omega_1 = \Omega_2$, the aforementioned decoupling takes place, and the state of the system goes to a non-symmetric two-mode squeezed thermal state with infinite squeezing, i.e. the ideal EPR (maximally entangled) state. We finally note that, as discussed in Appendix B.4, it is possible to find a approximate prediction for the critical T, given by Eq. (B.13). We found that this prediction is in the same order of magnitude (nK) for all numerical results presented.

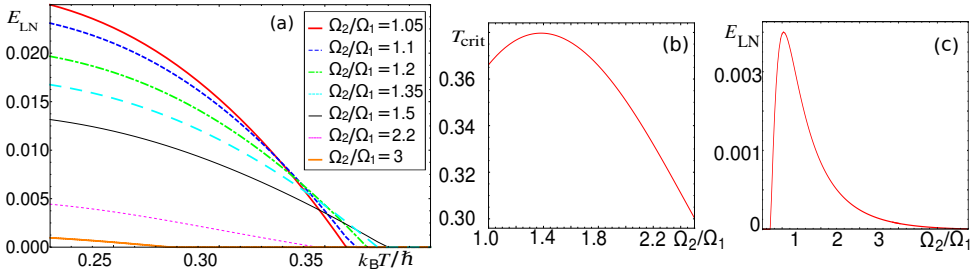

Fig. 5.7 *Trapping frequency dependence of the entanglement between the two kinds of impurities.* In (a) we study entanglement as a function of T for various ratios between the trap frequencies of each kind of impurity. For each Ω_2/Ω_1, at certain T_{crit}, the entanglement vanishes. The dependence of T_{crit} as function of Ω_2/Ω_1 is shown in (b). (c) illustrates that the entanglement at fixed T has a maximum value for certain value of Ω_2/Ω_1. The parameters $n_0 = 500(\mu m)^{-1}$ and $g_B = 9.75 \cdot 10^{-39} J \cdot m$ were used in this case. In all of the graphs, we are considering impurities of potassium K in a bath of particles of Rubidium Rb. The parameters used in these plots are: $\Omega_1 = 600\pi Hz$, $\eta_1 = 0.325$, $\eta_2 = 0.295$, $n_0 = 90(\mu m)^{-1}$, $T = 4.35nK$, $g_B = 2.36 \cdot 10^{-38} J \cdot m$ and $R_{12}/a_{HO} = 0$.

5.3 Summary

In the present chapter, we have applied the techniques developed in the previous chapters to a concrete physical system, evaluating quantities that can potentially be measured in experiments. In particular we studied a system of two impurities immersed in a common BEC bath. This treatment is based on the work in (Lampo *et al.*, 2017a) and the results presented in this chapter were published in (Charalambous *et al.*, 2019a). Our main results are:

- By starting from the physically motivated Hamiltonian describing two impurities interacting with a common homogeneous bath of bosons, through contact interactions, we derived after making the condensation assumption a Frohlich like Hamiltonian. Then by doing a Bogoliubov transformation and by further making the dipole approximation assumption, in the spirit of (Lampo *et al.*, 2017a), we transformed the Hamiltonian into a Caldeira-Leggett like Hamiltonian of two BP. Again, the role of the environment is represented by the surrounding Bogoliubov cloud. We note that no term is artificially introduced in the Hamiltonian in the process, in particular we do not introduce a counterterm to obtain the QBM Hamiltonian. This implies that the Hamiltonian is not bounded from below for all the parameter space, and for this reason we derive a condition on the parameters of the system for which the Hamiltonian remains positively defined.

- With the Hamiltonian at hand, we derive an expression for the spectral density of the bath, and we find it to depend cubically on the frequencies of the bath as in (Lampo *et al.*, 2017a). This implies that we again have non-markovian evolution of the system. However, the spectral density is now a 2×2 matrix for which the off-diagonal terms are also dependent on the distance between the impurities.

- At the level of the equations of motion (eom), derived from the Heisenberg equations, an effective interaction between the two impurities appears that depends on the distance between them. The equations are solved by considering their Laplace transform. Two distinct cases are considered, a free impurity and a harmonically trapped one. In the first case the eom can be solved by considering the long time limit at the level of the Laplace transform. For the second case, numerical Laplace inversion techniques are used, namely the Zakian method. We study entanglement and squeezing for the two cases for various parameters of the system, making sure that the Heisenberg Uncertainty principle holds. We find that this latter condition is not satisfied for all parameters, for our numerical investigations.

- The main result concerning the untrapped case, is that entanglement does not survive in the long time limit. We further proved that this does not happen because the two impurities move infinitely far away at the long time limit.

- The main result concerning the trapped case, is that entanglement and squeezing appear in the long time limit of the system. We focused on entanglement and studied this as a function of the various parameters of the system. We find that entanglement:

  - Decreases as a function of temperature, and is zero beyond a critical temperature. Squeezing behaves in the same way and in approximately the same

temperature regime.

  - Decreases as a function of distance between the two impurities.

  - Exhibits a non-monotonic behaviour as a function of the coupling constant between the impurities and the bath. Namely, increasing the coupling of one of the impurities to the bath appears to increase initially entanglement but beyond a certain value it contributes negatively to entanglement until a value of the coupling constant beyond which entanglement vanishes. We interpret this as following: Since entanglement requires some sort of interaction between the two impurities, even an effective one, the initial increase in the coupling constant helps establish this interaction. However, further increase of the interaction with the bath leads to probably a decoherence effect, where the impurities lose any quantum effects that they may exhibit.

  - Exhibits a non-monotonic behaviour with as a function of the density of the bosons, as well as a function of the inter-boson coupling. The interpretation again follows the same line as above.

  - Exhibits a resonance effect as a function of the trapping frequencies of the two impurities. Namely, when the two frequencies match entanglement is maximized. This is explained as following. When the two frequencies match, one can show that the two eom almost decouple, in the bases of center of mass and relative distance coordinates. This implies the existence of a decoherence free subspace, and according to (Ludwig *et al.*, 2010) this implies that the state of the two impurities is that of maximally entangled state.

- We also showed that at the long time limit, the two impurities are in a non-equilibrium state, in a sense that the two see an environment of a different effective temperature.

CHAPTER 6

CONTROL OF ANOMALOUS DIFFUSION OF A BOSE POLARON IN A COHERENTLY COUPLED TWO-COMPONENT BEC

In this work, we aim to study how an impurity in a coherently coupled two-component BEC can show a transient anomalous diffusing behaviour, and how this depends on the parameters of the system. We will study this phenomena under experimentally realistic conditions and we will show that this behaviour can be controlled through the strength of the interactions and the coherent coupling. To this end, we treat the Bose Polaron problem within an open quantum system framework. The open quantum system approach has been used recently in the context of ultracold quantum gases to study the diffusion of an impurity and two impurities in a BEC (Lampo *et al.*, 2017a, 2018, Charalambous *et al.*, 2019a), for the movement of a bright soliton in a superfluid in one dimension (Efimkin *et al.*, 2016a), among other examples (Hurst *et al.*, 2017b, Keser and Galitski, 2018, Bonart and Cugliandolo, 2012a)). On the other hand, the effect of contact interactions, dipole-dipole interactions and disorder on the diffusion properties of 1D dipolar two-component condensates were studied in (Bai and Xue, 2015), identifying again the conditions for subdiffusion, while the study for the diffusive behaviour of a 2D two-component BEC in a disordered potential was undertaken in (Xi *et al.*, 2014). Finally, an important study

on an impurity immersed in a two-component BEC was reported in (Ashida *et al.*, 2018).

To be specific, we consider here that an external field drives the population transfer (spin-flipping) between the two atomic levels. The population transfer between the two levels turns out to be described by Josephson dynamics, leading to what is known as internal Josephson effects (see, e.g. (Leggett, 2001)). This internal Josephson interaction controls the many-body physics of multicomponent phase coherent matter. We identify how under suitable assumptions, starting from the Hamiltonian describing the aforementioned system of an impurity in a coherently coupled two component BEC, one can equivalently describe the impurity as a Brownian particle in a bath, where the role of the bath is played by the Bogoliubov modes of the coherently coupled two-component BEC. Importantly, the Bogoliubov spectrum has to branches: the density mode, gapless and with a linear behaviour at low momenta; and the spin mode, gapped and with a parabolic behaviour even at low momenta. We consider two scenarios: same coupling among the impurity and the two bosonic components, and repulsive coupling to one component and attractive to the other. We show that these scenarios correspond to the impurity coupling either to the density or to the spin mode of the two-component BEC, respectively. We henceforth derive the relevant spectral densities. For the coupling to the density mode there is no qualitative difference in comparison to the case where the impurity in a single BEC (Lampo *et al.*, 2017a). For the coupling to the spin mode, we find a completely different spectral density, namely a gapped sub-ohmic spectral density. We derive and solve the equations of motion of the impurity, that are obtained through the corresponding Heisenberg equations for the bath and impurity particles. These have the form of Generalized Langevin equations with memory effects. By solving numerically these equations we find the effect of the gapped sub-ohmic spectral density on the Mean Square Displacement (MSD) of the impurity. We show that a transient subdiffusive behaviour occurs for experimentally feasible parameters, and study how the strength of the coherent coupling and interactions modify this subdiffusive behaviour.

The paper is organized as follows. In Section II we introduce the two-component Hamiltonian together with the assumptions that go with it, as well as the generalized Bogoliubov transformation that diagonalizes it. In Section III we present the impurity-bath Hamiltonian, where the bath is this time the coherently coupled two component BEC and transform it into the form of a Caldeira-Leggett one. In Section IV we derive the spectral densities for the cases of coupling to density or spin mode. In Section V we find and solve the Langevin equations and in Section VI we present the results. We end the paper with the discussion and outlook presented in Section VII.

6.1 Multicomponent BECs

Multi-component condensates are defined as systems where two or more internal quantum states are macroscopically populated. Such systems then possess internal degrees of freedom relating to the relative population and phase of each component, in addition to the usual external degrees of freedom of a single-component condensate. The interplay between these external and internal degrees of freedom in multi-component systems can then lead to a range of phenomena not present in scalar condensates. The reason for this, is that each component interacts with atoms both of the same and of the other species. As a result, for example, the various components can be spatially separated or mixed. This is dependent on the relative values of the different scattering lengths. This also determines the stability of the multicomponent BECs, as well as other fundamental properties of the system. Furthermore, these characteristics are fundamentally modified, if one introduces a radiation field that linearly couples the two components. Then, for example, an immiscible system can be tuned miscible by the radiation field (Merhasin *et al.*, 2005).

An example of such multicomponent BEC as was mentioned before is that composed of different hyperfine states of atoms of the same species. The dilute Bose-Einstein condensates created in atom traps (Davis *et al.*, 1995) consist of bosons with internal degrees of freedom: by taking advantage of this, the atoms can be trapped in different atomic hyperfine states. Soon after the first observation of atom trap BECs, experimentalists succeeded in trapping partly overlapping BECs of atoms in different hyperfine states that are (i) hyperfine split (Myatt *et al.*, 1997) or (ii) nearly degenerate and correspond to different orientations of the spin (Stamper-Kurn *et al.*, 1998).

In our work, we consider a two-component Bose gas with both one-body (field-field) and two-body (density-density) couplings, composed of such atoms in different hyperfine states. Furthermore, we assume that the two components are coupled through a Josephson (one-body) type of coupling. The two-body interaction results from short-range particle-particle interactions between atoms in different internal states, while the one-body interaction can be implemented by two-photon Raman optical coupling, which transfers atoms from one internal state to the other. In present-day BEC experiments, the internal Josephson or Rabi interactions that inter-convert atoms of different internal states are two-photon transitions, induced by a laser field or a combination of a laser field and oscillating magnetic field. For a perspective on the experimental relevance of our study, we refer to the work of (Miesner *et al.*, 1999, Stenger *et al.*, 1998, Matthews *et al.*, 1998, Myatt *et al.*, 1997). Finally, immersed in this two-component BEC, we assume an impurity which interacts with both components through contact interactions. In Fig. 6.1 a sketch of the set-up is shown.

Before introducing this additional impurity, in the following subsections, we introduce the theoretical description of coherently coupled interacting two-component Bose-Einstein condensates in the mean field approximation. We will discuss their ground state properties and excitation spectra along with the resulting dynamics. As in the single BEC case we focus in the 1D case, where in an actual experimental system, as was discussed for the single BEC case, the atomic clouds will be confined in an elongated trapping potential. However, as before, we simplify the description by assuming a homogeneous system without longitudinal confinement as it allows to derive many results analytically.

6.1.1 Hamiltonian of the weakly interacting coherently coupled two-component BEC

The Hamiltonian of a weakly interacting coherently coupled two-component BEC in one dimension reads

$$H = H_{\mathrm{B}}^{(1)} + H_{\mathrm{B}}^{(2)} + H_{\mathrm{B}}^{(12)}, \tag{6.1}$$

The terms of the individual bosonic species, labeled with the index $j = 1, 2$, are

$$H_{\mathrm{B}}^{(j)} = \int \Psi_j^\dagger(\mathbf{x}) \left[-\frac{\mathbf{p}_j^2}{2m_{\mathrm{B}}} + V(\mathbf{x}) \right] \Psi_j(\mathbf{x})\, \mathrm{d}\mathbf{x} + \frac{g_j}{2} \int \Psi_j^\dagger(\mathbf{x})\, \Psi_j^\dagger(\mathbf{x})\, \Psi_j(\mathbf{x})\, \Psi_j(\mathbf{x})\, \mathrm{d}\mathbf{x},$$

where the intra-species contact interactions have a strength given by the coupling constants g_j, the external potential is $V(x)$ and we assume the mass equal for both species, m_{B}. The coupling Hamiltonian between the two bosonic species consists of an inter-species contact interactions part, with coupling constant g_{12}, and a Rabi coupling Ω which exchanges atoms between components, i.e.,

$$H_{\mathrm{B}}^{(12)} = g_{12} \int \Psi_1^\dagger(\mathbf{x})\, \Psi_2^\dagger(\mathbf{x})\, \Psi_2(\mathbf{x})\, \Psi_1(\mathbf{x})\, \mathrm{d}\mathbf{x} + \hbar \boldsymbol{\Omega} \int \boldsymbol{\Psi}_{\mathbf{1}}^\dagger(\mathbf{x})\, \boldsymbol{\Psi}_{\mathbf{2}}(\mathbf{x})\, \mathrm{d}\mathbf{x} + \mathrm{H.c.} \tag{6.2}$$

Without loss of generality, we will only consider $\boldsymbol{\Omega}$ real and positive. This is because even if a complex Rabi frequency is assumed, this can always be canceled by introducing a counteracting phase for one of the BECs which can be shown that will have no effect on the energy spectrum of the bath. The latter part of the Hamiltonian, referred to as an internal Josephson interaction, is a two-photon transition that is induced by a laser field or a combination of a laser field and an oscillating magnetic field. This also introduces an effective energy difference between the two internal states/ species of the BEC, which assuming a low intensity driving field is simply equal to the detuning δ of the two-photon transition. This detuning does not affect our studies however, so for sake of clarity and simplicity, we will assume it to be zero. We also consider here only repulsive two-body term coupling, i.e. $g_{12} > 0$, for reasons that will become apparent soon.

From this point onwards, we assume that the BEC is one dimensional, which simplifies the analytical part of our studies. We assume a dilute gas of low depletion in order

to be able to apply the Bogoliubov diagonalization technique. By these assumptions, we are allowed in the low-density sub-milikelvin temperature regime of the atom trap experiments, to assume that the trapped atoms interact only in the partial s-wave channel and that the many-body properties are well described by assuming the particles to interact as hard spheres. The radius of those spheres is given by the scattering length a, which we assume it to be positive, as is the case in most experiments. We say that the system of particle density n is dilute if the packing fraction of space occupied by the spheres $na^3 \ll 1$. The assumption of low depletion means that almost all particles occupy, on average, the single particle state associated with the condensate ($k = 0$ where k is the momentum for the particular case of homogeneous BEC that we will be considering). This implies that the temperatures to be considered should be smaller than the critical temperature (the 1D case is peculiar, but we assume condensation occurs at some finite temperature as well). For a single BEC, all the bosons condensate at the same state. However this will not be the case for the two-component BEC and one has to determine the fraction of particles in each component, which will depend on the ground state of the system. This is determined by the parameters of the system.

Under the above assumptions, we can assume that our bosonic gases condensate. This means that we can apply mean field theory and further assuming that the ground state is coherent, the wavefunctions $\Psi_j(x), \Psi_j^\dagger(x)$ for a homogeneous BEC are given by

$$\Psi_j(x) = \Psi_{j,0}(x) + \delta\Psi_j(x), \tag{6.3}$$

where $\Psi_{j,0}(x) = \phi_0(x)\sqrt{N_j}e^{i\theta_j}$, with θ_j being the phase of the coherent j^{th} component, N_j the number of bosons of the j^{th} species and $\delta\Psi_j(x) = \sum_{k\neq 0}\phi_{j,k}(x)a_{j,k}$ with $\phi_k(x) = \frac{1}{\sqrt{V_j}}e^{ikx}$ the plane wave solutions, with V_j the corresponding bath's volume. From here onwards we assume for simplicity that $V_1 = V_2 = V$, i.e. that the two baths have the same volume, and that we are dealing with homogeneous BECs. Here $a_{j,k}$ and $a_{j,k}^\dagger$ are bosonic annihilation and creation operators. To proceed further, we write the Hamiltonian in terms of these operators. The bosonic parts read

$$\begin{aligned} H_{\mathrm{B}}^{(j)} &= \sum_{k\neq 0}\epsilon_k a_{j,k}^\dagger a_{j,k} + \frac{g_j}{2}\sum_{k,k',q\neq 0} a_{j,k+q}^\dagger a_{j,k'-q}^\dagger a_{j,k}a_{j,k'}, \\ H_{\mathrm{B}}^{(12)} &= g_{12}\sum_{k,k',q\neq 0} a_{1,k+q}^\dagger a_{2,k'-q}^\dagger a_{2,k}a_{1,k'} + \Omega\sum_{k\neq 0} a_{1,k}^\dagger a_{2,k} + \mathrm{H.c.}, \end{aligned}$$

with $\epsilon_k = k^2/2m_{\mathrm{B}}$. Here we set $\hbar = 1$ and we adimensionalized correspondingly. The zeroth order expectation value (or mean field value) of the Hamiltonian reads as

$$H_0 = \sum_j \frac{g_j}{2V}\Psi_{j,0}^4 + \frac{g_{12}}{V}\Psi_{1,0}^2\Psi_{2,0}^2 + \Omega\left(\Psi_{1,0}(\Psi_{2,0})^* + (\Psi_{1,0})^*\Psi_{2,0}\right) \tag{6.4}$$

Coupled Gross-Pitaevskii equations (CPGE)

The equations of motion governing the dynamics of a two-component condensate can be obtained from the Hamiltonian using the Heisenberg equation which yields the coupled pair of equations

$$i\hbar\frac{\partial}{\partial t}\Psi_j = \left[-\frac{\nabla^2}{2m} + g_j\left|\Psi_j\right|^2 + g_{12}\left|\Psi_{j'}\right|^2\right]\Psi_j - \frac{\Omega}{2}\Psi_{j'} \tag{6.5}$$

where $j' \neq j$ and $j, j' \in \{1, 2\}$. These equations are the main tool for modeling the dynamics of the two-component condensate in the mean field regime. All the conditions that applied in the single BEC case should be valid in order to obtain this CGPE. Namely, the diluteness and low temperature assumption, as well as the orthogonality of the many-body wavefunction (many-body ansatz in Eq. (4.19)). Finally the CGPE can only be used to investigate phenomena that take place over distances much larger then the scattering length a_{ij}, $j, i \in \{1, 2\}$.

Relative phase

The relative phase of two condensates is a measurable quantity and does not have a conceptual problem with respect to symmetry breaking. In this case, one can illustrate the relative phase, using a two-mode system where only two orthogonal states are allowed for particles. We designate the two states by Ψ_1 and Ψ_2, and the corresponding field operators are $a_1, a_1^\dagger$ and $a_2, a_2^\dagger$, respectively. Then, two sets of basis elements can be considered in order to express any given state of the condensate. These are the sets of coherent states and number (Fock) states:

$$\begin{aligned}\left|\Psi_{coh}\right\rangle &= \tfrac{1}{\sqrt{2^n n!}}\left(a_1^\dagger + e^{i\phi}a_2^\dagger\right)^N\left|0\right\rangle \\ \left|\Psi_{num}\right\rangle &= \tfrac{1}{(n/2)!}\left(a_1^\dagger\right)^{N/2}\left(a_2^\dagger\right)^{N/2}\left|0\right\rangle\end{aligned} \tag{6.6}$$

where $|0\rangle$ is a particle vacuum state and $N = N_1 + N_2$ the total particle number . In the coherent state, all particles stay in the same single-particle state, $\frac{1}{\sqrt{2}}\left(\Psi_1 + e^{i\phi}\Psi_2\right)$, and we say that two condensates represented by Ψ_1 and Ψ_2 have a well-defined relative phase ϕ. Even though for the two states the average particle numbers in each single-particle state are equal to $N/2$, the coherent state is a superposition of a number of number states with regular phase relations. Number states are states with fixed particle number in each single-particle state. Therefore, two condensates having a well-defined relative phase means that there is corresponding uncertainty in the particle numbers of the two condensates with strong correlation among number states. Furthermore, it was shown in (Lellouch *et al.*, 2013) that the relative phase fluctuations are maximally suppressed when $g_1 \approx g_2 = g$ and $g, g_{12} > 0$ where g_{12} approaches g from below. This is exactly the scenario we will assume in our work as well, which implies that the two BEC we will

consider will have a well-defined relative phase and uncertainty in the particle number. We will also assume the average particle number to be $N_1 = N_2 = N/2$ for reasons that will become apparent soon.

The Josephson effect One interesting phenomenon that has been observed with BECs is an analogue of the Josephson effect in condensed matter systems. The setting for the appearance of this phenomenon, is exactly the one we described above, i.e. that of two weakly coupled condensates, each of them with a modulus and a phase. Interestingly, the presence of a phase difference between them, yields the appearance of an oscillatory coherent tunneling of particles from one condensate to the other, through the weak link. This is what is known as Josephson effect in BEC.

This effect was predicted in 1962 by B. D. Josephson (Josephson, 1962) in the context of superconductivity. When two superconductors are separated by a thin insulating barrier, forming what is called a Josephson junction, there exists a finite current between them. This current is the macroscopic observation of tunneling of particles through a barrier, and is related to the phase difference between the two superconductors. This phenomenon is called direct current (d.c.) Josephson effect (Josephson, 1962) and was experimentally observed in 1963 by P. L. Anderson and J. W. Rowel (Anderson and Rowell, 1963). The idea of the manifestation of the Josephson effect in cold atoms was proposed by J. Javanainen in 1986 (Javanainen, 1986). One way of preparing such Bose-Josephson junctions experimentally is by confining a single BEC in a double-well potential (Gati and Oberthaler, 2007). In such system, the Josephson junction consists in the two localized matter wave packets in each well, that are weakly coupled via tunneling of particles through a potential barrier. In our case, we will consider instead of a double well potential, a spatially separated, i.e. miscible, two component BEC. The conditions to have such a BEC are specified below.

A common theoretical approach to study the dynamics of a bosonic Josephson junction within a mean-field approach, i.e. using Gross-Pitaevskii equations, was proposed in (Smerzi *et al.*, 1997). However, a mean-field description fails to fully capture correlations between atoms, and therefore, there are certain quantum effects that cannot be described. In contrast, the two-site Bose-Hubbard model (Fisher *et al.*, 1989), can overcome this problem, but in our work we'll restrict to the mean-field approach for its mathematical simplicity, and because it can already capture the effect we want to describe.

6.1.2 Ground state properties of a two-component BEC

To get a better understanding of the system of two coherently coupled interacting BECs we first focus on the simpler scenario of two interacting but uncoupled BEC, i.e. we set $\Omega = 0$. It can consist of condensates of two different elements, the condensate of

the same element being prepared in two different internal states, or the condensate in a double-well potential. We will assume a two-component BEC made out of two hyperfine states of Rb.

Miscibility condition for $\Omega = 0$

In a one-dimensional wave-guide the ground state can either be a spatially uniform superposition of the two components or a phase separated one, where the two components occupy different regions and their overlap is minimized. The following energetic consideration allows to derive a criterion determining which configuration is energetically favorable. For simplicity we ignore the kinetic energy contribution to the Hamiltonian and use a box potential of length L. The energy of the uniform superposition state with n_1 and n_2 atoms in the two components is given by (Pitaevskii and Stringari, 2016, Ao and Chui, 1998)

$$E_{unif} = \frac{g_1}{2}\frac{n_1^2}{L} + \frac{g_2}{2}\frac{n_2^2}{L} + g_{12}\frac{n_1 n_2}{L} \tag{6.7}$$

The corresponding expression for the phase-separated state reads

$$E_{sep} = \frac{g_1}{2}\frac{N_1^2}{L_1} + \frac{g_2}{2}\frac{N_2^2}{L_2} \tag{6.8}$$

The conditions of a fixed system size $L = L_1 + L_2$ and equal pressures $\partial E_{sep}/\partial L_1 = \partial E_{sep}/\partial L_2$ lead to

$$E_{sep} = \frac{g_1}{2}\frac{N_1^2}{L} + \frac{g_2}{2}\frac{N_2^2}{L} + \sqrt{g_1 g_2}\frac{N_1 N_2}{L} \tag{6.9}$$

Thus the phase separated state is energetically favorable if $E_{sep} < E_{unif}$ which implies $g_1 g_2 < g_{12}^2$. This is the condition for immiscibility (Pitaevskii and Stringari, 2016). In other words, the ground state of two components consists of two separate phases, if their inter-species repulsion is stronger than the geometric mean of the intra-species repulsion strengths.

Introducing a coherent coupling

To study the effect of the introduction of a coherent coupling, we follow a slightly different way. We first consider the ground state Hamiltonian of the two-component BEC H_0 given in Eq. (6.4). By minimizing H_0 with respect to the population imbalance $f = \frac{N_1 - N_2}{N}$, one can obtain the following conditions on the parameters of the system in order to have an extremum of the energy,

$$\Delta + Af - \cos\theta_{12}\frac{f}{(1-f^2)^{1/2}} = 0, \tag{6.10}$$

where $A = (g_1 + g_2 - 2g_{12})\, n/4\Omega$ is the mutual interaction parameter, while Δ is the effective detuning parameter $\Delta = 2\delta + (g_1 - g_2)\, n/4\Omega$, and

$$A - \cos\theta_{12} \frac{1}{(1-f^2)^{3/2}} > 0, \tag{6.11}$$

is the condition to have a minimum of the energy. In (Tommasini *et al.*, 2003), it was shown that to obtain the minimum energy of the system, without imposing any condition on the detuning δ, as is our case, then the relative phase should be chosen to be $\theta_{12} = \pi$, referred to as the π-state configuration. From here on we assume the symmetric case, i.e, $g_1 = g_2 = g$ as this will allow us to obtain analytically the spectral density in section B.1. After ignoring the detuning δ, the equilibrium condition Eq. (6.23) reads as

$$\left(g - g_{12} + \frac{\Omega}{\sqrt{n_1 n_2}}\right)(n_1 - n_2) = 0, \tag{6.12}$$

which has two solutions

$$\begin{aligned} n_1 - n_2 &= 0 && (GS1)\,, \\ n_1 - n_2 &= \pm n\sqrt{1 - \left(\tfrac{2\Omega}{(g-g_{12})n}\right)^2} && (GS2)\,, \end{aligned} \tag{6.13}$$

corresponding to neutral $GS1$ and polarized ground states $GS2$. Here, we make the strong Josephson junction assumption

$$|A| < 1, \tag{6.14}$$

which is also referred to as the miscibility condition. This implies that the minimum energy equilibrium ground state has to be $GS1$ as is shown in (Tommasini *et al.*, 2003, Abad and Recati, 2013). That this condition implies spatially separated BEC was proven theoretically in (Merhasin *et al.*, 2005) and in the numerical simulations of (Nicklas, 2013).

Finally, it is important to note that the extension to negative values of Ω does not have physical consequences in terms of the ground state of the system as all of its properties remain the same. One can show that the ground state of the system always has to have a relative phase of $\phi = 0$ between atomic states and the linear coupling. However, this phase ϕ after the introduction of the coherent coupling, is given as $\phi = \theta_{12} + \theta_{coh}$, where $\theta_{12} = \theta_1 - \theta_2$ where θ_j is the phase of the j^{th} component, and θ_{coh} is the phase of the coherent coupling. If the phase of the linear coupling θ_{coh} is changed by π this is 'compensated' by a phase flip in one of the components.

6.1.3 Generalized Bogoliubov transformation

The generalized Bogoliubov transformation serves the same purpose as the standard Bogoliubov transformation, i.e. to diagonalize the coherently coupled two-component BEC Hamiltonian and hence obtain the energy spectrum of the bath. We follow closely the results of (Tommasini *et al.*, 2003, Lellouch *et al.*, 2013, Abad and Recati, 2013) in

the rest of this subsection. This generalized Bogoliubov transformation is understood to be composed of

1. a rotation,
$$\begin{aligned} a_{1,k} &= d_{1,k}\cos\theta - d_{2,k}\sin\theta \\ a_{2,k} &= d_{1,k}\sin\theta + d_{2,k}\cos\theta \end{aligned} \tag{6.15}$$
where the $d_{j,k}$ are the dressed annihilation operators. The angle θ will be chosen in a way to eliminate the Ω term, namely,
$$\tan\theta = \begin{cases} \sqrt{n_1/n_2} & if\ \theta_{12} = \pi \\ \sqrt{n_2/n_1} & if\ \theta_{12} = 0 \end{cases} \tag{6.16}$$
with $0 < \theta < \pi/2$. Then one has to introduce the coordinate-like operators
$$\begin{aligned} x_{i,k} &= \tfrac{d_{i,-k}+d_{i,k}^{\dagger}}{\sqrt{2}} \\ p_{i,k} &= \tfrac{d_{i,k}-d_{i,-k}^{\dagger}}{\sqrt{2}} \end{aligned} \tag{6.17}$$

2. a scaling
$$\begin{aligned} x_{i,k} &= \overline{x}_{i,k}\sqrt{\tfrac{e_{i,k}}{\omega_{i,k}}} \\ p_{i,k} &= \overline{p}_{i,k}\sqrt{\tfrac{\omega_{i,k}}{e_{i,k}}} \end{aligned} \tag{6.18}$$
with
$$\begin{aligned} &e_{j,k} = \frac{k^2}{2m} \pm \frac{(1\mp\cos\theta_{12})\Omega n}{2n_1n_2}, \text{upper(lower) sign for } j = 1(2) \\ &\omega_{j,k} = \sqrt{e_{j,k}^2 + 2\Lambda_j n_j e_{j,k}}, \\ &\Lambda_1 n_1 = g_1 n_1 \cos^2(\theta) + g_2 n_2 \sin^2(\theta) + g_{12}\sin(2\theta)\cos(\theta_{12}), \\ &\Lambda_2 n_2 = g_1 n_1 \sin^2(\theta) + g_2 n_2 \cos^2(\theta) - g_{12}\sin(2\theta)\cos(\theta_{12}), \\ &\Lambda_{12}\sqrt{n_1 n_2} = \frac{g_2 n_2 - g_1 n_1}{2}\sin(2\theta) + g_{12}\sqrt{n_1 n_2}\cos(2\theta)\cos(\theta_{12}), \end{aligned}$$
where $n_j = \frac{N_j}{V}$ is the particle density of the j^{th} bath

3. and one more rotation,
$$\begin{aligned} \overline{x}_{1,k} &= \widehat{x}_{1,k}\cos\gamma_k - \widehat{x}_{2,k}\sin\gamma_k \\ \overline{x}_{2,k} &= \widehat{x}_{1,k}\sin\gamma_k + \widehat{x}_{2,k}\cos\gamma_k \\ \overline{p}_{1,k} &= \widehat{p}_{1,k}\cos\gamma_k - \widehat{p}_{2,k}\sin\gamma_k \\ \overline{p}_{2,k} &= \widehat{p}_{1,k}\sin\gamma_k + \widehat{p}_{2,k}\cos\gamma_k \end{aligned} \tag{6.19}$$
to cast the Hamiltonian in terms of new, decoupled, dressed bosons,

as is done in (Tommasini *et al.*, 2003). The derivation is based on a simple geometrical picture which results in a convenient parametrization of the transformation. Following the generalized Bogoliubov transformation, the initial bath operators are transformed as

$$\begin{aligned} a_{j,k} &= \mathcal{Q}^0_{j,+,k} b_{+,k} + \mathcal{Q}^1_{j,+,k} b^\dagger_{+,-k} + (-1)^{\delta_{j,-}} \left(\mathcal{Q}^0_{j,-,k} b_{-,k} + \mathcal{Q}^1_{j,-,k} b^\dagger_{-,-k} \right) \\ a^\dagger_{j,-k} &= \mathcal{Q}^1_{j,+,k} b_{+,k} + \mathcal{Q}^0_{j,+,k} b^\dagger_{+,-k} + (-1)^{\delta_{j,-}} \left(\mathcal{Q}^1_{j,-,k} b_{-,k} + \mathcal{Q}^0_{j,-,k} b^\dagger_{-,-k} \right), \end{aligned} \tag{6.20}$$

with $\delta_{1(2),-(+)} = 1$ and $\delta_{1(2),+(-)} = 0$ and

$$\begin{aligned} \mathcal{Q}^\phi_{j,s,k} =& R_{sj} \hat{\Gamma}_{j,s,k} \Big[(1-\delta_{j,s}) \cos(\gamma_k) + \delta_{j,s} \sin(\gamma_k) \Big] \cos\theta \\ &+ R_{sj'} \hat{\Gamma}_{j',s,k} \Big[(1-\delta_{j',s}) \cos(\gamma_k) + \delta_{j',s} \sin(\gamma_k) \Big] \sin\theta, \end{aligned} \tag{6.21}$$

where $j' \neq j$, $\phi \in \{0,1\}$, $s \in \{+,-\}$, $\hat{\Gamma}_{j(j'),s,k} = [\Gamma^2_{j(j'),s,k} + (-1)^\phi]/2\Gamma_{j(j'),s,k}$ and $R_{1+} = R_{2-} = (1,-1)^\top$, $R_{2+} = -R_{1-} = (1,1)^\top$. Also, in Eq. (6.21),

$$\sin(\gamma_k) = \sqrt{\frac{1}{2}\left[1 - \frac{[\omega^2_{1,k} - \omega^2_{2,k}]}{\sqrt{(\omega^2_{1,k} - \omega^2_{2,k})^2 + 16\Lambda^2_{12} n_1 n_2 e_{1,k} e_{2,k}}}\right]},$$

with $\cos(\gamma_k)$ defined accordingly, and $\Gamma_{j,s,k} = \sqrt{e_{j,k}/E_{s,k}}$ where

$$E_{\pm,k} = \left[\frac{\sum_j \omega^2_{j,k} \pm \sqrt{(\omega^2_{1,k} - \omega^2_{2,k})^2 + 16\Lambda^2_{12} n_1 n_2 e_{1,k} e_{2,k}}}{2}\right]^{\frac{1}{2}}, \tag{6.22}$$

In the literature, $(+)$ is referred to as the spin mode, and $(-)$ is referred to as the density mode. These correspond to two types of quasiparticles: one phonon mode $(-)$ in which the total density fluctuates and another mode $(+)$ in which the unlike particle densities fluctuate out of phase. The latter, in the presence of an internal Josephson interaction as in our case, is a Josephson plasmon (Paraoanu *et al.*, 2001). In addition, one gets that $\theta_{12} \in \{0, \pi\}$ by minimizing the mean-field value of the Hamiltonian per particle $\frac{H_0}{N}$ with respect to θ_{12}, where $N = N_1 + N_2$. By minimizing with respect to the population imbalance $f = \frac{N_1 - N_2}{N}$, one can obtain the following conditions on the parameters of the system in order to have an extremum of the energy,

$$\Delta + Af - \cos\theta_{12} \frac{f}{(1-f^2)^{1/2}} = 0, \tag{6.23}$$

where A and Δ are the mutual interaction parameter and the effective detuning parameter respectively, given in the previous section, and satisfy Eq. (6.11). In (Tommasini *et al.*, 2003), it was shown that to obtain the minimum energy of the system, without imposing any condition on the detuning δ, as is our case, then the relative phase should be chosen to be $\theta_{12} = \pi$, referred to as the π-state configuration. From here on we assume the

symmetric case, i.e, $g_1 = g_2 = g$ as this will allow us to obtain analytically the spectral density in section B.1. After ignoring the detuning δ, the equilibrium condition Eq. (6.23) reads as

$$\left(g - g_{12} + \frac{\Omega}{\sqrt{n_1 n_2}}\right)(n_1 - n_2) = 0, \tag{6.24}$$

which has two solutions

$$\begin{aligned} n_1 - n_2 &= 0 && (GS1)\,, \\ n_1 - n_2 &= \pm n\sqrt{1 - \left(\tfrac{2\Omega}{(g-g_{12})n}\right)^2} && (GS2)\,, \end{aligned} \tag{6.25}$$

corresponding to neutral $GS1$ and polarized ground states $GS2$. Here, we make the strong Josephson junction assumption

$$|A| < 1, \tag{6.26}$$

which is also referred to as the miscibility condition. This implies that the minimum energy equilibrium ground state has to be $GS1$ as is shown in (Tommasini *et al.*, 2003, Abad and Recati, 2013). Handleable expressions for the spectral density obtained section B.1 are possible over $GS1$. For the regime in which ground state is $GS2$ we expect similar qualitative behaviour, but we did not obtained a form for the spectral density which allows us to obtain the diffusive behaviour of the impurity. The study of the impurity diffusion over $GS2$, and even at the phase transition, falls out of the scope of this paper. Under the miscibility condition, the energy spectrum expressions simplifies into

$$E_{-,k} = \left(\frac{k^2}{2m_{\mathrm{B}}}\left(\frac{k^2}{2m_{\mathrm{B}}} + (g + g_{12})\,n\right)\right)^{\frac{1}{2}}, \tag{6.27}$$

$$E_{+,k} = \left[\frac{k^2}{2m_{\mathrm{B}}}\left(\frac{k^2}{2m_{\mathrm{B}}} + (g - g_{12})\,n + 4\Omega\right) + 2\Omega\left[(g - g_{12})\,n + 2\Omega\right]\right]^{\frac{1}{2}}. \tag{6.28}$$

In Fig.6.2 we plot the energy spectra as a function of k for specific parameters, to illustrate the spin and density branches. Furthermore, note that the Bogoliubov transformation elements satisfy the well-known relation

$$\mathcal{Q}^0_k(\mathcal{Q}^0_k)^T - \mathcal{Q}^1_k(\mathcal{Q}^1_k)^T = 1, \tag{6.29}$$

where $\mathcal{Q}^\phi_k = \begin{pmatrix} \mathcal{Q}^\phi_{1,+,k} & \mathcal{Q}^\phi_{1,-,k} \\ \mathcal{Q}^\phi_{2,+,k} & \mathcal{Q}^\phi_{2,-,k} \end{pmatrix}$ with $\phi \in \{0, 1\}$, that implies normalization. However, as is shown in (Lellouch *et al.*, 2013), these Bogoliubov operators, do not fulfill the bosonic commutations relations, which is understood as a consequence of the fact that they are not orthogonalized with respect to the quasicondensate functions $\Psi_{j,0} = \sqrt{N_j}e^{i\theta_j}$. In (Lellouch *et al.*, 2013) it is shown that to overcome this problem one needs to define some new transformation with components $\widehat{\mathcal{Q}}^0_{j,s,k}$, $\widehat{\mathcal{Q}}^1_{j,s,k}$, that are related to the previous ones as

$$\widehat{\mathcal{Q}}^\phi_{j,s,k} = \mathcal{Q}^\phi_{j,s,k} - \frac{\Psi_{j,0}}{N_j}\mathcal{Q}^\phi_{j,s,k}\Psi^*_{j,0}. \tag{6.30}$$

The elements of this transformation, these new Bogoliubov operators, are expressed in terms of the Bogoliubov wave functions of our system $f_{j,s,k}$, $\widetilde{f}_{j,s,k}$ as

$$\widehat{\mathcal{Q}}^{\phi}_{j,s,k} = \frac{f_{j,s,k} + (-1)^{\phi}\, \widetilde{f}_{j,s,k}}{2}, \tag{6.31}$$

where

$$\begin{aligned}
f_{1,-,k} = f_{2,-,k} &= \left[\frac{\epsilon_k}{2E_{-,k}}\right]^{1/2}, \\
\widetilde{f}_{1,-,k} = \widetilde{f}_{2,-,k} &= \left[\frac{E_{-,k}}{2\epsilon_k}\right]^{1/2}, \\
f_{1,+,k} = f_{2,+,k} &= \left[\frac{\epsilon_k + \Omega}{2E_{+,k}}\right]^{1/2}, \\
\widetilde{f}_{1,+,k} = \widetilde{f}_{2,+,k} &= \left[\frac{E_{+,k}}{2\left(\epsilon_k + \Omega\right)}\right]^{1/2}.
\end{aligned}$$

The spin mode branch is gapped while the density mode branch is gapless. For the latter, at low values of the momentum k the dispersion is linear, with a speed of sound $c_d = \sqrt{n\left(g + g_{12}\right)/(2m_{\mathrm{B}})}$. On the contrary for the gapped branch, the dispersion relation goes as k^2 for low k, and at $k = 0$, it has a gap

$$E_{\mathrm{gap}} = \sqrt{2\Omega\left(\left(g - g_{12}\right)n + 2\Omega\right)}. \tag{6.32}$$

This corresponds to the Josephson frequency for small amplitude oscillations. As we will see the fact that there are two branches in the spectrum will give rise to two different noise sources.

The assumption of equal populations amounts to selecting one of the two ground states of the system obtained through the solutions of the corresponding Gross-Pitaevskii equations, as is explained in (Abad and Recati, 2013). This is equivalent to assuming that we are in the "Strong Josephson coupling" regime as in (Tommasini *et al.*, 2003). More importantly, one should note that, if we had not introduced the Rabi coupling term in the Hamiltonian, the latter would commute with both n_1 and n_2 such that we would have two broken continuous symmetries and both branches would be gapless, which we can see this by the fact that $E_{\mathrm{gap}} \to 0$ when $\Omega \to 0$. In this case, the low momentum excitations would be both phase-like, as it has to be for Goldstone modes of the $U\left(1\right)$x$U\left(1\right)$ broken symmetries (Recati and Piazza, 2019). Hence the introduction of the Rabi coupling term, results in the system having only one continuous broken symmetry, namely only n has to be conserved now and not both n_1 and n_2. The long wavelength limit of the Goldstone mode corresponds to a low-amplitude phonon fluctuation in which the total density oscillates and the unlike atoms move in unison (i.e., with the same superfluid velocity). In contrast, in the long wavelength gap mode the unlike atoms move in opposite directions,

while their center of mass remains at rest. This fluctuation is then reminiscent of the motion of ions in an optical phonon mode, which also exhibits a gapped dispersion. At zero momentum, the gap mode corresponds to an infinitesimal Josephson-like oscillation of the populations in the distinguishable internal states. In the strong Josephson coupling regime we have closed orbits around a fixed point for the Josephson Hamiltonian, with vanishing mean polarisation (or population imbalance) and a phase difference around π if $\Omega \geq 0$, giving rise to plasma-like oscillations.

6.2 Impurity-Bath Hamiltonian

The Hamiltonian of an impurity interacting with a two-species bosonic mixture in one dimension reads

$$H = H_{\mathrm{I}} + H_{\mathrm{B}}^{(1)} + H_{\mathrm{B}}^{(2)} + H_{\mathrm{IB}} + H_{\mathrm{B}}^{(12)}, \tag{6.33}$$

where the impurity of mass m_{I} is described by $H_{\mathrm{I}} = \frac{\mathbf{p}^2}{2m_{\mathrm{I}}} + U(\mathbf{x})$, with $U(\mathbf{x})$ being the trapping potential, and its interactions with the bosons is H_{IB}. We will only study free impurities, hence we assume $U(\mathbf{x}) = 0$. The terms of the individual bosonic species, labeled with the index $j = 1, 2$, are given as above.

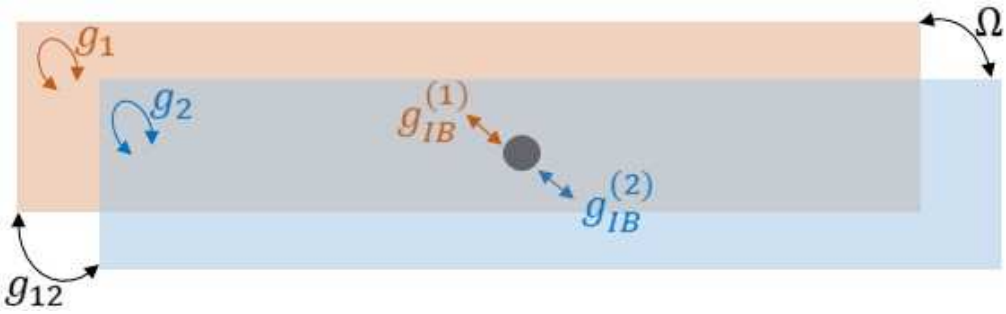

Fig. 6.1 We consider a set-up of a coherently coupled two-component BEC in which an impurity is immersed. By g_1 and g_2 we denote the intra-species contact interactions of the atoms of the first and second species respectively. g_{12} refers to the coupling strength of the interspecies contact interaction among atoms of the first and second species. By Ω we denote the Rabi frequency of the Raman coherent coupling between the two species. Finally $g_{IB}^{(1)}$ and $g_{IB}^{(2)}$ indicate the coupling of the impurity to the atoms of the first and second species respectively.

In what concerns the impurity-bosons interaction part of the Hamiltonian, we assume that the interaction is among the impurity and the densities of the bosons, i.e. it has the form of a contact interaction:

$$H_{\mathrm{IB}} = \left(\sum_{j=1,2} g_{\mathrm{IB}}^{(j)} \Psi_j^\dagger(\mathbf{x}) \Psi_j(\mathbf{x}) + h.c. \right). \tag{6.34}$$

The impurity-bath Hamiltonian in terms of the annihilation (creation) operators $a_{j,k}(a^{\dagger}_{j,k})$, and after making the condensation assumption, reads as

$$\begin{aligned} H_{\mathrm{IB}} &= \sum_{j} \frac{1}{V} \sum_{k,q} V^{(j)}_{\mathrm{IB}}(k)\, \rho_{\mathrm{I}}(q)\, a^{\dagger}_{j,k-q} a_{j,k} \\ &= \sum_{j} \sqrt{\frac{n_j}{V}} \sum_{k\neq 0} \rho_{\mathrm{I}}(k)\, V^{(j)}_{\mathrm{IB}} \left(a_{j,k} + a^{\dagger}_{j,-k}\right), \end{aligned} \tag{6.35}$$

with $\rho_I(q) = \int_{-\infty}^{\infty} e^{-iqx'} \delta(x'-x)\, dx'$, $V^{(j)}_{\mathrm{IB}}(k) = \mathcal{F}_k[g^{(j)}_{\mathrm{IB}} \delta(x-x')]$ and $g^{(j)}_{\mathrm{IB}} = 2\pi a^{(j)}_{\mathrm{IB}}/m_R$, where $\mathcal{F}$ is the Fourier transform, $a^{(j)}_{\mathrm{IB}}$ represents the scattering length of the impurity with the bosons of the j^{th} BEC, and $m_R = m_{\mathrm{B}} m_I/(m_{\mathrm{B}} + m_I)$ is the j^{th} reduced mass. Furthermore, n_j, with $j = 1, 2$, is the averaged density of the j^{th} bath. The second line of Eq. (6.35) is a consequence of the assumption that our bosons condensate. We will consider two cases:

1. $g^{(1)}_{\mathrm{IB}} = g^{(2)}_{\mathrm{IB}} = g_{\mathrm{IB}}$,
2. $g^{(1)}_{\mathrm{IB}} = -g^{(2)}_{\mathrm{IB}} = g_{\mathrm{IB}}$.

After the Bogoliubov transformation the impurity-bath term for each species is

1. $H^{(-)}_{IB} = \sqrt{\frac{n}{V}} \sum_{j,k\neq 0} \rho_I(k)\, g_{\mathrm{IB}} \left(\widehat{\mathcal{Q}}^0_{j,-,k} + \widehat{\mathcal{Q}}^1_{j,-,k}\right) x_{-,k}$,
2. $H^{(+)}_{IB} = \sqrt{\frac{n}{V}} \sum_{j,k\neq 0} \rho_I(k)\, g_{\mathrm{IB}} \left(\widehat{\mathcal{Q}}^0_{j,+,k} + \widehat{\mathcal{Q}}^1_{j,+,k}\right) x_{+,k}$,

where $x_{\pm,k} = \left(b_{\pm,k} + b^{\dagger}_{\pm,k}\right)$. These equations show that in case 1 the impurity only couples to the density $(-)$ mode of the bosonic baths, while in case 2 it couples only to the spin $(+)$ mode. We rewrite the impurity-bath terms as

$$H^{s}_{\mathrm{IB}} = \sum_{\substack{j,k\neq 0 \\ s\in\{+,-\}}} V_{j,s,k} e^{ikx} \left(b_{s,k} + b^{\dagger}_{s,-k}\right), \tag{6.36}$$

where

$$V_{j,s,k} = \sqrt{\frac{n}{V}} g_{\mathrm{IB}} \left(\widehat{\mathcal{Q}}^0_{j,s,k} + \widehat{\mathcal{Q}}^1_{j,s,k}\right). \tag{6.37}$$

We note here that $\widehat{\mathcal{Q}}^0_{1,s,k} + \widehat{\mathcal{Q}}^1_{1,s,k} = \widehat{\mathcal{Q}}^0_{2,s,k} + \widehat{\mathcal{Q}}^1_{2,s,k}$, such that $V_{1,s,k} = V_{2,s,k} = \widehat{V}_{s,k}$. We linearize the interaction (see (Lampo *et al.*, 2017a) for validity of this assumption) to get

$$H_{\mathrm{IB}} = \sum_{\substack{k\neq 0 \\ s\in\{+,-\}}} V_{s,k} (\mathbb{I} + ikx) \left(b_{s,k} + b^{\dagger}_{s,-k}\right). \tag{6.38}$$

where $V_{s,k} = 2\widehat{V}_{s,k}$. Thus, after a redefinition $b_{s,k} \to b_{s,k} - \frac{V_{s,k}}{E_{s,k}} \mathbb{I}$, the final total Hamiltonian reads as

$$H = H_{\mathrm{I}} + \sum_{\substack{k\neq 0 \\ s\in\{+,-\}}} E_{s,k} b^{\dagger}_{s,k} b_{s,k} + \sum_{\substack{k\neq 0 \\ s\in\{+,-\}}} g_{s,k} \pi_{s,k}, \tag{6.39}$$

with $g_{j,s,k} = \frac{kV_{s,k}}{\hbar}$ and $\pi_{s,k} = i\left(b_{k,s} - b_{k,s}^{\dagger}\right)$ the momentum of the bath particles. We see that as in (Lampo *et al.*, 2017a), the coupling is between the position of the impurity and the momentum of the bath particles.

6.3 Spectral densities

The spectral densities can be obtained from the self-correlation functions (Lampo *et al.*, 2017a) for each environment (corresponding to cases 1 and 2). These read

$$\mathcal{C}(t) = \sum_{\substack{k \neq 0 \\ s \in \{+,-\}}} g_{s,k}^2 \left\langle \pi_{s,k}(t)\, \pi_{s,k}(0) \right\rangle . \tag{6.40}$$

Using that the bath is composed of bosons for which

$$\left\langle b_{k,s}^{\dagger} b_{k,s} \right\rangle = \frac{1}{e^{\frac{\omega_k}{k_B T}} - 1}, \tag{6.41}$$

we obtain

$$\begin{aligned} \mathcal{C}(t) = & \sum_{\substack{k \neq 0 \\ s \in \{+,-\}}} g_{s,k}^2 \left[\coth\left(\frac{\omega_k}{2k_B T}\right) \cos(\omega_k t) - i \sin(\omega_k t) \right] \\ & = \nu(t) - i\lambda(t), \end{aligned} \tag{6.42}$$

where

$$\begin{aligned} \nu(t) &= \int_0^{\infty} \sum_{s \in \{+,-\}} J^D(\omega) \coth\left(\frac{\omega}{2k_B T}\right) \cos(\omega t)\, d\omega, \\ \lambda(t) &= \int_0^{\infty} \sum_{s \in \{+,-\}} J^D(\omega) \sin(\omega t)\, d\omega. \end{aligned} \tag{6.43}$$

In these definitions we used the spectral density,

$$J^D(\omega) = \sum_{k \neq 0} (g_{s,k})^2\, \delta(\omega - \omega_k). \tag{6.44}$$

The spectral density is evaluated in the continuous frequency limit as

$$J^D(\omega) = 4n g_{\mathrm{IB}}^2 \frac{D_d}{(2\pi)^d} \int dk\, k^{d+1} (\mathcal{U}_{s,k} + \mathcal{V}_{s,k})^2 \frac{\delta(k - k_{E_s}(\omega))}{\partial_k E_s(k)\,|_{k=k_{E_s}(\omega)}}, \tag{6.45}$$

where D_d is the surface of the hypersphere in the momentum space with radius k in d-dimensions. In the particular case of 1D becomes $D_1 = 2$.

To obtain the expression for the continuous frequency case, the inverse of the dispersion relation from Eq. (6.22) is needed. For this general energy spectrum, obtaining such inverse function is not easy. However this is indeed possible for the simplified case, Eqs. (6.28). The inverse of the density (-) branch which is the one to which the impurity couples for the case 1 type of coupling, reads

$$k_{E_-}(\omega) = \sqrt{m_{\mathrm{B}} n g}\left[\frac{g_{12}}{g} - 1 + \sqrt{1 - \frac{2g_{12}}{g} + \left(\frac{g_{12}}{g}\right)^2 + \left(\frac{2\omega}{ng}\right)^2}\right]^{\frac{1}{2}}. \tag{6.46}$$

With this, for the density $(-)$ branch (case 1 type of coupling), the spectral density is

$$J_-(\omega) = \tilde{\tau}_- \frac{G_-(\omega)^{3/2}}{\sqrt{F_-(\omega)}}, \tag{6.47}$$

with

$$F_-(\omega) = 1 + \left(\frac{\omega}{\Lambda_-}\right)^2, \tag{6.48}$$

$$G_-(\omega) = -1 + \sqrt{F_-(\omega)}, \tag{6.49}$$

$$\tilde{\tau}_- = \frac{(2g_{\mathrm{IB}})^2 n m_{\mathrm{B}}^{3/2}}{2^{1/2}\pi}\sqrt{\Lambda_-}, \tag{6.50}$$

and where $\Lambda_- = n(g + g_{12})/2$ is the cutoff frequency, which resembles the one in (Lampo *et al.*, 2017a) when g is replaced by $\frac{g+g_{12}}{2}$. In the limit of $\omega \ll \Lambda_-$, the spectral density can be simplified to

$$J_-(\omega) = \tau_- \omega^3, \tag{6.51}$$

where

$$\tau_- = \frac{(2\eta)^2}{2\pi}\left(\frac{m_{\mathrm{B}}}{n(g + g_{12})^{1/3}}\right)^{3/2}, \tag{6.52}$$

with $\eta_- = \frac{g_{\mathrm{IB}}}{g+g_{12}}$. Thus, for the the π-state equilibrium configuration one obtains a cubic spectral density.

For the spin $(+)$ branch (case 2 type of coupling), the inverse of the spectrum reads as

$$k_{E_+}(\omega) = \sqrt{m_{\mathrm{B}} n g}\left[\frac{g_{12}}{g} - 1 - \frac{4\Omega}{ng} + \sqrt{1 - \frac{2g_{12}}{g} + \left(\frac{g_{12}}{g}\right)^2 + \left(\frac{2\omega}{ng}\right)^2}\right]^{\frac{1}{2}}.$$

In this case, the spectral density is

$$J_+(\omega) = \widetilde{\tau}_+ \frac{G_+(\omega)}{\sqrt{F_+(\omega)}}, \tag{6.53}$$

where

$$
\begin{aligned}
F_{+}(\omega) &= 1+\left(\frac{\omega}{\Lambda_{+}}\right)^{2}, \\
G_{+}(\omega) &= W(\omega)\left(W(\omega)+\frac{1}{2}-\frac{1}{2}\sqrt{1+\left(\frac{E_{\mathrm{gap}}}{\Lambda_{+}}\right)^{2}}\right)^{1/2}, \\
W(\omega) &= -\frac{1}{2}+\sqrt{F_{+}(\omega)}-\frac{1}{2}\sqrt{1+\left(\frac{E_{\mathrm{gap}}}{\Lambda_{+}}\right)^{2}}, \\
\widetilde{\tau}_{+} &= \frac{(2g_{\mathrm{IB}})^{2} n m_{\mathrm{B}}^{3/2}}{2^{1/2}\pi}\sqrt{\Lambda_{+}},
\end{aligned}
\tag{6.54}
$$

with $\Lambda_{+}=n(g-g_{12})/2$. We note that to interpret $\widetilde{\tau}_{+}$ as a relaxation time, as is custom to do, see (Lampo *et al.*, 2017a), one has to impose $g \geq g_{12}$ to assure it remains a real quantity. In other case, the spectral density will be imaginary (note $\frac{G_{+}(\omega)}{\sqrt{F_{+}(\omega)}}$ is independent of the sign of $g-g_{12}$).

Let us find how the spectral density in Eq. (6.53) simplifies in two limiting cases. First, in the absence of coherent coupling, $\Omega=0$, the gap vanishes, $E_{\mathrm{gap}}=0$. In this case, Eq. (6.53) is equal to that of the density mode, upon the interchange $\Lambda_{-}\to\Lambda_{+}$. Therefore, on the long time limit $\omega \ll \Lambda_{+}$ we obtain the same cubic behaviour of the spectral density. We illustrate this case in Fig. 6.2. In panel (a) we show that the two branches of the energy spectra have the same behaviour, that is, linear at low k and parabolic for large k.

Second, we consider the case of finite Ω which implies $E_{\mathrm{gap}}>0$. For any Ω that satisfies (6.26), one finds that $E_{\mathrm{gap}}>\Lambda_{+}$. In this scenario, to study the long-time behaviour of the system, a first approach is to assume that it is determined by Λ_{+} , i.e. by $\omega \ll \Lambda_{+}$. In such case, the resulting spectral density is imaginary, and for this reason we exclude it. On the other hand, for $\omega \ll E_{\mathrm{gap}}$, the spectral density is also imaginary. Furthermore, a requirement which we impose on the spectral density is that one cannot consider frequencies lower than the gap energy E_{gap}. Physically, one can interpret this as follows: Since the energy spectrum of the bath is gapped, with a gap given by Eq. (6.32), the spectral density cannot assign a weight at frequencies lower than this, because the bath cannot excite the impurity with such frequencies since it is not part of its spectrum. Then, we simplify the spectral density as

$$
\widehat{J}_{+}(\omega)=\Theta(\omega-E_{\mathrm{gap}})\,J_{+}(\omega), \tag{6.55}
$$

with $\Theta(.)$ the step delta function.

Let us now comment on the frequency region right above the energy gap of our system. To this end, we replace $\omega=E_{\mathrm{gap}}+\epsilon$, where $\epsilon>0$. We use ϵ as the small value expansion

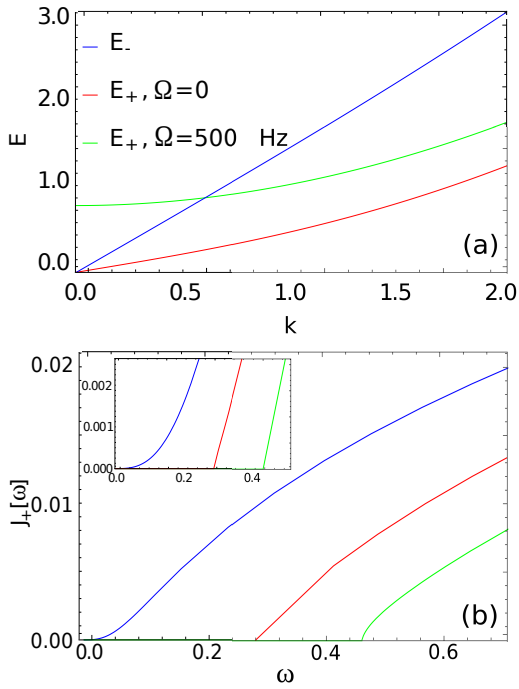

Fig. 6.2 (a) Energy spectrum for a coherently coupled two component BEC. There are two branches in the spectrum corresponding to the density (-) and spin modes (+). We plot both for different values of the coherent coupling, Ω. First, this illustrates that the gap opens for the spin mode (+); and second, it shows that, while for $\Omega = 0$ both branches behave similarly, i.e., linearly for low k and quadratically for large k, for finite Ω the (+) mode behaves quadratically even at low k. This has direct implications on the behaviour of the spectral density in case 2, plotted in (b). When the $\Omega = 0$ (blue line) the spectral density behaves as for the density mode (i.e. with a w^3-behaviour). The red and green lines (for $\Omega = 50\pi$ Hz, 100πHz, respectively) show instead a different behaviour. The inset shows a zoom, where we checked that it fits the simplified behaviour in Eq. (6.60), i.e. has a lower gap and behaves as $\sqrt{w}$ initially. In these plots we used $g = g_{12} = 2.15x10^{-37} J \cdot m$, $n = 7(\mu m)^{-1}$, $g_{\mathrm{IB}} = 0.5x10^{-37} J \cdot m$, with BEC and impurities made of Rb and K atoms, respectively.

parameter in our case, i.e. we consider the limit $\epsilon \ll E_{\mathrm{gap}}$, such that $\omega \approx E_{\mathrm{gap}}$. We furthermore introduce an arbitrary cutoff Λ, for which it holds that $\epsilon \ll \Lambda - E_{\mathrm{gap}}$. The

expressions in the spectral density will now read as

$$F_+(\epsilon) = 1 + \left(\frac{E_{\rm gap}}{\Lambda_+}\right)^2, \tag{6.56}$$
$$W(\epsilon) = -\frac{1}{2} + \frac{1}{2}\sqrt{1+\left(\frac{E_{\rm gap}}{\Lambda_+}\right)^2} + \frac{E_{\rm gap}}{\Lambda_+}\left(E_{\rm gap}^2 + \Lambda_+^2\right)^{-\frac{1}{2}}\epsilon,$$

such that

$$G_+(\epsilon) = \left[-\frac{1}{2} + \frac{1}{2}\sqrt{1+\left(\frac{E_{\rm gap}}{\Lambda_+}\right)^2}\right]\left(\frac{E_{\rm gap}}{\Lambda_+}\right)^{\frac{1}{2}}\left(E_{\rm gap}^2+\Lambda_+^2\right)^{-\frac{1}{4}}\epsilon^{\frac{1}{2}}. \tag{6.57}$$

Hence the spectral density is

$$\widehat{J}_+(\epsilon) = \Theta(\epsilon)\,\widehat{\tau}_+\epsilon^{1/2}, \tag{6.58}$$

with

$$\tau_+ = \widetilde{\tau}_+ \frac{\left(-\frac{1}{2} + \frac{1}{2}\sqrt{1+\left(\frac{E_{\rm gap}}{\Lambda_+}\right)^2}\right)(E_{\rm gap})^{\frac{1}{2}}}{\left(1+\left(\frac{E_{\rm gap}}{\Lambda_+}\right)^2\right)^{1/4}}. \tag{6.59}$$

The final form of the spectral density, after introducing a cutoff Λ, to avoid the related ultraviolet divergencies mentioned above, is

$$\widehat{J}_+(\omega) = \Theta(\omega - E_{\rm gap})\,\tau_+(\omega - E_{\rm gap})^{1/2}\,\Theta(\Lambda + E_{\rm gap} - \omega). \tag{6.60}$$

We introduced a hard cutoff to our spectral density as this better describes the physical system we study. Such a spectral density, i.e. with an exponent on the frequencies less than 1, is often associated to subdiffusive impurity dynamics. Note that in the results that we present below, we assume $g \approx g_{12}$ as in (Nicklas, 2013), which significantly simplifies the expression for the coefficient of the spectral density τ_+ without changing its behaviour. In particular in this case $\tau_+ = (2g_{\rm IB})^2\, n m_{\rm B}^{3/2}/2^{1/2}\pi$. In Fig. 6.2(b), we show how the approximate spectral density in Eq. (6.60), under the assumption $\epsilon \ll E_{\rm gap}$, compares to the original spectral density. For vanishingly small values of $E_{\rm gap}$ the spectral density approaches the form of that of the density mode, i.e. it goes as $\propto \omega^3$, as expected. In the limit we are interested, that is, for finite $E_{\rm gap}$, the spectral density behaves approximately as in Eq. (6.60) (see inset in panel Fig. 6.2(b)).

Such gapped spectral densities as in Eq. (6.60), have already been studied extensively in the literature. In general, they are usually related to semiconductors (John and Quang, 1994, Tan *et al.*, 2011, Prior *et al.*, 2013) or photonic crystals (PC) (Kofman *et al.*, 1994). In particular, the simplified form of the spectral density, Eq. (6.60), is related in particular with 3D photonic crystals. The latter, are artificial materials engineered with periodic dielectric structures (P Bykov, 1972). If one considers an atom embedded in such a

material, it is known that if the resonant frequency of the excited atom approaches the band gap edge of the PC, strong localization of light, atom-photon bound states, inhibition of spontaneous emission and fractionalized steady-state inversion appear (Yablonovitch, 1987, Lambropoulos *et al.*, 2000, Woldeyohannes and John, 2003, Quang *et al.*, 1997). The rapidly varying distribution of field modes near the band gap (Kofman *et al.*, 1994, Kofman and Kurizki, 2004) requires a non-Markovian description (Breuer and Petruccione, 2007a) of the reduced dynamics of quantum systems coupled to the radiation field of a PC (Woldeyohannes and John, 2003, Quang *et al.*, 1997, Rivas *et al.*, 2010, de Vega *et al.*, 2005, 2008). This enhanced appearance of Non-Markovian effects is also confirmed by a recent study based on exact diagonalization (Vasile *et al.*, 2014). In this study it was observed that for frequencies of the bath much larger than the band gap, energy transfer between the system and the bath is allowed and therefore information and energy flow irreversibly from system to bath appears leading to Markovian dynamics. On the other hand, at the edges of the gaps, one observes the largest backflow of information where the energy bounces between the system and bath leading to Non-Markovian evolution of the system. Furthermore, deep within the band gap, less excitations and energy are exchanged between the system and the bath, which is shown to lead to localized modes (Zhang *et al.*, 2012), expressed as dissipation-less oscillatory behaviour, plus non-exponential decays (such as for example fractional relaxations (Giraldi and Petruccione, 2014)).

From the work in (Zhang *et al.*, 2012), a relationship is suggested of such long-lived oscillations that appear in the dynamics of a system coupled to a bath with a gapped spectral density, with the fact that the Hamiltonian of the system might have thermodynamic and dynamic instabilities. This is the case when the Hamiltonian is unbounded from below, i.e. non-positive. Physically, this is the case for Hamiltonians that exhibit breakdown of particle number conservation, as is our case of the QBM, and which can induce dynamical instabilities in the long-time regime, where by long time limit, one implies the regime $\omega \ll \Lambda$, meaning for frequencies deep inside the band. As in the spirit of (Lampo *et al.*, 2017a), one can show that the effect of the bath on the impurity is not only to dissipate its energy, but as well to introduce an inverse parabolic potential in which the impurity is diffusing (which would work as a renormalization of the trapping frequency had we considered a harmonic trapping potential). This inverse parabolic potential is understood to be a consequence of the unboundedness of the Hamiltonian, and is what is resulting in the dynamical instability of the long time solution of the impurity dynamics. Unfortunately, contrary to the case in (Lampo *et al.*, 2017a), we will not consider a harmonic trap for the impurity, and hence the positivity of the Hamiltonian is violated irrespective of the strength of the coupling of the impurity to the bath. In practice one would study the impurity constrained in a box of a certain size, which if included in the modeling of the system, would result in a positively defined Hamiltonian, at the price of

complicating significantly the analytical solution for the impurity's dynamics. Hence we proceed with the current description of our system, but we assume that we are looking at timescales where the effect of the finite sized box are not manifested. Theoretically, there are also a number of other ways to circumvent this problem, even without referring to the presence of a box, such as taking into account bilinear terms in the impurity's or bath's operators in the Hamiltonian as in (Bruderer *et al.*, 2007, Rath and Schmidt, 2013, Christensen *et al.*, 2015a, Shchadilova *et al.*, 2016d). In any case, we will show below that for the regime of the transient effect that we are interested in, this will not change qualitatively our results.

Following the approach sketched above, we take advantage of the simplicity of the Fröhlich like Hamiltonian we are considering above. Furthermore, we remind that we will look at the long time dynamics of the impurity, i.e. $\omega \ll \Lambda$, as was implied by the above study on the spectral density's form. In addition, one should take into account the dissipationless oscillatory behaviour, which can also be expressed as an incomplete decay of the Green function impurity propagator which we will study below. In fact by identifying the equivalence of the appearance of these oscillations with the incomplete decay of the Green function, this provides us with a very simple condition upon which the long-live oscillations appear, that is that the Green function has at least one purely imaginary pole, which can be shown to only be possible for frequencies within the band gap (Kofman *et al.*, 1994). We will study this in the next section.

Finally, an important point to note, is that from the above considerations, we conclude also that our system could potentially be used to observe various phenomena traditionally linked to particles immersed in electromagnetic fields in quantum-optical systems. This idea goes in parallel to a previous attempt to simulate quantum optical phenomena with cold atoms in optical lattices as in (Navarrete-Benlloch *et al.*, 2011). It is yet important to state that this set-up could as well be used in simulating Bose-Hubbard Hamiltonian with extended hopping and Ising models with long-range interactions.

6.4 Heisenberg equations and their solution

In this section, we derive the equation of motion for the impurity, which will allow us to study its diffusive behaviour under the various scenarios. To do so, we begin with the Heisenberg equations of motion for both the impurity and the bath particles. The latter set of equations can be solved, and we use this solution to obtain a Langevin like equation

of motion for the impurity. The Heisenberg equations for the bath particles are

$$\begin{aligned}\frac{db_{s,k}(t)}{dt} &= \frac{i}{\hbar}[H, b_{s,k}(t)] = -\frac{i}{\hbar}\Omega_{s,k} b_{s,k}(t) - \sum_{j=1}^{2} g_{s,k}^{(j)} x(t),\\ \frac{db_{s,k}^{\dagger}(t)}{dt} &= \frac{i}{\hbar}\left[H, b_{s,k}^{\dagger}(t)\right] = \frac{i}{\hbar}\Omega_{s,k} b_{s,k}^{\dagger}(t) - \sum_{j=1}^{2} g_{s,k}^{(j)} x(t),\end{aligned} \tag{6.61}$$

and for the central particle

$$\begin{aligned}\frac{dx(t)}{dt} &= \frac{i}{\hbar}[H, x(t)] = \frac{p(t)}{m_I},\\ \frac{dp(t)}{dt} &= \frac{i}{\hbar}[H, p(t)] = \frac{i}{\hbar}[U(x), x(t)] - \hbar \sum_{\substack{k\neq 0\\ j=\{1,2\}\\ s=\{+,-\}}} g_{s,k}^{(j)} \pi_{s,k}(t).\end{aligned} \tag{6.62}$$

Substituting the solutions of the equations of motion for the bath into that of the central particle, one gets

$$\ddot{x}(t) + \frac{\partial}{\partial t}\int \Gamma(t-s)\, x(s)\, ds = \frac{B(t)}{m_I}, \tag{6.63}$$

where

$$\begin{aligned}\Gamma(\tau) &= \frac{1}{m_I}\int_0^{\infty} \frac{\sum_{\substack{j=\{1,2\}\\ s=\{+,-\}}} J_s^{(j)}(\omega)}{\omega} \cos(\omega\tau)\, d\omega,\\ B(t) &= \sum_{k\neq 0} i\hbar \sum_{\substack{j=\{1,2\}\\ s=\{+,-\}}} g_{s,k}^{(j)} \left(b_{s,k}^{\dagger}(t)\, e^{i\omega_k t} - b_{s,k}(t)\, e^{-i\omega_k t}\right),\end{aligned} \tag{6.64}$$

are the damping and noise terms, respectively. Note that in Eq. (6.63) we neglected a term $-\Gamma(0)\, x(t)$. This term may introduce dynamic instabilities in our system in the long time regime. As in (Lampo *et al.*, 2017a), we neglect it as these instabilities are unphysical, that is, will not occur in a physical realization of the system and will only occur in the long time behavior. To be more specific, for the coupling to the density mode this term reads as,

$$\Gamma_{-}(0) = \tau_{-}\frac{\Lambda_{-}^{3}}{3}. \tag{6.65}$$

For the coupling to the spin mode this term reads as

$$\Gamma_{+}(0) = \widehat{\tau}_{+}\left[-\pi E_{Gap}^{1/2} + 2(\Lambda + E_{Gap})^{0.5}\, F_{2,1}\left(-\frac{1}{2}, -\frac{1}{2}; \frac{1}{2}; \frac{E_{Gap}}{\Lambda + E_{Gap}}\right)\right].$$

As in (Lampo *et al.*, 2017a), the solution of Eq. (6.63) takes the form

$$x(t) = G_1(t)x(0) + G_2(t)\dot{x}(0) + \frac{1}{m_I}\int_0^t G_2(t-s)B(s)ds, \tag{6.66}$$

with the corresponding Green functions given by

$$\mathcal{L}_z\left[G_1(t)\right] = \frac{z}{z^2 + z\mathcal{L}_z\left[\Gamma(t)\right]} = \frac{1}{z + \mathcal{L}_z\left[\Gamma(t)\right]}, \tag{6.67}$$

$$\mathcal{L}_z\left[G_2(t)\right] = \frac{1}{z^2 + z\mathcal{L}_z\left[\Gamma(t)\right]}. \tag{6.68}$$

where $\mathcal{L}_z\left[\cdot\right]$ represents the Laplace transform. To obtain an expression for $G_1(t)$ and $G_2(t)$, one needs to consider the specific type of bath that is interested to study. For the first scenario (coupling to the density mode), this was studied in (Lampo *et al.*, 2017a), where $\Gamma(t)$ was found to be

$$\Gamma_-(t) = \frac{\tau_-}{t^3}\left[2\Lambda_- t\cos\left(\Lambda t\right) - 2\left(2 - \Lambda_-^2 t^2\right)\sin\left(\Lambda_- t\right)\right], \tag{6.69}$$

and under the long time limit assumption of $z \ll \Lambda_-$

$$\mathcal{L}_z\left[\Gamma_-(t)\right] = \tau_-\Lambda_- z + \mathcal{O}\left(z^2\right). \tag{6.70}$$

Then, one obtains

$$G_1\left(t\right) = \frac{1}{1 + \tau_-\Lambda_-} \tag{6.71}$$

and

$$\mathcal{L}_z\left[G_2(t)\right] = \frac{1}{\left(1 + \Lambda_-\tau_-\right)z^2}, \tag{6.72}$$

which results in

$$G_2(t) = \frac{t}{\left(1 + \Lambda_-\tau_-\right)}, \tag{6.73}$$

where we see that the Green functions have an identical form to that of (Lampo *et al.*, 2017a), which was shown to result in a ballistic diffusion. More importantly, this diverges at $t \to \infty$, a consequence of the fact that an equilibrium state is not reached at this limit.

The second case (coupling to the spin mode) is slightly more involved. We consider the scenario described in the previous section which results in the gapped spectral density of Eq. (6.60). To proceed, we first need an expression for the Laplace transform $\mathcal{L}_z\left[\Gamma_+(t)\right]$ which can be shown to read as

$$\begin{aligned}
\mathcal{L}_z\left[\Gamma_+(t)\right] &= \int_0^\infty \left(\int_0^\infty d\omega \frac{\widehat{J}_+\left(\omega\right)}{\omega}\cos\left(\omega t\right)\right) e^{-zt} dt \\
&= z\int_0^\infty d\omega \frac{\widehat{J}_+\left(\omega\right)}{\omega\left(\omega^2 + z^2\right)} \\
&= \frac{\widehat{\tau}_+}{z\left(E_{gap}^3 + E_{gap} z^2\right)}\Lambda^{1.5}\left[-\frac{E_{\rm gap}}{3}(E_{\rm gap} + iz)F_{2,1}\left(1, \frac{3}{2}; \frac{5}{2}; -\frac{\Lambda}{E_{\rm gap} - iz}\right)\right. \\
&\left. - \frac{E_{\rm gap}}{3}\left(E_{\rm gap} - iz\right)F_{2,1}\left(1, \frac{3}{2}; \frac{5}{2}; -\frac{\Lambda}{E_{\rm gap} + iz}\right) + \frac{2}{3}\left(E_{\rm gap}^2 + z^2\right)F_{2,1}\left(1, \frac{3}{2}; \frac{5}{2}; -\frac{\Lambda}{E_{\rm gap}}\right)\right],
\end{aligned} \tag{6.74}$$

where $F_{2,1}(\alpha,\beta;\gamma;z)$ is the hypergeometric function

$$F_{2,1}(\alpha,\beta;\gamma;z)=\sum_{n=0}^{\infty}\frac{(\alpha)_n(\beta)_n}{(\gamma)_n}\frac{z^n}{n!}, \tag{6.75}$$

with $(\cdot)_n$ being the Pochhammer symbol. Unfortunately, inverting the Laplace transform in Eq. (6.68), given Eq. (6.74), is rather complicated. For this reason we restrain ourselves to studying only the long-time limit, determined by $z \ll \Lambda$. In this case the inverse Laplace transform of the Green's function in Eq. (6.68), reads as

$$\begin{aligned} G_2(t) &= At, \qquad (6.76)\\ A &= E_{\rm gap}^5\left[E_{\rm gap}^5+\frac{2}{3}E_{\rm gap}^2\Lambda^{1.5}\widehat{\tau}_+F_{2,1}\left(1,\frac{3}{2};\frac{5}{2};-\frac{\Lambda}{E_{\rm gap}}\right)\right.\\ &\left.-\frac{4}{5}E_{\rm gap}\Lambda^{2.5}\widehat{\tau}_+F_{2,1}\left(2,\frac{5}{2};\frac{7}{2};-\frac{\Lambda}{E_{\rm gap}}\right)+0.285714\Lambda^{3.5}\widehat{\tau}_+F_{2,1}\left(3,\frac{7}{2};\frac{9}{2};-\frac{\Lambda}{E_{\rm gap}}\right)\right]^{-1}, \end{aligned}$$

which has the same time dependence as in case 1 (coupling to the density mode). Unfortunately this is as far as we can get analytically, as contrary to the coupling to the density mode, even though we have the Green function at hand, using it to obtain an analytic expression for the MSD of the impurity which is our ultimate goal is not possible.

Equation (6.73) as well as Eq. (6.74) have been both obtained at the long time limit, which implied expanding the Laplace transform of the damping kernel $\mathcal{L}_z\left[\Gamma_-(t)\right]$, $\mathcal{L}_z\left[\Gamma_+(t)\right]$ at the first order in $z/\Lambda_-, z/\Lambda$. In general, one could have considered higher orders of the aforementioned expansion, but should then be careful in inverting the Laplace transform to obtain the Green function in defining the relevant Bromwich integral in the complex plane in such a way as to not include the roots which correspond to divergent runaway solutions (Lampo *et al.*, 2017a). Even if one would do so, the result for the Green function would not change much, and this can be proven by considering a numerical inversion of the Laplace transform for the Green function, where the long time limit assumption is not made. For the coupling to the density mode this was shown using the Zakian method in (Lampo *et al.*, 2017a). For the spin mode, we checked this using the same method. Moreover, we contrasted its results to two other methods for numerically inverting a Laplace transform, in particular, the Fourier and the Stehfest methods (Wang and Zhan, 2015). The Zakian method, gives the inverse of the Laplace transform of a function $F(z)$ in the following form

$$f(t)=\frac{2}{t}\sum_{j=1}^{N}Re\left[k_jF\left(\frac{\beta_j}{t}\right)\right], \tag{6.77}$$

where k_j and β_j are real and complex constants given in (Wang and Zhan, 2015). With all of these methods the Green function behaves linearly with time for the range of parameters

we considered. In fact in the numerical results presented in the next section, the Zakian method was used to obtain the Green function, such that our results are not restricted just to the long time limit $z \ll \Lambda$.

In addition, we are also now in a position to check the presence of the long-lived oscillations in our system. As was mentioned before, this can only be the case if the Green function exhibits a purely imaginary pole, which if it exists, should correspond to a frequency within the bandgap. As is shown in (Lo *et al.*, 2015), this will be the case, for the frequency that is a solution of

$$\omega^2 + \Gamma(0) - \Delta(\omega) = 0, \tag{6.78}$$

where

$$\begin{aligned}\Delta(\omega) &:= P\int_0^\infty \frac{\widehat{J}_+(\omega')}{\omega - \omega'}d\omega' \\ &= -\frac{2\widehat{\tau}_+\Lambda^{1.5}F_{2,1}\left(1, \frac{3}{2}; \frac{5}{2}; -\frac{\Lambda}{E_{\text{gap}}-\omega}\right)}{3(E_{\text{gap}} - \omega)},\end{aligned} \tag{6.79}$$

is the bath self energy correction, where P denotes the principal value. One can show that the expression of Eq. (6.79) is always non-positive for $\omega < E_{\text{gap}}$ and hence the condition in Eq. (6.78) is never satisfied, such that we do not have to worry about these oscillations in the transient dynamics that we will study in the next section.

Finally, one can evaluate the validity of the linearity assumption which allowed us to consider a linear coupling between the BEC and the impurity (see Hamiltonian in Eq. (6.38)) in terms of the physical parameters of the system. This assumption reads as $kx \ll 1$. In (Lampo *et al.*, 2017a) it was shown that, as a function of the temperature, there exist a maximum time for which the linear assumption holds. In the system discussed here, since an expression for the MSD cannot be found, for each set of parameters one has to evaluate numerically the long-time behavior of the MDS and determine the maximum time for which the assumption holds. To this end, on has to note that differently to (Lampo *et al.*, 2017a), for the coupling to the spin mode the momenta grows parabolically with ω even for small k and there is an energy gap. Then, to evaluate the criteria ($kx \ll 1$), one has to use the expression for the energy, Eq. (6.28) together with the numerically evaluated MSD. We checked this condition in the numerical examples presented in next section.

6.5 Results

Mean square displacement With the Green propagator and the spectral density at hand, we are now in a position to evaluate the MSD. This, as shown in (Lampo *et al.*,

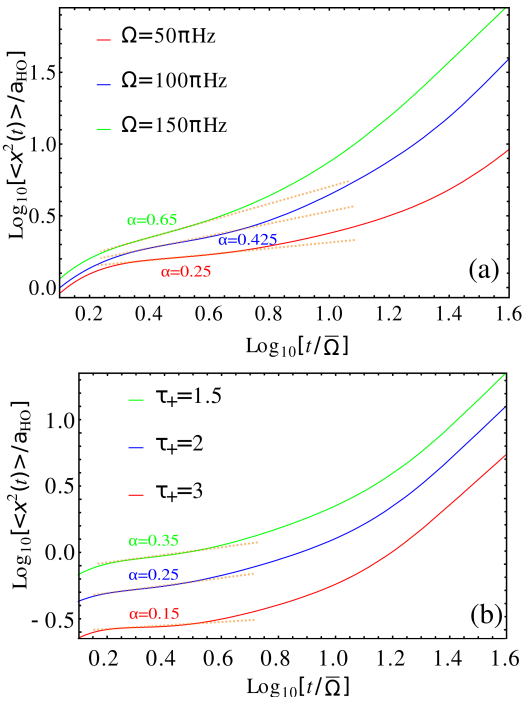

Fig. 6.3 MSD as a function of time for the case of coupling to the spin mode. A cutoff of $\Lambda = 10\bar{\Omega}$ was used, where $\bar{\Omega} = 1000\pi Hz$. In (a) we plot it for different coherent couplings Ω and in (b) for different couplings to the bath. The MSD shows three regimes, where it behaves approximately as $MSD\,(t) \propto t^{\alpha}$, and therefore linearly in log-log pots, with a different slope given by the anomalous exponent α: (i) an initial short time behavior, where $\alpha \approx 2$; (ii) a nontrivial transient subdiffusive behavior, where $\alpha < 1$. We plot a dashed orange line as a guide to the eye, to illustrate the different slopes in this regime; (iii) a long time ballistic regime, with $\alpha = 2$. In (a) we show that, as Ω is reduced, the subdiffusive plateau enlarges and α gets smaller. In (b) we show that increasing the couplings to the bath τ_+, also enlarges the plateau and reduces α. See main text for discussion of both effects. In both panels, we consider Rb and K atoms for BEC and impurities, respectively. We use intra- and inter-species coupling constant for the BEC $g = g_{12} = 2.15x10^{-37} J \cdot m$, density $n = 7(\mu m)^{-1}$, and impurity-BEC $g_{\mathrm{IB}} = 0.5x10^{-37} J \cdot m$; We take $\tau_+ = 1$ in (a) and $\Omega = 100\pi Hz$ in (b).

2017a), is evaluated in the long time limit $\omega \ll \Lambda_-, \Lambda$ as

$$\langle [x\,(t) - x\,(0)]^2 \rangle = MSD\,(t) = G_2^2(t)\langle \dot{x}^2\,(0)\rangle + \frac{1}{2}\int_0^t ds \int_0^t d\sigma G_2(s) G_2(\sigma) \langle \{B(s), B(\sigma)\} \rangle_{\rho_B}\,, \tag{6.80}$$

where we assumed that the impurity-bath are initially in a product state $\rho(0) = \rho_B \otimes \rho_S(0)$, where ρ_B is the thermal Gibbs state for the bath at temperature T. The initial conditions of the impurity and bath oscillators are then uncorrelated. Then, averages of the form $\langle \dot{x}(0) B(s) \rangle$ vanish. To treat the second term in Eq. (6.80), we note that

$$\langle \{B(s), B(\sigma)\} \rangle_{\rho_B} = 2\nu(s-\sigma), \tag{6.81}$$

where $\nu(t)$ is defined as in Eq. (6.43).

In case 1 (coupling to density mode) the spectral density reads as in Eq. (6.51). Then, the MSD behaves the same way as in (Lampo *et al.*, 2017a), with the only difference of replacing $g \to g + g_{12}$. Hence the impurity will again superdiffuse as

$$\langle [x(t) - x(0)]^2 \rangle = \left[\langle \dot{x}^2(0) \rangle + \frac{\tau_- \Lambda_-^2}{2} \right] \left(\frac{t}{\zeta} \right)^2, \tag{6.82}$$

where $\zeta = 1 + \tau_- \Lambda_-$. Note that the superdiffusive behavior $\langle x^2(t) \rangle \propto t^2$ appears for both low temperature ($\coth(\hbar\omega/2k_BT) \approx 1$) and high temperature ($\coth(\hbar\omega/2k_BT) \approx 2k_BT/\hbar\omega$) limits. Hence from Eq. (6.82) we see that, effectively, the contribution of the Bogoliubov modes to the MSD behavior in this case is just to modify the mass of the free particle.

In case 2 (coupling to the spin mode), analytical expressions for the Eq. (6.80) cannot be found. We remind again that we are interested in the transient effects attributed to the bath frequencies right above the band gap, after making the assumption for $\omega = E_{gap} + \epsilon$ that $\omega \approx E_{\rm gap}$ i.e. $\epsilon \ll E_{\rm gap}$. In this case the Green function reads as in Eq. (6.60), while the noise kernel at low temperatures, where $\coth\left(\frac{\omega}{2k_BT}\right) \to 1$, can be shown to be equal to

$$\begin{aligned} \nu(t) =& \widehat{\tau}_+ (\Lambda - E_{\rm gap})^{1.5} \left[\frac{2}{3} \cos(E_{\rm gap} t) F_{1,2}\left(\frac{3}{4}; \frac{1}{2}, \frac{7}{4}; -\frac{1}{4} t^2 (E_{\rm gap} - \Lambda)^2 \right) \right. \\ &\left. + \frac{2}{5} t (E_{\rm gap} - \Lambda) \cos(E_{\rm gap} t) F_{1,2}\left(\frac{5}{4}; \frac{3}{2}, \frac{9}{4}; -\frac{1}{4} t^2 (E_{\rm gap} - \Lambda)^2 \right) \right], \end{aligned} \tag{6.83}$$

where

$$F_{1,2}(\alpha; \beta, \gamma; z) = \sum_{n=0}^{\infty} \frac{(\alpha)_n}{(\beta)_n (\gamma)_n} \frac{z^n}{n!}. \tag{6.84}$$

In this case, we were not able to obtain an analytic solution for the MSD, as the integral in Eq. (6.80) is quite difficult to perform. We evaluate it numerically and present the results below.

Numerical results for case 2 These numerical calculations are only valid for finite Ω, as we used the simplified version of the spectral density, Eq. (6.60). In all calculations we checked that all assumptions made are fulfilled. We numerically find three regimes of

behavior for the MSD, and in each regime it behaves as $MSD\,(t) \propto t^{\alpha}$, where α, which is known as the anomalous exponent, is different at each regime. In regime (i), there is an initial short time behavior where, as expected, the MSD grows more or less ballistically with time. So here, $\alpha \approx 2$; In regime (ii), there is a plateau where $\alpha < 1$. This is a transient subdiffusive behavior; Finally, in regime (iii), which is the long time behavior, where the impurity superdiffuses with $\alpha = 2$. We interpret this behavior as follows: the impurity performs free motion initially. Then after interacting with the large frequencies of the bath, the impurity begins to perform a subdiffusive motion since it screens the part of the spectral density that depends on the square root of the bath modes frequencies. At long times, and after undergoing dissipation for some time, the impurity again effectively only interacts with the lower frequencies of the bath which has zero effect on the motion of the impurity and hence the impurity performs a ballistic motion.

In Fig. 6.3 we show the numerically evaluated MSD as a function of time according to Eq. (6.80) and different Rabi frequencies and interaction strengths. We remind that initially, $\langle \dot{x}^2\,(0)\rangle = 0$. In Fig. 6.3 (a) we show how decreasing Ω both enlarges the duration of the subdiffusive plateau and reduces the anomalous exponent α. We should note that the results are valid only for finite Ω: since we use the simplifies spectral density, Eq. (6.60), we are never able to describe the smooth transition to the cubic spectral density, which will show an smooth change to ballistic behavior for the whole range. Then, the effect of reducing Ω is merely to reduce the gap, not to change the form of the spectral density. As a consequence, the plateau is enlarged. In Fig. 6.3 (b) we show how the MSD varies as a function of the coupling strength of the impurity to the BECs. Here, we observe that increasing the coupling strength results in more subdiffusive motion and an increase in the time length of the subdiffusive plateau. Finally, note that, in Fig. 6.3, time is measured in units of $\bar{\Omega} = 1000\pi s$ and hence the transient subdiffusive phenomenon appears in time of the order of ms. Last but not least, in such a study one should be careful to avoid the phenomenon called initial jolts, a consequence of the initially uncorrelated state of the impurity and the bath (Hu *et al.*, 1992). In (Lombardo and Villar, 2007, Paavola *et al.*, 2009, Paavola and Maniscalco, 2010), is shown that for subdiffusive system, the initial jolts appear for times $t \ll \Lambda^{-1}$. In our studies, we used $\Lambda = 10\bar{\Omega}$, which implies that the results presented in Fig. 6.3, should be free of this issue.

6.6 Summary

In this work, we again studied BM in BEC but the environment we considered in this case was rather more complicated. In particular, we studied the scenario where the bath is composed of two condensed clouds of ultracold atoms of different types, where this means that they can either be of different species, or even of the same species but of different hyperfine states. On top of the usual inter-bosons interactions of each species, we also consider interspecies interactions. In addition, the two species can also interact

through a coherent coupling, possibly a laser, that allows atoms of one type to convert to atoms of the other. The main findings of our studies are the following:

- We used as our starting point, the physical Hamiltonian describing the coupling of an impurity to a coherently coupled two-component BEC, through a contact interaction. We then performed a so-called generalized Bogoliubov transformation to diagonalize the purely bath dependent Hamiltonian, which led to the appearance of two modes of this composite bath, the density mode and the bath mode.

- The energy spectrum of the density mode is of the same form as that of a single BEC. However the energy spectrum of the spin mode is fundamentally different, since this is a gapped spectrum. In addition the two spectra behave differently at low frequencies. While the density spectrum behaves linearly for low frequencies and quadratically for higher frequencies, the spin spectrum behaves quadratically in both regimes. We note that in our studies we take into account the orthogonality of the wavefunctions corresponding to these modes.

- The total Hamiltonian again has the form of a Frohlich type Hamiltonian, but the impurity now couples to two distinct baths. Hence under the dipole approximation, we again obtain a Caldeira-Leggett type Hamiltonian.

- We show that depending on how the impurity couples to the two original types of atoms, it sees a distinct spectral density for the bath. Namely, if the impurity is coupled in the same way tot he two type of atoms, i.e. if it couples to both of them attractively or to both of them repulsively, the impurity couples to the density mode of the diagonalized Hamiltonian. If on the other hand the impurity couples oppositely to the two types of atoms, namely attractively with one of them and repulsively with the other, then the impurity couples to the spin mode of the diagonalized energy spectrum. This is the main result of this work.

- We study the form of the spectral densities, in the same way as in A.1.2, and we find that while in the density case the spectral density remains cubic, but with a slightly modified relaxation time, in the spin case, the spectral density is gapped, with a gap equal to the gap in the energy spectrum. This is understood hence to be a direct consequence of the form of the energy spectrum, namely it means that when the impurity couples to the spin mode, it only receives energy from the bath in the form of excitations of energy larger than the gap. We furthermore determine the form of the spectral density close to the band gap, and we find it to increase as the square root of the bath frequencies.

- We then proceed to solve the equations of motion in the standard way of utilizing

Laplace transforms, assuming a free impurity.

- We focus then on the study of the MSD. For the cubic spectral density the MSD can be obtained analytically as before and the impurity is found to behave superdiffusively as before. On the other hand, the gapped spectral density was not possible to treat it analytically, and we obtained numerical results concerning the MSD behavior as a function of the parameters of the system. Namely we found that the impurity had a transiently subdiffusive behavior at short times, and a superdiffusive behavior at later times. In particular at long times, the impurity diffuses quadratically with time, which is expected since from the Tauberian theorem, we know that the low frequency part of the spectral density determines the motion at the long time. For this gapped spectral density then, one naturally expects that at long time the bath should not affect the motion, and the impurity should continue moving freely/ ballistically. For the transient part at short times, as a function of the parameters of the system, we find that:
  - The impurity behaves more subdiffusively when a larger coherent coupling is assumed.
  - The impurity behaves more subdiffusively when it couples stronger to the two types of atoms.

CHAPTER 7

USING BOSE POLARONS AS QUANTUM BROWNIAN PROBES FOR QUANTUM THERMOMETRY

In this chapter, we examine the possibility to use Bose polarons as probes in order to measure the temperature of a given BEC sample. As in previous works, we treat the Bose polaron within an open quantum system framework. Once again we make the dipole approximation that translates the Bose polaron system into a QBP. To make the chapter self consistent, we first make an overview of the necessary background material. We begin in Sec. 7.1 with a short presentation of the general framework and assumptions one makes in modern day quantum thermometry, and in particular what insights to this field has quantum estimation theory introduced. Then, in Sec. 7.2, we proceed with the main technical tools that are needed in order to be able to understand our work, namely a definition of the quantum Fisher information, a proof of the Quantum Cramer Rao bound as well as the introduction of the symmetric logarithmic derivative. The classical analogues of these are presented in parallel since they offer a better intuition about the physical meaning of these quantities. In Sec. 7.3, we continue with a short overview of the goals and limitations of quantum thermometry in equilibrium, just to understand the importance of the structure of the specific energy spectrum of the Hamiltonian. This is even more true in out of equilibrium quantum thermometry, which demonstrates the importance of studying quantum thermometry for a case by case model. We then comment

on the main results of a theoretical study (Correa *et al.*, 2017) of a quantum thermometry protocol with the probe-system being described by the Caldeira-Leggett Hamiltonian. There, having this concrete model at hand enabled the authors to elucidate the effect of the strength of the coupling between the probe and the system on the efficiency of this system as a thermometer. In Sec. 7.4, we present our results, where instead of referring to an arbitrary model of a quantum Brownian probe, we consider as our probe a concrete physical system, a Bose polaron, which is indeed described within the QBM framework as in (Lampo *et al.*, 2018). Finally in Sec. 7.5, we summarize the contents of the chapter. The material presented in this chapter was published in (Mehboudi *et al.*, 2019b).

7.1 Quantum thermometry and quantum estimation theory

7.1.1 Quantum thermometry

In the recent years, quantum technologies have attracted an ever increasing interest, both for the practical applications they may bring, as well as for the fact that they can allow us to study fundamental questions about nature, as for example in the study of quantum thermodynamics (Kosloff, 2013, Kosloff and Levy, 2014). In addition, exploiting the quantum nature of physical systems provides a remarkable advantage in enhancing the accuracy of estimation problems, and the resolution in the estimation of fundamental constants of nature. Exploring this possibility plays a pivotal role in the current swift development of quantum technology (Caves, 1981, Huelga *et al.*, 1997, Giovannetti *et al.*, 2006, Tóth and Apellaniz, 2014, Szczykulska *et al.*, 2016, Pezzè *et al.*, 2018). This quantum advantage, resides on the fact that, quantum estimation of parameters with a strategy that uses multiple resources simultaneously, provides better precision over individual estimation strategies with equivalent resources (Humphreys *et al.*, 2013, Baumgratz and Datta, 2016). However, for any quantum effects to be observed, systems have to be controlled down to very small scales, whether this is in terms of size or temperature or other quantities. For this reason, the relevant instruments of very high accuracy to monitor these systems have also to be constructed. Generally, identifying strategies for improving the measurement precision by means of quantum resources is the purpose of the field of quantum metrology (Paris, 2009, Giovannetti *et al.*, 2011), which as of now, has found applications in numerous fields, ranging from fundamental physics, (Udem *et al.*, 2002, Katori, 2011, Aspachs *et al.*, 2010, Ahmadi *et al.*, 2014, Schnabel *et al.*, 2010, Aasi *et al.*, 2013), to applied physics, such as thermometry (Correa *et al.*, 2015, De Pasquale *et al.*, 2016), spectroscopy (Schmitt *et al.*, 2017, Boss *et al.*, 2017), imaging (Tsang *et al.*, 2016, Nair and Tsang, 2016), magnetic field detection (Lupo and Pirandola, 2016, Taylor and Bowen, 2016) navigation (Bonato *et al.*, 2016, Cai and Barthel, 2013) and remote sensing (Komar *et al.*, 2014, Dowling and Seshadreesan, 2015) or sensing of biological systems

(Boto *et al.*, 2000, Wynands and Weyers, 2005, Lombardi *et al.*, 2001).

Quantum thermometry is the sub-field of quantum metrology where the quantity that one seeks to estimate is temperature. In doing so, knowledge and results are drawn from a number of fields, such as open quantum systems and many-body systems. From a theoretical point of view, the interest is focused on identifying bounds and scaling laws that restrict the precision of temperature estimation for both equilibrium and non-equilibrium systems. In terms of practical applications, quantum thermometry deals with the proposal of precise thermometric protocols for physically relevant experimental set-ups. In general, it is also the goal of quantum thermometry to reveal the role of quantum features, such as entanglement and coherence, in the achievable resolution of the aforementioned thermometric protocols with the aim of showing possible quantum enhancements. Thermometry is possible, thanks to the zeroth and second law of thermodynamics (McKeown, 1927), which guarantee, the former that for a given thermal equilibrium state corresponds a certain constant temperature, and the latter that, no absolute thermometric scale is needed to measure temperature differences. Quantum thermodynamics (Binder *et al.*, 2018) is precisely concerned with the challenge of consistently redefining the usual thermodynamic variables (Esposito *et al.*, 2010, Campisi *et al.*, 2011, Perarnau-Llobet *et al.*, 2017), among which is temperature, or even reformulating the laws of thermodynamics (Brandão *et al.*, 2015, Uzdin and Rahav, 2018, Kolář *et al.*, 2012, Levy *et al.*, 2012, Freitas and Paz, 2017, Masanes and Oppenheim, 2017, Bera *et al.*, 2019) to make them applicable to systems which are not macroscopic, but fully quantum.

Ultracold atomic gases are one of the key platforms for quantum technologies due to their potential for quantum simulation (Lewenstein *et al.*, 2012). Such promise has been reinforced by several breakthroughs which include, among others, the celebrated Mott insulator to superfluid quantum phase transition for bosons (Greiner *et al.*, 2002), as well as recent simulations of antiferromagnetic spin chains with both, bosonic (Simon *et al.*, 2011) and fermionic (Tarruell *et al.*, 2012) ultracold atomic gases. Nonetheless, operating a quantum simulator requires very precise tuning of the parameters of the experiment, so as to ensure that the simulated system behaves as intended. In particular, a precise temperature control is essential, for instance, for the reconstruction of the equation of state of the system (Greiner *et al.*, 2002). Hence recently, there has been an increasing interest both at the theoretical and experimental level, in obtaining accurate temperature readings with nanometric spatial resolution in such a context (Neumann *et al.*, 2013, Kucsko *et al.*, 2013, Toyli *et al.*, 2013). Beyond this, the development of such ultraprecise thermometric protocols, could in the long run also pave the way towards many groundbreaking applications in medicine, biology or material science. Motivated by the above, we set off to propose a thermometric protocol to measure the temperature of a BEC at sub-nK temperatures.

7.1.2 Quantum estimation theory

It is often the case, that important physical quantities can not be directly measured, either in principle or due to some technical obstructions, such that one can only infer their values from indirect measurements. One such case is also temperature. This is because it is a non-linear function of the density matrix, so it is not a (quantum) observable of the system. In addition if one seeks to study quantum effects in the precision of temperature measurements, i.e. where one needs to resort to quantum thermodynamics, then they encounter the additional difficulty of the fact that relevant quantities like entanglement and purity are nonlinear functions of the density matrix and cannot, even in principle, correspond to proper quantum observables. Furthermore, in high-precision measurements, and in the quantum regime, it is important to include also a proper accounting of the measurement process and apparatus. For all the above reasons, in these situations one should resort to indirect measurements, inferring the value of the quantity of interest by inspecting a set of data coming from the measurement of a different observable, or a set of observables. To do so one needs to introduce an ancillary physical system, the probe, over which a high degree of control is assumed.

The idea of the aforementioned probe is the following. Through the interactions of the system and the probe, information about the system parameter of interest λ is passed into the state of the probe. A measurement of the probe can be performed then, in order to infer the parameter λ. This can be summarized in the following protocol:

1. Initialization of the probe: the probing system is prepared in an assigned state ρ_0.

2. Evolution of the probe: the probe interacts with the system, and evolves according to a λ-dependent process described by a superoperator $\mathcal{E}_\lambda$, so as to imprint onto the probe state, via $\rho_\lambda = \mathcal{E}_\lambda(\rho_0)$.

3. Readout of the probe: a (quantum) measurement is performed on ρ_λ, followed by classical data processing on the outcomes. This is what is properly defined as the 'estimation step'.

This is repeated for N independent probes, where all of them are initialized in the same initial state ρ_0.

Hence, to properly address the problem of precise temperature measurements at the quantum level, as well as to place bounds on the precision of a given temperature-sensing protocol, one has to make use of the framework of quantum estimation theory (QET) (Helstrom, 1976, Holevo, 2003). This, provides analytical tools to find the optimal measurement according to some given criterion (Braunstein and Caves, 1994, Barndorff-Nielsen and Gill, 2000). From a fundamental perspective, it provides a gold standard upon which

to asses distinguishability of quantum states. Moreover, one can also single out which temperature dependent quantity is the most sensitive to thermal fluctuations and thus, produces the most accurate temperature estimates. In case that this aforementioned quantity is not measurable in practice, due to technological limitations, quantum thermometry can assist in identifying accessible (sub-optimal) alternatives which approximate the fundamental precision limits closely (Campbell *et al.*, 2017, Cavina *et al.*, 2018).

7.2 Preliminaries and Relevant quantities for Quantum thermometry from quantum estimation theory

We begin by a general overview of the traditional methods and tools employed in Quantum thermometry and quantum metrology in general in order to estimate the relevant parameters.

7.2.1 Classical parameter estimation toolbox

The solution of a parameter estimation problem amounts to find an estimator, i.e a mapping $\lambda = \lambda(x_1, x_2, ...)$ from the set $\mathbf{x}$ of measurement outcomes into the space of parameters M. Optimal estimators in classical estimation theory are those saturating the Cramer-Rao inequality (Cramér, 1999)

$$V(\lambda) \geq \frac{1}{NF(\lambda)} \tag{7.1}$$

(for a proof see App. C.1) which establishes a lower bound on the mean square error $V(\lambda) = E_\lambda\left[(\lambda(\mathbf{x}) - \lambda_{mean})^2\right]$ of any estimator of the parameter λ. The constant factor just follows from the central limit theorem, where N is the number of measurements. $F(\lambda)$ is the so-called Fisher Information (FI)

$$F(\lambda) = \int dx p(x \mid \lambda)\left(\frac{\partial \ln p(x \mid \lambda)}{\partial \lambda}\right)^2 = \int dx \frac{1}{p(x \mid \lambda)}\left(\frac{\partial p(x \mid \lambda)}{\partial \lambda}\right)^2 \tag{7.2}$$

where $p(x \mid \lambda)$ denotes the conditional probability of obtaining the value x when the parameter has the value λ. An interesting property of this quantity is that it is additive when the systems are independent. Equivalently, one can show that FI derives from the Fisher-Rao distance between probability distributions differing by an infinitesimal increment in λ, namely $p(x \mid \lambda)$ and $p(x \mid \lambda + \delta\lambda)$. The role of the Fisher information becomes clearer by considering its relation with the fidelity. The fidelity between two

probability distributions quantifies their closeness, and is defined as follows

$$Fid\left(p,q\right)=\sum_{\mathbf{x}}\sqrt{q_{\mathbf{x}}p_{\mathbf{x}}} \tag{7.3}$$

It is easy to see that $0 \leq Fid\left(p,q\right) \leq 1$, with the equality to one holding iff $p_{\mathbf{x}} = q_{\mathbf{x}}$, while equality to zero happens iff the two distributions have no common support, i.e., $p_{\mathbf{x}} \neq 0 \Rightarrow q_{\mathbf{x}} = 0$, and $q_{\mathbf{x}} \neq 0 \Rightarrow p_{\mathbf{x}} = 0$. Note that the appearance of the factor M in the CRB is due to the additivity of the Fisher Information for independent measurements as the ones we assume here. On the one hand, the probability distribution $p\left(x \mid \lambda\right)$ (and thus its sensitivity to small variations of the parameter of interest) depends on the chosen measurement: optimal measurements are those with conditional probability maximizing the Fisher Information. On the other hand, for any fixed measurement, an efficient estimator is the one that saturates the Cramer-Rao inequality. In our work, we will be interested in estimating the temperature of some system, and we will assume we have no information about this temperature. In this case, one assumes an unbiased estimator, for which the mean square error is equal to the variance $Var\left(T\right) = \langle T^2 \rangle_{p_T} - \langle T \rangle_{p_T}^2$. Furthermore, if the data sample is sufficiently large, it results that an efficient estimator is provided by the maximum-likelihood principle,based on the intuition that the observed data have been measured since they hold the highest probability to be obtained. This is a typical example of an asymptotically efficient estimator. There also exist special families of probability distributions allowing for the construction of an estimator with only a finite number of measurements.

Finally, let us comment on the scaling of the accuracy of the measurement protocol with the number of repetitions or the number of probes. If a large number of independent experiments is carried out one can define an estimate of the temperature T of the system just by taking the average of the measurements. Then, as a result of the central limit theorem, the corresponding statistical error $\delta T = \left\langle \left(T - \langle T \rangle\right)^2 \right\rangle$ in the estimation decreases as $\delta T \sim \frac{1}{\sqrt{N}}$ (Giovannetti *et al.*, 2004), where N is the number of repetitions (which equivalently can be seen as the number of uncorrelated and independent probes used in the estimation). This type of scaling is often referred-to as shot noise (usually when associated with classical systems) or standard quantum limit SQL (when associated with quantum systems) (Cramér, 1999). In optical experiments, the SQL manifests as a significant technical noise floor (e.g. in homodyne or heterodyne field measurements), and is a consequence of quantum shot noise, associated to the Poissonian arrival times of quantised photons in a coherent state.

7.2.2 Quantum metrology toolbox

While the fundamental objects in classical Fisher information are parameter-dependent probability-distribution of the data, the fundamental objects involved in the quantum es-

timation problem are the density matrices $\rho(\lambda)$ labeled by $\lambda \in M$. These $\rho(\lambda)$ is a family of quantum states defined on a given Hilbert space H and labeled by a parameter λ living on a d-dimensional manifold M, with the mapping $\lambda \to \rho(\lambda)$ providing a coordinate system. This is sometimes referred to as a quantum statistical model. The parameter λ does not, in general, correspond to a quantum observable and our aim is to estimate its values through the measurement of some observable on λ. In turn, a quantum estimator $O(\lambda)$ for λ is a self-adjoint operator, which describe a quantum measurement followed by any classical data processing performed on the outcomes. The indirect procedure of parameter estimation implies an additional uncertainty for the measured value, that cannot be avoided even in optimal conditions. The aim of quantum estimation theory is to optimize the inference procedure by minimizing this additional uncertainty.

In quantum mechanics, according to the Born rule we have $p(x \mid \lambda) = Tr[\Pi_x \rho_\lambda]$ where $\{\Pi_x\}_x$, $\int dx \Pi_x = I$, are the elements of a positive operator-valued measure (POVM) and λ is the density operator parametrized by the quantity we want to estimate. Note that x is a quantum operator, but for the sake of simplicity of notation from now on we omit the hat. To proceed with constructing a quantum analogue of the Fisher information presented above which will allow us to obtain a quantum Cramer theorem and hence identify the bounds in precision of measurements in the quantum regime one needs to introduce the Symmetric Logarithmic Derivative (SLD) L_λ. This is the self-adjoint operator satisfying the (Lyapunov) equation

$$\frac{L_\lambda \rho_\lambda + \rho_\lambda L_\lambda}{2} = \frac{\partial \rho_\lambda}{\partial \lambda} \tag{7.4}$$

for which we have that $\partial_\lambda p(x \mid \lambda) = Tr[\partial_\lambda \rho_\lambda \Pi_x] = Re(Tr[\rho_\lambda \Pi_x L_\lambda])$. The Fisher Information (7.2) is then rewritten as

$$F(\lambda) = \int dx \frac{Re(Tr[\rho_\lambda \Pi_x L_\lambda])^2}{Tr[\rho_\lambda \Pi_x]} \tag{7.5}$$

For a given quantum measurement, i.e. a POVM $\{\Pi_x\}_{x \in \mathbb{R}}$, the equations above establish the classical bound on precision, which may be achieved by a proper data processing, e.g. by maximum likelihood, which is known to provide an asymptotically efficient estimator. On the other hand, in order to evaluate the ultimate bounds to precision we have now to maximize the Fisher information over the quantum measurements. One can show that the Fisher information $F(\lambda)$ of any quantum measurement is bounded by the so-called Quantum Fisher Information (QFI)

$$F(\lambda) \leq H(\lambda) \equiv Tr\left[\rho_\lambda L_\lambda^2\right] = Tr[\partial_\lambda \rho_\lambda L_\lambda] \tag{7.6}$$

(see App. C.1 and App. C.2) leading the quantum Cramer-Rao bound (QCRB)

$$Var\left(\lambda\right) \geq \frac{1}{NH\left(\lambda\right)} \tag{7.7}$$

to the variance of any estimator. The quantum version of the Cramer-Rao theorem provides an ultimate bound: it does depend on the geometrical structure of the quantum statistical model and does not depend on the measurement. Optimal quantum measurements for the estimation of λ thus correspond to POVM with a Fisher information equal to the quantum Fisher information. Furthermore, notice that taking the trace on both sides of the Lyapunov equation above, one can see that $\langle L_\lambda \rangle = 0$. Therefore, the QFI is actually the variance of SLD operator, i.e.,

$$F\left(\lambda\right) = \left\langle \Delta^2 L_\lambda \right\rangle_{\rho_\lambda} \tag{7.8}$$

where $\Delta^2 L_\lambda \equiv \left(L_\lambda - \langle L_\lambda \rangle_{\rho_\lambda}\right)^2$.

From the above, we see that SLD is of fundamental importance for quantum estimation theory, for this reason it has been studied for years (Paris, 2009, Tóth and Apellaniz, 2014, Braunstein and Caves, 1994). It is important mainly for two reasons. First, it is obvious that the QFI can be directly obtained when the SLD operator is known. Second, the achievement of quantum Cramer-Rao bound strongly depends on the measurement, namely, it can only be achieved for some optimal measurements. The eigenvectors of SLD operator are such theoretical optimal measurements (Tóth and Apellaniz, 2014, Braunstein and Caves, 1994). Thus, the study of SLD operator could help us to construct or find optimal measurements for the achievement of the highest precision. Unfortunately, the SLD projections can be highly nonlocal and hence, very hard to implement, especially on large multipartite probes. Even finding L_λ analytically is sometimes a challenging task (Demkowicz-Dobrzański *et al.*, 2012, Escher *et al.*, 2011). For example when the space of the density matrix is infinitely large, the diagonalization could be very tricky. Therefore, in practice, one must consider more manageable sub-optimal estimators, which nonetheless allow for a comparatively small error. For some cases, Lyapunov representation could be used as an alternative method to obtain the SLD operator and has indeed applied in many scenarios (Paris, 2009). The defining equation of the SLD is actually a special form of Lyapunov equation, indicating that SLD operator is a corresponding solution.

Alternatively, the QFI can be given a geometric interpretation through the Bures metric. In the context of temperature estimation, the QFI can be interpreted as the infinitesimal distance, according to the Bures metric, between a thermal state at temperature T, and a thermal state at temperature $T + \delta$ (Braunstein and Caves, 1994). Intuitively, the more such a distance, the more the initial probe state is sensitive to a

small variation of temperature. Formally,

$$F(\rho_T) = -2\lim_{\delta\to 0}\frac{\partial^2 \mathbb{F}(\rho_T, \rho_{T+\delta})}{\partial \delta^2} \tag{7.9}$$

where $\mathbb{F}(\rho_1, \rho_2) \equiv \left(Tr\sqrt{\sqrt{\rho_1}\rho_2\sqrt{\rho_1}}\right)^2$ is the Uhlmann fidelity between states ρ_1 and ρ_2, which defines their respective Bures distance via $d_{Bures}(\rho_1, \rho_2) = 2\left(1 - \sqrt{\mathbb{F}(\rho_1, \rho_2)}\right)$ (Braunstein and Caves, 1994).

Further to the intuitive meaning of the QFI, we note that there exists an optimal estimator (i.e., an optimal measurement procedure on the final thermalized state) for which the bound in the QCRB becomes tight for an asymptotically large number of measurements, and can be indeed saturated by means of adaptive metrological schemes (Giovannetti *et al.*, 2011). We note here that it is known that the bound is achievable through estimation strategies exploiting only local operations and classical communication (Masahito, 2005). Therefore, the inverse of the QFI equivalently defines the minimum achievable variance in the estimation of T. We will then refer to $F(\rho_T)$ as "thermal sensitivity", and take its maximization as synonym of optimality in the following analysis (Sabín *et al.*, 2014, Brunelli *et al.*, 2011). By using the definition of the thermal sensitivity, we withdraw the statistical dependence on the number of times the sample is probed.

The advantage of using a quantum probe, can be seen once we study the scaling of the accuracy of the measurement with the number of repetitions (or equivalently the number of probes). In general, it can be shown that quantum states with particles exhibiting quantum correlations, or more precisely, quantum entanglement (Horodecki *et al.*, 2009b, Gühne and Tóth, 2009), provide a higher precision than an ensemble of uncorrelated particles. Hence, if the probes are prepared in an entangled state before locally interacting with the parameter, it can be shown that the statistical uncertainty can decrease, at most, as $\delta T \sim \frac{1}{N}$, which is customarily termed Heisenberg scaling (Giovannetti *et al.*, 2006). A qualitative argument for this is given in (De Pasquale *et al.*, 2016) where the temperature of a bath of M identical two-level atoms, is estimated through a proxy observable, namely the number of excited atoms m through $\langle m\rangle = M\frac{e^{-\beta\epsilon}}{1+e^{-\beta\epsilon}}$. This is in turn estimated by converting this counting problem into a phase estimation problem. Alternatively, this advantage in precision for entangled quantum states can be equivalently understood as changing the measurement protocol to use a total of nN probes, in which we entangle blocks of N probes, and repeat n times (De Pasquale *et al.*, 2016). Note that if the Hamiltonian of the dynamics has interaction terms then even better scaling is possible (see, e.g., (Luis, 2004, Napolitano *et al.*, 2011, Boixo *et al.*, 2007)). From various theoretical results (Roy and Braunstein, 2008, Rivas *et al.*, 2010), regarding for example k-body interactions or even nonclassicality, there are good reasons to believe

that properties of quantum systems can be employed as a useful "resource" for quantum metrology. Numerous experiments have indeed demonstrated conceivability of sub-shot noise limit error by using aspects of quantum mechanics; see, e.g., Refs. (Leibfried *et al.*, 2004, Brida *et al.*, 2010).

Finally, let us comment on the application of quantum estimation theory in an open quantum system setting. In open quantum systems, as it was indicated above, due to interaction with an environment, the underlying dynamics can become "noisy". As a result, formulation and analysis of quantum estimation also becomes more involved (Escher *et al.*, 2011, Watanabe *et al.*, 2010). In general, dynamics of an open system can be described as $\rho_S(t) = Tr_E\left[U_{SE}(t,t_0)\,\rho_{SE}(t_0)\,U_{SE}^{\dagger}(t,t_0)\right]$, where ρ_{SE} is the state of the systems and environment (SE), and $U_{SE}(t,t_0)$ is the corresponding unitary evolution (Alicki and Lendi, 2007, Breuer *et al.*, 2002). Thereby one can argue that in general there may exist a ow of information between the system and the environment (Lu *et al.*, 2010). Under some conditions, this dynamics can feature quantum Markovian or non-Markovian properties (Rivas *et al.*, 2010, Modi *et al.*, 2012, Fleming and Hu, 2012). The former case typically appears when the environment has a small decoherence time during which correlations disappear, whereas in the latter correlations (both classical and/or quantum (Pernice *et al.*, 2012)) with the environment would form and persist. Such correlations are in practice inevitable, which necessitates investigation of noisy quantum metrology (Giovannetti *et al.*, 2011, Demkowicz-Dobrzański *et al.*, 2012, Chin *et al.*, 2012, Escher *et al.*, 2011, Adesso *et al.*, 2009), and may in turn offer new resources for enhancing estimation tasks. However, developing relatively general frameworks for open-system metrology is still needed and is of fundamental and practical importance. In our work, we focus on a specific case of an open system metrological protocol for the estimation of the temperature of a BEC bath, namely one where the dynamics of the probe are described by a QBM Hamiltonian. We consider a quantum Langevin equation description of the dynamics, which allows for non-Markovian evolution of the probe.

7.3 Quantum thermometry in and out of thermal equilibrium

7.3.1 Quantum thermometry in thermal equilibrium

From the quantum Cramer-Rao bound for the specific case of a temperature estimation, one can relate the ultimate limit on the precision of the temperature measurement of a thermal state to the probe's heat capacity C_V (Zanardi *et al.*, 2008) since the QFI can be shown to be equal to (proof in App. C.3)

$$F(\rho_T) = \frac{\Delta H^2}{T^4} = \frac{C_V}{k_B T^2} \tag{7.10}$$

where $\Delta H^2 = \left(Tr\left(\rho_\beta H^2\right) - \left(Tr\left(\rho_\beta H\right)\right)^2\right) = \langle H^2\rangle_{\rho_\beta} - \langle H\rangle^2_{\rho_\beta}$ with $\beta = (k_B T)^{-1}$. In other words, the ultimate limit to the precision at which the temperature of a thermal state can be determined by the variance of an energy measure on ρ_β. Note that the averages that will appear from now on, are also with respect to ρ_β but we omit explicit reference to it. The above equality builds a first significant bridge between two apparently independent theoretical frameworks: quantum thermodynamics and quantum estimation theory. In particular, from the above expression, one can relate the amount of information in a state or the sensitivity of the measuring procedure based on the heat capacity of the probe. This simple picture will not hold in the nonequilibrium case, and a detailed description of the system will be needed, as we will see. From Eq. (7.10), for temperature estimation on a Gibbs state, maximizing the quantum Fisher information is equivalent to maximizing the variance of the Hamiltonian. Introducing the thermal energy as $k_B T$, it is possible to express the quantum Cramer-Rao bound in the form of an uncertainty relation (Correa *et al.*, 2015, Zanardi *et al.*, 2008), that for a single shot reads

$$\Delta H \frac{\Delta T}{T^2} \geq 1 \tag{7.11}$$

The proof essentially lies on the QCRB, the fact that the QFI is the variance of SLD and that the SLD is related to the Hamiltonian as in Eq. (C.9) in App. C.3. This provides a very useful insight to understand how the thermal energy, the energy spectrum of the Hamiltonian and the error on the temperature determination come into play. The main message here, is that, indeed, according to the the inequality above and Eq. (7.10), quantum states having a larger QFI can be estimated with a smaller error. In general, finding the corresponding QFI of a system is a very difficult task, and different bounds on the QFI that are easier to evaluate, as suggested in (Escher *et al.*, 2011, Alipour *et al.*, 2014). In the temperature estimation of a strongly correlated thermal state, the difficulty arises in the calculation of its intricate energy spectrum, and, in general, it is usually not possible to derive a closed expression for the QFI. It is important to note that, due to the Gibbs form of the state , the probability distribution resulting from projective measurements in the energy basis belongs to the exponential family and, therefore, it allows for the saturation of the CRB at finite N (Kolodynski, 2014) (even at $N = 1$).

Harmonic and finite-dimensional thermometers

From the discussion above, it is clear that the energy-level structure of H plays a central role in limiting thermometric precision (Correa *et al.*, 2015, Campbell *et al.*, 2017). This is also confirmed from the study in (Miller and Anders, 2018) where the scenario where the equilibrium properties of the probe depend on the interaction energy (i.e. for arbitrary coupling strength), giving rise to an effective internal energy of the probe, was considered. There, the authors also obtained an upper bound on the optimal signal-

to-noise ratio depending on the heat capacity of the probe as well as on a dissipative term depending on the effective internal energy. With their results it is made clear that to obtain a better understanding of how the QFI scales at low temperatures for strong couplings, one needs to study the properties of this effective internal energy. This is done so in this work for a damped harmonic oscillator with a Drude-Ullesma spectrum for the coupling constants and the reservoir frequencies are assumed to be equidistant and the continuum frequency limit is considered. This allows for analytical results to be obtained, but this is not the case for any form of the spectrum of the coupling constants, in particular it will not be for the system that we will study. Two cases of probes where analytical forms of the QFI can be obtained are the two-level system and a harmonic oscillator. The QFI for the two is briefly discussed in App. C.5. The most important points to note is that from these QFI, one can show that

1. the harmonic thermometer performs efficiently in a wider temperature range than any finite-dimensional probe, hence including the two-level system,

2. the harmonic thermometer and the two-level thermometer converge towards the same sensitivity as $T \to 0$. This is to be expected, since, at low-enough temperatures, a thermal oscillator can be reliably truncated to its first two energy levels.

7.3.2 Quantum thermometry out of thermal equilibrium

In quantum estimation theory, the value of a variable is obtained indirectly as it was mentioned above, and this is done so by performing measurements on a given probe attached to the system of interest. This probe is usually assumed to be weakly coupled to the system whose temperature we want to measure. As a result of this weak-coupling constraint and the comparatively large 'thermal mass' of the system, the probe eventually thermalizes at the system temperature T without disturbing it. Hence probe and system end up being uncorrelated, and knowledge about the internal structure of the sample, and the probe-sample coupling scheme are not so relevant. In this conventional picture of implementing thermometry, the Einstein theory of Fluctuations can be used to characterize the sensitivity of the procedure in terms of the heat capacity of S which represents its thermal susceptibility to the perturbation imposed by the bath. Since the latter is an equilibrium property, one should not expect it to hold in nonequilibrium regimes.

One additional issue that one might run into within the standard quantum thermometry at equilibrium is the following. One will only obtain a local measurement of only a small part of the equilibrium system, and the temperature would then have to be obtained by the marginal of the density operator, i.e. from its projection on the accessible subspace. Importantly, this marginal is not generally of the simple Gibbs form but will rather depend on the specific details of the internal interactions of the system-bath. This becomes distinguishably evident once the following observations are made. The QFI for

a single-mode finite dimensional non-degenerate equilibrium thermometer (note that at sufficiently low temperature even a harmonic oscillator can be approximated by a two level /single mode system) decays exponentially at low T (for $T/\Omega \ll 1$), as was shown in the previous section. This is not specific to harmonic probes, but generally applicable to, e.g., optimized finite-dimensional equilibrium thermometers (Correa *et al.*, 2015), as was explained above. That is, even an estimate based on the most informative measurements on an optimized equilibrium probe has an exponentially vanishing precision as $T/\Omega \to 0$. This low temperature behaviour is quite general for gapped systems, and is attributed to the monotonicity of the QFI under partial tracing (can be shown to hold even at the thermodynamic limit, see (Hovhannisyan and Correa, 2018)). However this is not the case for gapless systems, where the thermal sensitivity can be shown to decay polynomially (Hovhannisyan and Correa, 2018). This last point, can be proven by considering a concrete model as is explained in (Mehboudi *et al.*, 2019c). The conclusion here, is that before one uses the toolbox of quantum metrology for making statements about the accuracy of temperature estimates, one should determine a suitable description for the state of the temperature probe, which will in general depend on the particular problem at hand, hence an accurate description of the probe system interaction might be necessary.

In fact, indeed such a simple picture as the one described above runs into trouble if the sample is too cold, especially when using an individual quantum thermometer. The seemingly natural assumption of the probe reaching equilibrium at the sample temperature might break down at low T . In this limit, the two parties can build up enough correlations to eventually keep the probe from thermalizing (Nieuwenhuizen and Allahverdyan, 2002, Gogolin and Eisert, 2016). In addition, if the probe is too small, boundary effects become relevant and need to be taken into account to properly describe equilibration and thermalization (Gogolin and Eisert, 2016, Kliesch *et al.*, 2014). As a result, thermometry with nonequilibrium quantum probes inescapably demands some knowledge about the internal structure of the sample, and the probe-sample coupling scheme. Nevertheless, one could still assume thermalization in the standard sense, owing to a vanishing probe-sample coupling. However, in this limit, the thermal sensitivity of the probe, which is proportional to its heat capacity (Landau and Lifshitz, 1938, Mandelbrot, 1956), drops quickly as the temperature decreases (Debye, 1912) this is an inherent problem of low-temperature thermometry (De Pasquale *et al.*, 2016). A paradigmatic system where high precision measurements of temperature are of paramount importance for its near-future applications to be possible, are cold atomic gases. These, can presently be cooled down to the lowest temperatures in the Universe even below the nanokelvin regime which demands measurement protocols capable of high precision at very low temperatures. Hence one understands that the conventional weak coupling approach can not be employed to measure the temperature in such a set-up.

Insights in strong coupling quantum thermometry from the quantum Brownian motion model

An important attempt to quantitatively assess the impact of strong interactions on the achievable thermometric precision across different temperature regimes (and in particular at the low temperature regime) was made in (Correa *et al.*, 2017). In this work, quantum thermometry was extended to the strong coupling regime, by adopting a fully rigorous description of the probe's dynamics. To that end, the Caldeira-Leggett Hamiltonian was employed, which is one of the most common dissipation models (see, e.g., (Weiss, 2012). The equilibrium sample was hence represented by a bosonic reservoir (Caldeira and Leggett, 1983a) which was dissipatively coupled to a single harmonic oscillator, playing the role of the thermometer. Since the Hamiltonian of the Caldeira-Leggett model is quadratic in positions and momenta, the steady state of the probe is necessarily Gaussian (Grabert *et al.*, 1984) and hence, fully determined by the stationary second order moments $\sigma_x = \langle x^2 \rangle$, $\sigma_p = \langle p^2 \rangle$ and $\sigma_{xp} = \langle xp \rangle$ (the first moments vanish). In turn, these can be explicitly evaluated, as was explained in Chapter 3 without making any approximations beyond our assumption of an initially uncorrelated probe-system state. Hence before presenting any results obtained from this study, we briefly review the temperature estimation task in a Gaussian probe setting. Note that, to enable thermometry in the study that follows, the system whose temperature is to be measured, corresponds to a large Hamiltonian quantum system whose heat capacity is much larger than that of the probe, such that its energy follows a Boltzmann-Gibbs distribution with some well-defined temperature T. We will make the same assumption in our work that will be presented in the next section.

Temperature estimation in Gaussian systems

The simplicity and power of the Gaussian state formalism can bring enormous analytic advantage to the study of precision protocols in metrology (Weedbrook *et al.*, 2012). Gaussian state formalism has already proven its success and serves as an invaluable tool in describing quantum states of light and atomic ensembles, as well as providing useful insight and intuition. On the other hand, in quantum estimation theory, the nontrivial equations defining central objects of it, often forces to numerical methods (Adesso *et al.*, 2009, Dorner *et al.*, 2009) for computing precision bounds and determining optimal measurements, and these difficulties are only aggravated by the infinite-dimensional nature of bosonic systems. Nevertheless, in (Monras, 2013), a fully general phase-space formulation of the central quantities in quantum estimation theory, namely, the symmetric logarithmic derivative (SLD), and the SLD quantum Fisher information (which will presented in the next section), with focus on general Gaussian states, was given, allowing for the analytical results obtained later on in (Correa *et al.*, 2017), that also enabled the analytical results of our work.

Note that from above, we know already that the QFI is nothing but the variance of the

SLD (see App. C.4). Owing to the simple quadratic form of the Hamiltonian of Caldeira-Leggett, we can obtain an analytic form of the SLD and hence the QFI for temperature estimation solely in terms of the variances $\langle x^2 \rangle$ and $\langle p^2 \rangle$ (Monras, 2013), i.e.,

$$\begin{aligned} L_T &= C_x \left(x^2 - \langle x^2 \rangle\right) + C_p \left(p^2 - \langle p^2 \rangle\right) \\ F\left(\rho_T\right) &= 2C_x^2 \left\langle x^2 \right\rangle^2 + 2C_p^2 \left\langle p^2 \right\rangle^2 - \hbar^2 C_x C_p \end{aligned} \tag{7.12}$$

where the coefficients C_x are given by

$$C_x \equiv \frac{4 \left\langle p^2 \right\rangle^2 \partial_T \left\langle x^2 \right\rangle + \hbar^2 \partial_T \left\langle p^2 \right\rangle}{8 \left\langle x^2 \right\rangle^2 \left\langle p^2 \right\rangle^2 - \frac{\hbar^4}{2}} \tag{7.13}$$

where C_p can be obtained by simply exchanging $x \leftrightarrow p$. The proof of this can be found in App. C.6.

Probe-system interactions as a thermometric resource and a determining factor of the behaviour of the low temperature QFI

In this work above, by calculating the steady state of the probe exactly and analytically, it was possible to show that its low-T sensitivity is significantly enhanced by increasing the coupling strength. In this study in particular, an ohmic spectral density was considered, such that from the resulting equations of motion, one can perform a totally unrestricted analysis of the thermal sensitivity of the probe, including arbitrarily low temperatures and strong probe-system interactions. The resulting QFI is given as above. By studying the QFI as a function of the coupling between the probe and the system, it can be shown, that increasing the interactions can result in a significant enhancement of $F(T)$. In fact, in the limit $T/\Omega \ll 1$ the dissipation-driven thermometric advantage grows monotonically with the dissipation strength γ (Correa *et al.*, 2017) (where is the relaxation time or constant of proportionality in the Ohmic spectral density). It is also important to note that from the studies in (Correa *et al.*, 2017) the variance of the position quadrature, not only is experimentally feasible to measure (Poyatos *et al.*, 1996), but also outperforms the local energy measurements. The underlying physical mechanism responsible for this dissipation-driven enhancement can be understood by looking at the normal modes of the global probe-system composite. For the central Brownian thermometer (Correa *et al.*, 2017), it can be shown that the normal-mode frequencies below Ω decrease monotonically with γ; the corresponding collective degrees of freedom thus become more sensitive to small thermal fluctuations. Furthermore, an analysis of the residual spectrum of the system allows us to understand the observation in App. C.5, namely that the QFI of a system with a gapped spectrum decays exponentially while the QFI for a gapless system polynomially. In particular, this is because when the chain features a finite gap, a non-zero minimal frequency emerges in the residual spectrum of the system that is, the probe can no longer couple to arbitrarily low-frequency system

modes, which are the most informative ones at low T. This explains the switching between polynomial and exponential scaling of the performance of low-temperature thermometry in gapped many-body systems (Hovhannisyan and Correa, 2018).

Relative error of low-temperature estimates The reference to a concrete model such as that of the Caldeira- Leggett model above, can help us to gain insights on the relative error of low-temperature estimates. In practice, the low-T scaling of the relative error (multiplied by the length of the data set for convenience)

$$\frac{\Delta T}{T\sqrt{N}} \geq \frac{1}{T\sqrt{NF\left(T\right)}} \tag{7.14}$$

may be more relevant than that of ΔT alone. For instance, even under the benign scaling $F\left(T\right) \sim T^2$, the relative error still diverges as $1/T^2$ when $T \to 0$. As argued in (Hofer *et al.*, 2017) one can make use of the relation in Eq. (7.10) for the global thermal sensitivity, and invoke the third law of thermodynamics to require $\lim_{T\to 0} C_V = 0$ and thus $(\Delta T/T) \to \infty$, which would also hold for local estimates. Hence, measuring ultracold temperatures precisely seems to be an impossible task. Luckily, one might bypass this impediment in practice by choosing, e.g., a Brownian probe with 'sufficiently low' frequency Ω. Assuming an Ohmic spectrum, it can be rigorously proven from the exact steady-state solution of this model that

$$F\left(T \to 0\right) \sim 1/T^2 \ , \ \Omega \to 0 \tag{7.15}$$

so that the relative error $\sqrt{N}\left(\Delta T/T\right)$ converges to a constant in the low-T regime (Hovhannisyan and Correa, 2018). A small but finite Ω would allow for a constant relative error down to arbitrarily low temperatures, so long as Ω/T remains small. As Ω/T grows, however, the usual power law-like divergence should be expected to take over.

In the light of these observations above, that clearly demonstrate the numerous advantages of studying quantum thermometry questions in a concrete model such as the Caldeira-Leggett model, we highlight some recent results of some works exhibiting how one could study concrete physical systems such as impurities in BEC, as instances of quantum Brownian particles described by the aforementioned Caldeira-Leggett Hamiltonian. In particular, this was done in the works in (Lampo *et al.*, 2017a) for an impurity in a homogeneous BEC and in (Lampo *et al.*, 2018) for an impurity in a harmonically trapped BEC. By taking advantage of these studies as well as the aforementioned extension of quantum thermometry in the strong coupling regime, in this work we study these impurities as thermometers for BEC. However, we clarify here that in our work, we will not work in this regime of $T/\Omega \to 0$, such that the aforementioned results of (Correa *et al.*, 2017) do not apply.

7.4 Quantum thermometry using Bose Polarons

7.4.1 Motivation

In current experimental set-ups, the main thermometric techniques to measure the temperature of a BEC are based on time-of-flight measurements (via the study of noise correlations (Fölling *et al.*, 2005)) or in-situ imaging that are applied directly on the BEC (Leanhardt *et al.*, 2003). In these cases, information about quantum phases and temperature is usually obtained from momentum and density distributions or from density-density (or spin- spin) correlations. When time-of-flight techniques are applied directly on the BEC, temperatures of few nK, or even sub-nK might be estimated efficiently, although at the price of destroying the BEC. Alternatively, in-situ imaging can be implemented using single site addressability (Sherson *et al.*, 2010). Despite their huge relevance, these methods might suffer limitations in certain occasions, due to their destructive character. For instance, in order to study spin-spin correlations in currently available set-ups for single site imaging, one needs to remove all particles from one of the two spin components. In this sense, quantum non demolition (QND) methods can provide clear advantages (Eckert *et al.*, 2008). Lately, proposals have been made to perform such measurements by introducing impurities in the BEC (Olf *et al.*, 2015) and obtain information about the BEC through measurements on them. Such protocols are less destructive, albeit efficient at relatively large temperatures of $\sim 100nK$. Recent proposals have discussed minimally disturbing interferometric set-ups in which the temperature is mapped onto a relative phase on a probe (Sabín *et al.*, 2014), however, the underlying models are very simple. An effective non-demolition thermometric technique in the sub-nK regime is thus still missing. Furthermore, when dealing with Bose Einstein Condensates at low T, one can come upon another problem, namely that the seemingly natural assumption of the probe reaching equilibrium at the sample temperature might break down, as was discussed in the introduction. As a result, thermometry with nonequilibrium quantum probes inescapably demands some knowledge about the internal structure of the sample, and the probe-sample coupling scheme. Any such strategy should be build upon a comprehensive theoretical description and be capable of informing the choice of the most sensitive temperature-dependent quantities to be measured.

Here, we propose what is, to the best of our knowledge, the first experimentally feasible quantum non-demolition technique to measure the temperature of a BEC in the sub-nK domain. It is based on the Bose polaron problem, i.e., interrogation of an impurity that is embedded in the condensate, while causing minimal disturbance to the cold atomic gas. The impurity problem has been intensively studied in the context of polaron physics in strongly interacting Fermi (Schirotzek *et al.*, 2009b, Kohstall *et al.*, 2012b, Płodzień *et al.*, 2018) or Bose gases (Lampo *et al.*, 2017a, 2018, Rath and Schmidt, 2013, Guenther

et al., 2018b), as well as in solid state physics (Devreese and Alexandrov, 2009a), and mathematical physics (Lieb and Thomas, 1997b, Anapolitanos and Landon, 2013b). In the work presented here, we specifically avoid any unjustified simplifications such as complete thermalization of the impurities at the BEC temperature and investigate the problem in its full generality. The usefulness of our proposed technique is finally illustrated with typical experimental parameters. Note that in our work we use as a probe a harmonic oscillator, which even though it can be shown to be less sensitive probe since it has equispaced energy spectrum, it features a wider operation range. In our analysis, we benefit from the toolbox of the emergent field of quantum thermometry (Mehboudi *et al.*, 2019c). This will allow us to compare the ultimate precision bounds on temperature estimation with the thermal sensitivity of concrete experimentally feasible measurements. It is important also to stress that we are not limited by any of the simplifying assumptions usually adopted when dealing with open quantum systems, such as the Born-Markov or secular approximations, nor rely on perturbative expansions in the dissipation strength (Lieb and Thomas, 1997b). In fact, our methods are totally general and thus, not limited to a specific probe-sample coupling scheme. Finally, since the specific way we use to treat the Bose polaron problem through open quantum systems techniques, namely by employing the Quantum Brownian motion model for an impurity trapped in a harmonically trapped bath of harmonic oscillators described in Chapter [], the Hamiltonian of our system is linear, and hence the covariance matrix elements, in particular the steady-state variances in position x and momentum p, are enough to describe the state of our system, since we can assume $\langle x\rangle = \langle p\rangle = 0$. This gives us a great advantage in utilizing the quantum thermometry toolbox in order to devise a protocol to measure the temperature of the BEC, since we can write the SLD and the QFI for temperature estimation solely in terms of these variances as we will show later on.

7.4.2 Results

First let us make explicit that the Hamiltonian in this case is given as in (Lampo *et al.*, 2018), and hence also the spectral density as well as the position and momentum variances, $\langle x^2\rangle$ and $\langle p^2\rangle$. Furthermore, even though in order to give some concrete numerical results in our studies we worked with a BEC of K atoms containing Yb impurities, the qualitative picture would remain essentially unaltered regardless of the atomic species considered. Furthermore, before presenting our results, we should introduce a very important quantity, namely the static temperature susceptibility

$$\chi_T(O) \equiv \partial_T Tr(\rho_T O) = \frac{1}{2}\langle OL_T + L_T O\rangle - \langle O\rangle\langle L_T\rangle \tag{7.16}$$

where for $O = x$ this is equivalent to $\chi_T(x) \equiv \partial_T\langle x^2\rangle$ and analogously for p. That is, by repeatedly measuring the observable L_T on the impurity, the temperature of the BEC can be estimated with the minimum possible uncertainty. We are now in the position

to plug in realistic numbers into the exact steady-state marginal for the probe and explore the thermal sensitivity of our non-demolition thermometric protocol at ultra-low temperatures.

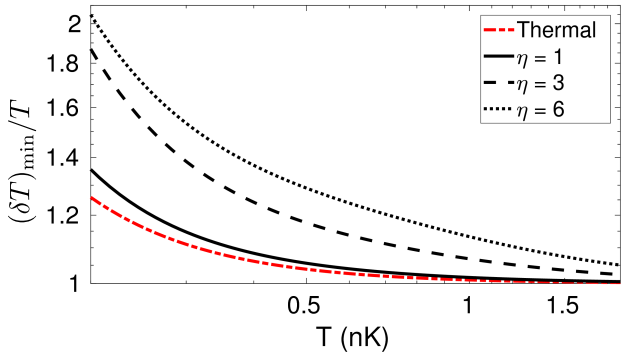

Fig. 7.1 (color online) (black) Optimal relative error $(\delta T)_{min}/T$ $(N=1)$ as a function of the temperature of the BEC in a logarithmic scale. Specifically, we work with impurities of Yb in a sea of ultracold K. The temperature range for the BEC is $200pK \leq T \leq 2nK$. The trapping frequency of the gas (with $N_{atoms} = 5000$ atoms) was set to $\omega_B = 2\pi 100Hz$, while $\Omega = 2\pi 10Hz$ ($g_{rmB} = 3 \times 10^{-39} Jm$). Different probe-sample coupling ratios $\eta = g_{IB}/g_B$ were considered, namely (solid) $\eta = 1$, (dashed) $\eta = 3$, and (dotted) $\eta = 6$. For comparison, we also depicted the relative error of a fully thermalized impurity (i.e., $\eta \to 0$) (dot-dashed red). Note that, for $\eta = 1$, the relative error can be kept below 14% from only 100 measurements. This is quantitatively close to state-of-the-art destructive experimental techniques. See text for discussion.

In Fig. 7.1, we plot the optimal relative error $\sqrt{N}\,(\delta T)_{min}/T = (TF(T))^{-1}$ for various probe-sample coupling strengths and temperatures ranging from $200pK$ to $2nK$. Here $(\delta T)_{min} \equiv \inf_{\widehat{O}} \delta T(O)$ where

$$\delta T(O) \equiv \frac{\Delta O}{\sqrt{N\chi_T^2(O)}} \tag{7.17}$$

with $\Delta^2 O = \langle O^2 \rangle - \langle O \rangle^2$. At this point we remind of the inequality Eq. (C.6), which implies that $(\delta T)_{min}$ can be obtained by the variance of SLD. We find that, keeping the interatomic and interspecies couplings comparable (i.e., $\eta = 1$) would allow to achieve a relative error below 14% from as few as 100 measurement outcomes. That is, polaron thermometry outperforms the interferometric technique proposed in Ref. (Sabín *et al.*, 2014) by an order of magnitude. More importantly, unlike state-of-the-art experimental methods (e.g., (Leanhardt *et al.*, 2003, Olf *et al.*, 2015)), ours provides a non-demolition measurement. We note, however, that the stronger the probe sample interaction, the

worse the estimation. Likewise, it can be clearly seen that, for strong dissipation, the impurity deviates significantly from a thermal state at the temperature of the sample. The first observation seems to be in striking contradiction with the main results of (Correa *et al.*, 2017), where a substantial dissipation driven enhancement was reported at low temperatures. Note however, that the temperature range considered in Fig. 7.1 does not qualify as low, according to the criteria of Ref. (Correa *et al.*, 2017), namely $T \ll \hbar\omega_B/k_B$ (here $T \sim \hbar\omega_B/k_B$). When it comes to the second observation, it is worth highlighting that the divergence between the exact steady state of the impurity and a fully thermalised probe can be sizeable in the pK range. This only comes to reinforce the idea that simple dissipation models, such as a Gorini-Kossakowski-Lindblad-Sudarshan master equation (Lindblad, 1976) are not suitable for this type of analysis. Recall that the above discussion assumes that the optimal measurement of L_T can be implemented. In practice, however, such a mixture of covariances with temperature dependent coefficients might be difficult to realize; the bare quadratures $\langle x^2\rangle$ or $\langle p^2\rangle$ being easier to measure.

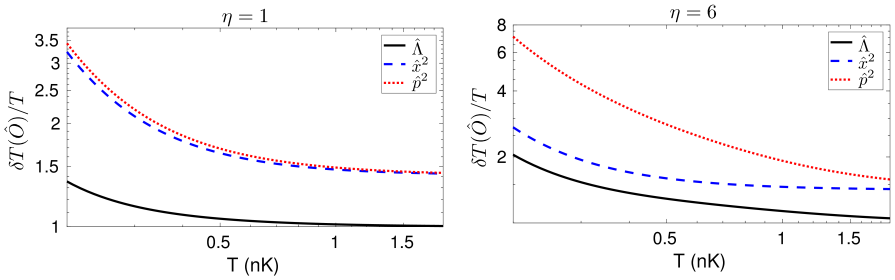

Fig. 7.2 (color online) (dashed blue) Relative error for the position quadrature $\delta_T(x^2)/T$ and (dotted red) the momentum quadrature $\delta_T(p^2)/T$ as a function of T for (left panel) $\eta = 1$ and (right panel) $\eta = 6$. All parameters are the same as in Fig. 7.1. The minimum relative error (solid black) is superimposed for reference. Even though both measurement schemes are sub-optimal, they still might allow to draw estimates with relative errors as low as 18% for 400. Note that for $T \geq 5nK$ and by using the same data size $N = 400$, one can achieve a relative error below 10%.

The relative error of estimates based on these is benchmarked against the ultimate lower bound in Figs. 7.2. Note that, at $\eta = 1$, $\langle x^2\rangle$ and $\langle p^2\rangle$ perform similarly, while at stronger coupling, the position quadrature becomes a significantly better temperature estimator. Also, under stronger dissipation, $\langle x^2\rangle$ gets closer to the optimal setting. Importantly, our approach remains practically useful regardless of the strict sub-optimality of x^2 temperature estimates with $\delta_T(x^2)/T < 18\%$ (or in the domain $T \geq 0.5nK$, with $\delta_T(x^2)/T < 10\%$ can still be constructed from relatively small datasets of 400.

7.5 Summary

In this chapter, we investigated how impurities immersed in a BEC can be exploited as temperature sensors for the BEC. The main points discussed are summarized in the following:

- A short introduction was given in quantum metrology, quantum thermometry and quantum estimation theory to set up the framework within which we worked and to motivate the studies we undertook. In particular, the main paradigm in quantum thermometry is the usage of a probe in order to measure the temperature of a bath considered to be of infinite heat capacity. The measurements on this probe are then analyzed through quantum estimation theory.

- We then presented the main tools from classical/quantum estimation theory that are usually used in this task. Namely, we presented the quantum Fisher information, the Quantum Cramer-Rao bound and the symmetric logarithmic derivative. We initially discussed their classical analogues in order to obtain an intuition for these quantities.

- We discussed about quantum thermometry in thermal equilibrium. Even though the case we studied does not fall into this category, it served us to show the importance of the structure of the energy spectrum of the Hamiltonian on the accuracy on the temperature measurement one can achieve.

- The scenario of out of equilibrium quantum thermometry was discussed, where we discussed the importance of having a concrete model in order to understand the achievable bounds on the temperature measurements, and we saw how in some works the QBM served as this concrete model. We commented on the importance of interactions between the probe and system on the temperature measurements.

- We finally presented our studies on temperature measurements on a harmonically trapped BEC confined in 1D, using as a probe an impurity treated as a QBP as in (Lampo *et al.*, 2018). We obtained the exact stationary state of the impurity from the corresponding quantum Langevin equation and, using standard tools from quantum estimation theory, we could eventually calculate the minimum possible statistical uncertainty for a temperature measurement. The key features of the thermometric scheme proposed are that

  - the temperature is estimated by monitoring the impurity atoms only. The BEC itself does not need to be measured destructively,

  - it can compete with state-of-the-art thermometric techniques in the sub-nK

range,

  - the underlying analysis does not assume thermalization of the impurity at the temperature of the BEC, but rather takes fully into account the strong correlations built up between probe and sample.

- Owing to our analysis being exact, we could verify that the usual assumption of full thermalization for the impurity at the temperature of the sample overestimates the performance of the scheme for typical parameters in the $pK - nK$ range.

- Furthermore, we showed that, with only 100 measurements, the relative error can be kept below 14% for temperatures as low as $200pK$. Importantly, we could also show that feasible sub-optimal quadrature measurements specifically, $\widehat{x}^2$ allow for similar performances with limited resources (i.e., datasets of just few hundreds of independent measurements).

- Interestingly, we found that increasing the probe-sample coupling does not improve the sensitivity of the protocol in the temperature range under study due to the comparatively low typical trapping frequencies $(60 - 70Hz)$.

CHAPTER 8

HEAT CURRENT CONTROL IN TRAPPED BOSE-EINSTEIN CONDENSATES

The primary aim of the work presented in (Charalambous *et al.*, 2019b) is to design a method to transfer heat between two Bose-Einstein condensates (BECs)—with a comprehensive analytical description. The BECs are confined in independent one-dimensional parabolic traps, and kept at a certain distance such that the two BECs do not spatially overlap. Our second aim is to create thermal devices in our platform, specifically a heat rectifier. In our platform, the working medium is constructed with two impurities, each of them immersed in one of these BECs. The two impurities interact through long-range dipolar interactions (see Fig. 8.1 for a schematic of the system considered). Heat transfer through dipolar interactions has been also proposed recently in two parallel layers of dipolar ultracold Fermi gases (Renklioglu *et al.*, 2016). We first show that the Hamiltonian of the impurities in their corresponding harmonically trapped BECs can be cast as that of two bilinearly coupled Quantum Brownian particles interacting bilinearly with the Bogoliubov excitations of each BEC—which play the role of heat baths for the corresponding impurities. We analytically derive the spectral density (SD) of the system and construct the quantum Langevin equations describing the out-of-equilibrium dynamics of the coupled impurities (Lampo *et al.*, 2019). We emphasize that, following this procedure we avoid approximations involved in an alternative conventional approach based on Lind-

blad master equations, such as the Born-Markov approximation and the rotating wave approximation. We solve the quantum Langevin equations and find the covariance matrix of the impurities. We henceforth focus on our two main aims. Firstly, we find exactly the steady state heat current between the BECs, and study how it can be manipulated by controlling relevant parameters, such as the trapping frequencies, dissipation strengths, and the physical distance of the BECs. Secondly, we introduce a periodic driving on the trapping frequency of one impurity and show that our setup can be used as a thermal rectifier. The setup that we present here can be used for implementing other thermal devices as well.

The paper is structured as follows: In section 2, we introduce the Hamiltonian of our system, present the main assumptions involved, and rewrite the Hamiltonian in a form analogous to that of two coupled Brownian particles. In section 3 we derive the Generalized Langevin equations of motion for the two impurities and study their solution in both static and periodically driven scenarios. In section 4 we present the relevant quantities of interest and in section 5 we present our main results, both for heat transfer and rectification. Finally we summarize the results and conclude in section 6.

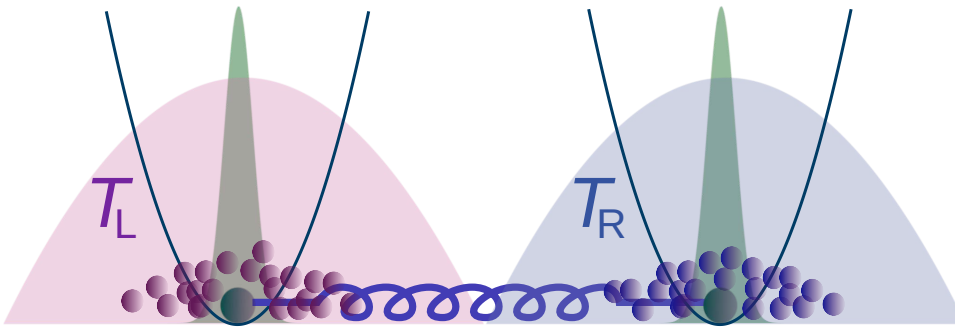

Fig. 8.1 Schematic of the system. The red and blue shaded profiles (and circles) represent the hot and cold Bose-Einstein condensates, respectively kept at T_L and T_R. The green profiles (and circles) represent the two impurities trapped in their corresponding parabolic potentials, plotted as blue lines – we omit the representation of the trap for the BECs. The spring-like blue line represents the long-range dipolar interaction among the impurities.

8.1 The Model

We consider a system composed of two interacting impurities of the same mass m. Each one of these impurities is embedded in a different BEC, which we label as L or R because they are trapped in parabolic potentials of frequencies $\Omega_{B,L}$ and $\Omega_{B,R}$, respectively, but one trapping potential is centered around a minimum located in $\mathbf{d}_L$ and the other around $\mathbf{d}_R$, with certain distance among them. Each BEC has, respectively, N_L and N_R

interacting atoms of the same species with mass m_{B}. The two impurities are also trapped in a parabolic potential of frequencies Ω_{L} and Ω_{R} located around the same minimum as their corresponding BEC. We allow for the scenario of these impurities being driven by an external periodic force. The two BECs do not overlap among themselves (we will specify later the condition over the distance between the minima of the trapping potential). With this, the Hamiltonian describing this setting is

$$H_{\mathrm{Tot}} = H_{\mathrm{S}} + \sum_{j\in\{\mathrm{L,R}\}} \left(H_{\mathrm{B,j}} + H_{\mathrm{BB,j}}\right) + \sum_{j\in\{\mathrm{L,R}\}} H_{\mathrm{Int.,j}} + H_{\mathrm{Drive}}\left(t\right), \tag{8.1}$$

where

$$H_{\mathrm{S}} = \sum_{\substack{i,j\,\in\,\{\mathrm{L,R}\}\,,\\ i\neq j}} \frac{\mathbf{p}_j^2}{2m} + \mathbf{V}_j\left(\mathbf{x}_j\right) + H_{\mathrm{int.}}, \tag{8.2}$$

$$H_{\mathrm{B,j}} = \int \mathbf{\Psi}_j^{\dagger}\left(\mathbf{x}_{\mathrm{B}}\right)\left[\frac{\mathbf{q}_j^2}{2m_{\mathrm{B}}} + \mathbf{V}_{\mathrm{B}}^{(j)}\left(\mathbf{x}_{\mathrm{B}}\right)\right]\mathbf{\Psi}_j\left(\mathbf{x}_{\mathrm{B}}\right)\mathrm{d}\mathbf{x}_{\mathrm{B}}, \tag{8.3}$$

$$H_{\mathrm{BB,j}} = g_{\mathrm{B}}^{(j)}\int \mathbf{\Psi}_j^{\dagger}\left(\mathbf{x}_{\mathrm{B}}\right)\mathbf{\Psi}_j^{\dagger}\left(\mathbf{x}_{\mathrm{B}}\right)\mathbf{\Psi}_j\left(\mathbf{x}_{\mathrm{B}}\right)\mathbf{\Psi}_j\left(\mathbf{x}_{\mathrm{B}}\right)\mathrm{d}\mathbf{x}_{\mathrm{B}}, \tag{8.4}$$

$$\begin{aligned} H_{\mathrm{Int.,j}} &= g_{\mathrm{IB}}^{(j)}\int \mathbf{\Psi}_j^{\dagger}\left(\mathbf{x}_{\mathrm{B}}\right)\mathbf{\Psi}_j\left(\mathbf{x}_{\mathrm{B}}\right)\delta\left(\mathbf{x}_j - \mathbf{x}_{\mathrm{B}}\right)\mathrm{d}\mathbf{x}_{\mathrm{B}}, \\ &= g_{\mathrm{IB}}^{(j)}\mathbf{\Psi}_j^{\dagger}\left(\mathbf{x}_j\right)\mathbf{\Psi}_j\left(\mathbf{x}_j\right), \end{aligned} \tag{8.5}$$

where $\mathbf{x}$ and $\mathbf{x}_{\mathrm{B}}$ are the three-dimensional position operators of the impurity and the bosons respectively. We assume contact interactions among the bosons and between the impurity and the bosons, with strength given by the coupling constants $g_{\mathrm{B}}^{(j)}$ and $g_{\mathrm{IB}}^{(j)}$ respectively. Here, $H_{\mathrm{int.}}$ denotes the interaction Hamiltonian between the two impurities, which we will specify later. For the rest of the paper we assume that the trapping frequencies in two directions are much larger than in the third one. Therefore, the dynamics in those directions is effectively frozen and we can study the system in one dimension. From here on we assume that the minima of the potential are located at $d_{\mathrm{L}} = -d/2$ and $d_{\mathrm{R}} = d/2$. We comment here that from the form of the Hamiltonian, one can see that since there is no direct interaction between the two BECs, any relative phase between them should not play any role in the dynamics of the system. It would be interesting to study the effects of allowing such an interaction, e.g. by introducing a coherent coupling between the two BECs or by studying heat transport in the experimental setting of homogeneous BEC in (Brantut *et al.*, 2013), but this goes beyond the scope of our work.

We next recast our initial Hamiltonian (8.1), in such a way as to describe the motion of two interacting Quantum Brownian particles in two separate BECs. The procedure, which is the same as that presented (Lampo *et al.*, 2018) for the case of a single impurity embedded in a harmonically trapped BEC, can be summarized as follows: (i) we make

the BEC assumption, i.e. that the condensate density greatly exceeds that of the above-condensate particles, which results to only quadratic terms in the Hamiltonian; (ii) we perform the Bogoliubov transformation appropriate for the case of a harmonically trapped BEC; (iii) we solve the relevant Bogoliubov-de-Gennes equations, in the limit of a one dimensional BEC that yields a Thomas-Fermi parabolic density profile, as in (D.S. Petrov *et al.*, 2004); (iv) we finally assume that the oscillations x_j of each one of the impurities are much smaller than the corresponding Thomas-Fermi radius R_j,

$$x_j \ll R_j, \tag{8.6}$$

which physically implies that we study the dynamics of the impurities in the middle of their corresponding bath traps, which allows us to obtain a bilinear interaction of the position of the impurities and the positions of their corresponding baths.

These steps bring the Hamiltonian in the form

$$H_{\rm Tot} = H_{\rm S}\left(t\right) + \sum_{j\in\{\rm L,R\}} \widetilde{H}_{\rm B,j} + \sum_{j\in\{\rm L,R\}} \widetilde{H}_{\rm Int.,j}, \tag{8.7}$$

where

$$\widetilde{H}_{\rm B,j} = \sum_q E_q^{(j)} b_{j,q}^\dagger b_{j,q}, \tag{8.8}$$

$$\widetilde{H}_{\rm Int.,j} = \sum_q \hbar g_q^{(j)} x_j \left(b_{j,q} + b_{j,q}^\dagger\right), \tag{8.9}$$

with

$$E_q^{(j)} = \hbar\Omega_{\rm B,j}\sqrt{q\left(q+1\right)}, \tag{8.10}$$

and

$$g_q^{(j)} = \frac{g_{\rm IB}^{(j)}\mu_j}{\hbar\pi^{3/2}}\left[\frac{1+2q}{\hbar\Omega_{\rm B,j}g_{\rm B}^{(j)}R_j^3}\right]^{1/2}\frac{\Gamma\left[\frac{1}{2}\left(1-q\right)\right]\Gamma\left[\frac{1}{2}\left(1+q\right)\right]\sin\left(\pi q\right)}{\left[q\left(q+1\right)\right]^{1/4}}. \tag{8.11}$$

The chemical potential μ_j of the $j^{\rm th}$ bath is

$$\mu_j = \left(\frac{3}{4\sqrt{2}}g_{\rm B}^{(j)}N_j\Omega_{\rm B,j}\sqrt{m_{\rm B}}\right)^{2/3}, \tag{8.12}$$

and the Thomas-Fermi radius R_j of the $j^{\rm th}$ bath is

$$R_j = \sqrt{\frac{2\mu_j}{m_{\rm B}\left(\Omega_{\rm B,j}\right)^2}}\,. \tag{8.13}$$

At this point, it is important to note that Hamiltonian in Eq. (8.7), which is indeed in the form of a Hamiltonian describing two coupled quantum Brownian particles, was derived from the physical initial Hamiltonian. Therefore, this Hamiltonian lacks the

renormalization term that guarantees that no "runaway" solutions appear in the system, which is often included in conventional open quantum system approaches (Coleman and Norton, 1962b). We are not going to introduce such a term in order to guarantee the positivity of the Hamiltonian and cast the system in the form of a minimal coupling theory with $U(1)$ gauge symmetry. Instead, we are going to determine in the next section a condition on the allowed parameters of the system that will guarantee this.

We assume dipole-dipole interactions among the two impurities. From (Lahaye *et al.*, 2009) we know that the form of dipole-dipole interaction is the following:

$$H_{\text{int.}} = A\frac{1}{r^3}, \tag{8.14}$$

where $A = \frac{C_{dd}\left(1-3(\cos\theta)^2\right)}{4\pi}$, with

$$C_{dd} = \mu^2\mu_0, \tag{8.15}$$

and $\mu_0 = 4\pi 10^{-7}\frac{J}{A^2 m}$ being the vacuum permeability, while μ is the magnetic moment of the dipole. The angle θ is that formed between the axis of the two dipoles and it can determined in experiments. Furthermore, in Eq. (8.14), $r = |(d_{\text{R}} + x_{\text{R}}) - (d_{\text{L}} + x_{\text{L}})|$ is the distance between the two oscillators, with d_{L} and d_{R} being the centers of the trapping potentials of the two oscillators. We then rewrite Eq. (8.14) as

$$H_{\text{int.}} = Ad^{-3}\left|1 + \frac{(x_{\text{L}} - x_{\text{R}})}{d}\right|^{-3}, \tag{8.16}$$

and we assume that the distance between the two oscillators centers d is much larger than the fluctuations $x_{\text{L}}, x_{\text{R}}$ and hence the fluctuations difference $x_{\text{L}} - x_{\text{R}}$, i.e. $x_{\text{L}}, x_{\text{R}} \ll d$. Importantly, let us emphasize that this is not an additional assumption, because we assumed right from the beginning that the two baths should not overlap. This indeed means that the sum of the Thomas-Fermi radius have to be smaller than the distance between the impurities, $R_{\text{L}} + R_{\text{R}} < d$. With the additional assumption we made before, namely that the impurities oscillations are much smaller than their corresponding Thomas-Fermi radius, Eq. (8.6), then one concludes that $x_{\text{L}}, x_{\text{R}} \ll d$. One could also tackle the problem of interacting baths, by making use of the work in (Li *et al.*, 2012a) where one needs to consider the surface Green functions, and in this case then the assumption $x_{\text{L}}, x_{\text{R}} \ll d$ should be made explicitly.

Finally, after expanding the binomial series, Eq. (8.16) is rewritten as

$$H_{\text{int.}} = Ad^{-3}\left(1 - 3\frac{(x_{\text{L}} - x_{\text{R}})}{d} + 6\frac{(x_{\text{L}} - x_{\text{R}})^2}{d^2}\right). \tag{8.17}$$

One can show that the first two terms in the parenthesis will not contribute to the dynamics of the impurities, since they are linear in the displacement operators $x_{\text{L}}, x_{\text{R}}$ and

hence they will appear only as constants in the equations of motion that we will study later on, which will be obtained from the Heisenberg equations of motion. The third term then is expanded as

$$\widehat{H}_{\text{int.}} = 6Ad^{-5}\left(x_{\text{L}}^2 - 2x_{\text{L}}x_{\text{R}} + x_{\text{R}}^2\right), \tag{8.18}$$

and we absorb the terms with x_{L}^2 and x_{R}^2 in the non-interacting part of the Hamiltonian by redefining the frequencies as

$$H_{\text{S}}^{\text{non-inter.}} = \frac{p_{\text{L}}^2}{2m} + \frac{p_{\text{R}}^2}{2m} + \frac{m}{2}\hat{\Omega}_{\text{L}}^2 x_{\text{L}}^2 + \frac{m}{2}\hat{\Omega}_{\text{R}}^2 x_{\text{R}}^2, \tag{8.19}$$

where

$$\begin{aligned} \hat{\Omega}_{\text{L}}^2 &= \Omega_{\text{L}}^2 + 6Ad^{-5}, \\ \hat{\Omega}_{\text{R}}^2 &= \Omega_{\text{R}}^2 + 6Ad^{-5}. \end{aligned} \tag{8.20}$$

From here on we omit the tilde in the frequencies to avoid unnecessary complications in the nomenclature. Therefore we can rewrite the interaction as

$$\widetilde{H}_{\text{int.}} = \kappa x_1 x_2, \tag{8.21}$$

which models a spring-like interaction among the two impurities with

$$\kappa = \frac{12C_{dd}\left(1 - 3\left(\cos\theta\right)^2\right)}{4\pi d^5}. \tag{8.22}$$

The angle θ can be experimentally controlled as was recently shown in (Tang *et al.*, 2018). This is possible thanks to a rotating magnetic field $\mathbf{B_{rot}}$ in the x-y plane that causes the dipoles to rotate at an angle θ with respect to a static magnetic field $\mathbf{B_z}$ along the z axis. The rotation angle is related to the magnitude of the two components by $\tan\theta = \mathbf{B_{rot}}/\mathbf{B_z}$. In practice, to achieve this in the experiment, the angle θ is controlled by using a calibration procedure that corrects for the effect of eddy currents. This allowed the authors to determine the amplitude of the *ac* current required to produce a given rotation angle θ. For this reason, to simplify our system, we considered the scenario where the angle is fixed. However, it is important to note here that the results that we present in this paper are valid even if the angle between the dipoles can not be experimentally controlled, but rather an average over the angle is considered. The constants in the interacting Hamiltonian as well as the power dependence on the relative distance will be different, but in the limit we consider, i.e. when $x_{\text{L}}, x_{\text{R}} \ll d$, qualitatively the results will be the same, with the difference being that the distance at which the oscillators should be kept will change (Reifenberger, 2016). This can be understood by considering the work by Keesom in (Keesom, 1921), where the angle-averaged interaction between two dipoles was evaluated. In this case, the initial expression for the distance dependent potential would depend on r^{-6}, but effectively the same procedure could be followed, that would just result in a modified expression for the spring constant k. We also note that, in most ultracold dipolar gases, the dipolar interaction is present together with the short range

interactions arising from low angular momentum scattering (Lahaye *et al.*, 2009, Giorgini *et al.*, 2008). Usually the latter is dominant and a Feshbach resonance is needed to probe the regimes where dipolar effects are prominent. However in the setting that we will consider in this work, as we maintain the two BEC baths spatially separated, the effect of the short range interactions is negligible, such that dipole interaction is the main process through which current is transferred.

Finally, there are a number of ways to drive our system, either by driving degrees of freedom of the central system, or degrees of freedom of the environment, or their coupling. In this work we focus on the first case. There are basically two types of driving that one could consider and would maintain the quadratic form of the Hamiltonian such that an analytic solution to the resulting equations of motion can be obtained. First we could consider applying a periodically driven ramp potential on the central particles degrees of freedom only, of the form $H_{\text{Drive}}(t) = \Theta(t-t_0)\,\mathbf{f}^T(t)\,\mathbf{X}(t)$ where $\mathbf{X}(t) = (x_1(t), x_1(t))^\intercal$ and $\mathbf{f}(t)$ is some periodic function, e.g. $\mathbf{f}(t) = \mathbf{f}_0 e^{-i\omega_d t} + c.c.$ with t_0 the time at which the driving begins, Ω_d the driving frequency and $\mathbf{f}_0$ a complex valued constant column vector, $\mathbf{f}_0 = (f_{0,\text{L}}, f_{0,\text{R}})^\intercal$. This type of driving was considered in (Agarwalla *et al.*, 2011), and can represent the force exerted on the system by a time dependent electromagnetic field. For this kind of driving however, it was shown in (Marathe *et al.*, 2007) that with the setup we assume above, neither a heat engine nor a heat pump can be constructed. Furthermore, our goal is to construct a phononic diode with our setup which means that the driving should be able to induce a unidirectional flow of heat current, and this is not the case for this type of driving. Therefore, in our work we consider the only other possible type of driving on our system that maintains our Hamiltonian in a quadratic form, i.e.

$$H_{\text{Drive}}(t) = \Theta(t-t_0)\,\frac{1}{2}\mathbf{X}^T \cdot \mathbf{V}(t)\,\mathbf{X}, \tag{8.23}$$

where the driving is either on the trapping frequency of the central oscillators or on their in-between coupling. It was recently shown in (Riera-Campeny *et al.*, 2019) that in such scenario one can observe the appearance of phenomenon of heat rectification, and also there is the potential to construct a heat engine as it was shown in (Hofer *et al.*, 2017), by introducing a coherently driven coupling between the two oscillators. We also assume the driving to be periodic, $\mathbf{V}(t+\tau) = \mathbf{V}(t)$ with τ being the time period, such that it can be Fourier expanded as

$$\mathbf{V}(t) = \sum_k \mathbf{V}_k e^{ik\Omega_d t}, \tag{8.24}$$

where $\Omega_d = 1/\tau$ being the driving frequency. This type of coupling could also be implemented by a laser.

8.2 Quantum Langevin equations

Let us now derive the equations of motion for the two impurities. First we write the Heisenberg equations of motion for the bath

$$\begin{aligned}\frac{db_{k,j}(t)}{dt} &= \tfrac{i}{\hbar}\left[H_{\mathrm{Tot}}, b_{k,j}^{\dagger}(t)\right] = -i\omega_{k,j}b_{k,j}(t) - g_{k,j}x_j(t),\\ \frac{db_{k,j}^{\dagger}(t)}{dt} &= \tfrac{i}{\hbar}\left[H_{\mathrm{Tot}}, b_{k,j}(t)\right] = i\omega_{k,j}b_{k,j}^{\dagger}(t) + g_{k,j}x_j(t),\end{aligned} \tag{8.25}$$

and impurity particles

$$\frac{dx_j(t)}{dt} = \frac{i}{\hbar}\left[H_{\mathrm{Tot}}, x_j(t)\right] = \frac{p_j(t)}{m}, \tag{8.26}$$

$$\frac{dp_j}{dt}(t) = \frac{i}{\hbar}\left[H_{\mathrm{Tot}}, p_j(t)\right] \tag{8.27}$$

$$= -m(\Omega_j^2 + \sum_k V_{k,jj}e^{ik\omega_d t})x_j(t) \tag{8.28}$$

$$-(\kappa + \sum_k V_{k,jj}e^{ik\omega_d t})x_q(t) - \hbar\sum_k g_{k,j}\left(b_{k,j}(t) + b_{k,j}^{\dagger}(t)\right),$$

where $j, q \in \{\mathrm{L}, \mathrm{R}\}$ and $j \neq q$. We first solve the bath particles equations of motion

$$b_{kj}(t) = b_{kj}(0)e^{-i\omega_k t} + \int_0^t \tfrac{g_{k,j}}{2}e^{i\omega_k(t-s)}x_j(s)\,\mathrm{ds}, \tag{8.29}$$

$$b_{kj}^{\dagger}(t) = b_{kj}(0)e^{i\omega_k t} + \int_0^t \tfrac{g_{k,j}}{2}e^{-i\omega_k(t-s)}x_j(s)\,\mathrm{ds}, \tag{8.30}$$

and we replace these in the impurities equations of motion (8.26)–(8.27), to obtain

$$\ddot{x}_j + (\Omega_j^2 + \sum_k V_{k,jj}e^{ik\omega_d t})x_j + (\kappa + \sum_k V_{k,jq}e^{ik\omega_d t})x_q - \int_0^t \lambda_j(t-s)\,x_j(s)\,\mathrm{ds} = \frac{1}{\mathrm{m}}\mathrm{B_j(t)}, \tag{8.31}$$

where $B_j(t)$ plays the role of the stochastic force and reads as

$$B_j(t) = \sum_k \hbar g_{k,j}\left(b_{kj}^{\dagger}e^{-i\omega_k t} + b_{kj}e^{i\omega_k t}\right). \tag{8.32}$$

Here $\lambda_j(t)$ is called the susceptibility or noise kernel. In this setting it can also be identified as the self-energy contributions coming from the bath, and it reads as

$$\lambda_j(t) = \frac{1}{m}\sum_k \hbar g_{k,j}^2 \sin(\omega_k t) = \frac{1}{m}\int_0^{\infty} J_j(\omega)\sin(\omega t)\,\mathrm{d}\omega, \tag{8.33}$$

with

$$J_j(\omega) = \sum_k \hbar g_{k,j}^2 \delta(\omega - \omega_k), \tag{8.34}$$

being the spectral density. Eq. (8.31) has the form of a Generalized Langevin equation which describes the evolution of a system with memory and under the influence of a

stochastic force. These terms, $B_j(t)$ and $\gamma_j(t)$, contain all the relevant information about the baths. Furthermore, let us assume the Feynman-Vermon initial state assumption, i.e. that the initial conditions of the impurities and the bath oscillators are uncorrelated,

$$\rho(0) = \rho_{\mathrm{S}}(0) \otimes \rho_{\mathrm{B}}, \tag{8.35}$$

where $\rho(0)$ is the total density state, $\rho_{\mathrm{S}}(0)$ is the initial density state of the system and ρ_{B} is the density state of the bath which is assumed to be thermal and hence is a Gibbs state. Then, it can be shown that the Fourier transform of $B_j(t)$ obeys the fluctuation dissipation relation

$$\frac{1}{2}\left\langle\left\{B_j(\omega), B_q(\omega')\right\}\right\rangle = \delta_{jq} Im\left[\lambda_j(\omega)\right] \coth\left(\frac{\hbar\omega}{2k_{\mathrm{B}}T}\right)\delta(\omega-\omega'), \tag{8.36}$$

where $\lambda_j(\omega)$ is the Fourier transform of $\lambda_j(t)$ and obeys (Valido *et al.*, 2013b)

$$Im\left[\lambda_j(\omega)\right] = -\hbar\left(\Theta(\omega) - \Theta(-\omega)\right) J_j(\omega). \tag{8.37}$$

Hence one concludes that, upon determination of the spectral density $J_j(\omega)$, one determines the influence of the baths on the impurities. In (Lampo *et al.*, 2018), it was shown that in the continuous frequency limit, the spectral density takes the following form

$$J_j(\omega) = m\tau_j \frac{\omega^4}{\Lambda_j^3}\Theta(\omega - \Lambda_j), \tag{8.38}$$

where

$$\tau_j = \frac{2g_{\mathrm{B}}^{(j)}}{m\widehat{\Omega}_{\mathrm{B,j}}R_j^3}\left(\frac{\eta_j\mu_j}{\hbar\widehat{\Omega}_{\mathrm{B,j}}}\right)^2,\ \eta_j = \frac{g_{\mathrm{IB}}^{(j)}}{g_{\mathrm{B}}^{(j)}},\ \Lambda_j = \widehat{\Omega}_{\mathrm{B,j}}. \tag{8.39}$$

Note that the ultraviolet cutoff, that is usually introduced to regularize the spectrum in the conventional QBM model, is now given in terms of a physical quantity, the trapping frequency of the potential well of the j^{th} bath. Here $\frac{\tau_j}{\Lambda_j^3}$ plays the role of a relaxation time. Heat transport with a superohmic spectral density was considered for example in the energy transport in the phenomenon of photosynthesis (Qin *et al.*, 2017). Note that Eq. (8.31) can be rewritten in terms of the damping kernel $\gamma_j(t)$ which is related to the susceptibility by $\frac{1}{m}\lambda_j(t) = -\frac{\partial}{\partial t}\gamma_j(t)$ (Dhar and Dandekar, 2015), as

$$\ddot{x}_j + \tilde{\Omega}_j^2 x_j - \gamma_j(0)\, x_j + \tilde{\kappa}_q x_q + \frac{\partial}{\partial t}\int_0^t \gamma_j(t-s)\, x_j(s)\,\mathrm{d}s = \frac{1}{\mathrm{m}}\mathrm{B_j}(t), \tag{8.40}$$

with $\tilde{\Omega}_j^2 = \Omega_j^2 + \sum_k V_{k,jj}e^{ik\omega_d t}$ and $\tilde{\kappa}_q = \kappa + \sum_k V_{k,jq}e^{ik\omega_d t}$, where the Leibniz rule was used as in (Charalambous *et al.*, 2019a). Moreover, in (Lampo *et al.*, 2018), it was also shown that the form of the damping kernel for such a spectral density reads as

$$\gamma_j(t) = \frac{\tau_j\left(6 + 3\left(\left(\widehat{\Omega}_{\mathrm{B,j}}\right)^2 t^2 - 2\right)\cos\left(\widehat{\Omega}_{\mathrm{B,j}}t\right)\right)}{t^4\left(\widehat{\Omega}_{\mathrm{B,j}}\right)^3} + \frac{\tau_j\widehat{\Omega}_{\mathrm{B,j}}\left(\left(\widehat{\Omega}_{\mathrm{B,j}}\right)^2 t^2 - 6\right)\sin\left(\widehat{\Omega}_{\mathrm{B,j}}t\right)}{t^3\left(\widehat{\Omega}_{\mathrm{B,j}}\right)^3}. \tag{8.41}$$

In the limit $t \to 0$ this damping kernel becomes

$$\gamma_j(0) = \lim_{t\to 0} \gamma_j(t) = \frac{\widehat{\Omega}_{\mathrm{B,j}} \tau_j}{4}. \tag{8.42}$$

In vector form the two coupled equations in (8.31) read as

$$\ddot{\mathbf{X}}(t) + \mathbf{K}\cdot\mathbf{X}(t) + \frac{\partial}{\partial t}\int_0^t \mathbf{D}(t-s)\cdot\mathbf{X}(s)\,\mathrm{ds} = \frac{1}{\mathrm{m}}\mathbf{B}^{\mathrm{T}}(\mathrm{t})\,\mathbb{I}, \tag{8.43}$$

where $\mathbb{I}$ is the identity matrix and

$$\mathbf{X}(t) = \begin{pmatrix} x_{\mathrm{L}}(t) \\ x_{\mathrm{R}}(t) \end{pmatrix},$$

$$\mathbf{K} = \begin{pmatrix} \Omega_{\mathrm{L}}^2 + \sum_k V_{k,LL} e^{ik\Omega_d t} - \gamma_{\mathrm{L}}(0) & \kappa + \sum_k V_{k,LR} e^{ik\Omega_d t} \\ \kappa + \sum_k V_{k,RL} e^{ik\Omega_d t} & \Omega_{\mathrm{R}}^2 + \sum_k V_{k,RR} e^{ik\Omega_d t} - \gamma_{\mathrm{R}}(0) \end{pmatrix},$$

$$\mathbf{D}(t) = \begin{pmatrix} \gamma_{\mathrm{L}}(t) & 0 \\ 0 & \gamma_{\mathrm{R}}(t) \end{pmatrix}, \text{ and } \mathbf{B}(t) = \begin{pmatrix} B_{\mathrm{L}}(t) \\ B_{\mathrm{R}}(t) \end{pmatrix}.$$

Static case. From the system of coupled equations (8.31), one can now identify the condition that guarantees the positivity of the Hamiltonian in the static case, where $H_{\mathrm{Drive}}(t) = 0$. To this end one first diagonalizes the Hamiltonian, and then requires that the normal mode frequencies are positive. We diagonalize the Hamiltonian by making the transformation $\mathbf{Q} = \mathbf{O}\cdot\mathbf{X}$, that brings Eq. (8.43) into

$$\ddot{\mathbf{Q}}(t) + \mathbf{K}_D\cdot\mathbf{Q}(t) + \frac{\partial}{\partial t}\int_0^t \mathbf{D}_D(t-s)\cdot\mathbf{Q}(s)\,\mathrm{ds} = \frac{1}{\mathrm{m}}\mathbf{B}_{\mathrm{D}}^{\mathrm{T}}(\mathrm{t})\,\underline{\mathrm{I}}, \tag{8.44}$$

where $\mathbf{D}_D(t) = \mathbf{O}\cdot\mathbf{D}(t)\cdot\mathbf{O}^T$, $\mathbf{B}_D^T(t) = \mathbf{O}\cdot\mathbf{B}^T(t)$, and the frequency matrix is diagonalized as

$$\mathbf{K}_D = \mathbf{O}\cdot\mathbf{K}\cdot\mathbf{O}^T = \begin{pmatrix} \Omega_{\mathrm{L}}^D & 0 \\ 0 & \Omega_{\mathrm{R}}^D \end{pmatrix}. \tag{8.45}$$

The positivity of the Hamiltonian condition is then guaranteed by requiring that $\{\Omega_{\mathrm{L}}^D, \Omega_{\mathrm{R}}^D\} > 0$ which in terms of the original frequencies reads as

$$\tfrac{1}{2}\Big[\gamma_{\mathrm{L}}(0) + \gamma_{\mathrm{R}}(0) - \Omega_{\mathrm{L}}^2 - \Omega_{\mathrm{R}}^2 + \Big[\left(\gamma_{\mathrm{L}}(0) + \gamma_{\mathrm{R}}(0) - \Omega_{\mathrm{L}}^2 - \Omega_{\mathrm{R}}^2\right)^2 \tag{8.46}$$

$$-4\left(\gamma_{\mathrm{L}}(0)\,\gamma_{\mathrm{R}}(0) - \kappa^2 - \gamma_{\mathrm{L}}(0)\,\Omega_{\mathrm{R}}^2 - \gamma_{\mathrm{R}}(0)\,\Omega_{\mathrm{L}}^2 + \Omega_{\mathrm{R}}^2\Omega_{\mathrm{L}}^2\right)\Big]^{1/2}\Big] < 0.$$

This condition guarantees that we do not have negative renormalized normal frequencies in the system and hence stability of the solution is guaranteed in the long-time limit. With this satisfied, we are in a position to safely neglect the effects of $\gamma_{\mathrm{L}}(0)$ and $\gamma_{\mathrm{R}}(0)$ in the dynamics of the system.

Upon rewriting the coupled equations of motion for the static case in a vector form as above, and considering it expressed in terms of the susceptibilities $\lambda_{\mathrm{L}}(t), \lambda_{\mathrm{R}}(t)$, one can obtain its solution by taking the Fourier transform of both sides

$$\mathbf{X}(\omega) = \mathbf{G}(\omega)\frac{\mathbf{B}(\omega)}{m}, \tag{8.47}$$

where

$$\mathbf{G}(\omega) = \left(-\omega^2\mathbf{I} + \mathbf{K} - \mathbf{L}(\omega)\right)^{-1}, \tag{8.48}$$

which is understood to play the role of a phonon Green function, and $\mathbf{L}(\omega)$ is the Fourier transform of $\mathbf{L}(t) = \begin{pmatrix} \lambda_{\mathrm{L}}(t) & 0 \\ 0 & \lambda_{\mathrm{R}}(t) \end{pmatrix}$, with diagonal elements

$$\begin{aligned} \lambda_j(\omega) &= Re[\lambda_j(\omega)] + iIm[\lambda_j(\omega)] \\ &= \frac{\tau_j\left(\Lambda_j^4+2\Lambda_j^2\omega^2+2\omega^4\left(i\pi+\log\left(-1+\frac{\Lambda_j^2}{\omega^2}\right)\right)\right)}{\pi^2} - i(\hbar(\Theta(\omega)-\Theta(-\omega))J_j(\omega)), \end{aligned} \tag{8.49}$$

where the real part of the susceptibility was obtained through the Kramers-Kronig relation $Re[\lambda_j(\omega')] = \mathcal{H}[Im[\lambda_j(\omega)]](\omega') = \frac{1}{\pi}P\int_{-\infty}^{\infty}\frac{Im[\lambda_j(\omega)]}{\omega-\omega'}\mathrm{d}\omega$. Here $\mathcal{H}[\cdot](\omega')$ denotes the Hilbert transform and P the principal value. In general, for the parameters we consider in our results, it will always hold that $\Omega_j^2 \gg Re[\lambda_j(\omega)]$ such that we safely neglect the effect of $Re[\lambda_{\mathrm{L}}(\omega)]$ and $Re[\lambda_{\mathrm{R}}(\omega)]$.

In terms of this solution of the static equations of motion, the positivity condition (8.46), can be interpreted in a different way: it guarantees that the phonon propagator, i.e. the Green function $\mathbf{G}(\omega)$, has no poles in the lower half plane of the complex plane. This implies that there are no divergencies in the integrals that will be performed later on and will involve these Green functions (Rzażewski and Żakowicz, 1980).

Driven case. Now we consider the case where a driving is applied on the central system. In particular we assume that the driving is either on the oscillators' frequencies or on their in-between coupling, as in (Riera-Campeny *et al.*, 2019). The analytic treatment of this case is slightly more involved than the static one. We are now dealing with a periodic differential equation, and the analysis of the stability of the long-time steady state solution of the equations of motion is not straightforward. To be able to perform the stability analysis, what one usually does is to convert the periodic differential equation to a linear one by resorting to Floquet theory. This is done by converting first all the terms in the equation of motion into periodic ones, and then study the stability of the Floquet-Fourier components of the resulting Green function. The basic assumption that enables us to employ the Floquet formalism is that even though some function $f(t)$ might not be periodic, another function defined based on this one as $\mathbf{W}(t,\omega) = \int_{\mathbb{R}} dt' f(t-t') e^{i\omega(t-t')}$ will indeed be periodic. Furthermore,

such periodic function can always be expressed in terms of its Fourier components as $\mathbf{W}(t,\omega) = \sum_k \mathbf{B}_k(\omega) e^{ik\Omega_d t}$. By performing these two transformations on the equations of motion, i.e. $\int_{\mathbb{R}} dt' e^{i\omega(t-t')}$ and Fourier expanding, one obtains a set of equations for the Fourier coefficients $\mathbf{A}_k(\omega)$ of $\mathbf{P}(t,\omega) = \int_{\mathbb{R}} dt' \mathbf{G}(t-t') e^{i\omega(t-t')} = \sum_k \mathbf{A}_k(\omega) e^{ik\Omega_d t}$ that can be self-consistently solved. By following this procedure, in (Riera-Campeny *et al.*, 2019) the authors were able to obtain expressions for these coefficients

$$\mathbf{A}_0(\omega) = \mathbf{G}(\omega) + \sum_{j\neq 0} \mathbf{G}(\omega)\cdot\mathbf{V}_j\cdot\mathbf{G}(\omega+j\Omega_d)\cdot\mathbf{V}_{-j}\cdot\mathbf{G}(\omega) + \mathcal{O}\left(\mathbf{V}_j^4\right), \tag{8.50}$$

$$\mathbf{A}_k(\omega) = -\mathbf{G}(\omega-k\Omega_d)\cdot\mathbf{V}_k\cdot\mathbf{G}(\omega) + \mathcal{O}\left(\mathbf{V}_j^3\right), \tag{8.51}$$

where $\mathbf{V}(t) = \sum_k \mathbf{V}_k e^{ik\Omega_d t}$. Note that we will assume that the driving strength coefficient is sufficiently small such that we can ignore terms of the order of $\mathcal{O}\left(\mathbf{V}_j^3\right)$ or higher. Furthermore, since the Fourier coefficients $\mathbf{A}_k(\omega)$ are related to the Green function, one can interpret them as describing the fundamental processes responsible for the phonon and hence heat transport. These coefficients tell us that the driving is responsible for a sudden change of the propagation frequency ω of the phonon by an amount of $k\Omega_d$. Finally, the solution of the equations of motion in this case would read as

$$X(t) = \sum_k \int_{-\infty}^{\infty} e^{-i(\omega-k\Omega_d)t} \mathbf{A}_k(\omega) \frac{\mathbf{B}(\omega)}{m}. \tag{8.52}$$

Uncertainty relation. Finally, we comment that we check that the uncertainty relation holds for both cases that we consider, static and driven. This is simply expressed by the condition

$$\nu_- \geq \frac{1}{2}, \tag{8.53}$$

where ν_- is the minimum standard eigenvalue of $\widetilde{\mathbf{C}}(0)$ ($\hbar$ is assumed to be equal to 1 in this case). In the above expression, $\widetilde{\mathbf{C}}(0) = i\mathbf{W}\cdot\mathbf{C}(0)$ with $\mathbf{W}$ the symplectic matrix and $\mathbf{C}(0)$ the covariance matrix, that both are defined in the appendix. Note that the covariance matrix can be expressed in terms of the Green's function and the spectral density, for both static and driven cases as is shown in the appendix.

8.3 Heat current control between the BECs

Here we present the thermodynamics quantities of interest, in order to evaluate the performance of our system as a heat current control platform and as a thermal diode. These quantities cannot be expressed in terms of analytically known functions, due to the non-ohmic spectral density that describes the baths. As such, the results in next section are obtained by numerically evaluating the integrals.

8.3.1 Static case

We begin with the static scenario with $H_{\text{Drive}}(t) = 0$, and we study the behaviour of heat current and the current-current correlations.

The heat current. When studying a heat engine, a key quantity is the average current J_{L} going from the left reservoir (assuming it to be the hot reservoir) to the left oscillator (Dhar, 2008, Lepri, 2016) (by conservation of current $J_{\mathrm{L}} = -J_{\mathrm{R}}$), or equivalently the average rate at which the left bath does work on the left particle (power). In general, there are two ways to define the heat current. The first one is derived from considerations of energy conservation on the system,

$$J_{\mathrm{L}} = \frac{d\left\langle H_{\mathrm{S}}\right\rangle}{dt} - \left\langle \frac{\partial}{\partial t} H_{\mathrm{S}} \right\rangle = \left\langle \frac{i}{\hbar}\left[\widetilde{H}_{Int.,L}, H'_{\mathrm{L}}\right]\right\rangle_{\rho}, \tag{8.54}$$

where $H'_{\mathrm{L}} = \frac{p_{\mathrm{L}}^2}{2m} + V_{\mathrm{L}}\left(x_{\mathrm{L}}\right) + \kappa x_{\mathrm{L}} x_{\mathrm{R}}$ and the average is over the total density state ρ. The second definition is expressed in terms of the rate of decrease of the bath energy (Kato and Tanimura, 2016)

$$\begin{aligned} \widehat{J}_{\mathrm{L}} &= -\frac{d\left\langle H_{B,L}\right\rangle_{\rho}}{dt} = \left\langle \tfrac{i}{\hbar}\left[H_{B,L}, H_{\mathrm{Tot}}\right]\right\rangle_{\rho} \\ &= \left\langle \tfrac{i}{\hbar}\left[\widetilde{H}_{Int.,L}, H'_{\mathrm{L}}\right]\right\rangle_{\rho} + \frac{d\left\langle \widetilde{H}_{Int.,L}\right\rangle_{\rho}}{dt} + \left\langle \left[\widetilde{H}_{Int.,L}, \widetilde{H}_{Int.,R}\right]\right\rangle_{\rho}. \end{aligned} \tag{8.55}$$

The second term vanishes under steady state conditions and weak system-bath coupling, where weak is understood in the sense of assumption (8.35) (and not of Markovian dynamics for the impurity), which is the case in our study. We are further considering that the correlations among the system bath interactions is negligible, i.e. $\left\langle \left[\widetilde{H}_{Int.,L}, \widetilde{H}_{Int.,R}\right]\right\rangle_{\rho_{\mathrm{B}}} = 0$, since we assume that each system interacts only with its own reservoir. Under these criteria the two definitions of heat current are equivalent. In other words, in our model, the rate at which the bath looses/gains energy is equal to the energy that the system gains/looses. The more general scenario of strong coupling and hence non-separability of the system-bath was considered for a spin-boson model in (Gelbwaser-Klimovsky and Aspuru-Guzik, 2015), while the case of interactions among the baths was studied in (Li *et al.*, 2012a). Therefore the heat current considered here is

$$J_{\mathrm{L}} = \left\langle \frac{i}{\hbar}\left[\widetilde{H}_{Int.,L}, H'_{\mathrm{L}}\right]\right\rangle_{\rho_{\mathrm{B}}} = \left\langle \eta_{\mathrm{L}}\left(t\right)\frac{p_{\mathrm{L}}\left(t\right)}{m}\right\rangle_{\rho_{\mathrm{B}}}, \tag{8.56}$$

where the second equality is valid in steady state with $\eta_{\mathrm{L}}\left(t\right) = \int_0^t \lambda_{\mathrm{L}}\left(t-s\right) x_{\mathrm{L}}\left(s\right) \mathrm{d}s + \frac{1}{\mathrm{m}} \mathrm{B}_{\mathrm{L}}\left(t\right)$, and it is obtained after solving the bath particles equations of motion. Note that in (8.56) the current is a scalar, which is the average current, and it is averaged under steady state condition i.e. at the long time limit which is independent of the initial state of the system. In (Dhar, 2008, Lepri, 2016, Dhar and Sriram Shastry, 2003), by using a direct solution of the equations of motion for a non-interacting system of bath particles, the average current is proven to be equal to

$$\left\langle J_{\mathrm{L}}\right\rangle_{\rho_{\mathrm{B}}} = \frac{1}{4\pi}\int_{-\infty}^{\infty} \mathrm{d}\omega \mathcal{T}\left(\omega\right)\hbar\omega\left[f\left(\omega, T_{\mathrm{L}}\right) - f\left(\omega, T_{\mathrm{R}}\right)\right] = -\left\langle J_{\mathrm{R}}\right\rangle \equiv \left\langle J\right\rangle, \tag{8.57}$$

with $f(\omega, T_j) = [e^{\frac{\hbar\omega}{k_B T_j}} - 1]^{-1}$, the phonon occupation number for the respective thermal reservoir and

$$\mathcal{T}(\omega) = 4Tr\left[\mathbf{G}(\omega)\, Im\left[\mathbf{L}_{\mathrm{L}}(\omega)\right] \mathbf{G}^{\dagger}(\omega)\, Im\left[\mathbf{L}_{\mathrm{R}}(\omega)\right]\right], \tag{8.58}$$

$$\mathbf{L}_{\mathrm{L}}(\omega) = \begin{pmatrix} \lambda_{\mathrm{L}}(\omega) & 0 \\ 0 & 0 \end{pmatrix}, \; \mathbf{L}_{\mathrm{R}}(\omega) = \begin{pmatrix} 0 & 0 \\ 0 & \lambda_{\mathrm{R}}(\omega) \end{pmatrix}, \tag{8.59}$$

being the transmission coefficient for phonons at frequency ω. You can find a proof of this in App. D.2. This is called the Landauer formula. Note that $\mathcal{T}(\omega)$ can be related to the transmittance of plane waves of frequency ω across the system as in (Das and Dhar, 2012). The transmission coefficient, interestingly, depends on all the parameters of the system. That is, it depends on the parameters of the baths (apart from temperature) as well as the parameters of the coupling between the system and the baths.

Eq. (8.57) describes the situation where the central region is small in comparison with the coherent length of the waves, which is the assumption we also abide to, so that it is treated as purely elastic scattering without energy loss. The dissipation resides solely in the heat baths. This implies ballistic thermal transport, which corresponds to direct point-to-point propagation of energy, contrary to the transport in bulk and disordered structures which is referred to as diffusive transport. Indeed, within the framework of modeling thermal baths by means of quantum Langevin equations, ballistic transport has been observed for chains of quantum harmonic oscillators (Zürcher and Talkner, 1990), and hence this is also our case. Furthermore, note that the Landauer formula can also capture phonon tunneling, i.e. the case when phonons off-resonance with the systems vibrations cross the "junction", showing features of quantum tunneling (Segal *et al.*, 2003). Finally, it is worth commenting on an implicit assumption we made. We assumed here that a unique steady state was reached, or equivalently that there are no bound states in our system, i.e., that no modes outside the bath spectrum are generated for the combined model of system and baths. The problem is that these modes are localized near the system and any initial excitation of the mode is unable to decay (Dhar and Sen, 2006).

It is interesting to comment on two limits of Eq. (8.57), namely the linear limit $\Delta T := T_{\mathrm{L}} - T_{\mathrm{R}} \ll T$ where $T = \frac{T_{\mathrm{L}}+T_{\mathrm{R}}}{2}$ and the classical limit, $\frac{\hbar\omega}{k_B T} \to 0$ where ω refers to the bath frequencies. In the first limit, the current reduces to

$$\langle J \rangle = \frac{\Delta T}{2\pi} \int_0^{\infty} \mathrm{d}\omega \mathcal{T}(\omega)\, \hbar\omega \frac{\partial f(\omega, T)}{\partial T}, \tag{8.60}$$

such that once the two baths are at the same temperature there is no current flow. In the second limit, it becomes

$$\langle J \rangle = \frac{k_B \Delta T}{2\pi} \int_0^{\infty} \mathrm{d}\omega \mathcal{T}(\omega), \tag{8.61}$$

where the current is independent of the temperature of the baths $T_{\mathrm{L}}, T_{\mathrm{R}}$ but it only depends on their difference ΔT.

We conclude with one last comment regarding our system and the role that entanglement could play on the amount of heat current transported from one BEC to the other. From (Riera-Campeny *et al.*, 2019), it is known that the static current can also be expressed in terms of the off-diagonal elements of the covariance matrix. This, might lead one to consider that entanglement, the presence of which is understood to be related to these off-diagonal elements might play a role in the amount of heat current transported. However, it was shown in (Liu and Goan, 2007, Vasile *et al.*, 2010a) that in a system of two harmonic oscillators coupled to distinct baths, as is our case, there is no long-time entanglement present.

Current-Current correlations. Next, we focus on the current-current correlations which is an easily accessible quantity from an experimental point of view. This is because these correlations are related to noise, which can be experimentally measured. They contain valuable information on the nature of the fundamental processes responsible for the heat transport. Furthermore, from the current-current correlation many other quantities can be obtained, such as the thermal conductance (Dhar, 2008, Lepri, 2016) and the local effective temperature of driven systems (Caso *et al.*, 2012).

The current-current time correlations $JJ_{\mathrm{LL}}(t,t')$, which is sometimes referred to as current fluctuations in time or current noise, is defined as the symmetrized correlation function of the current, that is

$$JJ_{\alpha\beta}(t,t') = \frac{1}{2}\left\langle \left[J_\alpha(t) - \langle J_\alpha(t)\rangle_{\rho_{\mathrm{B}}},\ J_\beta(t') - \langle J_\beta(t')\rangle_{\rho_{\mathrm{B}}} \right] \right\rangle_{\rho_{\mathrm{B}}}. \tag{8.62}$$

We are interested in the steady state correlations, for which an expression for this can be obtained using the non-equilibrium Green's functions as was mentioned above. Hence the correlation function of interest is a function only of the time difference, $JJ(t,t') = JJ(t-t')$. Therefore, the noise strength is characterized by the zero frequency component $JJ_{\alpha\beta} = \int_{-\infty}^{\infty} JJ_{\alpha\beta}(t)\,\mathrm{dt}$, which obeys $JJ_{\alpha\beta} \geq 0$ according to Wiener-Khinchine theorem. It is current conserving, i.e. the sum of currents entering the system from all reservoirs is equal to zero at each instant of time, and gauge invariant and hence physically meaningful (Blanter and Büttiker, 2000, Kohler *et al.*, 2005). Current conservation implies $JJ_{\mathrm{LL}} = JJ_{\mathrm{RR}}$.

One way to obtain such an expression is by first deriving the cumulant generating function $\chi(\mu)$, employing the non-equilibrium Green's functions technique within the Keldysh formalism, and noting that $JJ_{\alpha\beta} := \frac{\partial^2 \chi(\mu)}{\partial \mu^2}\,|_{\mu=0}$ (see e.g., (Dhar, 2008, Lepri, 2016, Saito and Dhar, 2007)). In this case, one can show that the current fluctuations

read as (Blanter and Büttiker, 2000, Kohler *et al.*, 2005)

$$\langle JJ_{\mathrm{LL}}\rangle_{\rho_{\mathrm{B}}}=\int_0^\infty \mathrm{d}\omega\frac{\hbar^2\omega^2}{2\pi}\Big\{\mathcal{T}(\omega)\left[\mathrm{f}(\omega,\mathrm{T_R})(1+\mathrm{f}(\omega,\mathrm{T_R}))+\mathrm{f}(\omega,\mathrm{T_L})(1+\mathrm{f}(\omega,\mathrm{T_L}))\right] \\ -\mathcal{T}(\omega)(1-\mathcal{T}(\omega))\left[f(\omega,T_{\mathrm{L}})-f(\omega,T_{\mathrm{R}})\right]^2\Big\}. \quad (8.63)$$

The first two terms of this expression correspond to the equilibrium noise, while the third corresponds to the non-equilibrium noise, also referred to as shot noise. At high energies, the latter is negligible. Note that the shot noise is negative and hence contributes to diminish the noise power in comparison with having the equilibrium noise alone. The expression above Eq. (8.63) is true only under the assumption of independence of the two baths.

Finally let us address the linear and the classical limits of the correlations. In the first limit, the current-current correlations read as

$$\langle JJ_{\mathrm{LL}}\rangle_{\rho_{\mathrm{B}}}=\int_0^\infty \mathrm{d}\omega\frac{\hbar^2\omega^2}{2\pi}\left\{\left[\mathcal{T}^2(\omega)\left(\Delta\mathrm{T}\frac{\partial\mathrm{f}(\omega,\mathrm{T})}{\partial\mathrm{T}}\right)^2+\frac{2\mathrm{T}^2\mathcal{T}(\omega)}{\omega}\frac{\partial\mathrm{f}(\omega,\mathrm{T})}{\partial\mathrm{T}}\right]\right\}. \quad (8.64)$$

In the classical limit it becomes

$$\langle JJ_{\mathrm{LL}}\rangle_{\rho_{\mathrm{B}}}=\frac{k_{\mathrm{B}}^2}{2\pi}\int_0^\infty \mathrm{d}\omega\mathrm{Tr}\left[\mathcal{T}^2(\omega)(\Delta\mathrm{T})^2+2\mathcal{T}(\omega)\mathrm{T_L}\mathrm{T_R}\right]. \quad (8.65)$$

Note that Eq. (8.64), contrary to the expression for the current Eq. (8.60) at the same limit, does not vanish when $\Delta T\to 0$, which results in non-zero fluctuations of the current even in the scenario that no average current flows in the system.

We comment here on the experimental feasibility of the measurements of the two proposed quantities above, namely the heat current and the current variance. As is proven in detail in (Riera-Campeny *et al.*, 2019) in Appendix C, the heat current depends on the covariance matrix element $C_{\mathbf{XP}}(0)$ defined in Appendix D.1 of our paper, where the nonzero elements of this matrix are $\langle x_i p_j\rangle$ with $i\neq j$. Hence one needs to measure simultaneously the position of one particle and the momentum of the other. It should be experimentally feasible to make this measurements almost instantaneously. For the former type of measurement, that of position, there are already experiments in which one is able to evaluate them (Catani *et al.*, 2012a). The idea is that, one measures the position of the particle using a time-of-flight experiment, by implementing a resonant in-situ absorption imaging technique, in a system with a two species ultracold gas, in which one of the species is much more dilute - dilute enough as to consider its atoms as impurities immersed in a much bigger BEC. A much more recent technique could be used to make measurements of both the position and the momentum. In particular, a quantum

gas microscope (Sherson *et al.*, 2010, Bakr *et al.*, 2009) may be an option. This technique uses optical imaging systems to collect the fluorescence light of atoms, and it has been used in the study of atoms in optical lattices, achieving much better spatial resolution (Sherson *et al.*, 2010, Bakr *et al.*, 2009), and avoiding the aforementioned problem with time-of-flight experiments. In the past such a technique has been used to study spatial entanglement between itinerant particles, by means of quantum interference of many body twins, which enables the direct measurement of quantum purity (Islam *et al.*, 2015). Finally, having these measurements at hand, one can evaluate the $C_{\mathbf{XP}}(0)$. The current-current correlation then is the variance of the current, which could be obtained by the data collected. This would be the protocol to follow in order to measure the heat current. Nevertheless, we can only give an idea of a measurement protocol, leaving open for future research the question of whether the resolution when measuring the correlations in current experimental set-ups would be enough as to infer the heat current.

8.3.2 The dynamic case

For the driven case, the steady-state averaged heat current is given by (Riera-Campeny *et al.*, 2019)

$$J_j^{(D)} = -\int_{\mathbb{R}} \mathrm{d}\omega \widehat{\mathrm{T}}_{\mathrm{j}}(\omega)\left(\mathrm{f}_{\mathrm{j}}(\omega)+\frac{1}{2}\right) + \sum_{q\neq j}\int_{\mathbb{R}} \mathrm{d}\omega\left[\widetilde{\mathrm{T}}_{\mathrm{qj}}(\omega)\left(\mathrm{f}_{\mathrm{j}}(\omega)+\frac{1}{2}\right)-\widetilde{\mathrm{T}}_{\mathrm{jq}}(\omega)\left(\mathrm{f}_{\mathrm{q}}(\omega)+\frac{1}{2}\right)\right], \tag{8.66}$$

where the new transmission coefficient reads as

$$\widetilde{T}_{jq}(\omega) = \sum_k \hbar(\omega - k\Omega_d)\, tr\left[Im\left[\mathbf{L}_j(\omega-k\Omega_d)\right]\mathbf{A}_k(\omega)\, Im\left[\mathbf{L}_q(\omega)\right]\mathbf{A}_k^{\dagger}(\omega)\right], \tag{8.67}$$

and

$$\widehat{T}_j(\omega) = \sum_\beta \widetilde{T}_{jq}(\omega). \tag{8.68}$$

A proof of this is given in App. D.3.This expression was also obtained in (Kohler *et al.*, 2005, Freitas and Paz, 2017, Camalet *et al.*, 2003, 2004), while in (Lehmann *et al.*, 2003) a similar expression was obtained for transport through quantum dots. Unlike the static case, these transmission coefficients are not symmetric, i.e., $\widetilde{T}_{jq}(\omega) \neq \widetilde{T}_{qj}(\omega)$. Crucially, this symmetry breaking, attributed to the driving that is now expressed in the form of the transmission coefficients, is responsible for the appearance of *heat rectification* as addressed in (Riera-Campeny *et al.*, 2019). To observe and quantify rectification, it is useful to evaluate the rectification coefficient

$$R := \frac{\left|J_j^{(D)} + J_{j,\mathrm{r}}^{(D)}\right|}{\max\left(\left|J_j^{(D)}\right|, \left|J_{j,\mathrm{r}}^{(D)}\right|\right)}, \tag{8.69}$$

Left BEC and impurity	Right BEC and impurity	Other parameters
$T_{\mathrm{L}} = 75nK$	$T_{\mathrm{R}} = 7.5nK$	$d = 9.5a_{\mathrm{ho}}$
$N_{\mathrm{L}} = 7.5 \times 10^4$	$N_{\mathrm{R}} = 7 \times 10^4$	$a_{\mathrm{ho}} = 0.7\mu m$
$\eta_{\mathrm{L}} = 0.5$	$\eta_{\mathrm{R}} = 0.5$	$\Omega = 200\pi Hz$
$g_{\mathrm{B}}^{(L)} = 2.5 \times 10^{-40} J \cdot m$	$g_{\mathrm{B}}^{(R)} = 2 \times 10^{-40} J \cdot m$	
$\Omega_{\mathrm{L}} = \Omega$	$\Omega_{\mathrm{R}} = \Omega$	
$\widehat{\Omega}_{B,L} = 3\Omega$	$\widehat{\Omega}_{B,R} = 3\Omega$	

Table 8.1 List of default parameters—unless otherwise mentioned—used in the static case, corresponding to Figures. 8.2 and 8.3.

where $J_{j,\mathrm{r}}^{(D)}$ is the value of the current, once the temperature gradient is reversed, i.e. when the two baths' temperatures are interchanged. Notice that this coefficient takes values between 0 and 2, namely, $R = 0$ when $J_j^{(D)} = -J_{j,\mathrm{r}}^{(D)}$, with the current being symmetric under reversing the temperature gradient. The upper bound is achieved when the current remains unaffected by reversing the temperature gradient. When either of the two currents is blocked, the coefficient is equal to one.

8.4 Main Results

Before presenting our main results, let us summarize the major assumptions we made for our system, and the restrictions that these impose on the parameter regimes that we can consider:

1. Linearization of the impurity-bath coupling, which is achieved by assuming that the impurity is in the middle of its corresponding trap (see Eq. (8.6)). This in practice imposes a restriction on the maximum temperature we can consider (Lampo *et al.*, 2018)
$$T_j \ll T_j^{\max} = \frac{m\Omega_j^2 R_j^2}{k_{\mathrm{B}}}. \tag{8.70}$$
Note that in the scenario when the impurity is driven, the frequency term Ω_j^2 is replaced by $\min_t \left(\Omega_j^2 + \sum_k V_{k,jj} e^{ik\Omega_d t}\right)$.

2. BEC independence condition $R_{\mathrm{L}} + R_{\mathrm{R}} < d$

3. Positivity condition, Eq. (8.46).

In our analysis below we consider the BECs of Rubidium (Rb) atoms. The impurities are Dysprosium (Dy) atoms, which are the atoms with the largest magnetic moment known at present, $\mu = 10\mu_{\mathrm{B}}$, where μ_{B} is the Bohr magneton.

8.4.1 Static system

Heat current

In Fig. 8.2 (a) we plot the heat current with the temperature difference $\Delta T = T_{\mathrm{L}} - T_{\mathrm{R}}$, where we keep fixed the temperature of the left reservoir T_{L}. As expected, the heat current increases with increasing temperature difference, while it is zero when there is no temperature gradient. We see that the current depends linearly on the temperature gradient. This is in accordance to the linear limit for the heat current in Eq. (8.60). In addition, we studied heat current in the scenario where the temperature difference between the two baths was fixed to some value, in particular $\Delta T = 10nK$, with $T_{\mathrm{L}} = T$ and $T_{\mathrm{R}} = T + \Delta T$, and we considered the simultaneous variation of the temperatures of both baths, in the temperature regime $T = 10\mathrm{nK} - 100\mathrm{nK}$. In this case we saw that the heat current remained constant as a function of T and hence we conclude that the regime in which we could study the system was that of the classical limit Eq. (8.61). A figure for this case is omitted since the current was just constant as a function of T. From Fig. 8.2 (a) we also observe that increasing the distance of the two impurities results in decreasing the heat current flow (red *vs* blue curves), while increasing the impurity-BEC couplings results in an increase of the current (red *vs* green curves).

Figure 8.2 (b) depicts the heat current against the trapping frequencies of the BECs. In particular we fix one of the trapping frequencies and vary the other. Firstly, we observe that the heat current is reaches a maximum when the trapping frequencies of the two impurities match, i.e., $\Omega_{\mathrm{R}} = \Omega_{\mathrm{L}}$. This is understood as follows. The current density, which we define as $J_{den.} := \frac{1}{4\pi}\mathcal{T}(\omega)\hbar\omega\left[f(\omega, T_{\mathrm{L}}) - f(\omega, T_{\mathrm{R}})\right]$ is maximized when the denominator of $\mathcal{T}(\omega)$, given by $\left(-\omega^2\mathbf{I} + \mathbf{K} - \mathbf{L}(\omega)\right)^{-1}\left(\left(-\omega^2\mathbf{I} + \mathbf{K} - \mathbf{L}(-\omega)\right)^{T}\right)^{-1}$ is minimized. In the regime we are looking, $\frac{\tau_j}{\tilde{\Omega}_j^3}$ come out to be of the order of 10^{-4}, while the values of κ that are allowed, are of the order of 10^{-5}. These are much smaller than the trapping frequencies Ω_{L}^2, Ω_{R}^2, such that the denominator is minimized whenever $\left(\omega^2 - \Omega_L^2\right)^2 + \left(\omega^2 - \Omega_R^2\right)^2$ is minimized. This happens when $\omega = \Omega_L = \Omega_R$. Secondly—for the specific parameters that we choose—contrary to Fig. 8.2 (a), increasing the impurity-BEC coupling strength results in reducing the current.

We study the dependence on the impurity-BEC coupling strength in Fig. 8.2 (c), where we see current reaches a maximum at some optimal coupling. Keeping the coupling constant of the left impurity fixed and varying that of the right impurity, we find that if the impurity is weakly coupled to the BECs, then current can not be carried from one BEC to the other through the vibrations of these impurities. If on the other hand, this is coupled too strongly, the effect of the noise induced by the baths (BECs) reduces the current that can be transmitted This is in agreement with the findings in Fig. 8.2 (a) and (b).

In Fig. 8.2 (d) we see how the heat current varies as a function of the distance between the two impurities. As expected, we see that increasing the distance between the impurities reduces the heat current. In particular, we find $\langle J \rangle \propto \kappa^2$—in the parameter regime that we study. It is possible that, at shorter distances, another resonance effect occurs between the value of the spring constant, which depends inversely on the distance between the impurities and the trapping frequencies of the impurities. Anyhow, we do not study the system at such small distances because the approximation of independence of the BECs breaks down.

Finally we remark here that one could also consider studying homogeneous gases instead of harmonically trapped ones and the induced heat current could be examined for this case, by studying the system in the spirit of (Lampo *et al.*, 2017a). Experimentally, homogeneous gases could be created as in (Gaunt *et al.*, 2013). From our studies, we observe that as expected one can still have current in this case, but since the spectral density is different in this case, even though still superohmic, there is a quantitative difference in the amount of current. Nevertheless we focused on the harmonically trapped case which is more conventionally implemented experimentally. From (Lampo *et al.*, 2018) it is known that the two spectral densities result in a different degree of non-markovianity, and it would be interesting in the future to study the effect of non-markovianity on the heat current. This however exits the scope of this paper.

Current-Current correlations.

In Fig. 8.3 (a) the behavior of the current-current correlations is illustrated as a function of temperature T while keeping the temperature difference ΔT constant. From the figure, we see that, for small ΔT, such that the first term of Eq. (8.65) prevailed, the current-current correlations are proportional to T^2. On the contrary when ΔT is large, and for relatively small T, the current-current correlations depended linearly on the temperature T. Nevertheless the behavior seems to be independent of ΔT as the temperature increases, and appears to depend on the square of T as expected in the classical limit.

In Fig. 8.3 (b) we study the dependence of current-current correlations on the temperature difference ΔT. At large temperature difference, i.e. beyond the linear limit considered in (8.64), the correlations depend linearly on ΔT. We comment here that this is not directly evident from the LogLog plot, but we checked that this is indeed the case of a linear relation from the corresponding current-current correlation versus temperature difference plot before taking the logarithms. For small ΔT, where (8.63) is well approximated by Eq. (8.64), indeed we find the saturation on the correlations predicted by the second term of Eq. (8.63). This implies that even as $\Delta T \to 0$—in which case current is zero— the fluctuations are still present. One might expect quantum effects to appear in this regime then, but we studied the entanglement in this system, by means of the

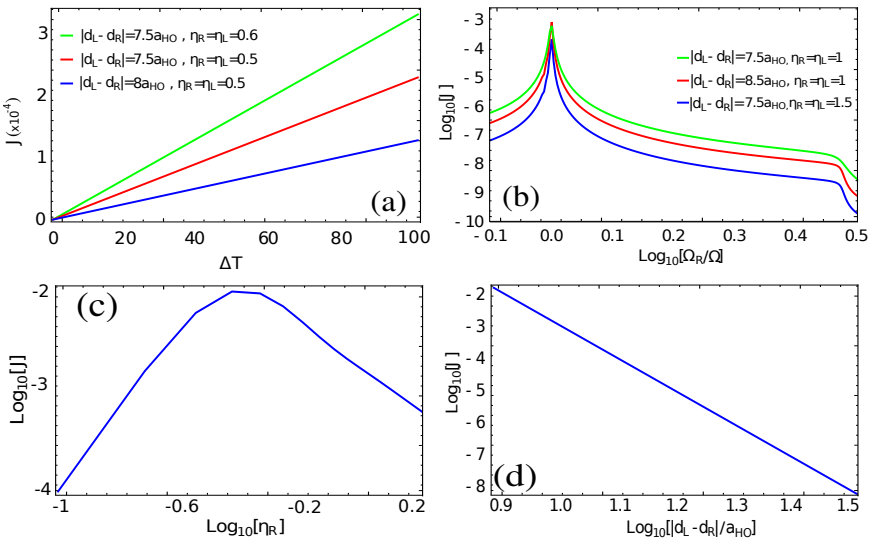

Fig. 8.2 **(a)** Heat current J against the temperature difference of the two baths ΔT, with fixed T_{R}. As expected current increases linearly with ΔT. Furthermore, the current decreases with increasing distance, and increases with increasing the coupling strength of the impurities to the bath. **(b)** Current as a function of the trapping frequency Ω_{R} of the right impurity. We observe resonance at $\Omega_{\mathrm{R}} = \Omega_{\mathrm{L}}$. Furthermore, for Ω_{R} larger than the trapping frequency of the bath—which is also the cutoff for the spectral density—the current vanishes quickly. Moreover, current decreases with distance as before. In this regime, current decreases as the impurities couple stronger to their respective baths (note that the coupling strengths are different from panel **(a)**). **(c)** Current as a function of the coupling strength of the right impurity. Current reaches a maximum in the range studied. **(d)** Current as a function of the distance between the impurities $|d_1 - d_2|$. Current decreases linearly with increasing distance in the regime we were allowed to study, that is under the restriction that is imposed on the lower distance in order to maintain the two BECs spatially independent. Current is found to scale as κ^2. See Table 8.1 for the parameters that we use here.

logarithmic negativity as in (Charalambous *et al.*, 2019a), and no entanglement could be detected in this regime.

8.4.2 Driven case: Heat rectification

Heat rectification is quantified by the heat rectification, Eq. (8.69). We use the particular form of driving

$$\mathbf{V}(t) = 2v\cos(\omega_d t)\begin{pmatrix} 1 & 0 \\ 0 & 0 \end{pmatrix}, \tag{8.71}$$

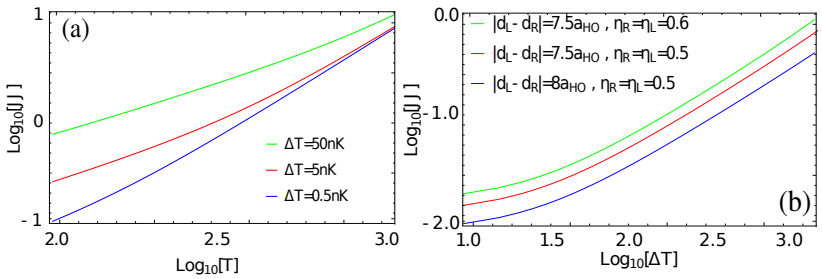

Fig. 8.3 (a) Current-current correlations against temperature T at constant ΔT. Here we observe that for small ΔT and at large temperatures T as expected from Eq. (8.65), current-current correlations scale as $\propto T^2$. At sufficiently large T this is expected to happen for large ΔT as well, however we were restricted on the range of maximum temperatures we could consider. **(b)** Current-current correlations as a function of the temperature difference of the two baths ΔT. For small values of ΔT, i.e., in the linear regime, the correlations have a nonzero value as predicted in Eq. (8.64). This implies that even as $\Delta T \to 0$, where current also vanishes, correlations still persist. For large enough values of ΔT the correlations increase linearly with ΔT. See Table 8.1 for the parameters that we use here.

Left BEC and impurity	Right BEC and impurity	Other parameters
$T_{\mathrm{L}} = 15nK$	$T_{\mathrm{R}} = 1nK$	$d = 35a_{\mathrm{ho}}$
$N_{\mathrm{L}} = 7.5 \times 10^4$	$N_{\mathrm{R}} = 7 \times 10^4$	$a_{\mathrm{ho}} = 0.7\mu m$
$\eta_{\mathrm{L}} = 0.5$	$\eta_{\mathrm{R}} = 0.5$	$\Omega = 200\pi Hz$
$g_{\mathrm{B}}^{(L)} = 5 \times 10^{-39} J \cdot m$	$g_{\mathrm{B}}^{(R)} = 4.5 \times 10^{-39} J \cdot m$	$v = 0.1\Omega$
$\Omega_{\mathrm{L}} = 2\Omega$	$\Omega_{\mathrm{R}} = 2\Omega$	
$\Omega_{B,L} = 2.5\Omega$	$\Omega_{B,R} = 2.5\Omega$	

Table 8.2 List of default parameters—unless otherwise mentioned—used in the dynamic case, corresponding to Fig. 8.4

i.e. we drive the frequency of the first oscillator. The parameters that we use are given in Table 8.2. The temperatures we choose are upper bounded by $\{T_L, T_R\} < 10^3 nK$.

In Fig. 8.4 we depict the heat rectification coefficient R as a function of Ω_d, the driving frequency. We find that it shows two maxima for two values of the driving frequency $\Omega_d \in \{\Omega, 3\Omega\}$. Note that, as shown in (Riera-Campeny *et al.*, 2019), heat rectification should be maximum at the following frequencies

$$\Omega_d = |\nu_j \pm \nu_i| \,. \tag{8.72}$$

Here $\{i,j\} \in \{\mathrm{L},\mathrm{R}\}$ with $i \neq j$ and ν_i's are the normal modes of the coupled impurities

$$\nu^2_{\mathrm{L,R}} = \Omega^2_{\mathrm{L}} + \kappa + \frac{\Delta}{2} \mp \left(\kappa^2 + \frac{\Delta^2}{4}\right)^{1/2}, \tag{8.73}$$

with $\Delta = \Omega^2_{\mathrm{R}} - \Omega^2_{\mathrm{L}}$. In our case, Eq. (8.72) indeed suggests that rectification should be maximum at $\Omega_d \in \{\Omega, 3\Omega\}$ which explains the results in Fig. 8.4. Note that we also studied dependence of the rectification coefficient on the other parameters of the system, apart from the driving frequency. In particular, we find that in the regime of parameters we study, maximum rectification decreases when the impurities couple more strongly to their respective baths. On the contrary, decreasing the number of atoms significantly increases R, in fact reaching $R > 1$. What is more, rectification could also be optimized with respect to the detuning between the trapping frequencies of the impurities as in (Riera-Campeny *et al.*, 2019).

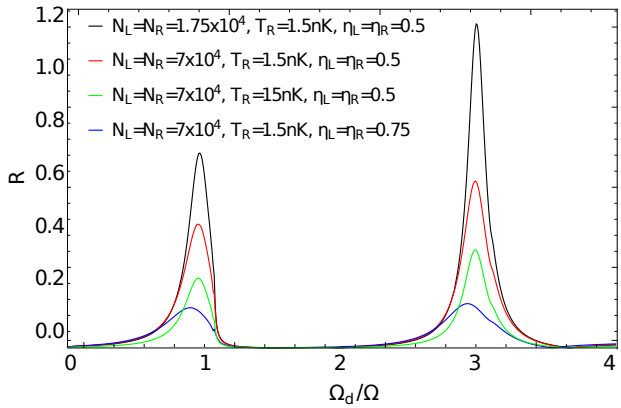

Fig. 8.4 Rectification coefficient against the driving frequency. As predicted analytically, we observe non-zero rectification at the vicinity of frequencies $\Omega_d = \{\Omega, 3\Omega\}$ corresponding to $|\nu_j \pm \nu_i|$. Furthermore, we see that rectification decreases with increasing coupling to the baths in this regime of parameters. See Table 8.2 for the parameters that we use here.

8.5 Summary

Here, we have applied once again the approach of treating impurities in BEC as QBP, and we used these impurities to establish a heat current between two BEC kept at different temperatures. We did so by making use of a dipole-dipole coupling between the two impurities. We also introduced a periodic driving on the trapping frequencies of the impurities, which allowed us to construct a thermal diode. The results were presented in (Charalambous *et al.*, 2019b). The main results of this study are the following:

- We begun with the standard physical Hamiltonian describing two harmonically trapped impurities coupled each one to its respective BEC through a contact in-

teraction. Following the treatment in (Lampo *et al.*, 2018), one can show how these can be treated as two QBP. However, we also introduced a dipole-dipole interaction between the two. We assumed the two impurities to be far enough, namely much farther than the Thomas-Fermi radii of the two BEC so that these can be assumed independent, and can be kept in two different temperatures.

- However we show that the advantage of the aforementioned assumption is two-fold, since it also permits us to approximate the interaction by a spring-like interaction which is bilinear on the variables of the impurities. This maintains the overall Hamiltonian quadratic and as a result the state of the system at any later point Gaussian, and permits us to solve the eom that will be derived.

- We derive the Langevin eom, from the Heisenberg equations, which describe two coupled oscillators, and we solve them through the Laplace transform technique.

- The above setup, is understood to enable a heat current to pass from the hot BEC to the cold one, in the form of phonons, mediated through the vibrations of the impurities. We then proceeded in evaluating the heat current and the current correlations as a function of the various parameters of the system. We find that:

  - The heat current increases as a function of the temperature gradient, but the dependence is linear on the temperature difference, a sign that we are working in the classical regime. As expected when there is no temperature gradient, the heat current is zero.

  - The heat current increases quadratically when we keep the temperature difference constant but increase temperature for both of the baths.

  - Heat current exhibits a non-monotonic behaviour with the coupling constant between the impurities and the bath. In particular, while increasing the coupling appears to increase the current for small values of the coupling constant, beyond a certain value, further increase, which implies also more noise, seems to have a negative effect on the current. In other words, we identify an optimal coupling constant.

  - Heat current is maximized when the trapping frequencies of the two impurities match, i.e. when the frequencies of the phonons emitted and received match.

  - The correlations of the current behave in a rather similar way, with the only difference being that even when the temperature gradient is zero, current fluctuations can still be finite.

- We then introduced a periodic driving on the trapping frequencies of the two im-

purities. By taking advantage of the theoretical results of (Riera-Campeny *et al.*, 2019), we showed how one can obtain a thermal diode in a real physical system. We studied then the ability of this device to unidirectionally direct the heat current as a function of the parameters of the system.

CHAPTER 9

CONCLUSIONS

In this thesis, we presented a number of projects regarding both applications as well as proof of concept ideas related to Bose polarons in 1D BEC. These Bose polarons were treated as quantum Brownian particles as in (Lampo *et al.*, 2017a). The main conclusions of each project are summarized at the end of each one of the relevant Chapters. Here we present a brief review of all of them.

9.1 Two distinguishable impurities in BEC: squeezing and entanglement of two Bose polarons

In this paper, we studied the emergent entanglement between two distinguishable polarons due to their common coupling to a BEC bath. To this end, we formulated the problem of two different kinds of impurities immersed in a BEC as a quantum Brownian motion model. The BEC is assumed to be confined in one dimension and homogeneous. The impurities do not interact among themselves, but only with the BEC. By means of a Bogoliubov transformation we diagonalize the part describing the BEC in the Hamiltonian. This brings the total Hamiltonian into a form in which one can identify the BEC part as a collection of oscillators with different frequencies, thus resembling a bath Hamiltonian. Also, we identify the impurities part of the Hamiltonian as the system Hamiltonian, in the usual terminology from open quantum systems. Finally, under the same physical constraints discussed in (Lampo *et al.*, 2017b) for the Bose polaron problem, we linearise the interaction Hamiltonian, which brings the Hamiltonian into a conventional

Caldeira-Leggett-like Hamiltonian, i.e., a quantum Brownian motion model.

We henceforth solve the associated coupled quantum Langevin equations system of motion, which encode the bath as a damping and a noise kernel. The damping kernel includes a non-diagonal term, often called hydrodynamic term in the context of Brownian particles, as it encodes the effect of the particles on one another. We find that the spectral density characterizing the bath is superohmic in 1D. We emphasize that in our work the properties of the bath, and particularly the spectral density, are not arbitrarily assumed but derived from physical considerations of the BEC. We solve these equations both for the case of untrapped and trapped impurities. We do not add artificial terms to the Hamiltonian as to make it non-negative. Instead we find a condition on the parameters of the system, for which the energy spectrum of the Hamiltonian is positive.

For the untrapped case we were able to solve the equations of motion analytically. Hence, we studied the MSD and the diffusive properties of the impurities, which are found to perform a super diffusive motion. In addition, we studied the momentum variance of the impurities, observing an energy back-flow from the bath, attributed to its non-Markovian nature. Moreover, we obtained the covariance matrix explicitly. By using the covariance matrix, we quantified entanglement between the two types of impurities using the logarithmic negativity. This is found to decrease linearly as a function of time. What is more, the relative distance and center of mass coordinates were considered for the case of identical impurities. The former becomes decoupled from the bath, such that it no more performs a superdiffusive motion, hence the variance of the distance between the impurities stays on average constant. Yet, we can detect a linearly decreasing with time entanglement between the two types of impurities, so we conjecture that the decrease of entanglement is attributed to their interaction with the bath rather than them running away from each other. This conjecture is further enhanced from our studies of the entanglement dependence on the rest of the parameters of the system, i.e. the density of the bosons n_0 in the BEC and their interaction strength g_{B}. In particular, we found that for any fixed finite time, and fixed n_0 (g_0), entanglement reaches a maximum value at some optimal g_0 (n_0). Increasing this value beyond the optimal reduces the entanglement until it vanishes.

For the trapped case, we obtained the covariance matrix elements numerically. We saw that the coherence correlations (off-diagonal terms of the covariance matrix) were linearly increasing with temperature, unless the parameters of the impurities were the same. Nevertheless, entanglement decreases as a function of temperature, which means that these correlations are not quantum. In the case of trapped impurities, entanglement was studied in detail as a function of the rest of the parameters of the system. It was found to decrease with increasing distance between the centers of the two trapping potentials.

Furthermore, entanglement was found to increase and then decrease as a function of both n_0 and g_B. Moreover, entanglement is maximized at resonance of the frequencies of the two trapping potentials as was seen in previous similar studies as well (Correa *et al.*, 2012).

Beyond entanglement, for all of these parameters the dependence of the critical temperature was also studied. In Appendix B.4 a rough estimate of the critical temperature is made, using the effective form of the Hamiltonian in the thermalized regime. The estimate is of the same order of magnitude as the critical temperature observed in our studies. Squeezing was also examined in this case as a function of all the parameters of the system, found to behave qualitatively the same as entanglement. In particular, it is seen that entanglement always appears if there is squeezing but the converse is not always true.

In summary, we have studied the emergence of entanglement of two types of impurities embedded in the same bath, starting from a Hamiltonian justified on physical grounds. We examined analytically the case of two untrapped impurities, and gave numerical results in the scenario of harmonically trapped impurities. The dependence of entanglement, squeezing as well as the critical temperature, i.e. the temperature beyond which entanglement vanishes, were studied as functions of the physical parameters of the system. The parameters of the system used were within current experimental settings and we believe that our results can be experimentally verified. These results on squeezing and entanglement in these setups are particularly interesting as the two phenomena represent resources for quantum information processing.

9.2 Control of anomalous diffusion of a Bose Polaron in a coherently coupled two-component Bose-Einstein condensate

In this work, we studied the diffusive behavior of an impurity immersed in a coherently coupled two-component BEC, that interacts with both of them through contact interactions. We showed how starting from the standard Hamiltonian that would describe such a scenario, one can recast the problem under certain assumptions and conditions into that of a quantum Brownian particle diffusing in a bath composed of the Bogoliubov modes of the two-component BEC. We found that the main difference of this scenario compared to that of the impurity being coupled to a single BEC studied in (Lampo *et al.*, 2017a), is that for the scenario of the impurity being coupled differently to the two BECs, namely coupled attractively to one of them and repulsively to the other but with the same magnitude, results in the impurity being coupled to the spin mode of the coherently coupled two-component BEC. This implies that its dynamics is determined by a qualitatively dif-

ferent spectral density. In particular this new spectral density is gapped and subohmic close to the gap. We demonstrate numerically, that such a spectral density can lead to a transient subdiffusive behavior. Furthermore, we show that this transient effect can be controlled by the magnitude of the Rabi frequency, as well as by the strength with which the impurity couples to the two BECs. These can control the duration of the time for which this subdiffusive behavior appears. A mechanism for inducing a transient controlled subdiffusion in Brownian motion has been also proposed in (Spiechowicz *et al.*, 2016), but with a completely different way for achieving it and most importantly not considering the system from a microscopic perspective. Moreover, we comment that the setup we studied, thanks to the appearance of this gapped subohmic spectral density, could also serve for simulating quantum-optical phenomena, phenomena that could be seen in photonic crystals, with cold atoms, as was proposed also in (Navarrete-Benlloch *et al.*, 2011) for the case of optical lattices. In addition, we note that our studies could be extended to the scenario of having two impurities in the coherently coupled two-component BEC, and study as in (Charalambous *et al.*, 2019a), the effects that the coupling to the spin mode could have on the bath-induced entanglement between the two impurities. Finally, we could also study the effect that this new gapped spectral density could have on the functioning of the impurity as a probe to measure the temperature of the two-component BEC, as in (Mehboudi *et al.*, 2019b).

9.3 Using polarons for sub-nK quantum nondemolition thermometry in a Bose-Einstein condensate

We have shown that impurities immersed in a BEC can be exploited as temperature sensors. The key features of such thermometric scheme are that (i) the temperature is estimated by monitoring the impurity atoms *only*-the BEC itself does not need to be measured destructively, (ii) it can compete with state-of-the-art thermometric techniques in the sub-nK range, and (iii) the underlying analysis does not assume thermalization of the impurity at the temperature of the BEC, but rather takes fully into account the strong correlations built up between probe and sample.

In particular, we considered a cold atomic gas and an impurity both harmonically confined in 1D at different trapping frequencies. Assuming that the impurity remains localised around the minimum of the potential, allowed us to "linearize" the model. We obtained the exact stationary state of the impurity from the corresponding quantum Langevin equation and, using standard tools from quantum estimation theory, we could eventually calculate the minimum possible statistical uncertainty for a temperature measurement. In particular, owing to our analysis being exact, we could verify that the usual assumption

of full thermalization for the impurity at the temperature of the sample overestimates the performance of the scheme for typical parameters in the pK–nK range.

We showed that, with only 100 measurements, the relative error can be kept below 14% for temperatures as low as $200\,nK$. Importantly, we could also show that feasible sub-optimal quadrature measurements—specifically, $\hat{x}^2$—allow for similar performances with limited resources (i.e., datasets of just few hundreds of independent measurements). Interestingly, we found that increasing the probe-sample coupling does not improve the sensitivity of the protocol in the temperature range under study due to the comparatively low typical trapping frequencies (60–$70Hz$).

Even though we illustrate our results with Yb impurities in a cold gas of K atoms, our approach is completely general and could be straightforwardly applied without limitations to other atomic species and temperature ranges. Similar results are also expected in the 2D and 3D cases. In particular, such an extension is straightforward for *homogeneous* BECs, the same position squeezing effects giving rise to the enhanced sensitivity of $\hat{x}^2$ are known to occur (Lampo *et al.*, 2017b); the main difference would be a larger degree of Ohmicity in the spectral density.

In order to bring these promising quantum non-demolition thermometers a step closer to experimental demonstrations, it would be interesting to study how the unavoidable non-linearities could affect our results. Exploring whether the entanglement between two impurities embedded in the BEC—recently studied in (Charalambous *et al.*, 2019a)—can be used to boost thermometric performance also remains an open challenge.

9.4 Heat current control in trapped BEC

In this work, we studied in detail the heat transport control and heat current rectification among two Bose Einstein Condensates (BEC). To this aim, we took an open quantum system approach, and focused on experimentally realistic conditions and parameter regimes. In particular we considered a system composed of two harmonically trapped interacting impurities immersed in two independent harmonically trapped 1D BECs kept at different temperatures. The impurities interact through a long range interaction, in particular a dipole-dipole coupling—that under suitable conditions we were able to treat as a spring-like interaction. In this work we considered the particular case of a fixed angle, motivated by the results in (Tang *et al.*, 2018), but the results should also hold under an angle-averaged scenario, by taking advantage of the results in (Keesom, 1921). We showed the dynamics of these impurities can be described within the framework of quantum Brownian motion, where the excitation modes of the gas play the role of the bath. In this analogy, the spectral density of the bath is not postulated, but it is rather derived

exactly from the Hamiltonian of the BEC, which turns out to be superohmic. By solving the relevant generalized Langevin equations, we find the steady state covariance matrix of the impurities, which contains all the information describing our Gaussian system. In particular, we use such information to study the heat currents and current-current correlations and their dependence on the controllable parameters of the system. We find that, the heat current scales linearly with temperature difference among the two BECs. Furthermore, we observe that heat current is maximum when the trapping frequencies of the impurities are at resonance. Finally, we showed the existence of an *optimal* coupling strength of the impurities on their respective baths.

What is more, by periodically driving one of the impurities, we can conduct heat asymmetrically, i.e., we achieve heat rectification—which is in full agreement with the recent proposal of (Riera-Campeny *et al.*, 2019). In particular, we see that one can achieve heat rectification at the driving frequencies predicted in (Renklioglu *et al.*, 2016), even though our bath is superohmic.

Motivated by recent developments on the usage of BECs as platforms for quantum information processing, as e.g. in (Charalambous *et al.*, 2019a), our work offers an alternative possibility to use this versatile setting for information transfer and processing, within the context of phononics. The possibility of quantum advantages using many-body impurities in our platform remains an interesting open question (see (Jaramillo *et al.*, 2016) too). Another future direction is to study heat control in 2D and 3D BECs. In principle this gives rise to a different spectral density, which opens a new window for further manipulation of heat current. Finally, it is desirable to investigate scenarios where the system is nonlinear, which raises difficulties in solving the problem analytically, nonetheless, it offers the opportunity to rectify heat even without periodic derivation. Moreover, motivated by the results in (Mehboudi *et al.*, 2019a,d) where the squeezing in position of a single impurity embedded in a BEC was used to measure the temperature of the BEC in the sub-nano-Kelvin regime, one may study if the present two-particle set-up can be used for applications in quantum thermometry.

Appendices

APPENDIX A

CHAPTER 3

A.1 Mathematical tools

A.1.1 Linear Response function

The goal of response theory is to figure out how a system reacts to outside time-dependent influences, e.g. applied electric and magnetic fields, or applied pressure, or an applied driving force. The main assumption in linear response theory is that the source is a small perturbation of the original system, such that the Hamiltonian reads as

$$H \to H + \delta H(t) = H + \sum_j \phi_j(t') O_j(t) \tag{A.1}$$

where $\mathcal{O}_i(t)$ is a set of observables of the system, $\phi_j(t')$ are some source fields of the perturbing forces. This has as a consequence that the change in the expectation value of any operator is linear in the perturbing source

$$\delta \langle \mathcal{O}_i(t) \rangle = \int dt' \chi_{ij}(t,t') \phi_j(t') \tag{A.2}$$

where $\chi_{ij}(t,t')$ is known as the response function, given by the Kubo formula.

Kubo formula The response function, within linear response theory, can be expressed in terms of the observables of the system. This is the main result of linear response theory

first derived by Kubo Kubo (1966). To obtain this result, we first need to consider the time evolved state of the system

$$\rho(t) = U(t)\,\rho(0)\,U^{\dagger}(t) \tag{A.3}$$

Then by taking the expectation value of some operator of the system $\langle \mathcal{O}_i(t) \rangle$ in the presence of a set of source field $\{\phi_j(t')\}_j$, and only considering terms up to first order in perturbation theory, one obtains that

$$\begin{aligned} \delta \langle \mathcal{O}_i(t) \rangle &= \langle \mathcal{O}_i(t) \rangle_{\phi} - \langle \mathcal{O}_i(t) \rangle_{\phi=0} \\ &= i \int_{-\infty}^{t} dt' \langle [\mathcal{O}_i(t), \mathcal{O}_j(t')] \rangle \phi_j(t') \\ &= i \int_{-\infty}^{\infty} dt' \Theta(t-t') \langle [\mathcal{O}_i(t), \mathcal{O}_j(t')] \rangle \phi_j(t') \end{aligned} \tag{A.4}$$

such that

$$\chi_{ji}(t,t') = i\Theta(t-t') \langle [\mathcal{O}_i(t), \mathcal{O}_j(t')] \rangle, \tag{A.5}$$

where we have used the step function to extend the range of the time integration to $+\infty$.

The response function In our work, we'll assume that the systems we will treat are invariant under time translations. In this case, we have $\chi_{ij}(t,t') = \chi_{ij}(t-t')$ and it is also useful to perform a Fourier transform to work in frequency space. Taking the Fourier transform of Eq. (A.2) gives

$$\delta \langle \mathcal{O}_i(\omega) \rangle = \chi_{ij}(\omega)\,\phi_j(\omega) \tag{A.6}$$

Hence we learn that the response is "local" in frequency space: if you shake something at frequency ω, it responds at frequency ω. Anything beyond this lies within the domain of nonlinear response.

If we work with a real source ϕ and a Hermitian operator $\mathcal{O}$ (which means a real expectation value $\langle \mathcal{O} \rangle$ then $\chi(t)$ must also be real. Let's see what this means for the Fourier transform $\chi(\omega)$. It's useful to introduce some new notation for the real and imaginary parts, $\chi(\omega) = Re[\chi(\omega)] + iIm[\chi(\omega)] \equiv \chi\prime(\omega) + i\chi\prime\prime(\omega)$.

- Imaginary Part: We can write the imaginary piece as

$$\begin{aligned} \chi''(\omega) &= -\tfrac{i}{2}[\chi(\omega) - \chi^{\dagger}(\omega)] \\ &= -\tfrac{i}{2} \int_0^{\infty} dt \chi(t) [e^{i\omega t} - e^{-i\omega t}] \\ &= -\tfrac{i}{2} \int_0^{\infty} dt e^{i\omega t} [\chi(t) - \chi(-t)] \end{aligned} \tag{A.7}$$

We see that the imaginary part of $\chi(\omega)$ is due to the part of the response function that is not invariant under time reversal $t \to -t$. In other words, $\chi''(\omega)$ knows about the arrow of time. Since microscopic systems are typically invariant under time reversal, the imaginary part $\chi''(\omega)$ must be arising due to dissipative processes. $\chi''(\omega)$ is called the dissipative or absorptive part of the response function. It is also known as the spectral function. It will turn out to contain information about the density of states in the system that take part in absorptive processes. Finally, notice that $\chi''(\omega)$ is an odd function, $\chi''(-\omega) = -\chi''(\omega)$.

- Real Part: The same analysis as above shows that

$$\chi^{''}(\omega) = \frac{1}{2}\int_0^\infty dt e^{i\omega t}[\chi(t) + \chi(-t)]. \tag{A.8}$$

The real part does not care about the arrow of time. It is called the reactive part of the response function. It is an even function, $\chi'(-\omega) = +\chi'(\omega)$.

Causality This statement of causality means that any response function must satisfy $\chi(t) = 0$ for all $t < 0$ For this reason, χ is often referred to as the causal Green's function or retarded Green's function for the susceptibility χ is related to the propagator/ Green function from the solution of the QGLE in Eq. (3.48). Let's see what this simple causality requirement means for the Fourier expansion of χ. When $t < 0$, we can perform the integral of the Fourier transform by completing the contour in the upper-half place (so that the exponent becomes $-i\omega(-i|t|) \to -\infty$). The answer has to be zero. Of course, the integral is given by the sum of the residues inside the contour. So if we want the response function to vanish for all $t < 0$, it must be that $\chi(\omega)$ has no poles in the upper-half plane. In other words, causality requires: $\chi(\omega)$ is analytic for $Im[\omega] > 0$.

Kramers-Kronig relation The fact that χ is analytic in the upper-half plane means that there is a relationship between the real and imaginary parts, χ' and χ''. This is called the Kramers-Kronig relation.

First define a new function $f(\omega)$ by the integral,

$$f(\omega) = \frac{1}{i\pi}\int_a^b \frac{\rho(\omega')}{\omega' - \omega} d\omega' \tag{A.9}$$

where $\rho(\omega')$ is a meromorphic function, which we will later identify as our linear response function from above, i.e. the susceptibility. To avoid the singularity $\omega' = \omega$, we can simply deform the contour of the integral into the complex plane, either running just above the singularity along $\omega' + i\epsilon$ or just below the singularity along $\omega' - i\epsilon$. The difference between

the two answers is given by Cauchy's residue theorem,

$$\frac{1}{2}\left[f(\omega+i\epsilon)-f(\omega-i\epsilon)\right]=\rho\left(\epsilon\right). \tag{A.10}$$

We can also define the average of the two functions either side of the discontinuity. This is usually called the principal value, and is denoted by adding the symbol $\mathcal{P}$ before the integral,

$$\frac{1}{2}\left[f(\omega+i\epsilon)+f(\omega-i\epsilon)\right]=\frac{1}{i\pi}\mathcal{P}\int_a^b\frac{\rho\left(\omega'\right)}{\omega'-\omega}d\omega'. \tag{A.11}$$

For a more intuitive explanation of the principal value look in King (2009). In our case, we'll be interested in the particular case of the integral being a complex plane integral over the susceptibility

$$\widehat{f}\left(\omega\right)=\frac{1}{i\pi}\oint_C\frac{\chi\left(\omega'\right)}{\omega'-\omega}d\omega'\ \omega\in\mathbf{R} \tag{A.12}$$

where the contour C skims just above the real axis, before closing at infinity in the upper-half plane. We'll need to make one additional assumption: that $\chi(\omega)$ falls off faster than $1/|\omega|$ at infinity. From the above discussion, we know that $\widehat{f}\left(\omega\right)=f(\omega-i\epsilon)$ with $\rho\to\chi$, such that by applying Eq. (A.10) and Eq. (A.11) we have

$$\widehat{f}\left(\omega\right)=f(\omega-i\epsilon)=\frac{1}{i\pi}\left[\mathcal{P}\int_{-\infty}^{\infty}\frac{\chi\left(\omega'\right)}{\omega'-\omega}d\omega'\right]-\chi\left(\omega\right). \tag{A.13}$$

But we know the integral in Eq. (A.12) has to be zero since $\chi(\omega)$ has no poles in the upper-half plane. This means that $f(\omega-i\epsilon)=0$, which leads to

$$\begin{array}{l} Re\left[\chi\left(\omega\right)\right]=\frac{1}{\pi}\mathcal{P}\int_{-\infty}^{\infty}\frac{Im[\chi(\omega')]}{\omega'-\omega}d\omega' \\ Im\left[\chi\left(\omega\right)\right]=\frac{1}{\pi}\mathcal{P}\int_{-\infty}^{\infty}\frac{Re[\chi(\omega')]}{\omega'-\omega}d\omega' \end{array} \tag{A.14}$$

These are the Kramers-Kronig relations.

Relation of the response function to the Green function The fluctuation-dissipation theorem holds for a general system in thermal equilibrium and for any Heisenberg picture observable. We focus here on the coordinate $x(t)$ of a Brownian particle in a harmonic potential. Since the commutator $[x(t),x(0)]$ is a c-number we can immediately determine the response function with the help of the exact solution of the Heisenberg equation of motion,

$$\chi\left(t\right)=\frac{i}{\hbar}\Theta\left(t\right)\left[x(t),x(0)\right]=\frac{i}{\hbar}\Theta\left(t\right)G_2\left(t\right)\left[\dot{x}(0),x(0)\right]=\frac{i}{\hbar}\Theta\left(t\right)G_2\left(t\right) \tag{A.15}$$

where $\Theta(t)$, the Heaviside theta function is introduced to guarantee that there is no influence in the motion from times before the initial time $t = 0$. Alternatively the above equivalency can be obtained by observing that adding the perturbation $-xF(t)$ to the total Hamiltonian of the system amounts to replacing $B(t)$ by $B(t)+F(t)$ in the equation of motion, Eq. (3.33). This replacement yields the additional term, $\int_0^t dsG_2(t-s)F(s)/m$ on the right-hand side of Eq. (3.48), which shows that the response function is in fact related to the fundamental solution $G_2(t)$. Expressing the Fourier transform of the response function in terms of its Laplace transform we therefore obtain

$$\chi(\omega) = \frac{1}{m}\int_0^\infty dte^{i\omega t}G_2(t) = \frac{1}{m}\widehat{G}_2(-i\omega) \tag{A.16}$$

A.1.2 Continuum limit of spectral density

In our work, we will assume that the environment of harmonic oscillators is so big that we can safely assume a continuous distribution of harmonic oscillator frequencies in the frequency domain, such that

$$\sum_k \to \int \frac{V}{(2\pi)^d}d^dk \tag{A.17}$$

with d the dimension of the bath and V the finite volume within which the Brownian motion takes place.

Then we make use of the following relation regarding the composition of a smooth function $g(x)$ with the delta function

$$\int_{\mathbf{R}} \delta(g(k))f(g(k))\left|\frac{\partial g(k)}{\partial k}\right|dk = \int_{g(\mathbf{R})}\delta(u)f(u)du \tag{A.18}$$

where it is assumed that f is a compactly supported test function, and that $g(x)$ is a continuously differentiable function with $\partial g(x)/\partial x$ nowhere 0. If g is nowhere 0 then $\delta(g(x)) = 0$, but if $g(x)$ has a real root at x_0 then it should hold that

$$\delta(g(k)) = \frac{\delta(k-k_0)}{\left|\frac{\partial g(k)}{\partial k}\right|_{k=k_0}} \tag{A.19}$$

In our case, where we are trying to evaluate the integral in Eq. (3.25), we will consider f as the function $Y(k) = \frac{\pi(c(k))^2}{2m\omega(k)}$ in the continuum limit of modes k, where for the sake of simplicity we assumed all the bosons of the bath to have the same mass m, and the delta function reads as $\delta(\omega-\omega(k))$ in the continuum limit. Hence in this case $g(k) \equiv \omega-\omega(k)$, i.e. is related to the dispersion relation of the energy spectrum of the bath. Note also

that we are only allowed to use this relation once we introduce the cutoff, since if not, the function f is not compactly supported. So the relation in Eq. (A.19) reads as

$$\delta\left(\omega-\omega\left(k\right)\right)=\frac{\delta\left(k-k\left(\omega\right)\right)}{\left|\frac{\partial\omega(k)}{\partial k}\mid_{k=k(\omega)}\right|} \tag{A.20}$$

where $k\left(\omega\right)$ is the inverse of the dispersion relation $\omega\left(k\right)$.

The last thing we need to have in mind in order to evaluate the integral in Eq. (3.25) is that an integral in d-dimensions can be rewritten in d-dimensional hyperspherical coordinates as

$$\int d^{d}k\rightarrow S_{d}\int dkk^{d-1} \tag{A.21}$$

where S_d is the surface area of a unit d-sphere in the momentum space. Hence finally, the relation for the spectral density is given by

$$J\left(\omega\right)=\frac{V}{\left(2\pi\right)^{d}}S_{d}\int dkk^{d-1}Y\left(k\right)\frac{\delta\left(k-k\left(\omega\right)\right)}{\left|\frac{\partial\omega(k)}{\partial k}\mid_{k=k(\omega)}\right|} \tag{A.22}$$

We will only focus on the 1D case where $S_1 = 1$.

A.1.3 Fluctuation dissipation theorem

The Quantum Fluctuation-Dissipation Theorem (QFDT) is an essential characteristic of quantum equilibrium states. It has been recognized since a long time that the QFDT is the key requirement for a stationary state being a quantum equilibrium state, in order to be consistent with the second fundamental theorem of quantum thermodynamics (Ford, 2017, Hanggi *et al.*, 2005). Indeed, recently, the conditions for which QFDT holds have been identified in (Aron *et al.*, 2018, Sieberer *et al.*, 2015). Moving away from the quantum equilibrium state will break this symmetry and the QFDT will cease to be valid. Therefore, the confirmation of the QFDT serves to distinguish quantum equilibrium states from any other type of stationary state.

The intuition behind the existence of such a theorem is the following. We have seen above that the imaginary part of the response function governs the dissipation in a system. Yet, the Kubo formula Eq. (A.5) tells us that the response formula can be written in terms of a two-point correlation function in the quantum theory. And we know that such two-point functions provide a measure of the variance, or fluctuations, in the system. This is the essence of the fluctuation-dissipation theorem which we'll now make more precise.

Let us give a brief derivation of QFDT in order to get a better grasp of the theorem.

For this, it is convenient to define the simplest possible two point correlation function

$$S_{ij}(t) := \langle \mathcal{O}_i(t)\,\mathcal{O}_j(0)\rangle \tag{A.23}$$

where we have used time translational invariance to set the time at which O_j is evaluated to zero. Then, we know from Eq. (A.7) that

$$\begin{gathered}\chi''_{ij}(t) = -\tfrac{i}{2}\left[\chi_{ij}(t) - \chi_{ji}(-t)\right] \\ = -\tfrac{1}{2}\Theta(t)\left[\langle \mathcal{O}_i(t)\,\mathcal{O}_j(0)\rangle - \langle \mathcal{O}_j(0)\,\mathcal{O}_i(t)\rangle\right] + \tfrac{1}{2}\Theta(-t)\left[\langle \mathcal{O}_j(-t)\,\mathcal{O}_i(0)\rangle - \langle \mathcal{O}_i(0)\,\mathcal{O}_j(-t)\rangle\right] \\ = \tfrac{1}{2}\left(\langle \mathcal{O}_j(-t)\,\mathcal{O}_i(0)\rangle - \langle \mathcal{O}_i(t)\,\mathcal{O}_j(0)\rangle\right)\end{gathered} \tag{A.24}$$

where in the second line we made use of the Kubo formula Eq. (A.5), and in the third line we applied time translation invariance. We are now going to re-order the operators in the first term of the last line. To do this, we need to be sitting in the canonical ensemble, so that the expectation value is computed with respect to the Boltzmann density matrix. We then have

$$\begin{gathered}\langle \mathcal{O}_j(-t)\,\mathcal{O}_i(0)\rangle = Tr\left[e^{-\beta H}\mathcal{O}_j(-t)\,\mathcal{O}_i(0)\right] \\ = Tr\left[e^{-\beta H}\mathcal{O}_j(-t)\,e^{\beta H}e^{-\beta H}\mathcal{O}_i(0)\right] \\ = Tr\left[e^{-\beta H}\mathcal{O}_i(0)\,\mathcal{O}_j(-t+i\beta)\right] \\ = \langle \mathcal{O}_i(0)\,\mathcal{O}_j(-t+i\beta)\rangle\end{gathered} \tag{A.25}$$

where we have treated the density matrix $e^{-\beta H}$ as a time evolution operator, but one which evolves the operator in the imaginary time direction. Then by taking the Fourier transform of $\chi''_{ij}(t)$ we get

$$\chi''_{ij}(\omega) = -\frac{1}{2}\left[1 - e^{-\beta\omega}\right]S_{ij}(\omega) = -\frac{1}{2}\left[1 + n_B(\omega)\right]S_{ij}(\omega) = \left(\coth(\beta\omega)\right)^{-1}S_{ij}(\omega) \tag{A.26}$$

where $n_B(\omega) = \left(e^{\beta\omega} - 1\right)^{-1}$ is the Bose-Einstein distribution function. This is the fluctuation-dissipation theorem, relating the fluctuations in frequency space, captured by $S(\omega)$, to the dissipation, captured by $\chi''(\omega)$. Indeed, a similar relationship holds already in classical physics; the most famous example is the Einstein relation that we saw in the previous chapter. To see this one needs to consider the limit $\beta\omega \ll 1$ where $n(\omega) \approx k_B T/\omega$, and also assume an ohmic spectral density. Finally, we notice that $S_{ij}(\omega) = S_{ij}(-\omega)$, such that its Fourier transform reads as

$$S_{ij}(t) = \int_{-\infty}^{\infty}\frac{d\omega}{2\pi}\hbar\cos(\omega t)\,S_{ij}(\omega)\,. \tag{A.27}$$

Fluctuation-dissipation relation for QBM First, we compute $\frac{1}{2}\langle\{B(\omega), B(\omega')\}\rangle = Re\langle B(\omega) B(\omega')\rangle$ from Eq. (3.24), where $B(\omega)$ is the Fourier transform of $B(t)$. Taking into account that

$$\begin{aligned}\langle x_k(0) x_{k'}(0)\rangle &= \delta_{kk'}(2m_k\omega_k)^{-1}[1+2n_k],\\ \langle p_k(0) p_{k'}(0)\rangle &= \delta_{kk'}m_k\omega_k[1+2n_k]/2,\\ \langle x_k(0) p_{k'}(0)\rangle &= \langle p_{k'}(0) x_k(0)\rangle^* = i\delta_{kk'}/2,\end{aligned}$$

where $n_k = (\coth(\omega_k/2T)-1)/2$ one has

$$\begin{aligned}\frac{1}{2}\langle\{B(t), B(t')\}\rangle &= \frac{1}{\pi}\sum_k \frac{\pi c_k^2}{2m_k\omega_k}[1+2n_k][\cos(\omega_k t)\cos(\omega_k t') + \sin(\omega_k t)\sin(\omega_k t')]\\ &= \frac{1}{\pi}\int_0^\infty d\omega J(\omega)\coth(\omega/2T)\cos(\omega(t-t'))\end{aligned} \tag{A.28}$$

Taking the Fourier transform of both sides

$$\begin{aligned}&\frac{1}{2}\langle\{B(\omega), B(\omega')\}\rangle = 2\pi\int_{-\infty}^\infty\frac{dt}{2\pi}e^{i\omega t}\int_{-\infty}^\infty\frac{dt'}{2\pi}e^{i\omega' t'}\int_0^\infty d\omega'' J(\omega'')\coth\left(\frac{\omega''}{2T}\right)\left(e^{i\omega''(t-t')}+e^{-i\omega''(t-t')}\right)\\ &= 2\pi\int_{-\infty}^\infty\frac{dt}{2\pi}\int_{-\infty}^\infty\frac{dt'}{2\pi}\int_0^\infty d\omega'' J(\omega'')\coth\left(\frac{\omega''}{2T}\right)\left(e^{it(\omega''+\omega)}e^{it'(\omega'-\omega'')} + e^{it(\omega-\omega'')}e^{it'(\omega'+\omega'')}\right)\\ &= 2\pi\int_0^\infty d\omega'' J(\omega'')\coth\left(\frac{\omega''}{2T}\right)[\delta(\omega''+\omega)\delta(\omega'-\omega'') + \delta(\omega-\omega'')\delta(\omega'+\omega'')]\\ &= 2\pi\delta(\omega+\omega')\coth\left(\frac{\omega}{2T}\right)[J(\omega)\Theta(\omega) - J(-\omega)\Theta(-\omega)]\end{aligned} \tag{A.29}$$

where we have used the identity $\int_{-\infty}^\infty dt e^{i\omega t} = 2\pi\delta(\omega)$. It is also possible to show that

$$\begin{aligned}Im[\chi(\omega)] &= Im\textstyle\sum_k \frac{c_k^2}{m_k\omega_k}\int_{-\infty}^\infty dt e^{i\omega t}\Theta(t)\sin\omega_k t\\ &= -\tfrac{1}{4}\textstyle\sum_k \frac{c_k^2}{m_k\omega_k}\int_0^\infty dt\left[e^{i(\omega+\omega_k)t} - e^{i(\omega-\omega_k)t} - e^{i(-\omega+\omega_k)t} + e^{-i(\omega+\omega_k)t}\right]\\ &= -\tfrac{1}{4}\textstyle\sum_k \frac{c_k^2}{m_k\omega_k}\left(\int_{-\infty}^\infty dt e^{i(\omega+\omega_k)t} - \int_{-\infty}^\infty dt e^{i(\omega-\omega_k)t}\right)\\ &= \tfrac{\pi}{2}\textstyle\sum_k \frac{c_k^2}{m_k\omega_k}(\delta(\omega-\omega_k) - \delta(\omega+\omega_k))\\ &= \textstyle\int_0^\infty d\omega' J(\omega')[\delta(\omega-\omega') - \delta(\omega+\omega')]\\ &= J(\omega)\Theta(\omega) - J(-\omega)\Theta(-\omega)\end{aligned} \tag{A.30}$$

which proves relation in Eq. (3.28).

APPENDIX B

CHAPTER 5

B.1 Spectral density

In this appendix we briefly present the derivation of the spectral density for a continuous spectrum of Bogoliubov modes, given in Eq. (5.51), following the work in (Lampo *et al.*, 2017b). In particular, the sum in Eq. (5.42) is turned into the integral

$$\sum_{k\neq 0} \to \int \frac{V}{(2\pi)^d} d^d k,$$

and using the relation

$$\delta\left(\omega - \omega_k\right) = \frac{1}{\partial_{\mathbf{k}}\omega_{\mathbf{k}}\mid_{\mathbf{k}=\mathbf{k}_\omega}} \delta\left(\mathbf{k} - \mathbf{k}_\omega\right),$$

we obtain

$$J_{jq}\left(\omega\right) = \frac{n_0 g_{\mathrm{IB}}^{(j)} g_{\mathrm{IB}}^{(q)} S_d}{\hbar\left(2\pi\right)^d} \int d\mathbf{k}\, \mathbf{k}^{d+1} \sqrt{\frac{\left(\xi\mathbf{k}\right)^2}{\left(\xi\mathbf{k}\right)^2 + 2}} \frac{\cos\left(\mathbf{k}R_{12}\right)}{\partial_{\mathbf{k}}\omega_{\mathbf{k}}\mid_{\mathbf{k}=\mathbf{k}_\omega}} \delta\left(\mathbf{k} - \mathbf{k}_\omega\right).$$

For a 1D environment $S_1 = 2$, so that the continuous form of the spectral density (5.51) is obtained.

B.2 Susceptibility

Here we evaluate the form of the susceptibility for the spectral density, given in Eq. (5.53). The imaginary part of the susceptibility is simply given by

$$Im\left[\lambda_{jq}\left(\omega\right)\right] = -\hbar\left(\Theta\left(\omega\right) - \Theta\left(-\omega\right)\right) J_{jq}\left(\omega\right),$$

while the real part is given by

$$\begin{aligned}
Re\left[\lambda_{jq}\left(\omega'\right)\right] &= \mathcal{H}\left[Im\left[\lambda_{jq}\left(\omega\right)\right]\right]\left(\omega'\right) \\
&= \frac{1}{\pi}P\int_{-\infty}^{\infty}\frac{Im\left[\lambda_{jq}\left(\omega\right)\right]}{\omega-\omega'}d\omega \\
&= -\frac{\hbar}{\pi}P\int_{-\infty}^{\infty}\frac{\left(\Theta\left(\omega\right)-\Theta\left(-\omega\right)\right)J_{jq}\left(\omega\right)}{\omega-\omega'}d\omega \\
&= -\frac{\hbar\widetilde{\tau}_{jq}}{\pi}P\int_{-\infty}^{\infty}\frac{\left(\Theta\left(\omega\right)-\Theta\left(-\omega\right)\right)\omega^3\cos\left(\frac{\omega}{c}R_{jq}\right)e^{-\frac{\omega}{\Lambda}}}{\omega-\omega'}d\omega \\
&= -\frac{\hbar\widetilde{\tau}_{jq}}{\pi}P\int_{0}^{\infty}\omega^3\cos\left(\frac{\omega}{c}R_{jq}\right)\left(\frac{1}{\omega-\omega'}+\frac{1}{\omega+\omega'}\right)d\omega,
\end{aligned}$$

where $\mathcal{H}$ represents the Hilbert transform, Θ is the Heaviside step function and P is the principal number. We first find

$$P\int_{0}^{\infty}\omega^3\frac{e^{-\frac{\omega}{\Lambda}}\cos\left(\frac{\omega}{c}R_{jq}\right)}{\omega-\omega'}d\omega,$$

as we can evaluate it with the property of the Hilbert transform

$$\mathcal{H}\left[\omega f\left(\omega\right)\right] = \omega\mathcal{H}\left[f\left(\omega\right)\right] + \frac{1}{\pi}\int_{-\infty}^{\infty}f\left(\omega\right)d\omega.$$

We apply this property three times to obtain

$$\begin{aligned}
P\int_{0}^{\infty}\omega^3\frac{e^{-\frac{\omega}{\Lambda}}\cos\left(\frac{\omega}{c}R_{jq}\right)}{\omega-\omega'}d\omega = \omega'^3P\int_{0}^{\infty}\frac{e^{-\frac{\omega}{\Lambda}}\cos\left(\frac{\omega}{c}R_{jq}\right)}{\omega-\omega'}d\omega + \omega'^2\frac{\Lambda}{1+\left(\Lambda\frac{R_{jq}}{c}\right)^2} \\
+\omega'\frac{\frac{1}{\Lambda^2}-\frac{R_{jq}^2}{c^2}}{\left(\frac{1}{\Lambda^2}+\frac{R_{jq}^2}{c^2}\right)^2}+2\frac{\left(\frac{1}{\Lambda^3}-3\frac{R_{jq}^2}{\Lambda c^2}\right)}{\left(\frac{1}{\Lambda^2}+\frac{R_{jq}^2}{c^2}\right)^3}.
\end{aligned} \tag{B.1}$$

We can then also show that:

$$P\int_{0}^{\infty}\frac{e^{-\frac{\omega}{\Lambda}+i\frac{\omega}{c}R_{jq}}}{\omega-\omega'}d\omega = \begin{cases} e^{-\frac{\omega'}{\Lambda}+i\frac{\omega'}{c}R_{jq}}\left(\Gamma\left[0,-\frac{\omega'}{\Lambda}+i\frac{\omega'}{c}R_{jq}\right]+i\pi\right) \\ e^{-\frac{\omega'}{\Lambda}+i\frac{\omega'}{c}R_{jq}}\Gamma\left[0,-\frac{\omega'}{\Lambda}+i\frac{\omega'}{c}R_{jq}\right] \end{cases},$$

where the top case corresponds to $\omega' \in (0,\infty)$ and the bottom to the complementary interval $\omega' \in (-\infty,0)$. Here $\Gamma\left[\alpha,z\right] = \int_z^\infty t^{\alpha-1}e^{-t}dt$ denotes the upper incomplete gamma function. After introducing (B.2) in the expression for the real part of the susceptibility

above, we obtain that

$$
\begin{aligned}
&Re\left[\lambda_{jq}\left(\omega'\right)\right] = \\
&-\frac{\hbar\widetilde{\tau}_{jq}}{\pi}\Bigg\{\omega'^{3}\mathrm{Re}\left[g\left(\omega'\right)-g\left(-\omega'\right)\right]+\pi\omega'^{3}Im\left[\Theta\left(\omega'\right)e^{-\frac{\omega'}{\Lambda}+i\frac{\omega'}{c}R_{jq}}+\left(\omega'\to-\omega'\right)\right] \\
&+2\omega'^{2}\frac{\Lambda}{1+\left(\Lambda\frac{R_{jq}}{c}\right)^{2}}+4\frac{\left(\frac{1}{\Lambda^{3}}-3\frac{R_{jq}^{2}}{\Lambda c^{2}}\right)}{\left(\frac{1}{\Lambda^{2}}+\frac{R_{jq}^{2}}{c^{2}}\right)^{3}}\Bigg\}
\end{aligned}
\tag{B.2}
$$

where $\left(\omega'\to-\omega'\right)$ stands for $\Theta\left(-\omega'\right)e^{\frac{\omega'}{\Lambda}-i\frac{\omega'}{c}R_{jq}}$ and

$$
g\left(\omega'\right)=e^{-\frac{\omega'}{\Lambda}+i\frac{\omega'}{c}R_{jq}}\Gamma\left[0,-\frac{\omega'}{\Lambda}+i\frac{\omega'}{c}R_{jq}\right].
$$

With this, the susceptibility takes the form in Eq. (5.73).

B.3 Study of an exact expression for the covariance matrix elements

In the particular case of $R_{12}=0$, it can be shown that the integral in Eq. (5.59) takes the following form:

$$
\int_{-\infty}^{+\infty}\frac{g_6(\omega)}{h_6(\omega)h_6(-\omega)}d\omega, \tag{B.3}
$$

where $h_6\left(\omega\right)$ is a 6th order polynomial, and $g_6(\omega)$ is a 7th order polynomial. An integral of this form was also obtained in (Correa *et al.*, 2012), for an ohmic spectral density. The criterion to use this formula, is that the roots of $h_6\left(\omega\right)$ lie in the upper half plane. Finding the roots of this polynomial requires finding expressions for 12 variables, 6 real and 6 imaginary. In our case one can show that the polynomial $h_6\left(\omega\right)$ can be written as

$$
h_6\left(\omega\right)=\sum_{j=0}^{6}A_j\left(2\pi i\omega\right)^{6-j}, \tag{B.4}
$$

with the coefficients A_j being all real, which implies that the roots of $h_6\left(\omega\right)$ are symmetrically located about the imaginary axis. This reduces the problem in finding just 6 variables, 3 real and 3 imaginary. Furthermore, by making use of the Vieta relations, one can show that

$$
\frac{Im[z_1]}{|z_1|^2}+\frac{Im[z_2]}{|z_2|^2}+\frac{Im[z_3]}{|z_3|^2}=0. \tag{B.5}
$$

This implies that not all roots of the polynomial can lie in the upper half plane. The reason for this can be traced back to the fact that there is no linear term in the polynomial $h_6\left(\omega\right)$,

which is an artifact of considering a super-ohmic spectral density as can be understood by comparing to the case in (Correa *et al.*, 2012). The issue of not all roots being in the upper half plane, can be resolved in the following way. The roots of $h_6(\omega)$ that are in the lower half plane, have mirrored roots in the upper half plane in the polynomial $h_6(-\omega)$. If the expressions for the roots could be derived, one could simply redefine polynomials $h_6(\omega)$ and $h_6(-\omega)$ to $\tilde{h}_6(\omega)$ and $\tilde{h}_6(-\omega)$ such that all the roots of $\tilde{h}_6(\omega)$ would lie in the upper half plane and all the roots of $\tilde{h}_6(-\omega)$ would lie in the lower half plane. However for a 6th order polynomial of the form we have, one can not find the roots. So this could perhaps only be applied in an algorithmic way, where one first selects a set of parameters and then makes the redefinition of the polynomials once the roots are found.

B.4 Equilibrium Hamiltonian

Here we discuss the thermalization properties of the system. We will use the fact that the two kinds of impurities are formally analogous to two oscillators. The bath dependent part of the Hamiltonian (5.18) is

$$\tilde{U}\left(x_1, x_2, \left\{b_k^\dagger, b_k\right\}_{k\neq 0}\right) = i\sum_{\substack{j=1\\k\neq 0}}^{2} \hbar g_k^{(j)}\left(e^{ikd_j}b_k - e^{-ikd_j}b_k^\dagger\right)x_j + \sum_{k\neq 0} E_k b_k^\dagger b_k.$$

For the system to thermalize, there should be no memory effects induced on the oscillator due to its coupling with the thermal bath. This means that the Hamiltonian will have to be independent of the bath variables $\{b_k^\dagger, b_k\}_{k\neq 0}$ evolution, i.e. $\forall k \neq 0$ the following should be fulfilled

$$\frac{\partial\tilde{U}\left(x_1, x_2, \left\{b_k^\dagger, b_k\right\}_{k\neq 0}\right)}{\partial b_k} = \frac{\partial\tilde{U}\left(x_1, x_2, \left\{b_k^\dagger, b_k\right\}_{k\neq 0}\right)}{\partial b_k^\dagger} = 0.$$

This results in the following conditions

$$b_k(t) = \frac{i\hbar}{E_k}\sum_{j=1}^{2} g_k^{(j)} e^{-ikd_j} x_j(t), \tag{B.6}$$

$$b_k^\dagger(t) = -\frac{i\hbar}{E_k}\sum_{j=1}^{2} g_k^{(j)} e^{ikd_j} x_j(t). \tag{B.7}$$

Replacing these expressions, for the bath degrees of freedom operators, in the initial Hamiltonian (5.18), it becomes:

$$H_{\mathrm{Lin}} = \sum_{j=1}^{2}\left[\frac{p_j^2}{2m_j} + \frac{1}{2}m_j\Omega_j^2\left(x_j + d_j\right)^2\right] + W\left(d_1, d_2\right)\left(x_1 + x_2\right)$$
$$- 2\hbar^2 \sum_{\substack{q,j=1 \\ k\neq 0}}^{2} \frac{1}{E_k} g_k^{(q)} g_k^{(j)} \cos\left(d_j - d_q\right) x_j x_q.$$

This can be rewritten as

$$H_{\mathrm{Lin}} = \sum_{j=1}^{2}\left[\frac{p_j^2}{2m_j} + \frac{1}{2}m_j\left(\Omega_j^2 - \widetilde{\Omega}_j^2\right)x_j^2\right] - 2Kx_1x_2 + \widehat{W}\left(d_1, d_2, x_1, x_2\right), \tag{B.8}$$

where $\widetilde{\Omega}_j^2 = \frac{1}{m_j} 2\hbar^2 \sum_{k\neq 0} \frac{1}{E_k}\left(g_k^{(j)}\right)^2$, $K = 2\hbar^2 \sum_{k\neq 0} \frac{1}{E_k} g_k^{(1)} g_k^{(2)} \cos\left(d_1 - d_2\right)$ and $\widehat{W}\left(d_1, d_2, x_1, x_2\right)$ is the function of the remaining constant terms and terms linear in x_1 and x_2. At thermal equilibrium, the terms in $\widehat{W}\left(d_1, d_2, x_1, x_2\right)$ will not affect the equilibrium state. Then, one can neglect them and consider the effective Hamiltonian

$$H_{\mathrm{eff}} = \sum_{j=1}^{2}\left[\frac{p_j^2}{2m_j} + \frac{1}{2}m_j\left(\Omega_j^2 - \widetilde{\Omega}_j^2\right)x_j^2\right] - 2Kx_1x_2. \tag{B.9}$$

This is formally analogous to two effectively coupled harmonic oscillators. To decouple them, we transform to the normal modes of the system, Q_1, Q_2. This is achieved by an orthogonal transformation of the form

$$\begin{pmatrix} Q_1 \\ Q_2 \end{pmatrix} = \begin{pmatrix} \cos\left(\theta\right) & -\sin\left(\theta\right) \\ \sin\left(\theta\right) & \cos\left(\theta\right) \end{pmatrix} \begin{pmatrix} x_1 \\ x_2 \end{pmatrix},$$

and

$$\begin{pmatrix} \Pi_1 \\ \Pi_2 \end{pmatrix} = \begin{pmatrix} \cos\left(\theta\right) & -\sin\left(\theta\right) \\ \sin\left(\theta\right) & \cos\left(\theta\right). \end{pmatrix} \begin{pmatrix} p_1 \\ p_2 \end{pmatrix}$$

With this, the effective Hamiltonian in terms of the normal modes is

$$H_{\mathrm{eff}} = \sum_{j=1}^{2}\left[\frac{1}{2}m\left(\Omega_j^2 - \widetilde{\Omega}_j^2\right)\left(\cos^2\left(\theta\right)Q_1^2 + \sin^2\left(\theta\right)Q_2^2 + 2\cos\left(\theta\right)Q_1Q_2\right)\right]$$
$$- 2K\left(-\cos\left(\theta\right)\sin\left(\theta\right)\left(Q_1^2 + Q_2^2\right) + \cos^2(\theta)\sin^2\left(\theta\right)Q_1Q_2\right) + \frac{\Pi_1^2}{2m} + \frac{\Pi_2^2}{2m}. \tag{B.10}$$

Here we made the assumption of $m_1 = m_2 = m$. To diagonalize the Hamiltonian, the condition on the rotation that should be performed reads as

$$\tan\left(2\theta\right) = \frac{2K}{\left(\Omega_1^2 - \widetilde{\Omega}_1^2\right) - \left(\Omega_2^2 - \widetilde{\Omega}_2^2\right)}.$$

For this rotation the Hamiltonian is

$$H_{\text{eff}} = \frac{1}{2}m\sum_{\substack{j,j'=1\\ j'\neq j}}^{2}\left[\left(\cos^2(\theta)\left(\Omega_j^2-\widetilde{\Omega}_j^2\right)+\sin^2(\theta)\left(\Omega_{j'}^2-\widetilde{\Omega}_{j'}^2\right)+K\sin(2\theta)\right)Q_j^2\right]+\frac{\Pi_1^2+\Pi_2^2}{2m}. \tag{B.11}$$

Hence the system has decoupled into two harmonic oscillators with frequencies

$$\begin{aligned}\nu_1^2 &= \cos^2(\theta)\left(\Omega_1^2-\widetilde{\Omega}_1^2\right)+\sin^2(\theta)\left(\Omega_2^2-\widetilde{\Omega}_2^2\right)+K\sin(2\theta),\\ \nu_2^2 &= \sin^2(\theta)\left(\Omega_2^2-\widetilde{\Omega}_2^2\right)+\cos^2(\theta)\left(\Omega_1^2-\widetilde{\Omega}_1^2\right)-K\sin(2\theta),\end{aligned}$$

and with the following second order moments

$$\begin{aligned}\left\langle Q_j^2\right\rangle &= \frac{\hbar}{2m\nu_j}\left(2\left\langle n_j\right\rangle+1\right)=\frac{\hbar}{m\nu_j}\coth\left(\frac{\nu_j}{2T}\right),\\ \left\langle \Pi_j^2\right\rangle &= \frac{\hbar m\nu_j}{2}\left(2\left\langle n_j\right\rangle+1\right)=\hbar m\nu_j\coth\left(\frac{\nu_j}{2T}\right),\end{aligned}$$

where the average is a statistical average over the bath variables. Also we find $\langle Q_jQ_q\rangle = \langle \Pi_j\Pi_q\rangle = 0$ for $j\neq q$. In the high temperature limit, $\coth(\nu_j\hbar/2k_{\text{B}}T)\sim\frac{2Tk_{\text{B}}}{\hbar\nu_j}$ and therefore

$$\begin{aligned}\left\langle Q_j^2\right\rangle &\sim \tfrac{2Tk_{\text{B}}}{m\nu_j^2},\\ \left\langle \Pi_j^2\right\rangle &\sim 2mTk_{\text{B}},\end{aligned}$$

One can now express the coherences or off-diagonal correlation functions at thermal equilibrium for the initial set of variables as:

$$\langle x_1x_2\rangle = \sin(\theta)\cos(\theta)\left(\left\langle Q_1^2\right\rangle-\left\langle Q_2^2\right\rangle\right). \tag{B.12}$$

In case that $\nu_1\neq\nu_2$, which happens when $\Omega_1\neq\Omega_2$ and/or $g_k^{(1)}\neq g_k^{(2)}$ for some k, then the coherence between x_1 and x_2 does not cancel out in the high temperature limit. Note however that this does not imply that entanglement survives at the high temperature limit, as this correlation is not necessarily a quantum correlation. This behaviour of $\langle x_1x_2\rangle$ is consistently verified in the numerical studies that we undertook using the original Hamiltonian. We note here that such behaviour, i.e. of asymptotic non–vanishing coherences at the high-temperature limit were identified in (Boyanovsky and Jasnow, 2017) but for the case of each particle attached to its own environment and both environments having an ohmic spectral density. The reason for the resemblance of the two cases is that in our case, one could argue that even though the two particles are coupled to a common bath contrary to (Boyanovsky and Jasnow, 2017), the particles effectively see the bath at different temperatures when $\nu_1\neq\nu_2$, in particular each one sees the bath at a temperature $\frac{T}{\nu_j^2}$. Hence our system in this case also reaches a non-equilibrium stationary state.

From these considerations, an estimate of the critical temperature can also be obtained. Notice that an important difference between the Hamiltonian in Eq. (B.11) and the original linear Hamiltonian in Eq. (5.18) is that the former has a spectrum that is bounded from below. In this case, and as the Hamiltonian is also self-adjoint, one can apply the results of Ref. (Anders and Winter, 2008), where it is proven that the critical temperature for such a symmetric system as the one we are considering is given by

$$(k_{\mathrm{B}}T_{\mathrm{crit}})^{-1} = \frac{1}{\hbar\nu_{\max}}\sigma(r), \tag{B.13}$$

where $\nu_{\max} = \max[\{\nu_j\}]$ with $j \in 1, 2$, $r = \nu_{\max}/\nu_{\min}$ where $\nu_{\min} = \min[\{\nu_j\}]$ and $\sigma(r) = ts(t)$ with $1 \leq t \leq r$ such that $s(t) = s(\frac{t}{r})$ with

$$s(x) := \frac{1}{x}\ln\left|\frac{1+x}{1-x}\right|. \tag{B.14}$$

For the general values of the parameters given in Sec. 5.2.2, the value of the critical temperature obtained assuming this effective Hamiltonian, was of the order of nK in agreement with our findings.

APPENDIX C

CHAPTER 7

C.1 Proof of CRB

Consider an unbiased estimator for which $\sum_{\mathbf{x}} p(x \mid \lambda)(\lambda_{est.}(\mathbf{x}) - \lambda) = 0$. By taking derivative of this equality with respect to λ one finds that

$$\begin{aligned} 0 &= \partial_\lambda \sum_{\mathbf{x}} p(x \mid \lambda)(\lambda_{est.}(\mathbf{x}) - \lambda) \\ &= -1 + \sum_{\mathbf{x}} (\lambda_{est.}(\mathbf{x}) - \lambda)\, \partial_\lambda p(x \mid \lambda) \\ \Rightarrow 1 &= \sum_{\mathbf{x}} (\lambda_{est.}(\mathbf{x}) - \lambda)\, p(x \mid \lambda)\, \partial_\lambda \log p(x \mid \lambda) \\ &= \sum_{\mathbf{x}} \left[(\lambda_{est.}(\mathbf{x}) - \lambda)\sqrt{p(x \mid \lambda)}\right] \left[\sqrt{p(x \mid \lambda)}\partial_\lambda \log p(x \mid \lambda)\right] \end{aligned} \tag{C.1}$$

Now using the Cauchy-Schwartz for the two terms inside the brackets one finds

$$\delta^2(\Pi_x, \lambda) \geq \frac{1}{\sum_x p(x \mid \lambda)(\partial_\lambda \log p(x \mid \lambda))^2} \tag{C.2}$$

where Π_x are the related set of POVM elements. Remembering that the term in the denominator of the right hand side is $F_{classical}(\lambda)$, the CRB for an unbiased estimator is proved.

C.2 Proof of QCRB

The QCRB can be proved with the help of the CRB, together with the Born rule, and the Cauchy-Schwartz inequality. We start by substituting $p(x \mid \lambda) = Tr(\rho(\lambda)\Pi_x)$ in the

expression of the Fisher information

$$F_{classical}(\lambda) = \sum_{\mathbf{x}} \frac{\left(\partial_\lambda Tr\left(\rho(\lambda)\Pi_x\right)\right)^2}{Tr\left(\rho(\lambda)\Pi_x\right)} \tag{C.3}$$

Next, we change the order of the derivative and the trace, and make use of the definition of the SLD

$$F_{classical}(\lambda) = \sum_{\mathbf{x}} \frac{\left(Re\left[Tr\left(L_\lambda \rho(\lambda)\Pi_x\right)\right]\right)^2}{Tr\left(\rho(\lambda)\Pi_x\right)} \leq \sum_{\mathbf{x}} \frac{\left|Tr\left(L_\lambda \rho(\lambda)\Pi_x\right)\right|^2}{Tr\left(\rho(\lambda)\Pi_x\right)} \tag{C.4}$$

By writing down $L_\lambda \rho(\lambda)\Pi_x = L_\lambda \sqrt{\rho(\lambda)}\sqrt{\rho(\lambda)}\sqrt{\Pi_x}\sqrt{\Pi_x}$ and with the help of the cyclic property of trace, a further use of Cauchy-Schwartz inequality gives

$$\begin{aligned} F_{classical}(\lambda) &\leq \textstyle\sum_{\mathbf{x}} \frac{Tr(\rho(\lambda)\Pi_x)Tr(L_\lambda\rho(\lambda)L_\lambda\Pi_x)}{Tr(\rho(\lambda)\Pi_x)} \\ &= Tr\left(L_\lambda \rho(\lambda) L_\lambda \textstyle\sum_{\mathbf{x}} \Pi_x\right) = F(\lambda) \end{aligned} \tag{C.5}$$

where in the last line we use the completeness of a POVM set, $\sum_{\mathbf{x}} \Pi_x = \mathbb{I}$, and the cyclic property of the trace.

C.3 Alternative Proof of QCRB by using static temperature susceptibility

The inherent errors from quantum measurements give rise to statistical uncertainty on the temperature estimate. Quantum estimation theory allows us to place fundamental limits on the error bars of the final temperature reading, and even to rank the various temperature dependent properties of the probe according to their thermal sensitivity. For instance, let us build our temperature estimate from a large set of outcomes of independent measurements of some impurity observable O [1]. We stress that these are either measurements performed on independent impurity atoms, or measurements on the same probe, but paced so that the BEC-impurity composite has time to reset to its stationary state every time. By mere propagation of errors, the uncertainty of the temperature inferred from such data set would read (Tóth and Apellaniz, 2014, Braunstein and Caves, 1994) as in Eq. (7.17). In order to assess the performance of O , it is essential to know which is the minimum possible uncertainty $(\delta T)_{min}$ defined from Eq. (7.17). To this end, one needs to consider the symmetric logarithmic derivative (SLD) defined by the Lyapunov equation in Eq. (7.4). Coming back to the definition of $\chi_T(O)$, we notice that $\chi_T(O) = \frac{1}{2}\langle OL_T + L_T O\rangle - \langle O\rangle\langle L_T\rangle$ while $\chi_T(O) = \Delta^2 L_T$. Making use of the fact that

[1] Note that we are not only assuming to work with a large data set, but also that the estimator which maps measurement outcomes to temperature estimates is unbiased (Braunstein and Caves, 1994).

$\Delta O \Delta L_T \geq \chi_T(O)$ allows to turn Eq. (7.17) into

$$\delta T(O) \geq \frac{1}{\sqrt{N\Delta^2 L_T}} = \frac{1}{\sqrt{NF(\rho_T)}} \tag{C.6}$$

where we have introduced the quantum Fisher information (QFI) $F(\rho_T) = \Delta^2 L_T$. The equation is nothing but the quantum Cramer-Rao bound (Braunstein and Caves, 1994), and sets the ultimate lower limit on the statistical error. Furthermore, by simply replacing O by L_T in Eq. (C.2), we can see that this bound is saturated by performing complete projective measurements onto the eigenbasis of the SLD.

C.4 Proof of Eq. (7.10)

The first equality in Eq. (7.10) is proven as following. From the definition of the SLD in Eq. (7.4), and having in mind that the expectation value of the SLD vanishes, it can be shown that

$$\partial_T \langle O \rangle = \partial_T Tr[O\rho_T] = Tr[O\partial_T \rho_T] = Tr\left[O\left(\frac{\rho_T L_T + L_T \rho_T}{2}\right)\right] = Cov(O, L_T) \tag{C.7}$$

where $Cov(A,B) \equiv \frac{1}{2}\langle AB + BA\rangle - \langle A\rangle\langle B\rangle$. We recall then the definition of $\chi_T\left(\widehat{O}\right)$ the static temperature susceptibility in Eq. (7.16) where $\partial_T \langle O\rangle \equiv \chi_T(O)$. However, it can also be shown that (Mehboudi *et al.*, 2019b)

$$\chi_T(O) = \frac{1}{T^2} Tr\left[O(H - \langle H\rangle) e^{-H/T} \mathcal{Z}^{-1}\right] = \frac{1}{T^2} Cov(O, H - \langle H\rangle) \tag{C.8}$$

where $\mathcal{Z}$ is the partition function, and hence it must be that

$$L_T = \frac{1}{T^2}(H - \langle H\rangle) \tag{C.9}$$

Having Eq. (7.8) in mind, the first equality of Eq. (7.10) is established. The second equality in Eq. (7.10) is simply a result of the fact that the temperature susceptibility of the Hamiltonian H is by definition the heat capacity of the probe $C_V \equiv \partial_T \langle H\rangle = (\Delta H/T)^2$.

C.5 Two-Level VS Harmonic Oscillator QFI

To see in practice what implications the structure of the energy level of a Hamiltonian might have on the thermometric precision of a given protocol, we will examine two distinct cases, the two-level probe and a probe described as a harmonic oscillator. It can be shown analytically (Mehboudi *et al.*, 2019b), that the first case corresponds to the optimal energy spectrum, i.e. the one that results to the most precise measurement of a given temperature T. In fact this spectrum for a finite dimensional N level spectrum, will correspond to an effectively two-level system, where the second level is $N-1$ fold degenerate. Furthermore,

it can be shown that taking the limit $N \to \infty$ yields a best-case relative error $(\Delta T/T)^2 \sim 4/\log N$ (Płodzień *et al.*, 2018). From the study of the QFI for this spectrum, given by

$$F_{N-level}(T) = \frac{\epsilon^2 e^{-\frac{\epsilon}{T}}}{T^4} \frac{N-1}{\left(N-1+e^{-\frac{\epsilon}{T}}\right)^2} \tag{C.10}$$

it is found that QFI drops rapidly in the low temperature limit, regardless of N, since at low-enough temperatures ($T/\epsilon \ll 1$), where is the fixed energy gap of the effectively two-level system, a probe with finite gap collapses into its ground state. Small variations of T would then be insufficient to pump population to the excited-state manifold and the probe would thus become insensitive to temperature changes.

The highly degenerate optimal spectra described above can be hard to craft in practice. Alternatively, one could try to realize more practical thermometers with a far less exotic energy spectrum. In particular, for this reason, we also consider the thermal responsiveness of a quantum harmonic oscillator with frequency Ω. At thermal equilibrium, its average energy is given by $\langle H_{ho}\rangle = \left(1-e^{-\frac{\Omega}{T}}\right)^{-1} e^{-\frac{\Omega}{T}}\Omega$. Deriving with respect to T leads to the energy variance, $\Delta H_{ho} = \left(1-e^{-\Omega/T}\right)^{-1} e^{-\frac{\Omega}{2T}}\Omega$. Therefore, the corresponding QFI can be written as

$$F_{ho}(T) = \frac{1}{T^4} \frac{\Omega^2 e^{-\Omega/T}}{\left(1-e^{-\Omega/T}\right)^2} \tag{C.11}$$

One can show then that the harmonic thermometer performs efficiently in a wider temperature range than any finite-dimensional probe as the one considered above. However, although harmonic oscillators are superior to two level thermometers at any temperature, the two types of probe converge towards the same sensitivity as $T \to 0$. This is to be expected, since, at low-enough temperatures, a thermal oscillator can be reliably truncated to its first two energy levels. More rigorously, one can prove that $F_{ho}(T) \sim F_{2-level}(T)\left(\Omega^2/T^4\right) e^{-\Omega/T}$. In fact, this holds also for any N-dimensional probe with equispaced spectrum (Campbell *et al.*, 2018). Many other type of probes and hence spectra can also be considered, for example a probe consisting of a mixture of two interacting species of fermions confined in a 1D harmonic potential, as in (Płodzień *et al.*, 2018).

C.6 Proof of Gaussian QFI

First we obtain an expression for the Gaussian SLD and remembering that QFI is just the variance of SLD, we obtain from that the QFI. Then, from Eq. (C.9), we know that the form of SLD should be the following

$$\begin{aligned} L_T &= C_x\left(x^2-\langle x^2\rangle\right) + C_p\left(p^2-\langle p^2\rangle\right) + d\left(xp+px-\langle xp+px\rangle\right) \\ &= C_x\left(x^2-\langle x^2\rangle\right) + C_p\left(p^2-\langle p^2\rangle\right) + d\left(xp+px\right) \end{aligned} \tag{C.12}$$

since by using $[x,p]=i\hbar$ we can prove that $\langle xp\rangle=-\langle px\rangle$. From this we also conclude that $\langle xp\rangle=i\hbar/2$. Furthermore, we recall the relation between the static temperature susceptibility of an observable O with the covariance of this observable with the SLD given in Eq. (C.7), and we apply it to the observables x^2 and p^2. This gives

$$\begin{gathered}\partial_T\langle x^2\rangle=Cov\left(x^2,L_T\right)=\tfrac{1}{2}\langle x^2L_T+L_Tx^2\rangle\\ =\tfrac{1}{2}\Big(C_x\langle x^4\rangle-C_x\langle x^2\rangle^2+C_p\langle x^2p^2\rangle-C_p\langle x^2\rangle\langle p^2\rangle+d\langle x^3p\rangle+d\langle x^2px\rangle\\ C_x\langle x^4\rangle-C_x\langle x^2\rangle^2+C_p\langle p^2x^2\rangle-C_p\langle p^2\rangle\langle x^2\rangle+d\langle xpx^2\rangle+d\langle px^3\rangle\Big)\\ =\tfrac{1}{2}\Big(4C_x\langle x^2\rangle^2+2C_p\left(\langle xp\rangle^2+\langle px\rangle^2\right)\Big)\\ =2C_x\langle x^2\rangle^2-\hbar^2C_p/2\end{gathered}\tag{C.13}$$

In the third step the Isserli's theorem was used. A similar expression for p^2 can be obtained

$$\partial_T\langle p^2\rangle=2C_p\langle p^2\rangle^2-\hbar^2C_x/2\tag{C.14}$$

Solving the two Eqs. (C.13)&(C.14) for C_x and C_p we obtain Eq. (7.13) and the analogous expression for p. Finally, we can also consider $0=\partial_T\langle xp\rangle=Cov\left(x^2,L_T\right)$ which will give us that $d=0$. This way we obtain the expression for L_T in Eq. (7.12).

For the expression of $F(\rho_T)$ we need to find the variance of SLD. This gives

$$\begin{gathered}F(\rho_T)=\Delta L_T^2=\left\langle\left[C_x\left(x^2-\langle x^2\rangle\right)+C_p\left(p^2-\langle p^2\rangle\right)\right]^2\right\rangle\\ =C_x^2\left\langle\left(x^2-\langle x^2\rangle\right)^2\right\rangle+C_p^2\left\langle\left(p^2-\langle p^2\rangle\right)^2\right\rangle\\ +C_xC_p\left\{\left(x^2-\langle x^2\rangle\right)\left(p^2-\langle p^2\rangle\right)+\left(p^2-\langle p^2\rangle\right)\left(x^2-\langle x^2\rangle\right)\right\}\\ =C_x^2\left(\langle x^4\rangle+\langle x^2\rangle^2-2\langle x^2\rangle^2\right)+C_p^2\left(\langle p^4\rangle+\langle p^2\rangle^2-2\langle p^2\rangle^2\right)\\ +C_xC_p\left\{\langle x^2p^2\rangle+\langle p^2x^2\rangle-2\langle x^2\rangle\langle p^2\rangle\right\}\end{gathered}\tag{C.15}$$

where after applying Isserli's theorem again, we obtain the expression for QFI in Eq. (7.12).

APPENDIX D

CHAPTER 8

D.1 The uncertainty relation

Here, we present how the covariance matrix of our system is obtained, (both for the static and driven cases) which we used in order to verify that our system fulfills the uncertainty principle. This allows us to guarantee that the system under study, for the parameters considered and according with the assumptions that we have imposed, is a physical system. To do so, one needs to obtain the covariance matrix of the system,

$$\mathbf{C}(0) = \begin{pmatrix} C_{\mathbf{XX}}(0) & C_{\mathbf{XP}}(0) \\ C_{\mathbf{PX}}(0) & C_{\mathbf{PP}}(0) \end{pmatrix}, \tag{D.1}$$

where $\mathbf{P} = (p_1(t), p_2(t))^T$ and

$$C_{\mathbf{AB}}(t-t') = \frac{1}{2}\left\langle \mathbf{A}(t)\mathbf{B}^T(t') + \mathbf{B}(t)\mathbf{A}^T(t')\right\rangle_{\rho_{\mathrm{B}}}. \tag{D.2}$$

We emphasize that the state of the system-bath is assumed to be a product state as in (8.35). Hence the average is taken over the thermal state of the bath, while the state of the system is assumed to have reached its unique equilibrium state by considering the long-time, steady state limit $t \to \infty$ which is equivalent to consider that $\omega \ll \Lambda_{\mathrm{L}}, \Lambda_{\mathrm{R}}$. The 4×4 matrix in (D.1) is constructed from the vector $\mathbf{Y}(t) = (x_1(t), x_2(t), p_1(t), p_2(t))^T$ as the product $\frac{1}{2}\left\langle \left\{ \mathbf{Y}^T(t)\mathbf{Y}(t'), \left(\mathbf{Y}^T(t)\mathbf{Y}(t')\right)^T \right\} \right\rangle_{\rho_{\mathrm{B}}}$.

The uncertainty relation will then be expressed as a condition on the symplectic transform of the covariance matrix $\widetilde{\mathbf{C}}(0)$, where the latter is obtained as $\widetilde{\mathbf{C}}(0) = i\mathbf{W}\cdot\mathbf{C}(0)$

with $\mathbf{W}$ the symplectic matrix $\mathbf{W} = \begin{pmatrix} 0 & 0 & 1 & 0 \\ 0 & 0 & 0 & 1 \\ -1 & 0 & 0 & 0 \\ 0 & -1 & 0 & 0 \end{pmatrix}$. The uncertainty relation then simply reads as

$$\nu_{-} \geq \frac{1}{2}, \tag{D.3}$$

where ν_{-} is the minimum standard eigenvalue of $\widetilde{\mathbf{C}}(0)$ ($\hbar$ is assumed to be equal to 1 in this case).

Static covariance matrix. The elements of the covariance matrix in the static case, in terms of the phonons propagator functions, can be expressed as

$$C_{x_j x_q}(0) = \frac{\hbar}{2\pi} \int_{-\infty}^{\infty} \mathrm{d}\omega \, \mathrm{Z_{jq}}(\omega), \tag{D.4}$$

$$C_{x_j x_q}(0) = \frac{\hbar}{2\pi} \int_{-\infty}^{\infty} \mathrm{d}\omega \, \mathrm{im}\omega \mathrm{Z_{jq}}(\omega), \tag{D.5}$$

$$C_{x_j x_q}(0) = \frac{\hbar}{2\pi} \int_{-\infty}^{\infty} \mathrm{d}\omega \, \mathrm{m}^2\omega^2 \mathrm{Z_{jq}}(\omega), \tag{D.6}$$

where

$$Z_{jq}(\omega) = \sum_{k,s=1}^{2} \left(\mathbf{G}(\omega)\right)_{js} \left(Im[\mathbf{L}(\omega)] \cdot \coth\left[\frac{\hbar\omega}{2k_{\mathrm{B}}\mathbf{T}}\right] \right)_{sk} \left(\mathbf{G}(-\omega)\right)_{kq}, \tag{D.7}$$

with $\mathbf{T} = \begin{pmatrix} T_{\mathrm{L}} & 0 \\ 0 & T_{\mathrm{R}} \end{pmatrix}$ being the temperatures of each bath.

Driven case. In the driven case, since the solution of the equations of motion is periodic, so are the elements of the covariance matrix as well. In particular, in terms of the Fourier components of the expansion of the periodic phonon Green function, the covariance matrix elements read as

$$C_{x_j x_q}(0) = \tfrac{\hbar}{2\pi} \textstyle\int_{-\infty}^{\infty} \mathrm{d}\omega \sum_{\mathrm{k,l}} \widetilde{\mathrm{Z}}_{\mathrm{jq,kl}}(\omega), \tag{D.8}$$

$$C_{x_j x_q}(0) = \tfrac{\hbar}{2\pi} \textstyle\int_{-\infty}^{\infty} \mathrm{d}\omega \sum_{\mathrm{k,l}} \mathrm{im}\left(\omega - \mathrm{l}\Omega_{\mathrm{d}}\right) \widetilde{\mathrm{Z}}_{\mathrm{jq,kl}}(\omega), \tag{D.9}$$

$$C_{x_j x_q}(0) = \tfrac{\hbar}{2\pi} \textstyle\int_{-\infty}^{\infty} \mathrm{d}\omega \sum_{\mathrm{k,l}} \mathrm{m}^2\left(\omega - \mathrm{k}\Omega_{\mathrm{d}}\right)\left(\omega - \mathrm{l}\Omega_{\mathrm{d}}\right) \widetilde{\mathrm{Z}}_{\mathrm{jq,kl}}(\omega), \tag{D.10}$$

where

$$\widetilde{Z}_{jq,kl}(\omega) = \sum_{n,s=1}^{2} \left(\mathbf{A}_k(\omega)\right)_{js} \left(Im[\mathbf{L}(\omega)] \cdot \coth\left[\frac{\hbar\omega}{2k_{\mathrm{B}}\mathbf{T}}\right] \right)_{sn} \left(\mathbf{A}_{\mathrm{L}}(-\omega)\right)_{nq} e^{i(k-l)\omega_d t}. \tag{D.11}$$

D.2 Proof of Landauer formula

Current The steady state current will be the same if we obtain it on any cross-section of the system. It is simplest to evaluate the current expression at the system reservoir interface. Let us consider the interface with the left reservoir. The steady state current can be shown (Dhar, 2008) to be just the expectation value of the rate at which the Langevin forces (which come from the bath) do work on the particles of the system

$$\langle J_L \rangle_{\rho_B} = \left\langle \dot{x}_L(t) \left[B_L(t) + \int_{-\infty}^{\infty} \lambda_L(t-s)\, x_L(s)\, ds \right] \right\rangle_{\rho_B} \tag{D.12}$$

where we set $m = 1$, which in matrix form reads as

$$\begin{aligned}
\langle J_L \rangle_{\rho_B} &= \left\langle \dot{\mathbf{X}}^T(t)\, \mathbf{B}(t)\, I_L \right\rangle_{\rho_B} + \int_{-\infty}^{\infty} ds \left\langle \dot{\mathbf{X}}^T(t)\, \mathbf{L}(t-s)\, I_L X(s) \right\rangle_{\rho_B} \\
&= -i \int_{-\infty}^{\infty} d\omega \int_{-\infty}^{\infty} d\omega' e^{-i(\omega+\omega')t} \omega \left\langle \mathbf{X}^T(\omega)\, \mathbf{B}(\omega')\, I_L + \mathbf{X}^T(\omega)\, \mathbf{L}(\omega')\, I_L \mathbf{X}(\omega') \right\rangle_{\rho_B} \\
&= -i \int_{-\infty}^{\infty} d\omega \int_{-\infty}^{\infty} d\omega' e^{-i(\omega+\omega')t} \omega \left\langle Tr\left[\mathbf{B}(\omega')\, I_L \mathbf{X}^T(\omega)\right] + Tr\left[\mathbf{L}(\omega')\, I_L \mathbf{X}(\omega')\, \mathbf{X}^T(\omega)\right] \right\rangle_{\rho_B}
\end{aligned} \tag{D.13}$$

where $I_L = \begin{pmatrix} 1 & 0 \\ 0 & 0 \end{pmatrix}$, $I_R = \begin{pmatrix} 0 & 0 \\ 0 & 1 \end{pmatrix}$

Using the solution of the QGLE in Eq. (3.48) written in vector form, we then get

$$\begin{aligned}
\langle J_L \rangle_{\rho_B} = -i \int_{-\infty}^{\infty} d\omega \int_{-\infty}^{\infty} d\omega' e^{-i(\omega+\omega')t} \omega \Big(& Tr\left[\mathbf{B}(\omega')\, I_L \mathbf{B}^T(\omega')\, \mathbf{G}(\omega)\right] \\
& + Tr\left[\mathbf{L}(\omega')\, I_L \mathbf{G}(\omega')\, \mathbf{B}(\omega')\, \mathbf{B}^T(\omega)\, \mathbf{G}(\omega)\right] \Big)
\end{aligned} \tag{D.14}$$

where we have used the fact that $\mathbf{G}(\omega)$ is a symmetric matrix. If we expand the above, and use the properties of the noise correlations (including the fact that the noise from the left and right baths are uncorrelated) , we notice that all terms depend either on the left, or on the right bath temperature, and no term depends on both temperatures. Let us collect those terms in $\langle J_L \rangle_{\rho_B}$ which depend only on the temperature T_R of the right reservoir, and not on that of the left. These give

$$\left\langle J_L^R \right\rangle_{\rho_B} = -i \int_{-\infty}^{\infty} d\omega \int_{-\infty}^{\infty} d\omega' e^{-i(\omega+\omega')t} \omega \left(Tr\left[\mathbf{L}(\omega')\, I_L \mathbf{G}(\omega') \left\langle \mathbf{B}(\omega')\, I_R \mathbf{B}^T(\omega)\, I_R \right\rangle_{\rho_B} \mathbf{G}(\omega) \right] \right) \tag{D.15}$$

Using the noise correlations in Eq. (3.28) or Eq. (8.36) we then get

$$\left\langle J_L^R \right\rangle_{\rho_B} = -\frac{i}{\pi} \int_{-\infty}^{\infty} d\omega \hbar\omega Tr\left[\mathbf{L}(-\omega)\, I_L \mathbf{G}(-\omega)\, Im\left[\mathbf{L}(\omega)\, I_R\right] \mathbf{G}(\omega)\right] f(\omega, T_R) \tag{D.16}$$

where we used the properties $1+f(-\omega,T_j)=-f(\omega,T_j)$ and $Im\left[\mathbf{L}(-\omega)I_R\right]=-Im\left[\mathbf{L}(\omega)I_R\right]$. Taking the complex conjugate of the above expression, using $Tr\left[A\right]^*=Tr\left[A^\dagger\right]$, $\mathbf{G}^\dagger(\omega)=-\mathbf{G}(\omega)$, and the cyclic property of trace, we get

$$\left\langle\left(J_L^R\right)^*\right\rangle_{\rho_B}=\frac{i}{\pi}\int_{-\infty}^{\infty}d\omega\hbar\omega Tr\left[\left(\mathbf{L}(-\omega)I_L\right)^*\mathbf{G}(-\omega)Im\left[\mathbf{L}(\omega)I_R\right]\mathbf{G}(\omega)\right]f(\omega,T_R) \quad \text{(D.17)}$$

The physical current is real, so we take $\left\langle J_L^{R,phys}\right\rangle_{\rho_B}=\left(\left\langle J_L^R\right\rangle_{\rho_B}+\left\langle\left(J_L^R\right)^*\right\rangle_{\rho_B}\right)/2$ we get

$$\left\langle J_L^{R,phys}\right\rangle_{\rho_B}=-\frac{1}{\pi}\int_{-\infty}^{\infty}d\omega\hbar\omega Tr\left[Im\left[\mathbf{L}(\omega)I_L\right]\mathbf{G}^\dagger(\omega)Im\left[\mathbf{L}(\omega)I_R\right]\mathbf{G}(\omega)\right]f(\omega,T_R) \quad \text{(D.18)}$$

From symmetry, and the requirement that $\left\langle J_L\right\rangle_{\rho_B}=0$ when $T_L=T_R$, it is clear that the contribution of the left reservoir to the current must have a similar form (this can be verified directly also) and hence we can now write the net current as in Eq. (8.57).

D.3 Proof of driven heat current

D.3.1 Heat current from the steady state covariance matrix

Suppose that the elements of the steady state covariance matrix as defined in Eq. (3.49) are given. We then want to know how the current $\left\langle J_L\right\rangle_{\rho_B}$ can be calculated from this. We first write the interaction Hamiltonian in the more compact form $\widetilde{H}_{int.,L}=\mathbf{Q}_L\mathbf{Y}_L$with $\mathbf{Q}_L$ a rectangular matrix of dimension $1\times N$ formed by the coupling constants $g_{q,L}$ of the N left bath particles with the left impurity and $\mathbf{Y}_L$ a rectangular matrix of dimension $N\times 1$ with the bath operators $b_{q,L}+b_{q,L}^\dagger$. Hence by using the definition of local heat currents $J_L=i/\hbar\left\langle\left[\widetilde{H}_{int.,L},H_L'\right]\right\rangle_\rho$, one can verify that

$$J_L=\frac{1}{2}\left(\left\langle\mathbf{P}^T\mathbf{Q}_L\mathbf{Y}_L\right\rangle_\rho+\left\langle\mathbf{Q}_L^T\mathbf{Y}_L^T\mathbf{P}\right\rangle_\rho\right) \quad \text{(D.19)}$$

Recall our assumption that each oscillator is at most coupled to one reservoir. We denote by Π_a the projector onto the space of the oscillator that is coupled to the bath a. Thus, using the Heisenberg equation of motion for the momentum of the left central particle, it follows that

$$J_L=\frac{1}{2}Tr\left[\Pi_L\frac{d}{dt}C_{\mathbf{PP}}\right]+Tr\left[\Pi_L\mathbf{V}(t)C_{\mathbf{XP}}\right] \quad \text{(D.20)}$$

where we have used the property of the bilinear product $\left\langle\Psi_1^TW\Psi_2\right\rangle=tr\left[W^T\left\langle\Psi_1\Psi_2^T\right\rangle\right]$ where Ψ_1 and Ψ_2 are vector operators and W a scalar matrix.

D.3.2 Driven heat current

Let us define the integrodifferential super-operator $\mathcal{L}_t[\cdot]=\frac{d^2}{dt^2}[\cdot]+\mathbf{V}(t)[\cdot]+\mathbf{L}(t)[\cdot]$ associated to the homogeneous quantum Langevin equation. The equation of motion of the Green's function is given by $\mathcal{L}_t\left[\widetilde{\mathbf{G}}(t,t')\right]=\mathbb{I}\delta(t-t')$. If the potential is $\tau-$periodic,

that is $\mathbf{V}(t+\tau)=\mathbf{V}(t)$, then $\mathcal{L}_t\left[\widetilde{\mathbf{G}}\left(t+\tau,t'+\tau\right)\right]=\mathbb{I}\delta\left(t-t'\right)$ and therefore $\widetilde{\mathbf{G}}\left(t,t'\right)=\widetilde{\mathbf{G}}\left(t+\tau,t'+\tau\right)$ in the steady state by uniqueness of the solution. Now, we define the periodic function $\mathbf{P}\left(t,\omega\right)=e^{i\omega t}\int_{\mathbb{R}}dt'e^{-i\omega t'}\widetilde{\mathbf{G}}\left(t,t'\right)$. It is easy to see that $P(t+\tau,\omega)=P(t,\omega)$. Since $\mathcal{L}_t$ is a linear superoperator, we have $e^{i\omega t}\int_{\mathbb{R}}dt'e^{-i\omega t'}\mathcal{L}_t\left[\widetilde{\mathbf{G}}\left(t,t'\right)\right]=\mathcal{L}_t\left[e^{-i\omega t}\mathbf{P}\left(t,\omega\right)\right]$ and using $\mathbf{P}\left(t,\omega\right)=\sum_k\mathbf{A}_k\left(\omega\right)e^{ik\Omega_d t}$, we have $\sum_k\mathcal{L}_t\left[e^{-i(\omega-k\Omega_d)t}\mathbf{A}_k\left(\omega\right)\right]=\mathbb{I}e^{-i\omega t}$. It follows

$$\sum_k\left[-\left(\omega-k\Omega_d\right)^2e^{ik\Omega_d t}+\sum_j\mathbf{V}_je^{i(j+k)\Omega_d t}+\mathbf{L}\left(\omega-k\Omega_d\right)e^{ik\Omega_d t}\right]\mathbf{A}_k\left(\omega\right)=\mathbb{I} \tag{D.21}$$

and projecting on k^{th} element of the Fourier expansion, one arrives at

$$\mathbf{G}^{-1}\left(\omega-k\Omega_d\right)\mathbf{A}_k\left(\omega\right)+\sum_{j\neq0}V_j\mathbf{A}_{k-j}\left(\omega\right)=\delta_{k,0}\mathbb{I} \tag{D.22}$$

We can use now the amplitudes $\{\mathbf{A}_k\left(\omega\right)\}$ to compute the steady state solution for

$$\begin{aligned}\mathbf{X}\left(t\right)&=\int_{\mathbb{R}}dt'\widetilde{\mathbf{G}}\left(t,t'\right)B\left(t'\right)=\sum_k\int_{\mathbb{R}}\tfrac{d\omega}{2\pi}e^{-i(\omega-k\Omega_d)t}\mathbf{A}_k\left(\omega\right)\mathbf{B}\left(\omega\right)\\ \dot{\mathbf{X}}\left(t\right)&=\tfrac{d}{dt}\int_{\mathbb{R}}dt'\widetilde{\mathbf{G}}\left(t,t'\right)B\left(t'\right)=-i\sum_k\int_{\mathbb{R}}\tfrac{d\omega}{2\pi}\left(\omega-k\Omega_d\right)e^{-i(\omega-k\Omega_d)t}\mathbf{A}_k\left(\omega\right)\mathbf{B}\left(\omega\right)\end{aligned} \tag{D.23}$$

The covariance matrix can be computed also using $\mathbf{A}_k\left(\omega\right)$ and it turns out to be τ-periodic. Let us take for instance

$$C_{\mathbf{XP}}=\sum_{jk}\left[i\sum_{\alpha\in\{L,R\}}\int_{\mathbb{R}}d\omega\hbar\left(\omega-k\Omega_d\right)\mathbf{A}_j\left(\omega\right)Im\left[\mathbf{L}\left(\omega\right)I_\alpha\right]\mathbf{A}_k^\dagger\left(\omega\right)\left(n_\alpha\left(\omega\right)+\frac{1}{2}\right)\right]e^{i(j-k)\Omega_d t} \tag{D.24}$$

We now take the average over a period of the heat currents. Notice that since $C_{\mathbf{PP}}$ is τ-periodic, the average of its derivative over a period vanishes. Then, $\overline{J_L}=Tr\left[\Pi_L\overline{\mathbf{V}\left(t\right)C_{\mathbf{XP}}}\right]$ which reads as

$$\begin{aligned}\overline{J_L}&=-\sum_\beta\int_{\mathbb{R}}d\omega\sum_k\hbar\left(\omega-k\Omega_d\right)Im\left\{Tr\left[\Pi_L\sum_j\mathbf{V}_j\mathbf{A}_{k-j}\left(\omega\right)Im\left[\mathbf{L}\left(\omega\right)I_\beta\right]\mathbf{A}_k^\dagger\left(\omega\right)\right]\right\}\left(n_\beta\left(\omega\right)+\frac{1}{2}\right)\\&=-\sum_\beta\int_{\mathbb{R}}d\omega\mathcal{T}_{L\beta}\left(n_\beta\left(\omega\right)+\frac{1}{2}\right)\end{aligned} \tag{D.25}$$

From Eq. (D.22) follows $\sum_j\mathbf{V}_j\mathbf{A}_{k-j}\left(\omega\right)=\delta_{k,0}\mathbb{I}+\left(\omega-k\Omega_d\right)^2\mathbf{A}_k\left(\omega\right)+\mathbf{L}\left(\omega-k\Omega_d\right)\mathbf{A}_k\left(\omega\right)$ which can be used to compute

$$\mathcal{T}_{\alpha\beta}\left(\omega\right)=\sum_k\hbar\left(\omega-k\Omega_d\right)\pi Tr\left[Im\left[\mathbf{L}\left(\omega-k\Omega_d\right)I_\alpha\right]\mathbf{A}_k\left(\omega\right)Im\left[\mathbf{L}\left(\omega\right)I_\beta\right]\mathbf{A}_k^\dagger\left(\omega\right)\right]$$

for $\beta\neq\alpha$. We define then $\widehat{\mathcal{T}}_\alpha=\sum_\beta\mathcal{T}_{\alpha\beta}\left(\omega\right)$ and one can hence shown that

$$\overline{J_L}=-\int_{\mathbb{R}}d\omega\widehat{\mathcal{T}}_L\left(n_L\left(\omega\right)+\frac{1}{2}\right)+\int_{\mathbb{R}}d\omega\mathcal{T}_{\beta L}\left(\omega\right)\left(n_L\left(\omega\right)+\frac{1}{2}\right)-\mathcal{T}_{L\beta}\left(\omega\right)\left(n_\beta\left(\omega\right)+\frac{1}{2}\right) \tag{D.26}$$

where we used $\sum_\beta\sum_{jk}\hbar\omega Im\left\{Tr\left[\Pi_\beta\mathbf{V}_{k-j}\mathbf{A}_j\left(\omega\right)Im\left[\mathbf{L}\left(\omega\right)I_\alpha\right]\mathbf{A}_k^\dagger\left(\omega\right)\right]\right\}=0$ for $\beta\neq\alpha$.

BIBLIOGRAPHY

Aasi, J., Abadie, J., Abbott, B., Abbott, R., Abbott, T., Abernathy, M., Adams, C., Adams, T., Addesso, P., Adhikari, R. *et al.* (2013). Enhanced sensitivity of the ligo gravitational wave detector by using squeezed states of light. *Nature Photonics*, **7**, 613.

Abad, M. and Recati, A. (2013). A study of coherently coupled two-component bose-einstein condensates. *The European Physical Journal D*, **67**, 148.

Abbott, D., Davies, P.C. and Pati, A.K. (2008). *Quantum aspects of life*. World Scientific.

Adesso, G. and Illuminati, F. (2005). Gaussian measures of entanglement versus negativities: Ordering of two-mode gaussian states. *Phys. Rev. A*, **72**, 032334.

Adesso, G. and Illuminati, F. (2007). Entanglement in continuous-variable systems: recent advances and current perspectives. *Journal of Physics A: Mathematical and Theoretical*, **40**, 7821–7880.

Adesso, G., Serafini, A. and Illuminati, F. (2004). Extremal entanglement and mixedness in continuous variable systems. *Phys. Rev. A*, **70**, 022318.

Adesso, G., Dell'Anno, F., De Siena, S., Illuminati, F. and Souza, L.A.M. (2009). Optimal estimation of losses at the ultimate quantum limit with non-gaussian states. *Phys. Rev. A*, **79**, 040305.

Agarwalla, B.K., Wang, J.S. and Li, B. (2011). Heat generation and transport due to time-dependent forces. *Phys. Rev. E*, **84**, 041115.

Ahmadi, M., Bruschi, D.E. and Fuentes, I. (2014). Quantum metrology for relativistic quantum fields. *Phys. Rev. D*, **89**, 065028.

Alexandrov, A. and Devreese, J. (2009). *Advances in Polaron Physics*. Springer Series in Solid-State Sciences, Springer.

Alexandrov, A.S. and Devreese, J.T. (2010). *Advances in polaron physics*, vol. 159. Springer.

Alicki, R. and Lendi, K. (2007). *Quantum dynamical semigroups and applications*, vol. 717. Springer.

Alipour, S., Mehboudi, M. and Rezakhani, A.T. (2014). Quantum metrology in open systems: Dissipative cramér-rao bound. *Phys. Rev. Lett.*, **112**, 120405.

Anapolitanos, I. and Landon, B. (2013a). The ground state energy of the multi-polaron in the strong coupling limit. *Lett. Math. Phys.*, **103**, 1347.

Anapolitanos, I. and Landon, B. (2013b). The ground state energy of the multi-polaron in the strong coupling limit. *Letters in Mathematical Physics*, **103**, 1347–1366.

Anders, J. and Winter, A. (2008). Entanglement and separability of quantum harmonic oscillator systems at finite temperature. *Quantum information and computation*, **8**.

Anderson, P.W. and Rowell, J.M. (1963). Probable observation of the josephson superconducting tunneling effect. *Phys. Rev. Lett.*, **10**, 230–232.

Anglin, J.R., Paz, J.P. and Zurek, W.H. (1997). Deconstructing decoherence. *Phys. Rev. A*, **55**, 4041–4053.

Ao, P. and Chui, S.T. (1998). Binary bose-einstein condensate mixtures in weakly and strongly segregated phases. *Phys. Rev. A*, **58**, 4836–4840.

Appel, J. (1968). Polarons. In *Solid State Physics*, vol. 21, 193–391, Elsevier.

Ardila, L.A.P. and Giorgini, S. (2016). Bose polaron problem: Effect of mass imbalance on binding energy. *Phys. Rev. A*, **94**, 063640.

Aron, C., Biroli, G. and Cugliandolo, L.F. (2018). (Non) equilibrium dynamics: a (broken) symmetry of the Keldysh generating functional. *SciPost Phys.*, **4**, 008.

Ashida, Y., Schmidt, R., Tarruell, L. and Demler, E. (2018). Many-body interferometry of magnetic polaron dynamics. *Phys. Rev. B*, **97**, 060302.

Aspachs, M., Adesso, G. and Fuentes, I. (2010). Optimal quantum estimation of the unruh-hawking effect. *Phys. Rev. Lett.*, **105**, 151301.

Aspect, A., Inguscio, M., Müller, C. and Delande, D. (2009). Anderson localization.

Physics today, **62**, 30–35.

Austin, I. and Mott, N. (1969). Polarons in crystalline and non-crystalline materials. *Advances in Physics*, **18**, 41–102.

Aycock, L.M., Hurst, H.M., Efimkin, D.K., Genkina, D., Lu, H.I., Galitski, V.M. and Spielman, I.B. (2017). Brownian motion of solitons in a bose–einstein condensate. *Proceedings of the National Academy of Sciences*, **114**, 2503–2508.

Bai, X.D. and Xue, J.K. (2015). Subdiffusion of dipolar gas in one-dimensional quasiperiodic potentials. *Chinese Physics Letters*, **32**, 010302.

Bakr, W.S., Gillen, J.I., Peng, A., Fölling, S. and Greiner, M. (2009). A quantum gas microscope for detecting single atoms in a hubbard-regime optical lattice. *Nature*, **462**, 74.

Barik, D. and Ray, D.S. (2005). Quantum state-dependent diffusion and multiplicative noise: A microscopic approach. *Journal of Statistical Physics*, **120**, 339–365.

Barndorff-Nielsen, O. and Gill, R. (2000). Fisher information in quantum statistics. *Journal of Physics A: Mathematical and General*, **33**, 4481.

Batchelor, G.K. (2000). *An Introduction to Fluid Dynamics*. Cambridge University Press.

Baumgratz, T. and Datta, A. (2016). Quantum enhanced estimation of a multidimensional field. *Phys. Rev. Lett.*, **116**, 030801.

Benatti, F., Floreanini, R. and Piani, M. (2003). Environment induced entanglement in markovian dissipative dynamics. *Phys. Rev. Lett.*, **91**, 070402.

Benatti, F., Floreanini, R. and Marzolino, U. (2010). Entangling two unequal atoms through a common bath. *Phys. Rev. A*, **81**, 012105.

Bennett, C.H., Bernstein, H.J., Popescu, S. and Schumacher, B. (1996a). Concentrating partial entanglement by local operations. *Phys. Rev. A*, **53**, 2046–2052.

Bennett, C.H., DiVincenzo, D.P., Smolin, J.A. and Wootters, W.K. (1996b). Mixed-state entanglement and quantum error correction. *Phys. Rev. A*, **54**, 3824–3851.

Bera, M.N., Riera, A., Lewenstein, M., Khanian, Z.B. and Winter, A. (2019). Thermodynamics as a Consequence of Information Conservation. *Quantum*, **3**, 121.

Bian, X., Kim, C. and Karniadakis, G.E. (2016). 111 years of brownian motion. *Soft Matter*, **12**, 6331–6346.

Billy, J., Josse, V., Zuo, Z., Bernard, A., Hambrecht, B., Lugan, P., Clément, D., Sanchez-Palencia, L., Bouyer, P. and Aspect, A. (2008). Direct observation of anderson localization of matter waves in a controlled disorder. *Nature*, **453**.

Binder, F., Correa, L., Gogolin, C., Anders, J. and Adesso, G. (2018). *Thermodynamics in the quantum regime Fundamental Theories of Physics*. Berlin: Springer.

Binder, F., Correa, L.A., Gogolin, C., Anders, J. and Adesso, G. (2019). Thermodynamics in the quantum regime. *Fundamental Theories of Physics (Springer, 2018)*.

Blanter, Y. and Büttiker, M. (2000). Shot noise in mesoscopic conductors. *Physics Reports*, **336**, 1 – 166.

Bloch, I., Greiner, M., Mandel, O., Hänsch, T.W. and Esslinger, T. (2001). Sympathetic cooling of ^{85}Rb and ^{87}Rb. *Phys. Rev. A*, **64**, 021402.

Bloch, I., Dalibard, J. and Zwerger, W. (2008). Many-body physics with ultracold gases. *Rev. Mod. Phys.*, **80**, 885–964.

Bloch, I., Dalibard, J. and Nascimbene, S. (2012). Quantum simulations with ultracold quantum gases. *Nature Physics*, **8**, 267.

Blum, J., Bruns, S., Rademacher, D., Voss, A., Willenberg, B. and Krause, M. (2006). Measurement of the translational and rotational brownian motion of individual particles in a rarefied gas. *Phys. Rev. Lett.*, **97**, 230601.

Bogolyubov, N.N. (1947). On the theory of superfluidity. *J. Phys.(USSR)*, **11**, 23–32.

Boixo, S., Flammia, S.T., Caves, C.M. and Geremia, J. (2007). Generalized limits for single-parameter quantum estimation. *Phys. Rev. Lett.*, **98**, 090401.

Bonart, J. and Cugliandolo, L.F. (2012a). From nonequilibrium quantum brownian motion to impurity dynamics in one-dimensional quantum liquids. *Phys. Rev. A*, **86**, 023636.

Bonart, J. and Cugliandolo, L.F. (2012b). From nonequilibrium quantum brownian motion to impurity dynamics in one-dimensional quantum liquids. *Phys. Rev. A*, **86**, 023636.

Bonart, J. and Cugliandolo, L.F. (2013). Effective potential and polaronic mass shift in a trapped dynamical impurity–luttinger liquid system. *EPL (Europhysics Letters)*, **101**, 16003.

Bonato, C., Blok, M., Dinani, H., Berry, D., Markham, M., Twitchen, D. and Hanson, R. (2016). Optimized quantum sensing with a single electron spin using real-time adaptive

measurements. *Nature nanotechnology*, **11**, 247—252.

Bose, S. (1924). Planck's law and light quantum hypothesis. *Z. Phys*, **26**, 178.

Boss, J.M., Cujia, K.S., Zopes, J. and Degen, C.L. (2017). Quantum sensing with arbitrary frequency resolution. *Science*, **356**, 837–840.

Boto, A.N., Kok, P., Abrams, D.S., Braunstein, S.L., Williams, C.P. and Dowling, J.P. (2000). Quantum interferometric optical lithography: exploiting entanglement to beat the diffraction limit. *Physical Review Letters*, **85**, 2733.

Bouchaud, J.P. and Georges, A. (1990). Anomalous diffusion in disordered media: Statistical mechanisms, models and physical applications. *Physics Reports*, **195**, 127 – 293.

Boyanovsky, D. and Jasnow, D. (2017). Coherence of mechanical oscillators mediated by coupling to different baths. *Phys. Rev. A*, **96**, 012103.

Brandão, F., Horodecki, M., Ng, N., Oppenheim, J. and Wehner, S. (2015). The second laws of quantum thermodynamics. *Proceedings of the National Academy of Sciences*, **112**, 3275–3279.

Brantut, J.P., Grenier, C., Meineke, J., Stadler, D., Krinner, S., Kollath, C., Esslinger, T. and Georges, A. (2013). A thermoelectric heat engine with ultracold atoms. *Science*, **342**, 713–715.

Braun, D. (2002). Creation of entanglement by interaction with a common heat bath. *Phys. Rev. Lett.*, **89**, 277901.

Braunstein, S.L. and Caves, C.M. (1994). Statistical distance and the geometry of quantum states. *Phys. Rev. Lett.*, **72**, 3439–3443.

Breuer, H. and Petruccione, F. (2007a). *The Theory of Open Quantum Systems*. OUP Oxford.

Breuer, H. and Petruccione, F. (2007b). *The Theory of Open Quantum Systems*. OUP, Oxford.

Breuer, H.P., Petruccione, F. *et al.* (2002). *The theory of open quantum systems*. Oxford University Press on Demand.

Breuer, H.P., Laine, E.M. and Piilo, J. (2009). Measure for the degree of non-markovian behavior of quantum processes in open systems. *Phys. Rev. Lett.*, **103**, 210401.

Brida, G., Genovese, M. and Berchera, I.R. (2010). Experimental realization of sub-shot-

noise quantum imaging. *Nature Photonics*, **4**, 227.

Brown, E.G., Martín-Martínez, E., Menicucci, N.C. and Mann, R.B. (2013). Detectors for probing relativistic quantum physics beyond perturbation theory. *Phys. Rev. D*, **87**, 084062.

Brown, R. (1828). Xxvii. a brief account of microscopical observations made in the months of june, july and august 1827, on the particles contained in the pollen of plants; and on the general existence of active molecules in organic and inorganic bodies. *The Philosophical Magazine*, **4**, 161–173.

Bruderer, M., Klein, A., Clark, S.R. and Jaksch, D. (2007). Polaron physics in optical lattices. *Phys. Rev. A*, **76**, 011605.

Brunelli, M., Olivares, S. and Paris, M.G.A. (2011). Qubit thermometry for micromechanical resonators. *Phys. Rev. A*, **84**, 032105.

Bunde, A. and Havlin, S. (1994). *Fractals in science*. Springer-Verlag Berlin Heidelberg.

Cai, Z. and Barthel, T. (2013). Algebraic versus exponential decoherence in dissipative many-particle systems. *Phys. Rev. Lett.*, **111**, 150403.

Cañizares, J.S. and Sols, F. (1994). Translational symmetry and microscopic preparation in oscillator models of quantum dissipation. *Physica A: Statistical Mechanics and its Applications*, **212**, 181 – 193.

Caldeira, A. and Leggett, A. (1983a). Path integral approach to quantum brownian motion. *Physica A: Statistical Mechanics and its Applications*, **121**, 587 – 616.

Caldeira, A. and Leggett, A. (1983b). Quantum tunnelling in a dissipative system. *Annals of Physics*, **149**, 374–456.

Caldeira, A.O. and Leggett, A.J. (1981). Influence of dissipation on quantum tunneling in macroscopic systems. *Phys. Rev. Lett.*, **46**, 211–214.

Callen, H.B. and Welton, T.A. (1951). Irreversibility and generalized noise. *Phys. Rev.*, **83**, 34–40.

Camacho-Guardian, A., Pena Ardila, L.A., Pohl, T. and G.M., B. (2018). Bipolarons in a bose-einstein condensate. *arxiv:1804.00402.pdf*.

Camalet, S., Lehmann, J., Kohler, S. and Hänggi, P. (2003). Current noise in ac-driven nanoscale conductors. *Phys. Rev. Lett.*, **90**, 210602.

Camalet, S., Kohler, S. and Hänggi, P. (2004). Shot-noise control in ac-driven nanoscale

conductors. *Phys. Rev. B*, **70**, 155326.

Campbell, S., Mehboudi, M., Chiara, G.D. and Paternostro, M. (2017). Global and local thermometry schemes in coupled quantum systems. *New Journal of Physics*, **19**, 103003.

Campbell, S., Genoni, M.G. and Deffner, S. (2018). Precision thermometry and the quantum speed limit. *Quantum Science and Technology*, **3**, 025002.

Campisi, M., Hänggi, P. and Talkner, P. (2011). Colloquium: Quantum fluctuation relations: Foundations and applications. *Rev. Mod. Phys.*, **83**, 771–791.

Caso, A., Arrachea, L. and Lozano, G. (2012). *Eur. Phys. J. B*, **85**, 266.

Casteels, W., Tempere, J. and Devreese, J.T. (2012). Polaronic properties of an impurity in a bose-einstein condensate in reduced dimensions. *Phys. Rev. A*, **86**, 043614.

Casteels, W., Tempere, J. and Devreese, J.T. (2013). Bipolarons and multipolarons consisting of impurity atoms in a bose-einstein condensate. *Phys. Rev. A*, **88**, 013613.

Catani, J., Lamporesi, G., Naik, D., Gring, M., Inguscio, M., Minardi, F., Kantian, A. and Giamarchi, T. (2012a). Quantum dynamics of impurities in a one-dimensional bose gas. *Phys. Rev. A*, **85**, 023623.

Catani, J., Lamporesi, G., Naik, D., Gring, M., Inguscio, M., Minardi, F., Kantian, A. and Giamarchi, T. (2012b). Quantum dynamics of impurities in a one-dimensional bose gas. *Phys. Rev. A*, **85**, 023623.

Caves, C.M. (1981). Quantum-mechanical noise in an interferometer. *Phys. Rev. D*, **23**, 1693–1708.

Cavina, V., Mancino, L., De Pasquale, A., Gianani, I., Sbroscia, M., Booth, R.I., Roccia, E., Raimondi, R., Giovannetti, V. and Barbieri, M. (2018). Bridging thermodynamics and metrology in nonequilibrium quantum thermometry. *Phys. Rev. A*, **98**, 050101.

Celi, A., Sanpera, A., Ahufinger, V. and Lewenstein, M. (2016). Quantum optics and frontiers of physics: the third quantum revolution. *Physica Scripta*, **92**, 013003.

Chang, C.W., Okawa, D., Majumdar, A. and Zettl, A. (2006). Solid-state thermal rectifier. *Science*, **314**, 1121–1124.

Chang, L.D. and Chakravarty, S. (1985). Dissipative dynamics of a two-state system coupled to a heat bath. *Phys. Rev. B*, **31**, 154–164.

Charalambous, C., Muñoz Gil, G., Celi, A., Garcia-Parajo, M.F., Lewenstein, M., Manzo,

C. and García-March, M.A. (2017). Nonergodic subdiffusion from transient interactions with heterogeneous partners. *Phys. Rev. E*, **95**, 032403.

Charalambous, C., Garcia-March, M., Lampo, A., Mehboudi, M. and Lewenstein, M. (2019a). Two distinguishable impurities in BEC: squeezing and entanglement of two Bose polarons. *SciPost Phys.*, **6**, 10.

Charalambous, C., Garcia-March, M.A., Mehboudi, M. and Lewenstein, M. (2019b). Heat current control in trapped bose–einstein condensates. *New Journal of Physics*, **21**, 083037.

Cherstvy, A.G. and Metzler, R. (2013). Population splitting, trapping, and non-ergodicity in heterogeneous diffusion processes. *Phys. Chem. Chem. Phys.*, **15**, 20220–20235.

Cherstvy, A.G., Chechkin, A.V. and Metzler, R. (2013). Anomalous diffusion and ergodicity breaking in heterogeneous diffusion processes. *New Journal of Physics*, **15**, 083039.

Cherstvy, A.G., Chechkin, A.V. and Metzler, R. (2014). Particle invasion, survival, and non-ergodicity in 2d diffusion processes with space-dependent diffusivity. *Soft Matter*, **10**, 1591–1601.

Chin, A.W., Huelga, S.F. and Plenio, M.B. (2012). Quantum metrology in non-markovian environments. *Phys. Rev. Lett.*, **109**, 233601.

Christensen, R.S., Levinsen, J. and Bruun, G.M. (2015a). Quasiparticle properties of a mobile impurity in a bose-einstein condensate. *Phys. Rev. Lett.*, **115**, 160401.

Christensen, R.S., Levinsen, J. and Bruun, G.M. (2015b). Quasiparticle properties of a mobile impurity in a bose-einstein condensate. *Phys. Rev. Lett.*, **115**, 160401.

Chruściński, D. and Maniscalco, S. (2014). Degree of non-markovianity of quantum evolution. *Phys. Rev. Lett.*, **112**, 120404.

Chubynsky, M.V. and Slater, G.W. (2014). Diffusing diffusivity: A model for anomalous, yet brownian, diffusion. *Phys. Rev. Lett.*, **113**, 098302.

Cirone, M.A., Chiara, G.D., Palma, G.M. and Recati, A. (2009). Collective decoherence of cold atoms coupled to a bose–einstein condensate. *New Journal of Physics*, **11**, 103055.

Claude, C.t. and David, G.o. (2011). *Advances In Atomic Physics: An Overview*. World Scientific.

Cohen, D. (1997). Unified model for the study of diffusion localization and dissipation.

Phys. Rev. E, **55**, 1422–1441.

Coleman, S. and Norton, R.E. (1962a). Runaway modes in model field theories. *Phys. Rev.*, **125**, 1422–1428.

Coleman, S. and Norton, R.E. (1962b). Runaway modes in model field theories. *Phys. Rev.*, **125**, 1422–1428.

Cornish, S.L. and Cassettari, D. (2003). Recent progress in bose-einstein condensation experiments. *Philosophical Transactions of the Royal Society of London. Series A: Mathematical, Physical and Engineering Sciences*, **361**, 2699–2713.

Correa, L.A., Valido, A.A. and Alonso, D. (2012). Asymptotic discord and entanglement of nonresonant harmonic oscillators under weak and strong dissipation. *Phys. Rev. A*, **86**, 012110.

Correa, L.A., Mehboudi, M., Adesso, G. and Sanpera, A. (2015). Individual quantum probes for optimal thermometry. *Phys. Rev. Lett.*, **114**, 220405.

Correa, L.A., Perarnau-Llobet, M., Hovhannisyan, K.V., Hernández-Santana, S., Mehboudi, M. and Sanpera, A. (2017). Enhancement of low-temperature thermometry by strong coupling. *Phys. Rev. A*, **96**, 062103.

Côté, R., Kharchenko, V. and Lukin, M.D. (2002). Mesoscopic molecular ions in bose-einstein condensates. *Phys. Rev. Lett.*, **89**, 093001.

Cramér, H. (1999). *Mathematical methods of statistics*, vol. 9. Princeton university press.

Cucchietti, F.M. and Timmermans, E. (2006a). Strong-coupling polarons in dilute gas bose-einstein condensates. *Phys. Rev. Lett.*, **96**, 210401.

Cucchietti, F.M. and Timmermans, E. (2006b). Strong-coupling polarons in dilute gas bose-einstein condensates. *Phys. Rev. Lett.*, **96**, 210401.

D. Durr, S.G. and Lebowitz, J.L. (1981). A mechanical model of brownian motion. *Commun. Math. Phys.*, **78**, 507–530.

Dalfovo, F., Giorgini, S., Pitaevskii, L.P. and Stringari, S. (1999). Theory of bose-einstein condensation in trapped gases. *Rev. Mod. Phys.*, **71**, 463–512.

Das, S. and Dhar, A. (2012). Landauer formula for phonon heat conduction: relation between energy transmittance and transmission coefficient. *The European Physical Journal B*, **85**, 372.

Davies, E.B. (1974). Markovian master equations. *Comm. Math. Phys.*, **39**, 91–110.

Davis, K.B., Mewes, M.O., Andrews, M.R., van Druten, N.J., Durfee, D.S., Kurn, D.M. and Ketterle, W. (1995). Bose-einstein condensation in a gas of sodium atoms. *Phys. Rev. Lett.*, **75**, 3969–3973.

de Broglie, L. (1925). Researches on the quantum theory. *Annalen der Physik*, **3**, 22–32.

de Faria, J.G.P. and Nemes, M.C. (1998). Phenomenological criteria for the validity of quantum markovian equations. *Journal of Physics A: Mathematical and General*, **31**, 7095–7103.

De Gennes, P. (1966). Superconductivity of metals and alloys wa benjamin. *Inc., New York*.

de Groot, S. and Mazur, P. (1962). Non-equilibrium thermodynamics, corrected reprint by dover publications. *Inc., New York, NY, USA*.

De Pasquale, A., Rossini, D., Fazio, R. and Giovannetti, V. (2016). Local quantum thermal susceptibility. *Nature communications*, **7**, 12782.

de Vega, I. and Alonso, D. (2017a). Dynamics of non-markovian open quantum systems. *Rev. Mod. Phys.*, **89**, 015001.

de Vega, I. and Alonso, D. (2017b). Dynamics of non-markovian open quantum systems. *Rev. Mod. Phys.*, **89**, 015001.

de Vega, I., Alonso, D. and Gaspard, P. (2005). Two-level system immersed in a photonic band-gap material: A non-markovian stochastic schrödinger-equation approach. *Phys. Rev. A*, **71**, 023812.

de Vega, I., Porras, D. and Ignacio Cirac, J. (2008). Matter-wave emission in optical lattices: Single particle and collective effects. *Phys. Rev. Lett.*, **101**, 260404.

Debarba, T. and Fanchini, F.F. (2017). Non-markovianity quantifier of an arbitrary quantum process. *Phys. Rev. A*, **96**, 062118.

Debye, P. (1912). Zur theorie der spezifischen wärmen. *Annalen der Physik*, **344**, 789–839.

Deffner, S., Jarzynski, C. and del Campo, A. (2014). Classical and quantum shortcuts to adiabaticity for scale-invariant driving. *Phys. Rev. X*, **4**, 021013.

Dehkharghani, A.S., Volosniev, A.G. and Zinner, N.T. (2018). Interaction-driven coalescence of two impurities in a one-dimensional bose gas. *arXiv:1712.01538*.

Deissler, B., Zaccanti, M., Roati, G., D'Errico, C., Fattori, M., Modugno, M., Modugno, G. and Inguscio, M. (2010). Delocalization of a disordered bosonic system by repulsive

interactions. *Nature Physics*, **6**.

Demkowicz-Dobrzański, R., Kołodyński, J. and Guţă, M. (2012). The elusive heisenberg limit in quantum-enhanced metrology. *Nature communications*, **3**, 1063.

Devreese, J. (1996). Encyclopedia of applied physics. **14**.

Devreese, J. (2016). Fr\" ohlich polarons. lecture course including detailed theoretical derivations. *arXiv preprint arXiv:1611.06122*.

Devreese, J.T. and Alexandrov, A.S. (2009a). Fröhlich polaron and bipolaron: recent developments. *Reports on Progress in Physics*, **72**, 066501.

Devreese, J.T. and Alexandrov, A.S. (2009b). Fröhlich polaron and bipolaron: recent developments. *Reports on Progress in Physics*, **72**, 066501.

Dhar, A. (2008). Heat transport in low-dimensional systems. *Advances in Physics*, **57**, 457–537.

Dhar, A. and Dandekar, R. (2015). Heat transport and current fluctuations in harmonic crystals. *Physica A: Statistical Mechanics and its Applications*, **418**, 49 – 64, proceedings of the 13th International Summer School on Fundamental Problems in Statistical Physics.

Dhar, A. and Sen, D. (2006). Nonequilibrium green's function formalism and the problem of bound states. *Phys. Rev. B*, **73**, 085119.

Dhar, A. and Sriram Shastry, B. (2003). Quantum transport using the ford-kac-mazur formalism. *Phys. Rev. B*, **67**, 195405.

Dhont, J. (1996). An introduction to dynamics of colloids, volume 2 of. *Studies in Interface Science*.

Diósi, L. (1993). On high-temperature markovian equation for quantum brownian motion. *Europhysics Letters (EPL)*, **22**, 1–3.

Doll, R., Wubs, M., Hänggi, P. and Kohler, S. (2007). Incomplete pure dephasing of n-qubit entangled w states. *Phys. Rev. B*, **76**, 045317.

Doll, R., Wubs, M., Hänggi, P. and Kohler, S. (2006). Limitation of entanglement due to spatial qubit separation. *Europhys. Lett.*, **76**, 547–553.

Donsa, S., Hofstätter, H., Koch, O., Burgdörfer, J. and Březinová, I. (2017). Long-time expansion of a bose-einstein condensate: Observability of anderson localization. *Phys. Rev. A*, **96**, 043630.

Dorner, U., Demkowicz-Dobrzanski, R., Smith, B.J., Lundeen, J.S., Wasilewski, W., Banaszek, K. and Walmsley, I.A. (2009). Optimal quantum phase estimation. *Phys. Rev. Lett.*, **102**, 040403.

Dowling, J.P. and Seshadreesan, K.P. (2015). Quantum optical technologies for metrology, sensing, and imaging. *J. Lightwave Technol.*, **33**, 2359–2370.

D.S. Petrov, D.M. Gangardt and G.V. Shlyapnikov (2004). Low-dimensional trapped gases. *J. Phys. IV France*, **116**, 5–44.

Duarte, O.S. and Caldeira, A.O. (2006). Effective coupling between two brownian particles. *Phys. Rev. Lett.*, **97**, 250601.

Duarte, O.S. and Caldeira, A.O. (2009). Effective quantum dynamics of two brownian particles. *Phys. Rev. A*, **80**, 032110.

Dubi, Y. and Di Ventra, M. (2011). Colloquium: Heat flow and thermoelectricity in atomic and molecular junctions. *Rev. Mod. Phys.*, **83**, 131–155.

Dümcke, R. and Spohn, H. (1979). The proper form of the generator in the weak coupling limit. *Zeitschrift für Physik B Condensed Matter*, **34**, 419–422.

Eckern, U., Schön, G. and Ambegaokar, V. (1984). Quantum dynamics of a superconducting tunnel junction. *Phys. Rev. B*, **30**, 6419–6431.

Eckern, U., Lehr, W., Menzel-Dorwarth, A., Pelzer, F. and Schmid, A. (1990). The quasiclassical langevin equation and its application to the decay of a metastable state and to quantum fluctuations. *Journal of Statistical Physics*, **59**, 885–934.

Eckert, K., Romero-Isart, O., Rodriguez, M., Lewenstein, M., Polzik, E.S. and Sanpera, A. (2008). Quantum non-demolition detection of strongly correlated systems. *Nature Physics*, **4**, 50.

Efimkin, D.K., Hofmann, J. and Galitski, V. (2016a). Non-markovian quantum friction of bright solitons in superfluids. *Phys. Rev. Lett.*, **116**, 225301.

Efimkin, D.K., Hofmann, J. and Galitski, V. (2016b). Non-markovian quantum friction of bright solitons in superfluids. *Phys. Rev. Lett.*, **116**, 225301.

Einstein, A. (1905). Uber die von der molekularkinetischen theorie der warme geforderte bewegung von in ruhenden flussigkeiten suspendierten teilchen. *Ann. Phys.*, **17**, 549–560.

Einstein, A. (1906). Zur theorie der brownschen bewegung. *Annalen der Physik*, **324**,

371–381.

Einstein, A. (1907). Theoretische bemerkungen Über die brownsche bewegung. *Zeitschrift für Elektrochemie und angewandte physikalische Chemie*, **13**, 41–42.

Einstein, A. (1908). Elementare theorie der brownschen) bewegung. *Zeitschrift für Elektrochemie und angewandte physikalische Chemie*, **14**, 235–239.

Einstein, A. (1925). Sitzungsber. *Kgl. Preuss. Akad. Wiss*, **3**, 261.

Escher, B., de Matos Filho, R. and Davidovich, L. (2011). General framework for estimating the ultimate precision limit in noisy quantum-enhanced metrology. *Nature Physics*, **7**, 406.

Esposito, M., Lindenberg, K. and den Broeck, C.V. (2010). Entropy production as correlation between system and reservoir. *New Journal of Physics*, **12**, 013013.

Fadel, M., Zibold, T., Décamps, B. and Treutlein, P. (2018). Spatial entanglement patterns and einstein-podolsky-rosen steering in bose-einstein condensates. *Science*, **360**, 409.

Ferialdi, L. (2017). Dissipation in the caldeira-leggett model. *Phys. Rev. A*, **95**, 052109.

Feynman, R.P. (1955). Slow electrons in a polar crystal. *Phys. Rev.*, **97**, 660–665.

Fisher, M.P.A., Weichman, P.B., Grinstein, G. and Fisher, D.S. (1989). Boson localization and the superfluid-insulator transition. *Phys. Rev. B*, **40**, 546–570.

Flach, S., Krimer, D.O. and Skokos, C. (2009). Universal spreading of wave packets in disordered nonlinear systems. *Phys. Rev. Lett.*, **102**, 024101.

Fleming, C. and Hu, B. (2012). Non-markovian dynamics of open quantum systems: Stochastic equations and their perturbative solutions. *Annals of Physics*, **327**, 1238 – 1276.

Fleming, C.H. and Cummings, N.I. (2011). Accuracy of perturbative master equations. *Phys. Rev. E*, **83**, 031117.

Fleming, C.H., Roura, A. and Hu, B. (2011). Exact analytical solutions to the master equation of quantum brownian motion for a general environment. *Annals of Physics*, **326**, 1207.

Fleming, C.H., Cummings, N.I., Anastopoulos, C. and Hu, B.L. (2012). Non-markovian dynamics and entanglement of two-level atoms in a common field. *Journal of Physics A: Mathematical and Theoretical*, **45**, 065301.

Fölling, S., Gerbier, F., Widera, A., Mandel, O., Gericke, T. and Bloch, I. (2005). Spatial quantum noise interferometry in expanding ultracold atom clouds. *Nature*, **434**, 481.

Ford, G.W. (2017). The fluctuation–dissipation theorem. *Contemporary Physics*, **58**, 244–252.

Ford, G.W. and Kac, M. (1987). On the quantum langevin equation. *Journal of Statistical Physics*, **46**, 803–810.

Ford, G.W., Kac, M. and Mazur, P. (1965). Statistical mechanics of assemblies of coupled oscillators. *Journal of Mathematical Physics*, **6**, 504–515.

Ford, G.W., Lewis, J.T. and O'Connell, R.F. (1988). Quantum langevin equation. *Phys. Rev. A*, **37**, 4419–4428.

Frank, R.L., Lieb, E.H., Seiringer, R. and Thomas, L.E. (2010). Bi-polaron and n-polaron binding energies. *Phys. Rev. Lett.*, **104**, 210402.

Freitas, N. and Paz, J.P. (2017). Fundamental limits for cooling of linear quantum refrigerators. *Phys. Rev. E*, **95**, 012146.

Fröhlich, H. (1954). Electrons in lattice fields. *Advances in Physics*, **3**, 325–361.

Fröhlich, H., Pelzer, H. and Zienau, S. (1950). Xx. properties of slow electrons in polar materials. *The London, Edinburgh, and Dublin Philosophical Magazine and Journal of Science*, **41**, 221–242.

Fröhlich, H. (1963). Polarons and excitons. *edited by CG Kuper and GD Whitfield, Plenum, New York*.

Galperin, M., Nitzan, A. and Ratner, M.A. (2007). Heat conduction in molecular transport junctions. *Phys. Rev. B*, **75**, 155312.

Galve, F. and Zambrini, R. (2018). Coherent and radiative couplings through two-dimensional structured environments. *Phys. Rev. A*, **97**, 033846.

Gardiner, C. (2009). *Stochastic methods*, vol. 4. Springer Berlin.

Gardiner, C. and Zoller, P. (2004). *Quantum Noise: A Handbook of Markovian and Non-Markovian Quantum Stochastic Methods with Applications to Quantum Optics*. Springer Series in Synergetics, Springer, Berlin.

Gati, R. and Oberthaler, M.K. (2007). A bosonic josephson junction. *Journal of Physics B: Atomic, Molecular and Optical Physics*, **40**, R61–R89.

Gati, R., Hemmerling, B., Fölling, J., Albiez, M. and Oberthaler, M.K. (2006). Noise thermometry with two weakly coupled bose-einstein condensates. *Phys. Rev. Lett.*, **96**, 130404.

Gauger, E.M., Rieper, E., Morton, J.J.L., Benjamin, S.C. and Vedral, V. (2011). Sustained quantum coherence and entanglement in the avian compass. *Phys. Rev. Lett.*, **106**, 040503.

Gaunt, A.L., Schmidutz, T.F., Gotlibovych, I., Smith, R.P. and Hadzibabic, Z. (2013). Bose-einstein condensation of atoms in a uniform potential. *Phys. Rev. Lett.*, **110**, 200406.

Gelbwaser-Klimovsky, D. and Aspuru-Guzik, A. (2015). Strongly coupled quantum heat machines. *The journal of physical chemistry letters*, **6**, 3477–3482.

Gerlach, B. and Löwen, H. (1991). Analytical properties of polaron systems or: Do polaronic phase transitions exist or not? *Rev. Mod. Phys.*, **63**, 63–90.

Gühne, O. and Tóth, G. (2009). Entanglement detection. *Physics Reports*, **474**, 1 – 75.

Giazotto, F., Heikkilä, T.T., Luukanen, A., Savin, A.M. and Pekola, J.P. (2006). Opportunities for mesoscopics in thermometry and refrigeration: Physics and applications. *Rev. Mod. Phys.*, **78**, 217–274.

Giorgini, S., Pitaevskii, L.P. and Stringari, S. (2008). Theory of ultracold atomic fermi gases. *Rev. Mod. Phys.*, **80**, 1215–1274.

Giovanazzi, S., Görlitz, A. and Pfau, T. (2002). Tuning the dipolar interaction in quantum gases. *Phys. Rev. Lett.*, **89**, 130401.

Giovannetti, V. and Vitali, D. (2001). Phase-noise measurement in a cavity with a movable mirror undergoing quantum brownian motion. *Phys. Rev. A*, **63**, 023812.

Giovannetti, V., Lloyd, S. and Maccone, L. (2004). Quantum-enhanced measurements: beating the standard quantum limit. *Science*, **306**, 1330–1336.

Giovannetti, V., Lloyd, S. and Maccone, L. (2006). Quantum metrology. *Phys. Rev. Lett.*, **96**, 010401.

Giovannetti, V., Lloyd, S. and Maccone, L. (2011). Advances in quantum metrology. *Nature photonics*, **5**, 222.

Giraldi, F. and Petruccione, F. (2014). Fractional relaxations in photonic crystals. *Journal of Physics A: Mathematical and Theoretical*, **47**, 395304.

Gogolin, C. and Eisert, J. (2016). Equilibration, thermalisation, and the emergence of statistical mechanics in closed quantum systems. *Reports on Progress in Physics*, **79**, 056001.

Goychuk, I. (2012). *Viscoelastic Subdiffusion: Generalized Langevin Equation Approach*, 187–253. John Wiley Sons, Ltd.

Goychuk, I. and Hänggi, P. (2007). Anomalous escape governed by thermal $1/f$ noise. *Phys. Rev. Lett.*, **99**, 200601.

Grabert, H., Weiss, U. and Talkner, P. (1984). Quantum theory of the damped harmonic oscillator. *Zeitschrift für Physik B Condensed Matter*, **55**, 87–94.

Grabert, H., Schramm, P. and Ingold, G.L. (1988). Quantum brownian motion: The functional integral approach. *Physics Reports*, **168**, 115 – 207.

Green, M.S. (1952). Markoff random processes and the statistical mechanics of time-dependent phenomena. *The Journal of Chemical Physics*, **20**, 1281–1295.

Green, M.S. (1954). Markoff random processes and the statistical mechanics of time-dependent phenomena. ii. irreversible processes in fluids. *The Journal of Chemical Physics*, **22**, 398–413.

Greiner, M., Mandel, O., Esslinger, T., Hänsch, T.W. and Bloch, I. (2002). Quantum phase transition from a superfluid to a mott insulator in a gas of ultracold atoms. *nature*, **415**, 39.

Greiner, W. (2009). *Classical mechanics: systems of particles and Hamiltonian dynamics*. Springer Science & Business Media.

Grifoni, M. and Hänggi, P. (1998). Driven quantum tunneling. *Physics Reports*, **304**, 229 – 354.

Gross, E.P. (1961). Structure of a quantized vortex in boson systems. *Il Nuovo Cimento (1955-1965)*, **20**, 454–477.

Grossmann, S. and Holthaus, M. (1995a). Bose-einstein condensation and condensate tunneling. *Zeitschrift für Naturforschung A*, **50**, 323–326.

Grossmann, S. and Holthaus, M. (1995b). On bose-einstein condensation in harmonic traps. *Physics Letters A*, **208**, 188–192.

Groth, S., Krüger, P., Wildermuth, S., Folman, R., Fernholz, T., Schmiedmayer, J., Mahalu, D. and Bar-Joseph, I. (2004). Atom chips: Fabrication and thermal properties.

Applied Physics Letters, **85**, 2980–2982.

Grusdt, F. and Demler, E. (2015). New theoretical approaches to bose polarons. *Quantum Matter at Ultralow Temperatures*, 325–411.

Grusdt, F., Shashi, A., Abanin, D. and Demler, E. (2014). Bloch oscillations of bosonic lattice polarons.

Grusdt, F., Shchadilova, Y.E., Rubtsov, A.N. and Demler, E. (2015). Renormalization group approach to the fröhlich polaron model: application to impurity-bec problem. *Scientific reports*, **5**, 12124.

Grusdt, F., Astrakharchik, G.E. and Demler, E. (2017a). Bose polarons in ultracold atoms in one dimension: beyond the fröhlich paradigm. *New Journal of Physics*, **19**, 103035.

Grusdt, F., Schmidt, R., Shchadilova, Y.E. and Demler, E. (2017b). Strong-coupling bose polarons in a bose-einstein condensate. *Phys. Rev. A*, **96**, 013607.

Guarnieri, G., Uchiyama, C. and Vacchini, B. (2016). Energy backflow and non-markovian dynamics. *Phys. Rev. A*, **93**, 012118.

Guenther, N.E., Massignan, P., Lewenstein, M. and Bruun, G.M. (2018a). Bose polarons at finite temperature and strong coupling. *Phys. Rev. Lett.*, **120**, 050405.

Guenther, N.E., Massignan, P., Lewenstein, M. and Bruun, G.M. (2018b). Bose polarons at finite temperature and strong coupling. *Phys. Rev. Lett.*, **120**, 050405.

Haake, F. (1982). Systematic adiabatic elimination for stochastic processes. *Zeitschrift für Physik B Condensed Matter*, **48**, 31–35.

Haake, F. and Lewenstein, M. (1983). Adiabatic drag and initial slip in random processes. *Phys. Rev. A*, **28**, 3606–3612.

Haake, F., Lewenstein, M. and Reibold, R. (1985). Adiabatic drag and initial slips for random processes with slow and fast variables. In L. Accardi and W. von Waldenfels, eds., *Quantum Probability and Applications II*, 268–275, Springer Berlin Heidelberg, Berlin, Heidelberg.

Haikka, P., McEndoo, S., De Chiara, G., Palma, G.M. and Maniscalco, S. (2011). Quantifying, characterizing, and controlling information flow in ultracold atomic gases. *Phys. Rev. A*, **84**, 031602.

Hakim, V. and Ambegaokar, V. (1985). Quantum theory of a free particle interacting with a linearly dissipative environment. *Phys. Rev. A*, **32**, 423–434.

Hänggi, P. (1997). Generalized langevin equations: A useful tool for the perplexed modeller of nonequilibrium fluctuations? In *Stochastic dynamics*, 15–22, Springer.

Hänggi, P., Talkner, P. and Borkovec, M. (1990). Reaction-rate theory: fifty years after kramers. *Rev. Mod. Phys.*, **62**, 251–341.

Hanggi, P., Marchesoni, F. and Nori, F. (2005). *Annalen der Physik*, **14**, 51.

Heaney, L., Anders, J., Kaszlikowski, D. and Vedral, V. (2007). Spatial entanglement from off diagonal long range order in a bose-einstein condensate. *Phys. Rev. A*, **76**, 053605.

Helstrom, C.W. (1976). *Quantum detection and estimation theory*. Academic press.

Hänggi, P. and Thomas, H. (1982). Stochastic processes: Time evolution, symmetries and linear response. *Physics Reports*, **88**, 207 – 319.

Ho, T.L. (1998). Spinor bose condensates in optical traps. *Phys. Rev. Lett.*, **81**, 742–745.

Hofer, P.P., Perarnau-Llobet, M., Miranda, L.D.M., Haack, G., Silva, R., Brask, J.B. and Brunner, N. (2017). Markovian master equations for quantum thermal machines: local versus global approach. *New Journal of Physics*, **19**, 123037.

Hohenberg, P.C. (1967). Existence of long-range order in one and two dimensions. *Phys. Rev.*, **158**, 383–386.

Holevo, A.S. (2003). *Statistical structure of quantum theory*, vol. 67. Springer Science & Business Media.

Holland, M.J. and Burnett, K. (1993). Interferometric detection of optical phase shifts at the heisenberg limit. *Phys. Rev. Lett.*, **71**, 1355–1358.

Hörhammer, C. and Büttner, H. (2008). Environment-induced two-mode entanglement in quantum brownian motion. *Phys. Rev. A*, **77**, 042305.

Horodecki, M., Horodecki, P. and Horodecki, R. (1996). Separability of mixed states: necessary and sufficient conditions. *Physics Letters A*, **223**, 1 – 8.

Horodecki, M., Horodecki, P. and Horodecki, R. (1998). Mixed-state entanglement and distillation: Is there a "bound" entanglement in nature? *Phys. Rev. Lett.*, **80**, 5239–5242.

Horodecki, R., Horodecki, P., Horodecki, M. and Horodecki, K. (2009a). Quantum entanglement. *Rev. Mod. Phys.*, **81**, 865–942.

Horodecki, R., Horodecki, P., Horodecki, M. and Horodecki, K. (2009b). Quantum entan-

glement. *Rev. Mod. Phys.*, **81**, 865–942.

Hottovy, S., Volpe, G. and Wehr, J. (2012). Noise-induced drift in stochastic differential equations with arbitrary friction and diffusion in the smoluchowski-kramers limit. *Journal of Statistical Physics*, **146**, 762–773.

Hovhannisyan, K.V. and Correa, L.A. (2018). Measuring the temperature of cold many-body quantum systems. *Phys. Rev. B*, **98**, 045101.

Hsiang, J.T. and Hu, B. (2015). Quantum entanglement at high temperatures? bosonic systems in nonequilibrium steady state.

Hu, B. and Yang, L. (2005). Heat conduction in the frenkel–kontorova model. *Chaos: An Interdisciplinary Journal of Nonlinear Science*, **15**, 015119.

Hu, B., Yang, L. and Zhang, Y. (2006). Asymmetric heat conduction in nonlinear lattices. *Phys. Rev. Lett.*, **97**, 124302.

Hu, B.L., Paz, J.P. and Zhang, Y. (1992). Quantum brownian motion in a general environment: Exact master equation with nonlocal dissipation and colored noise. *Phys. Rev. D*, **45**, 2843–2861.

Huang, R., Chavez, I., Taute, K.M., Lukić, B., Jeney, S., Raizen, M. and Florin, E.L. (2011). Direct observation of the full transition from ballistic to diffusive brownian motion in a liquid. *Nature Physics*, **7**, 576–580.

Huelga, S.F., Macchiavello, C., Pellizzari, T., Ekert, A.K., Plenio, M.B. and Cirac, J.I. (1997). Improvement of frequency standards with quantum entanglement. *Phys. Rev. Lett.*, **79**, 3865–3868.

Humphreys, P.C., Barbieri, M., Datta, A. and Walmsley, I.A. (2013). Quantum enhanced multiple phase estimation. *Phys. Rev. Lett.*, **111**, 070403.

Hurst, H.M., Efimkin, D.K., Spielman, I.B. and Galitski, V. (2017a). Kinetic theory of dark solitons with tunable friction. *Phys. Rev. A*, **95**, 053604.

Hurst, H.M., Efimkin, D.K., Spielman, I.B. and Galitski, V. (2017b). Kinetic theory of dark solitons with tunable friction. *Phys. Rev. A*, **95**, 053604.

Ingen-Housz, J. (1785). *Nouvelles expériences et observations sur divers objets de physique*. chez Théophile Barrois le jeune.

Ingold, G.L. (2002). Path integrals and their application to dissipative quantum systems. In *Coherent Evolution in Noisy Environments*, 1–53, Springer.

Ingold, G.L. and Nazarov, Y.V. (1992). Charge tunneling rates in ultrasmall junctions. In *Single charge tunneling*, 21–107, Springer.

Inouye, S., Andrews, M., Stenger, J., Miesner, H.J., Stamper-Kurn, D. and Ketterle, W. (1998). Observation of feshbach resonances in a bose–einstein condensate. *Nature*, **392**, 151.

Iomin, A. (2010). Subdiffusion in the nonlinear schrödinger equation with disorder. *Phys. Rev. E*, **81**, 017601.

Islam, R., Ma, R., Preiss, P.M., Tai, M.E., Lukin, A., Rispoli, M. and Greiner, M. (2015). Measuring entanglement entropy in a quantum many-body system. *Nature*, **528**, 77.

Jacobs, K., Tittonen, I., Wiseman, H.M. and Schiller, S. (1999). Quantum noise in the position measurement of a cavity mirror undergoing brownian motion. *Phys. Rev. A*, **60**, 538–548.

Jaramillo, J., Beau, M. and del Campo, A. (2016). Quantum supremacy of many-particle thermal machines. *New Journal of Physics*, **18**, 075019.

Javanainen, J. (1986). Oscillatory exchange of atoms between traps containing bose condensates. *Phys. Rev. Lett.*, **57**, 3164–3166.

Jendrzejewski, F., Bernard, A., Müller, K., Cheinet, P., Josse, V., Piraud, M., Pezzé, L., Sanchez-Palencia, L., Aspect, A. and Bouyer, P. (2012). Three-dimensional localization of ultracold atoms in an optical disordered potential. *Nature Physics*, **8**.

John, S. and Quang, T. (1994). Spontaneous emission near the edge of a photonic band gap. *Phys. Rev. A*, **50**, 1764–1769.

Jørgensen, N.B., Wacker, L., Skalmstang, K.T., Parish, M.M., Levinsen, J., Christensen, R.S., Bruun, G.M. and Arlt, J.J. (2016). Observation of attractive and repulsive polarons in a bose-einstein condensate. *Phys. Rev. Lett.*, **117**, 055302.

Josephson, B. (1962). Possible new effects in superconductive tunnelling. *Physics Letters*, **1**, 251 – 253.

Jozsa, R. and Linden, N. (2003). On the role of entanglement in quantum computational speed up. **459**, 2011–2032.

Kadio, D., Gajda, M. and Rzażewski, K. (2005). Phase fluctuations of a bose-einstein condensate in low-dimensional geometry. *Phys. Rev. A*, **72**, 013607.

Kajari, E., Wolf, A., Lutz, E. and Morigi, G. (2012). Statistical mechanics of entanglement

mediated by a thermal reservoir. *Phys. Rev. A*, **85**, 042318.

Kane, J.W. and Kadanoff, L.P. (1967). Long-range order in superfluid helium. *Phys. Rev.*, **155**, 80–83.

Kato, A. and Tanimura, Y. (2016). Quantum heat current under non-perturbative and non-markovian conditions: Applications to heat machines. *The Journal of Chemical Physics*, **145**, 224105.

Katori, H. (2011). Optical lattice clocks and quantum metrology. *Nature Photonics*, **5**, 203.

Kawasaki, K. (1970). Kinetic equations and time correlation functions of critical fluctuations. *Annals of Physics*, **61**, 1 – 56.

Keesom, W. (1921). Van der waals attractive force. *Physikalische Zeitschrift*, **22**, 129–141.

Keser, A.C. and Galitski, V. (2018). Analogue stochastic gravity in strongly-interacting bose–einstein condensates. *Annals of Physics*, **395**, 84 – 111.

Ketterle, W. and van Druten, N.J. (1996). Bose-einstein condensation of a finite number of particles trapped in one or three dimensions. *Phys. Rev. A*, **54**, 656–660.

Kheifets, S., Simha, A., Melin, K., Li, T. and Raizen, M.G. (2014). Observation of brownian motion in liquids at short times: Instantaneous velocity and memory loss. *Science*, **343**, 1493–1496.

Kim, C. and Karniadakis, G.E. (2013). Microscopic theory of brownian motion revisited: The rayleigh model. *Phys. Rev. E*, **87**, 032129.

King, F.W. (2009). *Hilbert transforms*, vol. 2. Cambridge University Press Cambridge.

Kirsten, K. and Toms, D.J. (1996). Bose-einstein condensation of atomic gases in a general harmonic-oscillator confining potential trap. *Phys. Rev. A*, **54**, 4188–4203.

Kleinert, H. (2004). *Path Integrals in Quantum Mechanics, Statistics, Polymer Physics, and Financial Markets*.

Kliesch, M., Gogolin, C., Kastoryano, M.J., Riera, A. and Eisert, J. (2014). Locality of temperature. *Phys. Rev. X*, **4**, 031019.

Kofman, A., Kurizki, G. and Sherman, B. (1994). Spontaneous and induced atomic decay in photonic band structures. *Journal of Modern Optics*, **41**, 353–384.

Kofman, A.G. and Kurizki, G. (2004). Unified theory of dynamically suppressed qubit

decoherence in thermal baths. *Phys. Rev. Lett.*, **93**, 130406.

Kohen, D., Marston, C.C. and Tannor, D.J. (1997). Phase space approach to theories of quantum dissipation. *The Journal of Chemical Physics*, **107**, 5236–5253.

Kohler, H. and Sols, F. (2013). Minimal coupling in oscillator models of quantum dissipation. *Physica A: Statistical Mechanics and its Applications*, **392**, 1989 – 1993.

Kohler, S., Lehmann, J. and Hänggi, P. (2005). Driven quantum transport on the nanoscale. *Physics Reports*, **406**, 379 – 443.

Kohstall, C., Zaccanti, M., Jag, M., Trenkwalder, A., Massignan, P., Bruun, G.M., Schreck, F. and Grimm, R. (2012a). Metastability and coherence of repulsive polarons in a strongly interacting fermi mixture. *Nature*, **485**, 615–618.

Kohstall, C., Zaccanti, M., Jag, M., Trenkwalder, A., Massignan, P., Bruun, G.M., Schreck, F. and Grimm, R. (2012b). Metastability and coherence of repulsive polarons in a strongly interacting fermi mixture. *Nature*, **485**, 615.

Kolář, M., Gelbwaser-Klimovsky, D., Alicki, R. and Kurizki, G. (2012). Quantum bath refrigeration towards absolute zero: Challenging the unattainability principle. *Phys. Rev. Lett.*, **109**, 090601.

Kolodynski, J. (2014). Precision bounds in noisy quantum metrology. *arXiv preprint arXiv:1409.0535*.

Komar, P., Kessler, E.M., Bishof, M., Jiang, L., Sørensen, A.S., Ye, J. and Lukin, M.D. (2014). A quantum network of clocks. *Nature Physics*, **10**, 582.

Kopidakis, G., Komineas, S., Flach, S. and Aubry, S. (2008). Absence of wave packet diffusion in disordered nonlinear systems. *Phys. Rev. Lett.*, **100**, 084103.

Koschorreck, M., Pertot, D., Vogt, E., Fröhlich, B., Feld, M. and Köhl, M. (2012). Attractive and repulsive Fermi polarons in two dimensions. *Nature*, **485**, 619–622.

Kosloff, R. (2013). Quantum thermodynamics: A dynamical viewpoint. *Entropy*, **15**, 2100–2128.

Kosloff, R. and Levy, A. (2014). Quantum heat engines and refrigerators: Continuous devices. *Annual Review of Physical Chemistry*, **65**, 365–393, pMID: 24689798.

Kubo, R. (1957). Statistical-mechanical theory of irreversible processes. i. general theory and simple applications to magnetic and conduction problems. *Journal of the Physical Society of Japan*, **12**, 570–586.

Kubo, R. (1966). The fluctuation-dissipation theorem. *Reports on Progress in Physics*, **29**, 255–284.

Kubo, R. and Tomita, K. (1954). A general theory of magnetic resonance absorption. *Journal of the Physical Society of Japan*, **9**, 888–919.

Kucsko, G., Maurer, P.C., Yao, N.Y., Kubo, M., Noh, H.J., Lo, P.K., Park, H. and Lukin, M.D. (2013). Nanometre-scale thermometry in a living cell. *Nature*, **500**, 54.

Kunkel, P., Prüfer, M., Strobel, H., Linnemann, D., Frölian, A., Gasenzer, T., Gärttner, M. and Oberthaler, M.K. (2018). Spatially distributed multipartite entanglement enables epr steering of atomic clouds. *Science*, **360**, 413.

Lahaye, T., Menotti, C., Santos, L., Lewenstein, M. and Pfau, T. (2009). The physics of dipolar bosonic quantum gases. *Reports on Progress in Physics*, **72**, 126401.

Laine, E.M., Breuer, H.P., Piilo, J., Li, C.F. and Guo, G.C. (2012). Nonlocal memory effects in the dynamics of open quantum systems. *Phys. Rev. Lett.*, **108**, 210402.

Lambropoulos, P., Nikolopoulos, G.M., Nielsen, T.R. and Bay, S. (2000). Fundamental quantum optics in structured reservoirs. *Reports on Progress in Physics*, **63**, 455–503.

Lampo, A., Lim, S.H., García-March, M.Á. and Lewenstein, M. (2017a). Bose polaron as an instance of quantum Brownian motion. *Quantum*, **1**, 30.

Lampo, A., Lim, S.H., García-March, M.Á. and Lewenstein, M. (2017b). Bose polaron as an instance of quantum Brownian motion. *Quantum*, **1**, 30.

Lampo, A., Charalambous, C., García-March, M.A. and Lewenstein, M. (2018). Non-markovian polaron dynamics in a trapped bose-einstein condensate. *Phys. Rev. A*, **98**, 063630.

Lampo, A., March, M.Á.G. and Lewenstein, M. (2019). *Quantum Brownian motion revisited: extensions and applications*. Springer.

Lan, J. and Li, B. (2006). Thermal rectifying effect in two-dimensional anharmonic lattices. *Phys. Rev. B*, **74**, 214305.

Lan, Z. and Lobo, C. (2014). A single impurity in an ideal atomic Fermi gas: current understanding and some open problems. *J. Indian I. Sci.*, **94**, 179.

Landau, L. and Lifshitz, E. (1938). *Statistical Mechanics (Clarendon*. Oxford.

Landau, L. and Pekar, S. (1948a). Effective mass of a polaron. *Zh. Eksp. Teor. Fiz*, **18**, 419–423.

Landau, L.D. (1933). Electron motion in crystal lattices. *Phys. Z. Sowjet.*, **3**, 664.

Landau, L.D. and Lifshitz, E. (1965). *Quantum mechanics (volume 3 of a course of theoretical physics)*. Pergamon Press Oxford, UK.

Landau, L.D. and Pekar, S.I. (1948b). Effective mass of a polaron. *Zh. Eksp. Teor. Fiz.*.

Lange, K., Peise, J., Lücke, B., Kruse, I., Vitagliano, G., Apellaniz, I., Kleinmann, M., Tóth, G. and Klempt, C. (2018). Entanglement between two spatially separated atomic modes. *Science*, **360**, 416.

Langevin, P. (1908). Sur la theorie de mouvement brownien. *C. R. Acad. Sci. Paris.*, **146**.

Laptyeva, T.V., Bodyfelt, J.D., Krimer, D.O., Skokos, C. and Flach, S. (2010). The crossover from strong to weak chaos for nonlinear waves in disordered systems. *EPL (Europhysics Letters)*, **91**, 30001.

Larcher, M., Dalfovo, F. and Modugno, M. (2009). Effects of interaction on the diffusion of atomic matter waves in one-dimensional quasiperiodic potentials. *Phys. Rev. A*, **80**, 053606.

Leanhardt, A.E., Pasquini, T.A., Saba, M., Schirotzek, A., Shin, Y., Kielpinski, D., Pritchard, D.E. and Ketterle, W. (2003). Cooling bose-einstein condensates below 500 picokelvin. *Science*, **301**, 1513–1515.

Lebowitz, J.L. and Rubin, E. (1963). Dynamical study of brownian motion. *Phys. Rev.*, **131**, 2381–2396.

Leggett, A.J. (2001). Bose-einstein condensation in the alkali gases: Some fundamental concepts. *Rev. Mod. Phys.*, **73**, 307–356.

Leggett, A.J., Chakravarty, S., Dorsey, A.T., Fisher, M.P.A., Garg, A. and Zwerger, W. (1987). Dynamics of the dissipative two-state system. *Rev. Mod. Phys.*, **59**, 1–85.

Lehmann, J., Kohler, S., Hänggi, P. and Nitzan, A. (2003). Rectification of laser-induced electronic transport through molecules. *The Journal of Chemical Physics*, **118**, 3283–3293.

Leibfried, D., Barrett, M.D., Schaetz, T., Britton, J., Chiaverini, J., Itano, W.M., Jost, J.D., Langer, C. and Wineland, D.J. (2004). Toward heisenberg-limited spectroscopy with multiparticle entangled states. *Science*, **304**, 1476–1478.

Lellouch, S., Dao, T.L., Koffel, T. and Sanchez-Palencia, L. (2013). Two-component bose gases with one-body and two-body couplings. *Phys. Rev. A*, **88**, 063646.

Lepri, S. (2016). *Thermal transport in low dimensions: from statistical physics to nanoscale heat transfer*, vol. 921. Springer.

Lepri, S., Livi, R. and Politi, A. (2003). Thermal conduction in classical low-dimensional lattices. *Physics Reports*, **377**, 1 – 80.

Levinsen, J. and Parish, M.M. (2014). Strongly interacting two-dimensional Fermi gases.

Levinsen, J., Parish, M.M. and Bruun, G.M. (2015). Impurity in a bose-einstein condensate and the efimov effect. *Phys. Rev. Lett.*, **115**, 125302.

Levy, A., Alicki, R. and Kosloff, R. (2012). Quantum refrigerators and the third law of thermodynamics. *Phys. Rev. E*, **85**, 061126.

Lewenstein, M., Sanpera, A. and Ahufinger, V. (2012). *Ultracold Atoms in Optical Lattices: Simulating quantum many-body systems*. Oxford University Press.

Leyvraz, F., Adler, J., Aharony, A., Bunde, A., Coniglio, A., Hong, D.C., Stanley, H.E. and Stauffer, D. (1986). The random normal superconductor mixture in one dimension. *Journal of Physics A: Mathematical and General*, **19**, 3683–3692.

Li, B., Wang, L. and Casati, G. (2004). Thermal diode: Rectification of heat flux. *Phys. Rev. Lett.*, **93**, 184301.

Li, B., Lan, J. and Wang, L. (2005). Interface thermal resistance between dissimilar anharmonic lattices. *Phys. Rev. Lett.*, **95**, 104302.

Li, B., Wang, L. and Casati, G. (2006). Negative differential thermal resistance and thermal transistor. *Applied Physics Letters*, **88**, 143501.

Li, H., Agarwalla, B.K. and Wang, J.S. (2012a). Generalized caroli formula for the transmission coefficient with lead-lead coupling. *Phys. Rev. E*, **86**, 011141.

Li, J., Fogarty, T., Campbell, S., Chen, X. and Busch, T. (2018). An efficient nonlinear feshbach engine. *New Journal of Physics*, **20**, 015005.

Li, N., Ren, J., Wang, L., Zhang, G., Hänggi, P. and Li, B. (2012b). Colloquium: Phononics: Manipulating heat flow with electronic analogs and beyond. *Rev. Mod. Phys.*, **84**, 1045–1066.

Li, T. and Raizen, M.G. (2013). Brownian motion at short time scales. *Annalen der Physik*, **525**, 281–295.

Li, T., Kheifets, S., Medellin, D. and Raizen, M.G. (2010). Measurement of the instantaneous velocity of a brownian particle. *Science*, **328**, 1673–1675.

Lieb, E.H. and Liniger, W. (1963). Exact analysis of an interacting bose gas. i. the general solution and the ground state. *Phys. Rev.*, **130**, 1605–1616.

Lieb, E.H. and Thomas, L.E. (1997a). Exact ground state energy of the strong-coupling polaron. *Comm. Math. Phys.*, **183**, 511.

Lieb, E.H. and Thomas, L.E. (1997b). Exact ground state energy of the strong-coupling polaron. *Communications in Mathematical Physics*, **183**, 511–519.

Lieb, E.H. and Yamazaki, K. (1958). Ground-state energy and effective mass of the polaron. *Phys. Rev.*, **111**, 728.

Lim, S.H., Wehr, J., Lampo, A., García-March, M.Á. and Lewenstein, M. (2018). On the small mass limit of quantum brownian motion with inhomogeneous damping and diffusion. *Journal of Statistical Physics*, **170**, 351–377.

Lindblad, G. (1976). Brownian motion of a quantum harmonic oscillator. *Reports on Mathematical Physics*, **10**, 393 – 406.

Liu, B.H., Hu, X.M., Huang, Y.F., Li, C.F., Guo, G.C., Karlsson, A., Laine, E.M., Maniscalco, S., Macchiavello, C. and Piilo, J. (2016). Efficient superdense coding in the presence of non-markovian noise. *EPL (Europhysics Letters)*, **114**, 10005.

Liu, J., Lu, X.M. and Wang, X. (2013). Nonunital non-markovianity of quantum dynamics. *Phys. Rev. A*, **87**, 042103.

Liu, K.L. and Goan, H.S. (2007). Non-markovian entanglement dynamics of quantum continuous variable systems in thermal environments. *Phys. Rev. A*, **76**, 022312.

Lo, P.Y., Xiong, H.N. and Zhang, W.M. (2015). Breakdown of bose-einstein distribution in photonic crystals. *Scientific Reports*, **5**.

Lombardi, M.A., Nelson, L.M., Novick, A.N. and Zhang, V.S. (2001). Time and frequency measurements using the global positioning system. *Cal Lab: International Journal of Metrology*, **8**, 26–33.

Lombardo, F.C. and Villar, P.I. (2007). Noise induced energy excitation by a general environment. *Physics Letters A*, **371**, 190–200.

Lorenzo, S., Plastina, F. and Paternostro, M. (2013). Geometrical characterization of non-markovianity. *Phys. Rev. A*, **88**, 020102.

Louisell, W.H. and Louisell, W.H. (1973). *Quantum statistical properties of radiation*, vol. 7. Wiley New York.

Lu, X.M., Wang, X. and Sun, C.P. (2010). Quantum fisher information flow and non-markovian processes of open systems. *Phys. Rev. A*, **82**, 042103.

Lucioni, E., Deissler, B., Tanzi, L., Roati, G., Zaccanti, M., Modugno, M., Larcher, M., Dalfovo, F., Inguscio, M. and Modugno, G. (2011). Observation of subdiffusion in a disordered interacting system. *Phys. Rev. Lett.*, **106**, 230403.

Ludwig, M., Hammerer, K. and Marquardt, F. (2010). Entanglement of mechanical oscillators coupled to a nonequilibrium environment. *Phys. Rev. A*, **82**, 012333.

Luis, A. (2004). Nonlinear transformations and the heisenberg limit. *Physics Letters A*, **329**, 8 – 13.

Luo, S., Fu, S. and Song, H. (2012). Quantifying non-markovianity via correlations. *Phys. Rev. A*, **86**, 044101.

Lupo, C. and Pirandola, S. (2016). Ultimate precision bound of quantum and subwavelength imaging. *Phys. Rev. Lett.*, **117**, 190802.

Mandelbrot, B. (1956). An outline of a purely phenomenological theory of statistical thermodynamics–i: Canonical ensembles. *IRE Transactions on Information Theory*, **2**, 190–203.

Mandelbrot, B.B. and Van Ness, J.W. (1968). Fractional brownian motions, fractional noises and applications. *SIAM review*, **10**, 422–437.

Manzo, C., Torreno-Pina, J.A., Massignan, P., Lapeyre, G.J., Jr., Lewenstein, M. and García-Parajo, M.F. (2014). Weak ergodicity breaking of receptor motion in living cells stemming from random diffusivity.

Marathe, R., Jayannavar, A.M. and Dhar, A. (2007). Two simple models of classical heat pumps. *Phys. Rev. E*, **75**, 030103.

Markov, A. (1906). Rasprostranenie zakona bol'shih chisel na velichiny, zavisyaschie drug ot druga. *Izvestiya Fiziko-matematicheskogo obschestva pri Kazanskom universitete*, **15**, 135–156.

Martín-Martínez, E., Dragan, A., Mann, R.B. and Fuentes, I. (2013). Berry phase quantum thermometer. *New Journal of Physics*, **15**, 053036.

Masahito, H. (2005). *Asymptotic theory of quantum statistical inference: selected papers*. World Scientific.

Masanes, L. and Oppenheim, J. (2017). A general derivation and quantification of the

third law of thermodynamics. *Nature communications*, **8**, 14538.

Massignan, P., Pethick, C.J. and Smith, H. (2005). Static properties of positive ions in atomic bose-einstein condensates. *Phys. Rev. A*, **71**, 023606.

Massignan, P., Zaccanti, M. and Bruun, G.M. (2014a). Polarons, dressed molecules and itinerant ferromagnetism in ultracold fermi gases. *Reports on Progress in Physics*, **77**, 034401.

Massignan, P., Zaccanti, M. and Bruun, G.M. (2014b). Polarons, dressed molecules and itinerant ferromagnetism in ultracold fermi gases. *Reports on Progress in Physics*, **77**, 034401.

Mathey, L., Wang, D.W., Hofstetter, W., Lukin, M.D. and Demler, E. (2004). Luttinger liquid of polarons in one-dimensional boson-fermion mixtures. *Phys. Rev. Lett.*, **93**, 120404.

Matthews, M.R., Hall, D.S., Jin, D.S., Ensher, J.R., Wieman, C.E., Cornell, E.A., Dalfovo, F., Minniti, C. and Stringari, S. (1998). Dynamical response of a bose-einstein condensate to a discontinuous change in internal state. *Phys. Rev. Lett.*, **81**, 243–247.

Mattuck, R.D. (1992). *A guide to Feynman diagrams in the many-body problem*. Courier Corporation.

Mazo, R.M. (2002). *Brownian motion: fluctuations, dynamics, and applications*, vol. 112. Oxford University Press on Demand.

Mazur, P. and Oppenheim, I. (1970). Molecular theory of brownian motion. *Physica*, **50**, 241 – 258.

McEndoo, S., Haikka, P., Chiara, G.D., Palma, G.M. and Maniscalco, S. (2013). Entanglement control via reservoir engineering in ultracold atomic gases. *EPL (Europhysics Letters)*, **101**, 60005.

McKeown, A. (1927). I.—treatise on thermodynamics. by dr. max planck. third english edition, translated from the seventh german edition by dr. a. ogg. pp. xiv+297. london: Longmans, green & co., ltd., 1927. price 15s. net. *Journal of the Society of Chemical Industry*, **46**, 408–408.

Mehboudi, M., Lampo, A., Charalambous, C., Correa, L., García-March, M.A. and Lewenstein, M. (2019a). Using polarons for sub-nk quantum nondemolition thermometry in a bose-einstein condensate. *Phys. Rev. Lett.*, **122**, 030403.

Mehboudi, M., Lampo, A., Charalambous, C., Correa, L.A., García-March, M.A. and

Lewenstein, M. (2019b). Using polarons for sub-nk quantum nondemolition thermometry in a bose-einstein condensate. *Phys. Rev. Lett.*, **122**, 030403.

Mehboudi, M., Sanpera, A. and Correa, L.A. (2019c). Thermometry in the quantum regime: recent theoretical progress. *Journal of Physics A: Mathematical and Theoretical*, **52**, 303001.

Mehboudi, M., Sanpera, A. and Correa, L.A. (2019d). Thermometry in the quantum regime: recent theoretical progress. *Journal of Physics A: Mathematical and Theoretical*, **52**, 303001.

Merhasin, I.M., Malomed, B.A. and Driben, R. (2005). Transition to miscibility in a binary bose–einstein condensate induced by linear coupling. *Journal of Physics B: Atomic, Molecular and Optical Physics*, **38**, 877–892.

Mermin, N.D. and Wagner, H. (1966). Absence of ferromagnetism or antiferromagnetism in one- or two-dimensional isotropic heisenberg models. *Phys. Rev. Lett.*, **17**, 1133–1136.

Metzler, R. and Klafter, J. (2000). The random walk's guide to anomalous diffusion: a fractional dynamics approach. *Physics Reports*, **339**, 1 – 77.

Miesner, H.J., Stamper-Kurn, D.M., Stenger, J., Inouye, S., Chikkatur, A.P. and Ketterle, W. (1999). Observation of metastable states in spinor bose-einstein condensates. *Phys. Rev. Lett.*, **82**, 2228–2231.

Miller, H.J. and Anders, J. (2018). Energy-temperature uncertainty relation in quantum thermodynamics. *Nature communications*, **9**, 2203.

Min, B., Li, T., Rosenkranz, M. and Bao, W. (2012). Subdiffusive spreading of a bose-einstein condensate in random potentials. *Phys. Rev. A*, **86**, 053612.

Modi, K., Brodutch, A., Cable, H., Paterek, T. and Vedral, V. (2012). The classical-quantum boundary for correlations: Discord and related measures. *Rev. Mod. Phys.*, **84**, 1655–1707.

Modugno, G. (2010). Anderson localization in bose–einstein condensates. *Reports on Progress in Physics*, **73**, 102401.

Modugno, G., Modugno, M., Riboli, F., Roati, G. and Inguscio, M. (2002). Two atomic species superfluid. *Phys. Rev. Lett.*, **89**, 190404.

Monras, A. (2013). Phase space formalism for quantum estimation of gaussian states. *arXiv preprint arXiv:1303.3682*.

Mori, H. (1965). Transport, Collective Motion, and Brownian Motion. *Progress of Theoretical Physics*, **33**, 423–455.

Mulansky, M. and Pikovsky, A. (2010). Spreading in disordered lattices with different nonlinearities. *EPL (Europhysics Letters)*, **90**, 10015.

Mulligan, B.P.J. (2007). Quasiprobability density diffusion equations for the quantum brownian motion in a potential.

Myatt, C.J., Burt, E.A., Ghrist, R.W., Cornell, E.A. and Wieman, C.E. (1997). Production of two overlapping bose-einstein condensates by sympathetic cooling. *Phys. Rev. Lett.*, **78**, 586–589.

Nair, R. and Tsang, M. (2016). Far-field superresolution of thermal electromagnetic sources at the quantum limit. *Phys. Rev. Lett.*, **117**, 190801.

Nakajima, S. (1958). On Quantum Theory of Transport Phenomena: Steady Diffusion. *Progress of Theoretical Physics*, **20**, 948–959.

Napolitano, M., Koschorreck, M., Dubost, B., Behbood, N., Sewell, R. and Mitchell, M.W. (2011). Interaction-based quantum metrology showing scaling beyond the heisenberg limit. *Nature*, **471**, 486.

Navarrete-Benlloch, C., de Vega, I., Porras, D. and Cirac, J.I. (2011). Simulating quantum-optical phenomena with cold atoms in optical lattices. *New Journal of Physics*, **13**, 023024.

Neumann, P., Jakobi, I., Dolde, F., Burk, C., Reuter, R., Waldherr, G., Honert, J., Wolf, T., Brunner, A., Shim, J.H. *et al.* (2013). High-precision nanoscale temperature sensing using single defects in diamond. *Nano letters*, **13**, 2738–2742.

Nicklas, E. (2013). A new tool for miscibility control: Linear coupling. *PhD thesis*.

Niemczyk, T., Deppe, F., Huebl, H., Menzel, E., Hocke, F., Schwarz, M., García-Ripoll, J.J., Zueco, D., Hümmer, T., Solano, E. *et al.* (2010). Beyond the jaynes-cummings model: circuit qed in the ultrastrong coupling regime. *arXiv preprint arXiv:1003.2376*.

Nieuwenhuizen, T.M. and Allahverdyan, A.E. (2002). Statistical thermodynamics of quantum brownian motion: Construction of perpetuum mobile of the second kind. *Phys. Rev. E*, **66**, 036102.

Nyquist, H. (1928). Thermal agitation of electric charge in conductors. *Phys. Rev.*, **32**, 110–113.

Ohmi, T. and Machida, K. (1998). Bose-einstein condensation with internal degrees of freedom in alkali atom gases. *Journal of the Physical Society of Japan*, **67**, 1822–1825.

Olf, R., Fang, F., Marti, G.E., MacRae, A. and Stamper-Kurn, D.M. (2015). Thermometry and cooling of a bose gas to 0.02 times the condensation temperature. *Nature Physics*, **11**, 720.

Olshanii, M. (1998). Atomic scattering in the presence of an external confinement and a gas of impenetrable bosons. *Phys. Rev. Lett.*, **81**, 938–941.

Onsager, L. (1931). Reciprocal relations in irreversible processes. i. *Phys. Rev.*, **37**, 405–426.

Ott, H., Fortagh, J., Schlotterbeck, G., Grossmann, A. and Zimmermann, C. (2001). Bose-einstein condensation in a surface microtrap. *Phys. Rev. Lett.*, **87**, 230401.

Ozpineci, A. and Ciraci, S. (2001). Quantum effects of thermal conductance through atomic chains. *Phys. Rev. B*, **63**, 125415.

P Bykov, V. (1972). Spontaneous emission in a periodic structure. *Journal of Experimental and Theoretical Physics*, **35**, 269.

Paavola, J. and Maniscalco, S. (2010). Decoherence control in different environments. *Phys. Rev. A*, **82**, 012114.

Paavola, J., Piilo, J., Suominen, K.A. and Maniscalco, S. (2009). Environment-dependent dissipation in quantum brownian motion. *Phys. Rev. A*, **79**, 052120.

Paraoanu, G.S., Kohler, S., Sols, F. and Leggett, A.J. (2001). The josephson plasmon as a bogoliubov quasiparticle. *Journal of Physics B: Atomic, Molecular and Optical Physics*, **34**, 4689–4696.

Paris, M.G.A. (2009). Quantum estimation for quantum technology. *International Journal of Quantum Information*, **07**, 125–137.

Pastukhov, V. (2017). Impurity states in the one-dimensional bose gas. *Phys. Rev. A*, **96**, 043625.

Paz, J.P. and Roncaglia, A.J. (2008). Dynamics of the entanglement between two oscillators in the same environment. *Phys. Rev. Lett.*, **100**, 220401.

Paz, J.P., Habib, S. and Zurek, W.H. (1993). Reduction of the wave packet: Preferred observable and decoherence time scale. *Phys. Rev. D*, **47**, 488–501.

Pekar, S. (1946). Autolocalization of the electron in an inertially polarizable dielectric

medium. *Zh. Eksp. Teor. Fiz*, **16**, 335.

Peotta, S., Rossini, D., Polini, M., Minardi, F. and Fazio, R. (2013). Quantum breathing of an impurity in a one-dimensional bath of interacting bosons. *Phys. Rev. Lett.*, **110**, 015302.

Perarnau-Llobet, M., Bäumer, E., Hovhannisyan, K.V., Huber, M. and Acin, A. (2017). No-go theorem for the characterization of work fluctuations in coherent quantum systems. *Phys. Rev. Lett.*, **118**, 070601.

Peres, A. (1996). Separability criterion for density matrices.

Pernice, A., Helm, J. and Strunz, W.T. (2012). System–environment correlations and non-markovian dynamics. *Journal of Physics B: Atomic, Molecular and Optical Physics*, **45**, 154005.

Perrin, J.B. (1909). Mouvement brownien et realite moleculaire. *Ann. de Chim. et de Phys. (VIII)*, **18**, 5–114.

Petrov, D.S., Shlyapnikov, G.V. and Walraven, J.T.M. (2001). Phase-fluctuating 3d bose-einstein condensates in elongated traps. *Phys. Rev. Lett.*, **87**, 050404.

Pezzè, L., Smerzi, A., Oberthaler, M.K., Schmied, R. and Treutlein, P. (2018). Quantum metrology with nonclassical states of atomic ensembles. *Rev. Mod. Phys.*, **90**, 035005.

Pikovsky, A.S. and Shepelyansky, D.L. (2008). Destruction of anderson localization by a weak nonlinearity. *Phys. Rev. Lett.*, **100**, 094101.

Pitaevskii, L. (1961). Vortex lines in an imperfect bose gas. *Sov. Phys. JETP*, **13**, 451–454.

Pitaevskii, L. and Stringari, S. (2016). *Bose-Einstein condensation and superfluidity*, vol. 164. Oxford University Press.

Plenio, M.B. (2005). Logarithmic negativity: A full entanglement monotone that is not convex. *Phys. Rev. Lett.*, **95**, 090503.

Plenio, M.B. and Huelga, S.F. (2002). Entangled light from white noise. *Phys. Rev. Lett.*, **88**, 197901.

Płodzień, M., Demkowicz-Dobrzański, R. and Sowiński, T. (2018). Few-fermion thermometry. *Phys. Rev. A*, **97**, 063619.

Poyatos, J.F., Walser, R., Cirac, J.I., Zoller, P. and Blatt, R. (1996). Motion tomography of a single trapped ion. *Phys. Rev. A*, **53**, R1966–R1969.

Prigogine, I. (1967). Thermodynamics of irreversible processes 3rd edition.

Prior, J., de Vega, I., Chin, A.W., Huelga, S.F. and Plenio, M.B. (2013). Quantum dynamics in photonic crystals. *Phys. Rev. A*, **87**, 013428.

Pu, H. and Bigelow, N.P. (1998). Properties of two-species bose condensates. *Phys. Rev. Lett.*, **80**, 1130–1133.

Qin, M., Shen, H.Z., Zhao, X.L. and Yi, X.X. (2017). Effects of system-bath coupling on a photosynthetic heat engine: A polaron master-equation approach. *Phys. Rev. A*, **96**, 012125.

Quang, T., Woldeyohannes, M., John, S. and Agarwal, G.S. (1997). Coherent control of spontaneous emission near a photonic band edge: A single-atom optical memory device. *Phys. Rev. Lett.*, **79**, 5238–5241.

Raab, E.L., Prentiss, M., Cable, A., Chu, S. and Pritchard, D.E. (1987). Trapping of neutral sodium atoms with radiation pressure. *Phys. Rev. Lett.*, **59**, 2631–2634.

Rahman, A. (1964). Correlations in the motion of atoms in liquid argon. *Phys. Rev.*, **136**, A405–A411.

Rajagopal, A.K., Usha Devi, A.R. and Rendell, R.W. (2010). Kraus representation of quantum evolution and fidelity as manifestations of markovian and non-markovian forms. *Phys. Rev. A*, **82**, 042107.

Rashba, E. (1957). Theory of strong interactions of electron excitations with lattice vibrations in molecular crystals. *Optika i Spektroskopiya*, **2**, 75–87.

Rath, S.P. and Schmidt, R. (2013). Field-theoretical study of the bose polaron. *Phys. Rev. A*, **88**, 053632.

Reatto, L. and Chester, G.V. (1967). Phonons and the properties of a bose system. *Phys. Rev.*, **155**, 88–100.

Recati, A. and Piazza, F. (2019). Breaking of goldstone modes in a two-component bose-einstein condensate. *Phys. Rev. B*, **99**, 064505.

Reifenberger, R. (2016). *Fundamentals of Atomic Force Microscopy: Part I: Foundations*. World Scientific Publishing Company Pte. Limited.

Ren, J., Hänggi, P. and Li, B. (2010). Berry-phase-induced heat pumping and its impact on the fluctuation theorem. *Phys. Rev. Lett.*, **104**, 170601.

Renklioglu, B., Tanatar, B. and Oktel, M.O. (2016). Heat transfer through dipolar cou-

pling: Sympathetic cooling without contact. *Phys. Rev. A*, **93**, 023620.

Rentrop, T., Trautmann, A., Olivares, F.A., Jendrzejewski, F., Komnik, A. and Oberthaler, M.K. (2016). Observation of the phononic lamb shift with a synthetic vacuum. *Phys. Rev. X*, **6**, 041041.

Riera-Campeny, A., Mehboudi, M., Pons, M. and Sanpera, A. (2019). Dynamically induced heat rectification in quantum systems. *Phys. Rev. E*, **99**, 032126.

Rivas, A., Huelga, S.F. and Plenio, M.B. (2010). Entanglement and non-markovianity of quantum evolutions. *Phys. Rev. Lett.*, **105**, 050403.

Roati, G., D'Errico, C., Fallani, L., Fattori, M., Fort, C., Zaccanti, M., Modugno, G., Modugno, M. and Inguscio, M. (2008). Anderson localization of a non-interacting bose–einstein condensate. *Nature*, **453**.

Robertson, H.P. (1929). The uncertainty principle. *Phys. Rev.*, **34**, 163–164.

Roy, S.M. and Braunstein, S.L. (2008). Exponentially enhanced quantum metrology. *Phys. Rev. Lett.*, **100**, 220501.

Rzażewski, K. and Żakowicz, W. (1980). Initial value problem for two oscillators interacting with electromagnetic field. *Journal of Mathematical Physics*, **21**, 378–388.

Sabín, C., White, A., Hackermuller, L. and Fuentes, I. (2014). Impurities as a quantum thermometer for a bose-einstein condensate. *Scientific reports*, **4**, 6436.

Sacha, K. and Timmermans, E. (2006). Self-localized impurities embedded in a one-dimensional bose-einstein condensate and their quantum fluctuations. *Phys. Rev. A*, **73**, 063604.

Saira, O.P., Meschke, M., Giazotto, F., Savin, A.M., Möttönen, M. and Pekola, J.P. (2007). Heat transistor: Demonstration of gate-controlled electronic refrigeration. *Phys. Rev. Lett.*, **99**, 027203.

Saito, K. and Dhar, A. (2007). Fluctuation theorem in quantum heat conduction. *Phys. Rev. Lett.*, **99**, 180601.

Sanchez-Palencia, L. and Lewenstein, M. (2010). Disordered quantum gases under control. *Nature Physics*, **6**.

Sarkar, S., McEndoo, S., Schneble, D. and Daley, A.J. (2018). Interspecies entanglement with impurity atoms in a bosonic lattice gas. *arXiv:1805.01592*.

Sarovar, M., Ishizaki, A., Fleming, G.R. and Whaley, K.B. (2010). Quantum entanglement

in photosynthetic light-harvesting complexes. *Nature Physics*, **6**, 462.

Saxton, M.J. (1993). Lateral diffusion in an archipelago. single-particle diffusion. *Biophys J*, **64**.

Saxton, M.J. (1997). Single-particle tracking: the distribution of diffusion coefficients. *Biophys J*, **72**.

Scher, H. and Montroll, E.W. (1975). Anomalous transit-time dispersion in amorphous solids. *Phys. Rev. B*, **12**, 2455–2477.

Schirotzek, A., Wu, C.H., Sommer, A. and Zwierlein, M.W. (2009a). Observation of fermi polarons in a tunable fermi liquid of ultracold atoms. *Phys. Rev. Lett.*, **102**, 230402.

Schirotzek, A., Wu, C.H., Sommer, A. and Zwierlein, M.W. (2009b). Observation of fermi polarons in a tunable fermi liquid of ultracold atoms. *Phys. Rev. Lett.*, **102**, 230402.

Schlosshauer, M. (2005). Decoherence, the measurement problem, and interpretations of quantum mechanics. *Rev. Mod. Phys.*, **76**, 1267–1305.

Schlosshauer, M. (2007a). *Decoherence and the Quantum To Classical Transition*. The Frontiers Collection, Springer.

Schlosshauer, M.A. (2007b). *Decoherence: and the quantum-to-classical transition*. Springer Science & Business Media.

Schmid, A. (1982). On a quasiclassical langevin equation. *Journal of Low Temperature Physics*, **49**, 609–626.

Schmidt, R., Enss, T., Pietilä, V. and Demler, E. (2012). Fermi polarons in two dimensions. *Phys. Rev. A*, **85**, 021602.

Schmitt, S., Gefen, T., Stürner, F.M., Unden, T., Wolff, G., Müller, C., Scheuer, J., Naydenov, B., Markham, M., Pezzagna, S., Meijer, J., Schwarz, I., Plenio, M., Retzker, A., McGuinness, L.P. and Jelezko, F. (2017). Submillihertz magnetic spectroscopy performed with a nanoscale quantum sensor. *Science*, **356**, 832–837.

Schön, G. and Zaikin, A. (1990). Quantum coherent effects, phase transitions, and the dissipative dynamics of ultra small tunnel junctions. *Physics Reports*, **198**, 237 – 412.

Schnabel, R., Mavalvala, N., McClelland, D.E. and Lam, P.K. (2010). Quantum metrology for gravitational wave astronomy. *Nature communications*, **1**, 121.

Schneider, S., Kasper, A., vom Hagen, C., Bartenstein, M., Engeser, B., Schumm, T., Bar-Joseph, I., Folman, R., Feenstra, L. and Schmiedmayer, J. (2003). Bose-einstein

condensation in a simple microtrap. *Phys. Rev. A*, **67**, 023612.

Schrodinger, E. (1930). About heisenberg uncertainty relation (english translation). *Ber. Kgl. Akad. Wiss*, 296–296.

Schumaker, B.L. (1986). Quantum mechanical pure states with gaussian wave functions. *Physics Reports*, **135**, 317 – 408.

Schwabl, F. (2002). *Statistical mechanics*. Berlin.

Schwartz, M. (1977). Off-diagonal long-range behavior of interacting bose systems. *Phys. Rev. B*, **15**, 1399–1403.

Segal, D. and Nitzan, A. (2005a). Heat rectification in molecular junctions. *The Journal of Chemical Physics*, **122**, 194704.

Segal, D. and Nitzan, A. (2005b). Spin-boson thermal rectifier. *Phys. Rev. Lett.*, **94**, 034301.

Segal, D., Nitzan, A. and Hänggi, P. (2003). Thermal conductance through molecular wires. *The Journal of Chemical Physics*, **119**, 6840–6855.

Serafini, A. (2006). Multimode uncertainty relations and separability of continuous variable states. *Phys. Rev. Lett.*, **96**, 110402.

Shashi, A., Grusdt, F., Abanin, D.A. and Demler, E. (2014a). Radio-frequency spectroscopy of polarons in ultracold bose gases. *Phys. Rev. A*, **89**, 053617.

Shashi, A., Grusdt, F., Abanin, D.A. and Demler, E. (2014b). Radio-frequency spectroscopy of polarons in ultracold bose gases. *Phys. Rev. A*, **89**, 053617.

Shchadilova, Y.E., Grusdt, F., Rubtsov, A.N. and Demler, E. (2016a). Polaronic mass renormalization of impurities in bose-einstein condensates: Correlated gaussian-wave-function approach. *Phys. Rev. A*, **93**, 043606.

Shchadilova, Y.E., Grusdt, F., Rubtsov, A.N. and Demler, E. (2016b). Polaronic mass renormalization of impurities in bose-einstein condensates: Correlated gaussian-wave-function approach. *Phys. Rev. A*, **93**, 043606.

Shchadilova, Y.E., Schmidt, R., Grusdt, F. and Demler, E. (2016c). Quantum dynamics of ultracold bose polarons. *Phys. Rev. Lett.*, **117**, 113002.

Shchadilova, Y.E., Schmidt, R., Grusdt, F. and Demler, E. (2016d). Quantum dynamics of ultracold bose polarons. *Phys. Rev. Lett.*, **117**, 113002.

Shepelyansky, D.L. (1993). Delocalization of quantum chaos by weak nonlinearity. *Phys. Rev. Lett.*, **70**, 1787–1790.

Sherson, J.F., Weitenberg, C., Endres, M., Cheneau, M., Bloch, I. and Kuhr, S. (2010). Single-atom-resolved fluorescence imaging of an atomic mott insulator. *Nature*, **467**, 68.

Shiokawa, K. (2009). Non-markovian dynamics, nonlocality, and entanglement in quantum brownian motion. *Phys. Rev. A*, **79**, 012308.

Sieberer, L.M., Chiocchetta, A., Gambassi, A., Täuber, U.C. and Diehl, S. (2015). Thermodynamic equilibrium as a symmetry of the schwinger-keldysh action. *Phys. Rev. B*, **92**, 134307.

Simon, J., Bakr, W.S., Ma, R., Tai, M.E., Preiss, P.M. and Greiner, M. (2011). Quantum simulation of antiferromagnetic spin chains in an optical lattice. *Nature*, **472**, 307.

Simon, R. (2000). Peres-horodecki separability criterion for continuous variable systems. *Phys. Rev. Lett.*, **84**, 2726–2729.

Simon, R., Sudarshan, E.C.G. and Mukunda, N. (1987). Gaussian-wigner distributions in quantum mechanics and optics. *Phys. Rev. A*, **36**, 3868–3880.

Simon, R., Mukunda, N. and Dutta, B. (1994). Quantum-noise matrix for multimode systems: U(n) invariance, squeezing, and normal forms. *Phys. Rev. A*, **49**, 1567–1583.

Skokos, C., Krimer, D.O., Komineas, S. and Flach, S. (2009). Delocalization of wave packets in disordered nonlinear chains. *Phys. Rev. E*, **79**, 056211.

Smerzi, A., Fantoni, S., Giovanazzi, S. and Shenoy, S.R. (1997). Quantum coherent atomic tunneling between two trapped bose-einstein condensates. *Phys. Rev. Lett.*, **79**, 4950–4953.

Săndulescu, A. and Scutaru, H. (1987). Open quantum systems and the damping of collective modes in deep inelastic collisions. *Annals of Physics*, **173**, 277–317.

Sokolov, I.M. and Klafter, J. (2005). From diffusion to anomalous diffusion: A century after einstein's brownian motion. *Chaos: An Interdisciplinary Journal of Nonlinear Science*, **15**, 026103.

Spiechowicz, J., Łuczka, J. and Hänggi, P. (2016). Transient anomalous diffusion in periodic systems: ergodicity, symmetry breaking and velocity relaxation. *Scientific Reports*, **6**.

Spiegelhalder, F.M., Trenkwalder, A., Naik, D., Hendl, G., Schreck, F. and Grimm, R. (2009). Collisional stability of ^{40}**K** immersed in a strongly interacting fermi gas of ^{6}Li. *Phys. Rev. Lett.*, **103**, 223203.

Stace, T.M. (2010). Quantum limits of thermometry. *Phys. Rev. A*, **82**, 011611.

Stamper-Kurn, D.M., Andrews, M.R., Chikkatur, A.P., Inouye, S., Miesner, H.J., Stenger, J. and Ketterle, W. (1998). Optical confinement of a bose-einstein condensate. *Phys. Rev. Lett.*, **80**, 2027–2030.

Stenger, J., Inouye, S., Stamper-Kurn, D., Miesner, H.J., Chikkatur, A. and Ketterle, W. (1998). Spin domains in ground-state bose–einstein condensates. *Nature*, **396**, 345.

Stockburger, J.T. (2003). Stochastic and numerical approaches to dissipative quantum dynamics: path integrals and beyond. *physica status solidi (b)*, **237**, 146–158.

Strunz, W.T., Diósi, L., Gisin, N. and Yu, T. (1999). Quantum trajectories for brownian motion. *Phys. Rev. Lett.*, **83**, 4909–4913.

Svensmark, H. and Flensberg, K. (1993). Squeezing of thermal and quantum fluctuations: Universal features. *Phys. Rev. A*, **47**, R23–R26.

Szczykulska, M., Baumgratz, T. and Datta, A. (2016). Multi-parameter quantum metrology. *Advances in Physics: X*, **1**, 621–639.

Talkner, P. (1986). The failure of the quantum regression hypothesis. *Annals of Physics*, **167**, 390–436.

Tan, H.T., Zhang, W.M. and Li, G.x. (2011). Entangling two distant nanocavities via a waveguide. *Phys. Rev. A*, **83**, 062310.

Tang, Y., Kao, W., Li, K.Y. and Lev, B.L. (2018). Tuning the dipole-dipole interaction in a quantum gas with a rotating magnetic field. *Phys. Rev. Lett.*, **120**, 230401.

Tarruell, L., Greif, D., Uehlinger, T., Jotzu, G. and Esslinger, T. (2012). Creating, moving and merging dirac points with a fermi gas in a tunable honeycomb lattice. *Nature*, **483**, 302.

Taylor, M.A. and Bowen, W.P. (2016). Quantum metrology and its application in biology. *Physics Reports*, **615**, 1–59.

Tempere, J., Casteels, W., Oberthaler, M.K., Knoop, S., Timmermans, E. and Devreese, J.T. (2009). Feynman path-integral treatment of the bec-impurity polaron. *Phys. Rev. B*, **80**, 184504.

Terraneo, M., Peyrard, M. and Casati, G. (2002). Controlling the energy flow in nonlinear lattices: A model for a thermal rectifier. *Phys. Rev. Lett.*, **88**, 094302.

Toda, M., Kubo, R., Saitō, N., Hashitsume, N. *et al.* (1991). *Statistical physics II: nonequilibrium statistical mechanics*, vol. 30. Springer Science & Business Media.

Tommasini, P., de Passos, E.J.V., de Toledo Piza, A.F.R., Hussein, M.S. and Timmermans, E. (2003). Bogoliubov theory for mutually coherent condensates. *Phys. Rev. A*, **67**, 023606.

Torrontegui, E., Ibáñez, S., Martínez-Garaot, S., Modugno, M., del Campo, A., Guéry-Odelin, D., Ruschhaupt, A., Chen, X. and Muga, J.G. (2013). Chapter 2 - shortcuts to adiabaticity. **62**, 117 – 169.

Tóth, G. and Apellaniz, I. (2014). Quantum metrology from a quantum information science perspective. *Journal of Physics A: Mathematical and Theoretical*, **47**, 424006.

Toyli, D.M., de las Casas, C.F., Christle, D.J., Dobrovitski, V.V. and Awschalom, D.D. (2013). Fluorescence thermometry enhanced by the quantum coherence of single spins in diamond. *Proceedings of the National Academy of Sciences*, **110**, 8417–8421.

Tsang, M., Nair, R. and Lu, X.M. (2016). Quantum theory of superresolution for two incoherent optical point sources. *Phys. Rev. X*, **6**, 031033.

Udem, T., Holzwarth, R. and Hänsch, T.W. (2002). Optical frequency metrology. *Nature*, **416**, 233.

Uhlenbeck, G.E. and Ornstein, L.S. (1930). On the theory of the brownian motion. *Phys. Rev.*, **36**, 823–841.

Ullersma, P. (1966). An exactly solvable model for brownian motion: I. derivation of the langevin equation. *Physica*, **32**, 27 – 55.

Unruh, W.G. and Zurek, W.H. (1989). Reduction of a wave packet in quantum brownian motion. *Phys. Rev. D*, **40**, 1071–1094.

Uzdin, R. and Rahav, S. (2018). Global passivity in microscopic thermodynamics. *Phys. Rev. X*, **8**, 021064.

Valido, A.A., Alonso, D. and Kohler, S. (2013a). Gaussian entanglement induced by an extended thermal environment. *Phys. Rev. A*, **88**, 042303.

Valido, A.A., Alonso, D. and Kohler, S. (2013b). Gaussian entanglement induced by an extended thermal environment. *Phys. Rev. A*, **88**, 042303.

Vasile, R., Giorda, P., Olivares, S., Paris, M. and Maniscalco, S. (2010a). Nonclassical correlations in non-markovian continuous-variable systems. *Phys. Rev. A*, **82**, 012313.

Vasile, R., Giorda, P., Olivares, S., Paris, M.G.A. and Maniscalco, S. (2010b). Nonclassical correlations in non-markovian continuous-variable systems. *Phys. Rev. A*, **82**, 012313.

Vasile, R., Galve, F. and Zambrini, R. (2014). Spectral origin of non-markovian open-system dynamics: A finite harmonic model without approximations. *Phys. Rev. A*, **89**, 022109.

Veksler, H., Krivolapov, Y. and Fishman, S. (2009). Spreading for the generalized non-linear schrödinger equation with disorder. *Phys. Rev. E*, **80**, 037201.

Vidal, G. and Werner, R.F. (2002). Computable measure of entanglement. *Phys. Rev. A*, **65**, 032314.

von Smoluchowski, M. (1906). Zur kinetischen theorie der brownschen molekularbewegung und der suspensionen. *Annalen der Physik*, **326**, 756–780.

Vulpiani A., C.M.P.A., Cecconi F. and D., V. (2014). *Large Deviations in Physics: The Legacy of the Law of Large Numbers*. Lect. Notes in Phys. Springer Berlin Heidelberg.

W. T. Coffey, Y.P.K. and Waldron, J.T. (2004). *The Langevin equation*. World Scientific, Singapore.

Wallraff, A. (2001). *Fluxon dynamics in annular Josephson junctions: From Relativistic Strings to quantum particles*. Lehrstuhl für Mikrocharakterisierung, Friedrich-Alexander-Universität.

Wang, J., He, J. and Ma, Y. (2018).

Wang, J.S., Wang, J. and Zeng, N. (2006). Nonequilibrium green's function approach to mesoscopic thermal transport. *Phys. Rev. B*, **74**, 033408.

Wang, L. and Li, B. (2007). Thermal logic gates: Computation with phonons. *Phys. Rev. Lett.*, **99**, 177208.

Wang, L. and Li, B. (2008a). Phononics gets hot. *Physics World*, **21**, 27–29.

Wang, L. and Li, B. (2008b). Thermal memory: A storage of phononic information. *Phys. Rev. Lett.*, **101**, 267203.

Wang, M.C. and Uhlenbeck, G.E. (1945). On the theory of the brownian motion ii. *Rev. Mod. Phys.*, **17**, 323–342.

Wang, Q. and Zhan, H. (2015). On different numerical inverse laplace methods for solute transport problems. *Advances in Water Resources*, **75**, 80 – 92.

Watanabe, Y., Sagawa, T. and Ueda, M. (2010). Optimal measurement on noisy quantum systems. *Phys. Rev. Lett.*, **104**, 020401.

Weedbrook, C., Pirandola, S., García-Patrón, R., Cerf, N.J., Ralph, T.C., Shapiro, J.H. and Lloyd, S. (2012). Gaussian quantum information. *Rev. Mod. Phys.*, **84**, 621–669.

Weiss, U. (2012). *Quantum dissipative systems*, vol. 13. World scientific.

Wernsdorfer, W. (2001). Classical and quantum magnetization reversal studied in nanometer-sized particles and clusters. *Adv. in Chem. Phys.*, **118**, 99–190.

Williamson, J. (1936). On the algebraic problem concerning the normal forms of linear dynamical systems. *American Journal of Mathematics*, **58**, 141–163.

Woldeyohannes, M. and John, S. (2003). Coherent control of spontaneous emission near a photonic band edge. *Journal of Optics B: Quantum and Semiclassical Optics*, **5**, R43–R82.

Wolf, A., Chiara, G.D., Kajari, E., Lutz, E. and Morigi, G. (2011). Entangling two distant oscillators with a quantum reservoir. *EPL (Europhysics Letters)*, **95**, 60008.

Wolf, M.M., Eisert, J., Cubitt, T.S. and Cirac, J.I. (2008). Assessing non-markovian quantum dynamics. *Phys. Rev. Lett.*, **101**, 150402.

Wynands, R. and Weyers, S. (2005). Atomic fountain clocks. *Metrologia*, **42**, S64–S79.

Xi, K.T., Li, J. and Shi, D.N. (2014). Localization of a two-component bose–einstein condensate in a two-dimensional bichromatic optical lattice. *Physica B: Condensed Matter*, **436**, 149 – 156.

Yablonovitch, E. (1987). Inhibited spontaneous emission in solid-state physics and electronics. *Phys. Rev. Lett.*, **58**, 2059–2062.

Yang, N., Li, N., Wang, L. and Li, B. (2007). Thermal rectification and negative differential thermal resistance in lattices with mass gradient. *Phys. Rev. B*, **76**, 020301.

Ye, Z., Hu, Y., He, J. and Wang, J. (2017). Universality of maximum-work efficiency of a cyclic heat engine based on a finite system of ultracold atoms. *Scientific reports*, **7**, 6289.

Yoshida, S.M., Endo, S., Levinsen, J. and Parish, M.M. (2018). Universality of an impurity in a bose-einstein condensate. *Phys. Rev. X*, **8**, 011024.

Zanardi, P., Paris, M.G.A. and Campos Venuti, L. (2008). Quantum criticality as a resource for quantum estimation. *Phys. Rev. A*, **78**, 042105.

Zell, T., Queisser, F. and Klesse, R. (2009). Distance dependence of entanglement generation via a bosonic heat bath. *Phys. Rev. Lett.*, **102**, 160501.

Zhang, W.M., Lo, P.Y., Xiong, H.N., Tu, M.W.Y. and Nori, F. (2012). General non-markovian dynamics of open quantum systems. *Phys. Rev. Lett.*, **109**, 170402.

Zürcher, U. and Talkner, P. (1990). Quantum-mechanical harmonic chain attached to heat baths. ii. nonequilibrium properties. *Phys. Rev. A*, **42**, 3278–3290.

Zurek, W.H. (2003). Decoherence, einselection, and the quantum origins of the classical. *Rev. Mod. Phys.*, **75**, 715–775.

Zwanzig, R. (1960). Ensemble method in the theory of irreversibility. *The Journal of Chemical Physics*, **33**, 1338–1341.

Zwanzig, R. (1961). Memory effects in irreversible thermodynamics. *Phys. Rev.*, **124**, 983–992.

Zwanzig, R. (1965). Time-correlation functions and transport coefficients in statistical mechanics. *Annual Review of Physical Chemistry*, **16**, 67–102.

Zwanzig, R. (1973). Nonlinear generalized langevin equations. *Journal of Statistical Physics*, **9**, 215–220.

Zwanzig, R. (2001). *Nonequilibrium statistical mechanics*. Oxford : New York : Oxford University Press, includes index.